Interactions of the OX-2 lymphoid/neuronal glycoprotein

Gavin James Wright

Balliol College

University of Oxford

A thesis submitted for the degree of Doctor of Philosophy,
Michaelmas Term, 1999

For Mum and Dad

CONTENTS

Abstract

Gavin James Wright, Balliol College, University of Oxford.
A thesis submitted for the degree of Doctor of Philosophy, Michaelmas Term, 1999

Interactions of the OX-2 lymphoid/neuronal glycoprotein

Lymphocytes play a key role in the mammalian immune system and migrate around the body interacting with both soluble factors and tissues in their role of detecting and eliminating disease causing pathogens. These interactions are mediated by the molecules expressed at the cell surface of the leukocyte which have become a popular paradigm for the study of intercellular communication. Proteins which belong to the immunoglobulin superfamily (IgSF) are the most abundant of these cell surface molecules and one of these (OX-2) is the major focus of this thesis.

The OX-2 glycoprotein is expressed in both the neuronal and lymphoid compartments of rats and has no known function. However, a highly avid OX-2 binding reagent was previously shown to specifically interact with a cell surface receptor expressed by macrophages. A monoclonal antibody, MRC OX-102, which bound rat macrophages and blocked the binding of OX-2 was raised and used to molecularly identify the receptor on the macrophage by a combination of protein purification and PCR-based strategies.

The rat OX-2 receptor (OX-2R) was identified as a novel member of the IgSF and had a close evolutionary relationship to the OX-2 protein itself. The two glycoproteins interacted with an affinity of 2.5μM and K_{off} 0.8 sec^{-1}, values typical of interactions between cell surface proteins. A mouse form of the OX-2 receptor was also cloned. The cytoplasmic region of the OX-2R contained conserved tyrosine residues which were shown to be phosphorylated upon pervanadate treatment of macrophages. Preliminary distribution data suggest that the receptor is restricted to cells of myeloid origin and the functional consequences of the interaction are discussed.

A monoclonal antibody, MRC OX-104, was raised to the human OX-2 protein to initiate the translation of this work from rodent models to humans. OX-2 showed highly conserved patterns of expression between the two species.

Acknowledgements

I am very grateful to my supervisors Neil Barclay and Marion Brown for all their advice and guidance and providing me with so many opportunities over the past three years.

I am also very grateful to the many members of the MRC Cellular Immunology Unit and Sir William Dunn School of Pathology who have helped me in this project. I am especially grateful to Mike Puklavec for his hybridoma expertise (and performing what seemed impossible) and Steve Simmonds for many immunisations and animal help. A big thank you also goes to Kate and Gill for cheerily taking care of the mountains of washing up, Vanessa Grimwade for help with fusion screens and to Liz Davis for providing answers when no-one else could.

I feel very lucky to have shared many scientific discussions and Halifax House beers with all past and present members of the CIU. I am very grateful to Douglas Brodie for European football nights, Nick Hutchings for 2D discussions and Tony Symons for his biochemical experience and many opening partnerships at Mansfield Road. A big thank you to Peter, Emma, Debbi, Lisa, Leigh, Debbie and Nasim for creating a memorable place to learn.

I am indebted to Diana Zelenika for timely cloning advice and Paul Fairchild and Gordon McPherson for dendritic cells. I am also grateful to members of both Professor Siamon Gordon's and Professor Geoff Smith's laboratories for their willingness to explain the mysteries of macrophages and viruses to a biochemist and their generosity in supplying reagents. Also, a big thank you to Amarjit Bhomra for much DNA sequencing and Tony Willis for protein analysis.

Away from the bench, thanks to all occupants of 11 George Moore Close for friendship and listening, especially to Yat for fried rice and JJ for computer expertise. Also, to everyone who either played in or supported the victorious 1999 cricket team -winning the Jack Cox Trophy will always bring back fond memories.

Finally, for the people who really made all this possible. Thank you to Mum and Dad for all their love and enthusiastic support over the years in everything that I turn my hand to.

Marieke, I am deeply grateful for all your patience, understanding and love.

Abbreviations

Ag	antigen
APC	antigen presenting cell
ATP	adenosine 5'-triphosphate
BirA	biotin protein ligase
bp	base pair
BSA	bovine serum albumin
CAM	cell adhesion molecule
CCP	complement control protein superfamily
CD4d3+4	rat CD4 domains 3 and 4
CD4d3+4-bio	CD4d3+4 biotinylated at C-terminus
cDNA	complementary DNA
C-domain	constant domain
CFA	complete Freund's adjuvant
CHO	Chinese hamster ovary
CIP	calf intestinal phosphatase
cM	centi Morgans
ConA	concanavalin A
CV	column volumes
Da	daltons
DEPC	diethyl pyrocarbonate
DNA	deoxyribonucleic acid
dNTPs	deoxynucleotide triphosphates
DOC	deoxycholate
DTT	dithiotheitol
EDTA	ethylenediaminetetraacetic acid
EGF	epidermal growth factor
ELISA	enzyme linked immunosorbant assay
EST	expressed sequence tag
FACS	fluorescence activated cell sorting
FCS	foetal calf serum
FITC	fluorescein isothiocyanate
FnIII	fibronectin type III
FPLC	fast performance liquid chromatography
g	gravitational constant
GPI	glycosyl-phosphatidylinositol
HAT	hypoxanthine, aminopterin, thymidine
HBS	hepes buffered saline
HEK	human endothelial kidney
HHV	human herpes virus
HPLC	high performance liquid chromatography
HPRT	hypoxanthine phosphoribosyl transferase
i.p.	intraperitoneally
i.v.	intravenously
IAA	iodoacetamide
IFA	incomplete Freund's adjuvant
IFN	interferon
IgSF	immunoglobulin superfamily
IL	interleukin
ITAM	immunoreceptor tyrosine based activation motif
ITIM	immunoreceptor tyrosine based inhibitory motif
K_d	dissociation constant
K_{off}	off rate constant
K_{on}	on rate constant
KSHV	Kaposi's sarcoma associated herpesvirus
LB	Luria-Bertini
LPS	lipoylpolysaccharide
mAb	monoclonal antibody
MCS	multiple cloning site
M-MLTV	Moloney murine leukaemia virus
mRNA	messenger RNA
MSX	methionine sulphoximine
MWCO	molecular weight cut off
NCAM	neural cell adhesion molecule
NR	non-reducing
OD	optical density
ORF	open reading frame
PAGE	polyacrylamide gel elecrophoresis
PBS	phosphate buffered saline
PCR	polymerase chain reaction
PEC	peritoneal exudate cells
PEG	polyethylene glycol
PMSF	phenylmethylsulphonyl fluoride
polyA	poly adenylate
R	reducing
r,m,hOX-2	rat, mouse, human OX-2
r,m,hOX-2R	rat, mouse, human OX-2 receptor
RACE	rapid amplification of cDNA ends
RNA	ribonucleic acid
rpm	revolutions per minute
rRNA	ribosomal RNA
RT	reverse transcriptase
RU	response units
s.c.	subcutaneously
SDS	sodium dodecylsulphate
SMART	switching mechanism at the 5' end of the RNA transcript
SPR	surface plasmon resonance
$t_{1/2}$	half life
TBAC	tris buffered ammonium chloride
TBE	tris borate EDTA
TCS	tissue culture supernatant
TE	tris EDTA
TEMED	N,N,N',N',-tetramethylethylene diamide
Tm	melting temperature
TNFRSF	tumour necrosis factor receptor superfamily
TNFSF	tumour necrosis factor superfamily
UTR	untranslated region
U	unit
V-domain	variable domain
YLDV	Yabba-like disease virus

Nomenclature:

MRC OX-102 is the name given to the cell hybrid that secretes the MRC OX-102 monoclonal antibody (mAb). The antigen recognised by the MRC OX-102 mAb is termed the OX-102 antigen. This same nomenclature is applied to the MRC OX-2 antibody and antigen.

Chapter One

General Introduction

1.1 The evolution of intercellular communication

The evolutionary success of multicellular organisms and advent of cellular specialisation generated the need for very sophisticated types of intercellular communication to appropriately co-ordinate the genetic programs of individual cells within an organism or population. Initially, these forms of communication would have been very simple, perhaps extracellular structures which would simply adhere like cells with like, but formed the basis for the highly complex communicative networks found in higher organisms. The one uniting feature of all forms of communication is the central role of the cell surface, which contains structures able to propagate and integrate signals through an insoluble lipid barrier. A brief analysis of the number of proteins containing membrane spanning regions present in a prokaryote, a single celled eukaryote and a multicellular organism, reveals that the relative number of these proteins increases in evolutionary "more advanced" organisms (Table 1-1). It is one of the major goals of biology to elucidate the function of these membrane proteins and thus understand how they co-ordinate the behaviour of all the individual cells within a multicellular organism.

Organism	T.M.	No. of ORFs	%T.M./total proteins	Reference
E. coli	666	4,288	15.5	(Blattner et al., 1997)
S. cerevisiae	1397	5,885	23.7	(Goffeau et al., 1996)
C. elegans	5687	19,099	29.8	(consortium, 1998)

Table 1-1. The relative number of predicted proteins containing transmembrane regions from a prokaryote, a single celled eukaryote and a multicellular organism. The number of open reading frames containing at least one transmembrane spanning segment (T.M.) were obtained by Dr Richard Copley (Comparative sequence analysis group, EMBL) using the TopPred algorithm http://www.biokemi.su.se/~server/toppred2/toppredServer.cgi from each of the fully sequenced organisms. A percentage of the total predicted open reading frames (orfs) that are T.M. containing proteins was calculated.

1.2 Communication: the molecular mechanism of information transfer

The amount and profile of proteins associated with the cell membrane is unique to a particular differentiated cell type and thus suggests a biochemical explanation for cellular functional heterogeneity (Stryer, 1988). Indeed, the different communicative properties of different cell types are achieved by proteins associated with the cellular membranes. These proteins can mediate communication by two distinct mechanisms:

1) Soluble factors, e.g. polypeptides (cytokines, growth factors) and ions (electrical impulses in the nervous system).
2) Direct cell:cell contact, e.g. cell surface molecules and gap junctions.

These mechanisms differ in that soluble factors have the potential to influence whole populations of cells capable of receiving and responding to the signal whereas communication initiated by direct cell contact is generally a more intimate form of communication involving just the interacting cells.

Membrane proteins which play a primarily architectural role such as those involved in the maintenance of tissue structure such as the cadherin family of proteins (Vleminckx and Kemler, 1999) will not be considered here. Instead, proteins specialised in intercellular communication will be the main focus.

Proteins involved in the initiation of intracellular signalling cascades have been shown to perform this function using a variety of different mechanisms:

1) Conformational changes of membrane proteins (usually multipass proteins) e.g. bacterial four-pass transmembrane receptor (Ottemann et al., 1999) and G-protein coupled receptors (Bockaert and Pin, 1999).

2) Redistribution of cell surface molecules, e.g. receptor clustering and segregation (Davis and van der Merwe, 1996), receptor oligomerisation (particularly dimerisation), (Weiss and Schlessinger, 1998; Heldin, 1995), lipid rafts (Simons and Ikonen, 1997).
3) Changes in membrane potential, e.g. ligand gated ion channels e.g. Acetylcholine receptor (Unwin, 1995), voltage gated ion channels (Choe et al., 1999).

Membrane proteins (with the exception of lipid linked proteins) are unique in that they bridge the lipid bilayer and are thus able to mediate interactions both in the extracellular and intracellular compartments. The environment in which these two types of interaction occur are quite different. Interactions occurring in the extracellular region do so in the lymph or blood serum which has a protein concentration of only 60 to 80 $mgml^{-1}$ compared to a concentration of ~300 $mgml^{-1}$ in the interior of a cell. Also, the two environments have a different redox potential, the exterior of the cell is a more oxidising environment to the interior. The transmembrane and cytoplasmic region of membrane proteins are often responsible for the initiation of an intracellular signal as a consequence of a specific binding event at the cell surface made by the extracellular region of the protein and are thus an integral part of the protein function.

The vast variety of signals that a single cell is capable of receiving by different mechanisms poses a hugely complex problem. If we are to understand how a single cell biologically responds to the barrage of inputs then we must elucidate all of the signals that are generated. Such a task requires a gargantuan effort and thus there is a need to define paradigms in order to achieve this goal.

1.3 The immune system and T-cell activation –a paradigm for complex intercellular communication

The membranes of leukocytes, and especially that of the T-lymphocyte, have been the subject of intensive study and thus the surfaces of these cells are now very well characterised in terms of their molecular composition, architecture (Barclay et al., 1997) and, in the case of the T-lymphocyte, functional dynamics (Grakoui et al., 1999). The highly characterised nature of the T-cell membrane has made it a popular paradigm in understanding the mechanisms of complex intercellular communication and this knowledge will provide the rationale for the work described in this thesis.

1.3.1 Functions of leukocyte cell surface proteins

The number of different leukocyte specific membrane proteins currently numbers just over 200 and the final figure is estimated to be not significantly greater than this (Barclay et al., 1997). Efforts are therefore being concentrated into identifying the functions of these characterised proteins. An analysis of the functions of the characterised leukocyte cell surface proteins is very revealing:

Function	Representation in the leukocyte membrane
Enzymatic activity in extracellular region	3%
Receptor for soluble factor	23%
Others (e.g. ion channels and transporters)	1%
Receptors for other cell surface proteins	25%
UNKNOWN	49%

Table 1-2. Relative frequency of the roles of leukocyte cell surface proteins. Adapted from Barclay et al., 1997.

A characteristic of leukocyte function is their highly migratory behaviour and ability to interact and communicate with the many other tissues in the body and this is reflected by the function of their cell surface proteins. A quarter are involved in cell surface to cell surface mediated adhesion/communication and over a fifth confer an ability to respond to soluble factors (Table 1-2). In contrast, very few contain an enzymatic activity and the immunological function afforded by this activity is often obscure. The remarkable finding is that the function of half of the leukocyte restricted antigens is unknown, although function can be predicted by identifying sequence similarities to proteins of known function. These predictions suggest that the majority of these unknown functions are receptors for other cell surface proteins and thus represent a large gap in our understanding of the leukocyte cell surface.

The major focus of this thesis is to further the understanding of the biological role of a membrane glycoprotein called OX-2 which belongs to the 50% of proteins which had no known function but was predicted to mediate a specific recognition event at the cell surface with another cell surface receptor. This protein attracted the interest of our laboratory for two basic reasons:

1) OX-2 belongs to the immunoglobulin superfamily (IgSF) which represents the most common structural family of cell surface proteins expressed by leukocytes (section 1.3.2.1) and thus the discovery of any general principles regarding the function of these molecules could be applied to a whole family of other proteins of unknown function.
2) OX-2 is expressed on tissues of both the immune and nervous systems (section 1.6.2).

OX-2 thus belongs to a small group of cell surface proteins which are both members of the IgSF and expressed in the immune and nervous systems such as CD90 (Thy-1) (Williams

and Gagnon, 1982), CD56 (NCAM), L1 (Hortsch, 1996), and CD166 (ALCAM) (Bowen et al., 1997; Tanaka et al., 1991). L1 is known to be important in neural function, since mutations in any of the six IgSF domains are associated with neuropathy (Hortsch, 1996). Members of this group are able to mediate both homophilic and heterophilic interactions, e.g. L1 (Tanaka et al., 1991; Hortsch, 1996) and NCAM (Ranheim et al., 1996) and interact with proteins from other structural families such as integrins (L1) (Hortsch, 1996) or scavenger receptor domains (ALCAM) (Bowen et al., 1995).

A significant step forward in understanding the function of OX-2 would be to molecularly characterise the OX-2 receptor and this was the primary aim of this thesis. The fact that OX-2 is a member of the IgSF facilitated the work since many predictions regarding the structural features of the protein could be made with confidence. However, no similar predictions could be made regarding the molecular nature of the OX-2 receptor since IgSF proteins mediate a huge variety of different types of interaction (see above).

1.3.2 Structural aspects of leukocyte cell surface proteins

The function of any protein is intimately associated with its structure and thus an appreciation of certain structural aspects of cell surface proteins is essential.

1.3.2.1 Domain frequencies in leukocyte cell surface molecules

It is convenient to group proteins which contain sequence similarities to each other into "superfamilies". The regions of similarity between proteins within a superfamily are often only 15-25% identical. Thus, the proteins are grouped together largely because they contain a number of structurally critical "signature" residues that typify the superfamily, although statistical tests are usually performed to support the argument. It is now known

through structural studies that these regions of homology define discrete structural units or domains. Thus, the classification of leukocyte proteins into separate superfamilies has allowed both structural and functional information to be implied. There are just under 20 different domains which have been identified in leukocyte cell surface proteins and the relative frequencies of some are shown in Table 1-3.

Domain	Frequency of leukocyte proteins where domain is present
IgSF	34%
FnIII	12%
Cytokine receptor	8%
Integrin	8%
Lectin type-C	6%
CCP	5%
EGF	4%
TNFSF	3%
TNFRSF	3%

Table 1-3. Frequency of different domain types present in leukocyte cell surface proteins. Adapted from Barclay et al., 1997.

It is quite clear from Table 1-3 that the immunoglobulin superfamily (IgSF) structural unit is by far the most common found in leukocyte cell surface proteins and is discussed in more detail below (section 1.4). In addition, proteins belonging to the IgSF have been identified at the cell surface of many other tissues indicating that the communicative mechanisms used by the leukocyte may well be used by many other cell types. Furthermore, despite sequence differences, both the Fibronectin type III (Fn III) and cytokine receptor domain fold into very similar tertiary structures (Barclay et al., 1997) and thus a greater understanding of the role of these superfamilies would enhance our understanding of intercellular communication.

1.3.2.2 Architecture of the cell surface

Structural studies of cell surface proteins have been used to build scale cartoons of what the cell surface might look like -one of which is shown in Figure 1-2. The first striking observation is that the individual components which constitute the cell surface vary enormously in their size and shape, ranging from small molecules such as CD80 and CD86 which project only ~7nm from the cell surface, to large, heavily glycosylated structures such as CD43 and CR1 which can extend up to 45nm (Cyster et al., 1991) and 85nm (Weisman et al., 1990) away from the cell surface. Secondly, note that the abundance of the immunoglobulin domain (ovals) which is present in a wide variety of proteins and that proteins composed of just two IgSF domains are the most common structural class of proteins on these cells. Indeed, around half of all leukocyte restricted proteins belonging to the IgSF have this 2 domain organisation and they account for 15% of all leukocyte cell surface proteins (Brown et al., 1998). OX-2 belongs to this structural class of proteins and is one of the smaller structures found at the leukocyte cell surface. In addition, leukocyte cell surface molecules rarely contain just a single domain but rather contain multiple copies of either the same domain or a mixture of different structural units. For example, the neural molecule L1 contains six IgSF domains but also five fibronectin type III domains (Hortsch, 1996). These multi hetero-domain containing proteins are often termed mosaic proteins (Barclay et al., 1997).

The relative abundance of membrane molecules is critical in constructing a model of the cell surface. Figures have been obtained for selected antigens present on rat thymocytes using labelled Fab fragments and site numbers are estimated to vary between 10^6 for an abundant molecule such as Thy-1 to 10^4 for the OX-2 antigen (Williams and Barclay, 1986). However, the abundance of some cell surface molecules are significantly lower than this,

such as the pre-TCR which is difficult to detect but known to have a significant biological role (Bruno et al., 1999).

What is becoming increasingly clear is that the overall dimensions of many interacting protein pairs between cells span a similar distance (~15nm) which corresponds to approximately four IgSF domains aligned in a row. The realisation that the dimensions within which an interaction could occur at the cell surface came from structural studies of ligand pairs, most notably TCR:peptide MHC (Garboczi et al., 1996; Garcia et al., 1996) and CD58:CD2 complex (Wang et al., 1999) and supported by the modelled dimensions of the rat CD2:CD48 interaction (van der Merwe et al., 1995). This conservation of four IgSF domains in the interaction distance has been extended to other interactions which now include the CD48:2B4 (Brown et al., 1998) and the SIRP(OX-41):CD47 interaction (Elizabeth Vernon-Wilson *et.al.* manuscript submitted). The importance of cell surface molecule dimensions has been studied by altering the dimensions of the CD48:CD2 adhesion complex and studying its effect on T-cell activation (Wild et al., 1999). In addition, it is clear from structural considerations alone, that in order for the smaller proteins to interact, the larger, often more abundant proteins, must be structurally reorganised or simply excluded from the region of contact. This suggests that the leukocyte cell surface must be able to redistribute the molecules at the cell surface and this has now been shown (Grakoui et al., 1999).

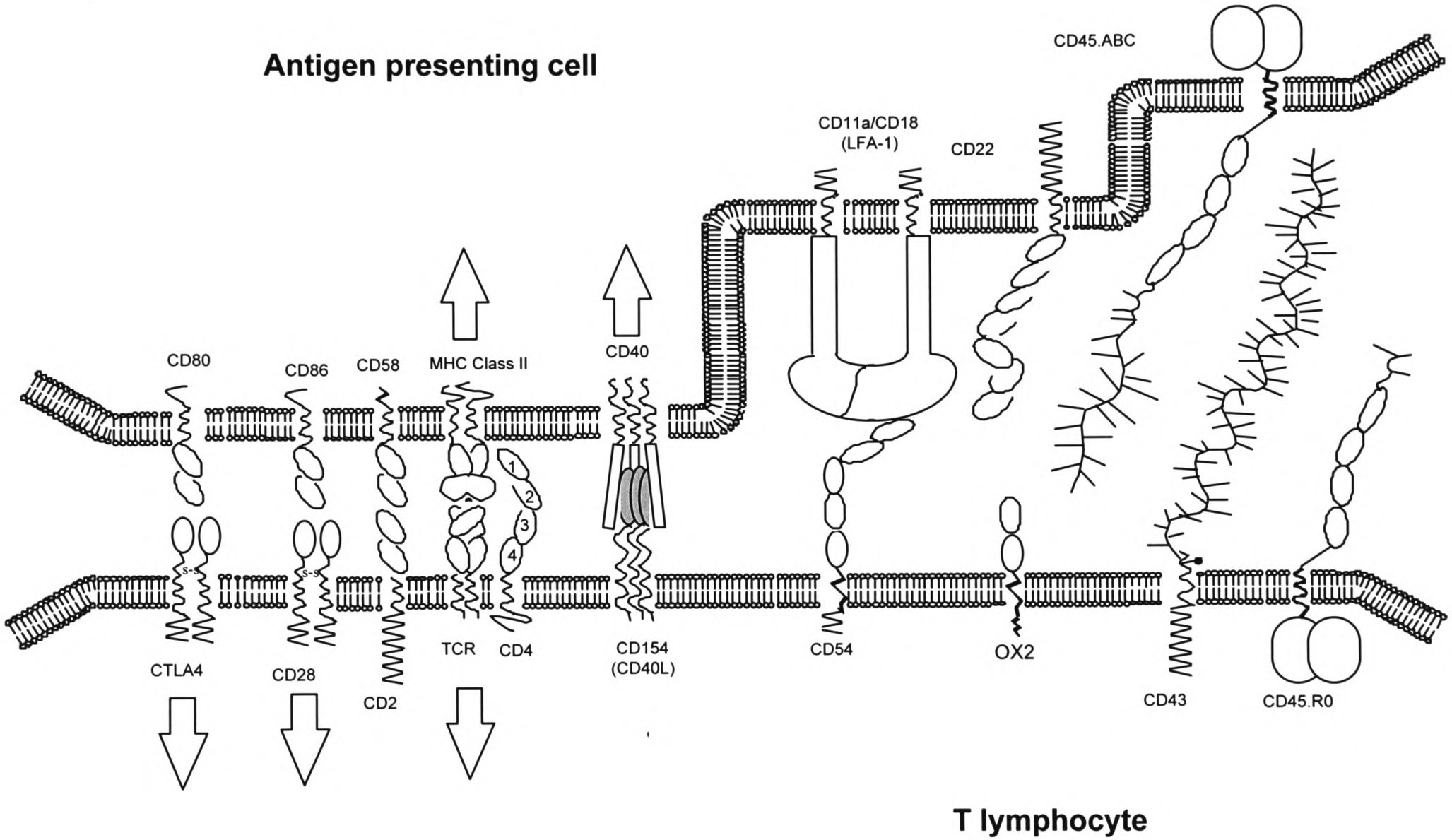

Figure 1-2. A schematic diagram of the leukocyte cell surface. The diagram illustrates the molecules involved in the interaction between a T-lymphocyte and an antigen presenting cell (APC). The molecules are drawn to scale and IgSF domains are represented by ovals.

1.3.2.3 Transmembrane and cytoplasmic regions

The cytoplasmic regions of membrane proteins generally consist of either an enzymatic activity e.g. phosphatase CD45, kinase CD135 (FLT3) or a region specialised in mediating further protein:protein interactions. An example of these regions are the ITAM and ITIM (immunoreceptor tyrosine-based activation/inhibition motif) which can be reversibly phosphorylated on tyrosine residues within a consensus motif and provide ligands for SH-2 domain containing signal transduction proteins making the phosphorylation state of the molecule critical for the initiation of signal transduction. Signals can be broadly defined as either activating or inhibitory and are usually associated with tyrosine kinase or phosphatase enzymatic activities respectively. Thus, ITAM containing receptors recruit kinases such as Syk or Zap (Cambier, 1995) and ITIMs recruit phosphatases such as SHP-1 or SHP-2 (Unkeless and Jin, 1997). Thus, although this is a gross oversimplification, signal initiation is thought to originate from the generation of localised microenvironments created due to receptor ligation at the cell surface and is dependent on the balance of the local tyrosine phosphatase and kinase activities.

The transmembrane regions of cell surface molecules are often stretches of hydrophobic residues between 17 and 25 amino acids long which span the lipid bilayer and are thought to adopt an α-helical secondary structure. However, some transmembrane regions are found to contain one or two charged residues which are thought to form stable multi-protein complexes within the membrane. Classically, this explained the association of the CD3 signalling complex with the T-cell receptor but has been found in a growing number of cell surface proteins such as the short forms of the killer immunoglobulin receptors (KIRs) with DAP-12 (Lanier et al., 1998) and CD147 with monocarboxylate transporters (Juel and Halestrap, 1999). Additionally, contributions from both the

transmembrane and extracellular regions can lead to the formation of a complex e.g. the B-cell CD19/CD21/CD81/leu-13 complex (Tedder et al., 1994).

Some membrane associated molecules do not wholly traverse the lipid bilayer but are modified by the covalent addition of hydrophobic lipid moieties which insert into one of the leaflets of the phospholipid bilayer. Proteins modified in this way present on the surface of cells contain a glycosyl-phosphatidylinositiol (GPI) anchor which is added to the protein shortly after synthesis. Several leukocyte cell surface proteins such as CD48 and the Thy-1 antigen contain this feature and have recently been found to associate within membrane microdomains or rafts (Friedrichson and Kurzchalia, 1998; Varma and Mayor, 1998) which contain a high local concentration of cholesterol and sphingolipids (Simons and Ikonen, 1997). These microdomains are also enriched in lipid-modified intracellular proteins such as the Src family of protein kinases and their reorganisation within the membrane have been shown to initiate signal transduction (Moran and Miceli, 1998; Viola et al., 1999).

1.4 The Immunoglobulin superfamily (IgSF)

It is now clear that proteins belonging to the IgSF have a major role to play in intercellular communication in both the immune system and a wide variety of other tissues (section 1.3.2.1). Therefore, it seems reasonable that studying these proteins and understanding some of the general principles by which they function will lead to significant advances in the understanding of intercellular communication in organisms as a whole. Since this is the principle adopted by our laboratory, a more detailed description of proteins belonging to the IgSF is relevant to this thesis.

The biochemical and structural analysis of antibodies formed the concept of a structurally discrete unit of around 100 amino acids stabilised by a conserved intra-chain disulphide bond (Edelman, 1970). The subsequent discovery that this protein fold was

present in cell surface proteins and not just in immunoglobulins suggested that the Ig-fold might have evolved to mediate interactions with other cell surface structures (Williams, 1984; Williams, 1985). Proteins containing an immunoglobulin-like fold represent one of the largest known protein families. The functions of these proteins are remarkably diverse but are generally thought to mediate intercellular communication, when expressed extracellularly (Williams and Barclay, 1988), or in the structural organisation of muscle, when expressed intracellularly (Pfuhl and Pastore, 1995).

1.4.1 The IgSF domain

IgSF domains from different proteins often show very little overall sequence similarity. However, closer inspection usually identifies key signature residues which enable the placing of the domain in this structural class. IgSF domains can be further sub-divided into structural sets which group together individual domains sharing sequence and structural features distinct from other IgSF sets. Originally, IgSF domains were grouped into variable (V) or constant (C) domains (Williams and Barclay, 1988) since they consistently differed in their length: a V-domain (9 to 10 β-strands ~110 amino acids) and C-domains (7 β-strands ~90 to 100 amino acids) and were originally observed in immunglobulin variable and constant domain regions respectively. A further division of the C domains into C1- or C2-set domains has been justified by significant differences in their tertiary structures. Further set classifications (I –intermediate (Harpaz and Chothia, 1994), S –switched and H –hybrid (Bork et al., 1994), C3- and C4-set (Halaby et al., 1999)) have been assigned as more sequence and structural data becomes available but the unequivocal placing of a given domain in a certain set is a matter of esoteric debate and is generally of limited use in assigning biological functions.

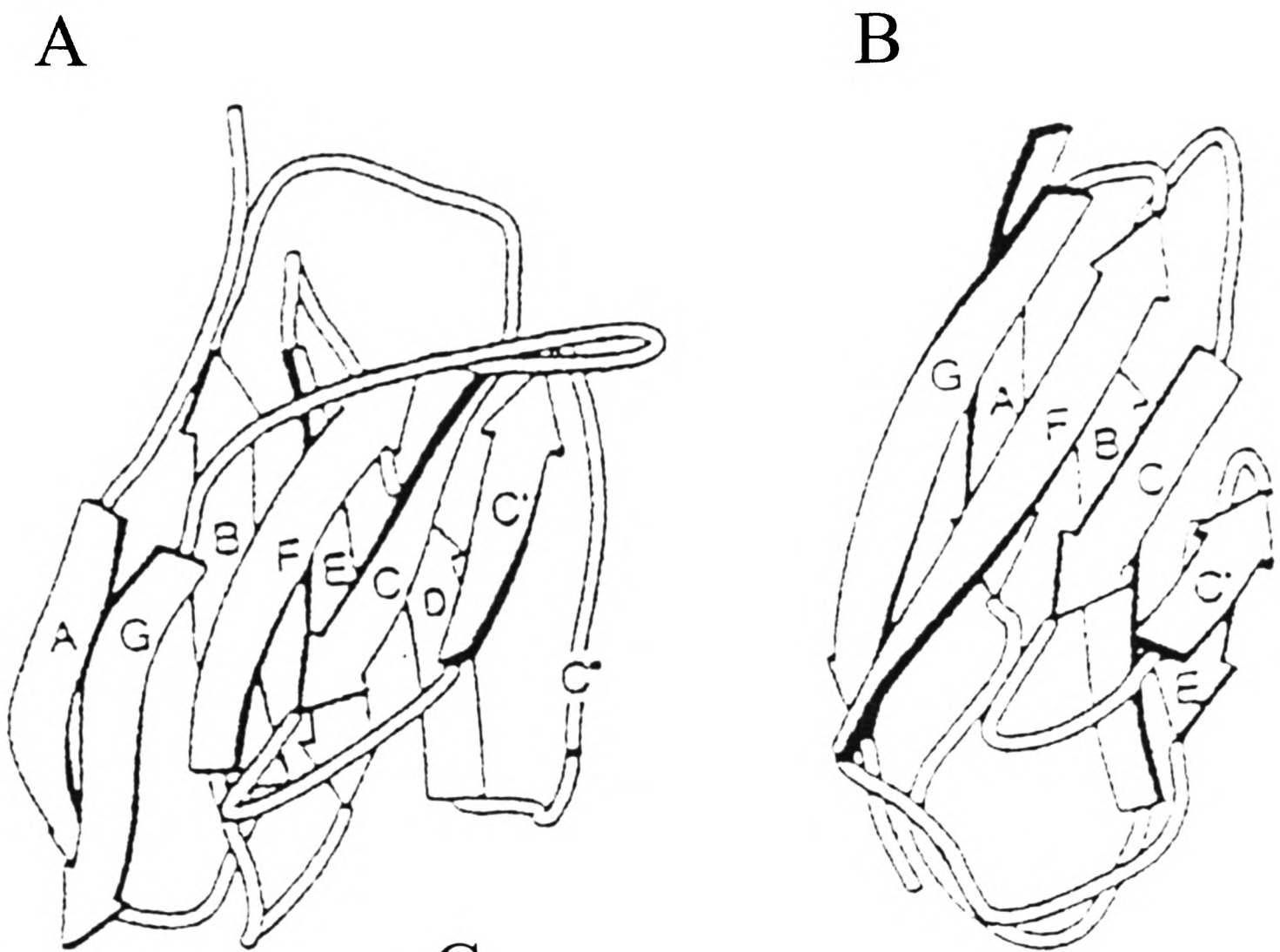

C

Figure 1-3. Structural and sequence features of the Ig-fold. (A) and (B) represent schematic diagrams of an IgSF V- (V_H of the human NEW Fab) and C2-set (human CD4 domain 2) folds respectively (taken from Barclay et al., 1997.) (C) shows how the IgSF signature residues form the core of the fold. The figure is adapted from Lange et al., 1994 and shows an antibody V_L domain (REI) and the Ig-fold signature residues are indicated in bold.

1.4.2 The sequence and structure of IgSF domains

The structure of many IgSF domains have been determined by both X-ray crystallography and nuclear magnetic resonance. The Ig fold consists of two sheets of anti-parallel β-strands which are usually referred to as the BED and GFCC'C" faces. These two sheets are usually covalently bridged by a disulphide bond formed by conserved cysteine residues located in the B and F β-strands. A representative schematic structure of both a V and C2- set domain are shown in Figure 1-3A and B which are orientated so the reader is looking directly at the GFCC'C" face. Other sequence similarities are mainly found at residues which have their functional groups pointing inwards on either face and form the hydrophobic core of the protein where the two sheets are sandwiched together. The core of an Ig V-set fold is shown in Figure 1-3C and illustrates how these conserved residues pack into the tertiary structure. The disulphide bond, formed between the B and F β-strands, joins the two sheets together. The B strand usually contains a L-X-**C** sequence and the F strand a D-X-G-X-Y-X-**C** (where X is any amino acid) around the disulphide forming cysteines and a conserved tryptophan (W) located at the start of the C-strand packs into the heart of the fold. Additionally, a salt bridge is usually formed between the aspartic acid (D) in the F strand with a basic residue (usually arginine (R)) present at the start of the D-strand. It is thought that these conserved residues are responsible for stabilising the central core of the fold. The Ig-fold can then interact through out-pointing residues from both the β-strands or the loop regions.

The structural relationship between two or more IgSF domains within a protein is a key question regarding the final dimensions of the molecule. Structural studies have shown that almost any orientation of two tandem IgSF domains is possible ranging from a straight rod-like structure in CD2 (Bodian et al., 1994) and CD4 (domains 3 and 4) (Lange et al., 1994), a highly bent structure found in the KIRs (Fan et al., 1997) to almost looping back on

itself as shown in both the $Fc_{\varepsilon}R1$ (Garman et al., 1998) and hemolin (Su et al., 1998). Despite the large number of solved Ig-fold structures, it is difficult to predict with confidence the orientation and folding pattern of any given IgSF protein. However, proteins containing two IgSF domains involved in cell surface:cell surface recognition events are often thought to project in a rod-like manner from the membrane.

1.4.3 Protein glycosylation

Virtually all leukocyte cell surface proteins are co-translationally modified by the covalent addition of carbohydrate moieties to the protein backbone by O- and/or N-linked mechanisms (Kornfeld and Kornfeld, 1985; Jentoft, 1990). IgSF domains are known to contain from zero (CD8α) to six (CD66) N-linked glycosylation sites. N-linked glycosylation is restricted to asparagine residues located in the extracellular regions of the molecule conforming to the sequon N-X-T-X or N-X-S-X, where X is any amino acid with the exception of proline. Proline (an imino acid) imposes a structural conformation on the nascent polypeptide chain preventing glycan attachment. There is no single function which can be attributed to protein glycosylation and many proteins can perform all known functions glycan-free (van der Merwe et al., 1993) but roles such as protecting immunogenic sites, protease resistance, involvement in the folding pathway and protein orientation have all been suggested. However, protein glycosylation is known to be centrally important for the function of some cell surface proteins. The selective expression of the α1,3-fucosyltransferase, FucT-VII in Th1 but not Th2 polarised $CD4^+$ T-cells accounts for the differential migratory properties of these cells by binding to E and P-selectin expressed on the cell surfaces of inflammed tissue (Wagers et al., 1998).

A typical N-linked glycan group will add an average of 3 kDa on to the overall mass of the protein but larger sugar moieties are possible (up to 6 to 7 kDa), usually by the introduction of repeating poly-lactosamine structures and thus carbohydrate can be a major structural feature of glycoproteins.

1.5 Furthering our knowledge of the leukocyte cell surface

In an attempt to further our knowledge of the leukocyte, the focus of our laboratory has been the structurally most abundant molecules, the IgSF proteins containing two domains, which account for 15% of all leukocyte cell surface proteins (section 1.3.2.3). Sequence similarities to proteins of known function suggest that they are involved in mediating specific recognition events at the cell surface and thus large steps forward in understanding the function of these proteins would be to identify the factors or molecules with which they interact.

1.5.1 Interactions made by leukocyte cell surface proteins

The measurement of the affinities and dissociation rate constants of cell surface protein interactions with either soluble factors or other cell surface ligands have revealed a striking dichotomy. In general, soluble factors such as cytokines bind to their receptors with high affinity and with long interaction half-lives (hours) whilst cell surface:cell surface interactions are typified by extremely low affinities and these interactions have half-lives of fractions of a second (van der Merwe and Barclay, 1994) (Table 1-4).

Interacting Pair	Kd	K_{off} (s^{-1})	$t_{1/2}$	Reference
Soluble ligands				
IL-1:IL-1R	10^{-10} M	10^{-4}	~2 hours	(Dower et al., 1985)
mAb to antigen	$5x10^{-10}$ M	$2x10^{-4}$	~1 hour	(Mason and Williams, 1986)
Cell surface ligands				
CD2:CD58	~20 μM	4	0.2 seconds	(van der Merwe et al., 1994)
CD80:CD28	4.0 μM	1.6	0.4 seconds	(van der Merwe et al., 1997)
CD80:CTLA-4	0.4 μM	0.43	1.6 seconds	(van der Merwe et al., 1997)
GlyCAM-1:CD62L	108 μM	10	0.07seconds	(Nicholson et al., 1998)

Table 1-4. Comparison of the monomeric affinities and kinetics of soluble versus cell surface ligand interactions at the leukocyte cell surface.

The difference in interaction kinetics are directly related to the functional consequences of the two interaction types. The high interaction affinity and slow dissociation rate of a soluble cytokine with its receptor factor will allow a high level of receptor occupancy at very low cytokine concentrations and allow sufficient time to initiate signal transduction. In contrast, the interactions mediated between cell surface molecules are of very low affinity and are highly transient. This low affinity is thought to be biologically relevant since cell surface proteins do not interact in a monomeric fashion but rather whole arrays of proteins individually contribute to the interaction, increasing the interaction avidity and yet still allowing de-adhesion so that leukocytes can continue their migration around the body in search of disease causing pathogens. One practical consequence of this transient adhesion is that these interactions are difficult to detect using conventional binding assays, since any assay requiring intermediate wash steps will simply wash away the ligand probe (Fig. 1-4). It is suggested that the practical difficulties presented by these transient interactions are the reason that around half of the characterised leukocyte cell surface proteins have no known function. Thus, the development of new techniques which can detect these transient interactions may allow further characterisation of the leukocyte cell surface.

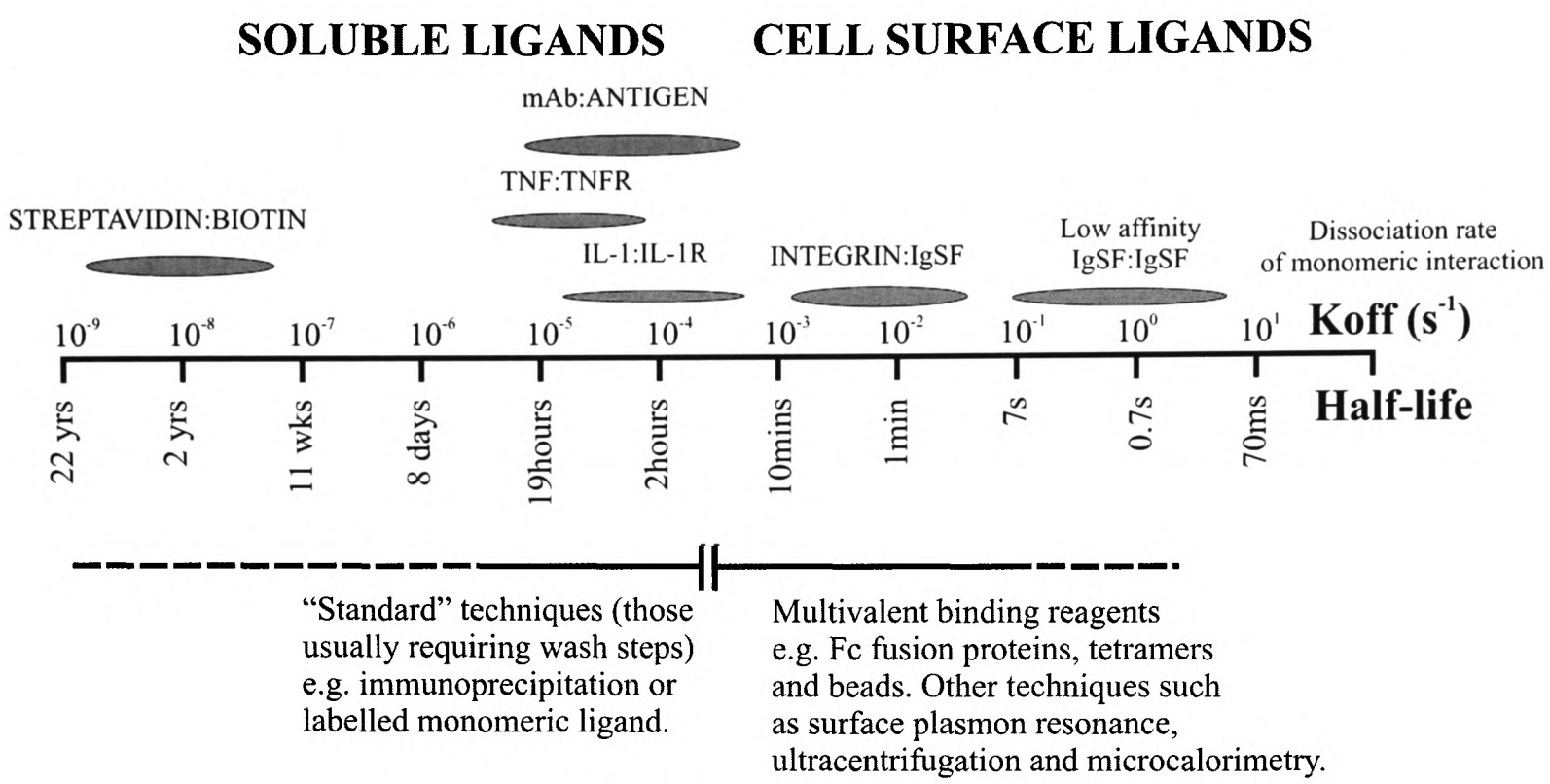

Figure 1-4. Comparison of different types of interaction and the techniques used to detect them. The dissociation rate of the monomeric interaction is shown as both a dissociation rate constant (K_{off}) and as a half-life on a log scale. The interactions can be broadly split into soluble and cell surface ligands and then examples of measured interactions are indicated above the scale. Using the same scale, the extent of the ability of "standard" techniques (i.e. those usually requiring washing steps) to detect certain interactions is compared to the use of multivalent binding reagents.

1.5.2 Techniques used to characterise low affinity interactions

Most techniques used to identify novel low affinity interactions are based around the principle used by the cell itself, i.e. making the interaction multivalent. Increasing the avidity of the interaction has been achieved using a variety of techniques which are outlined below. These techniques rely on producing soluble forms of the molecule and expressing the extracellular domains alone.

1.5.2.1 Ig fusion proteins

Perhaps the most widely used and therefore most numerically successful method of identifying protein interactions of extracellular regions of membrane proteins has been the

generation of Fc fusion proteins. These constructs recombinantly fuse the extracellular domains of the molecule of interest to the Fc portion of immunoglobulins. This both creates a dimeric, or in the case of an IgM fusion protein, decameric form of the molecule and additionally allows the purification of the construct using standard procedures used to purify antibodies via their Fc portion. In a comparative study (Brown et al., 1995), the rat CD48 cell adhesion molecule interacted with rat CD2 with half-lives of 0.2 seconds (monomer), 10 to 20 minutes (dimer-IgG Fc fusion protein) and 10 to 60 minutes (decamer-IgM Fc fusion protein). However, despite the 10,000-fold slower dissociation rate, binding to cells transfected with rat CD2 could not be detected using both high and low stringency washing. In addition, the problem of Fc receptor binding can lead to difficulties in interpreting binding data with certain cell types.

1.5.2.2 Tetramer technology

The extracellular regions of cell surface proteins can be displayed in a tetrameric form by enzymatically biotinylating a soluble form of the protein of interest and displaying it in a multivalent array around streptavidin. This involves engineering an additional stretch of 19 amino acids to the polypeptide which can then be specifically biotinylated on a lysine residue using the protein-biotin ligase (BirA) (O'Callaghan C et al., 1999). This technique is widely used to display complexes of MHC Class I molecules, produced in bacteria, purified, and refolded around chemically synthesised peptides and associated with a chemically biotinylated β2-microglobulin before display around streptavidin (Ogg and McMichael, 1998). These "tetramers" are then able to stain antigen specific T-lymphocytes and have been a useful tool in studying the biology of $CD8^+$ cytotoxic T-cells (McMichael and O'Callaghan, 1998). The increases in affinity due to multimerisation around streptavidin

have also been measured by surface plasmon resonance using the MHC I-E^k/moth cytochrome C peptide to its ligand, the T-cell receptor 2B4. The calculated half-lives were 9.5s (monomer), 3.1min (dimer) and 32min (tetramer) (Boniface et al., 1998) representing only a 200-fold decrease in dissociation rate resulting from the multimerisation. It is possible that the staining, seen using the tetramers might be due to larger multivalent aggregates of the purified complexes rather than true tetramers, suggesting that the efficacy of this type of reagent in detecting very transient interactions (i.e. those with half-lives of less than one second) might be inconsistent due to the unpredictable nature of protein aggregation.

1.5.2.3 Beads

In order to reliably detect low affinity interactions at the cell surface, a technique was developed whereby soluble recombinant membrane proteins are displayed as a highly multivalent array around a fluorescent bead. This assay was developed using the rat CD2:CD48 interaction (one of the weakest protein:protein interactions known) and was shown to be very successful in specifically detecting this interaction at the cell surface (Brown et al., 1995). Originally, this technique involved recombinantly fusing domains 3 and 4 of rat CD4 (CD4d3+4) to the extracellular regions of the protein of interest, thereby making the cell surface protein soluble. Rat CD4d3+4 was chosen because it is expressed by eukaryotic cells as a discrete unit, its structure is known from crystallographic studies (Brady et al., 1993; Lange et al., 1994) and several high affinity monoclonal antibodies binding to this protein were available, providing an antigenic "tag" which could be used in quantitative assays, purification and the appropriate display of the molecule for ligand binding (Brown and Barclay, 1994) (Fig. 1-5). Approximately 10^4 molecules of soluble CD4d3+4 protein can be presented on a single bead which represents ~40 to 400 fold greater surface density than at the cell surface (Brown et al., 1995). An important aspect of this system is that the

constructs are expressed by eukaryotic cells and therefore all post-translational modifications are present including disulphide bonds and the covalent addition of carbohydrate. The technique has recently been modified by the addition of the biotinylatable tag to the C-terminus of the CD4 portion allowing the proteins to be directly immobilised on avidin coated fluorescent beads thereby omitting the requirement for the anti-CD4 mAb.

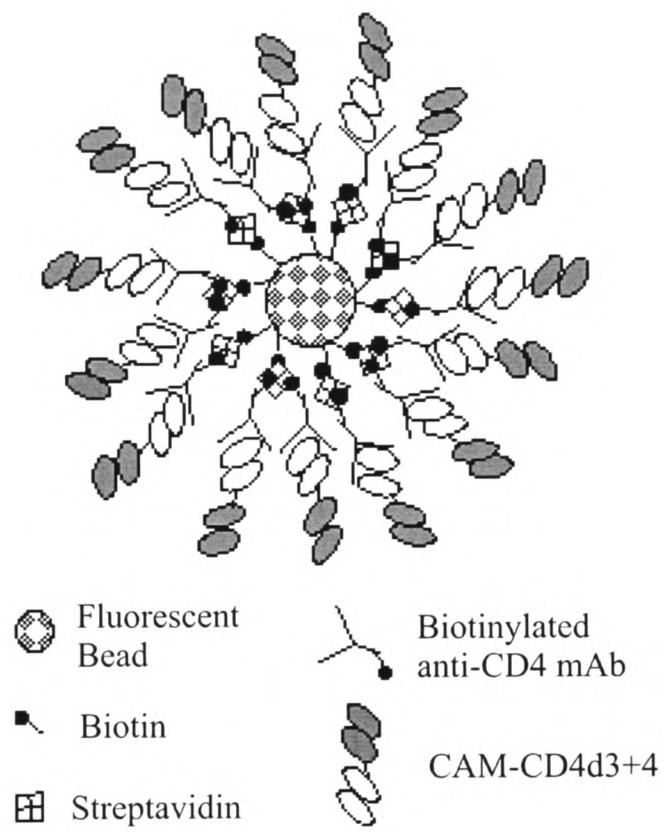

Figure 1-5. Using fluorescent beads as highly avid binding reagents. Biotinylated, fluorescent beads are coated with sequential layers of streptavidin, biotinylated anti-rat CD4d3+4 mAb and finally a soluble chimaeric protein of a cell adhesion molecule (CAM) which is consequently displayed as a highly multimeric array suitable for receptor binding.

1.6 The lymphoid/neuronal cell surface glycoprotein OX-2

The use of monoclonal antibodies to probe the structure and function of leukocyte cell surface proteins was pioneered by Williams in 1977 (Williams et al., 1977) and is still widely in use today. The MRC OX-2 antibody was raised in 1978 from mice immunised with glycoproteins prepared from rat thymocytes by lectin affinity chromatography and was

one of the first monoclonal antibodies to be made (McMaster and Williams, 1979). The antigen recognised by the MRC OX-2 mAb (OX-2) was initially of interest due to biochemical and tissue distribution similarities with another thymocyte glycoprotein, Thy-1 (Barclay and Ward, 1982). Both Thy-1 and OX-2 are expressed in the lymphoid and neuronal compartments (Barclay, 1981). This antigen and attempts to characterise its function is the major focus of this thesis.

1.6.1 Structure and biochemistry of OX-2

The gene corresponding to the antigen recognised by MRC OX-2 was cloned in 1985 by Clark (Clark et al., 1985) and was shown to be a 2 IgSF domain containing molecule which is structurally highly typical of leukocyte cell surface proteins (Barclay et al., 1997). The homologues in both human (McCaughan et al., 1987a; McCaughan et al., 1987b) and mouse (Borriello et al., 1998) have been identified at the genomic level (chromosomes 3q13.1 (human) and the syntenic chromosome 16 in mouse) and are not closely linked to any known disease locus. The protein products of the OX-2 gene from human and rodent models are aligned in Figure 1-6.

OX-2 contains several unusual features:

1) Its primary sequence is unusually highly conserved for a lymphoid antigen (GJW unpublished observations) and this includes the conservation of six potential N-linked glycosylation sites.

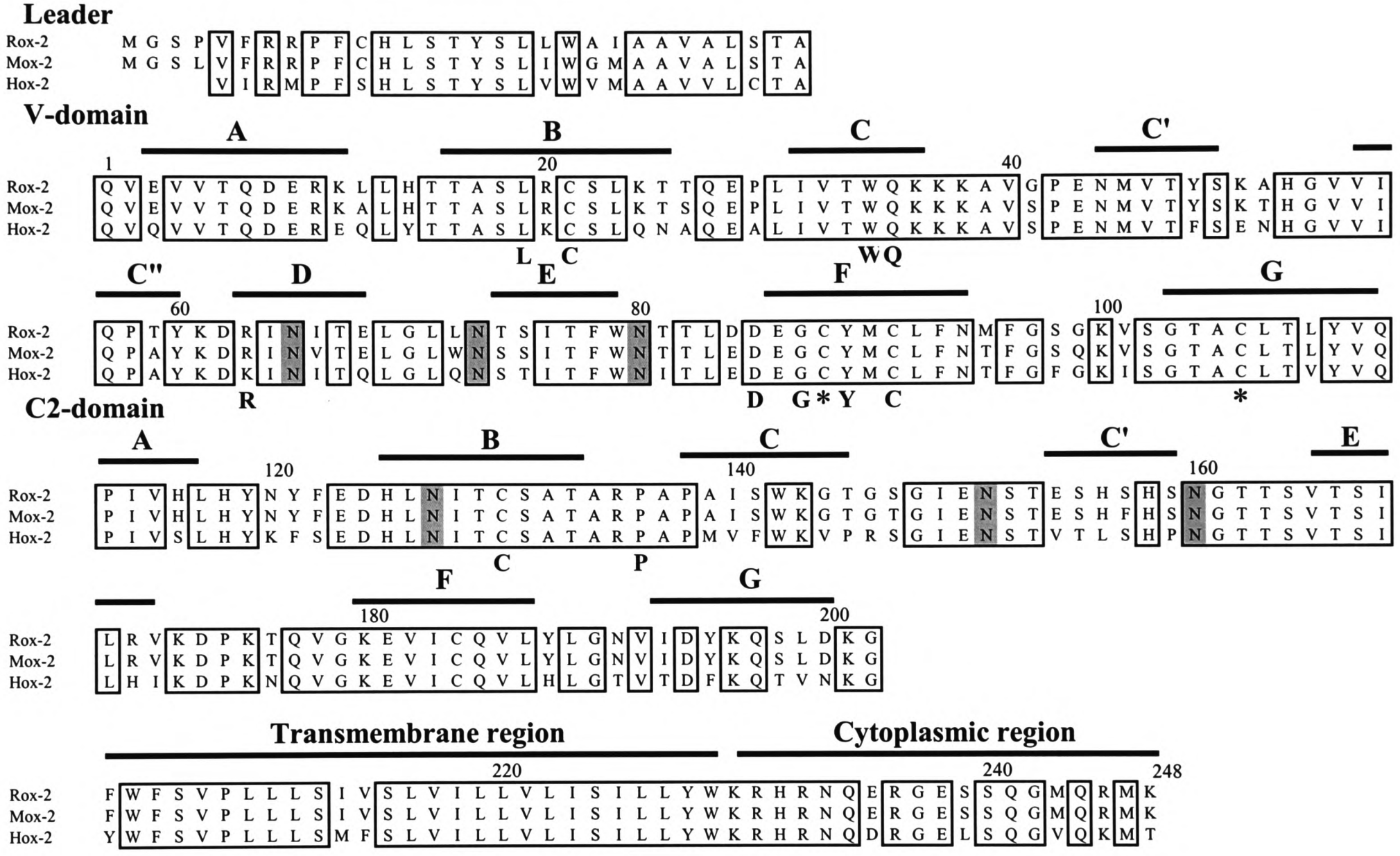

Figure 1-6. An alignment of the rat, mouse and human OX-2 amino acid sequences. The three sequences have been split according to their predicted domain organisation and topology. The superscripted bars in the extracellular regions predict the extent of the β-strands characteristic of the immunoglobulin fold by comparison to solved structures and the position of IgSF signature residues are indicated in bold beneath the sequences. Asparagines conforming to N-linked glycosylation sequons have been lightly shaded and the cysteines marked (*) are thought to form an unusual F to G strand disulphide.

2) It contains the characteristic signature residues of an IgSF domain including the B to F β-strand disulphide but also a highly characteristic and unusual pair of conserved cysteines which are predicted to form a F to G β-strand disulphide (Fig. 1-6).

3) A high level of mis-splicing events is abundant in lymphoid tissue. This was first described in the cloning of the rat molecule and also more recently in the mouse (Borriello et al., 1998). Remarkably, this mis-splicing event appears to be restricted to lymphoid tissue and is observed in T and B cells but not in mRNA isolated from neural sources (Clark, 1986; Barclay, 1986).

4) The OX-2 glycoprotein purified from neural tissue (brain) has a lower (41kDa) and more homogenous apparent molecular mass than OX-2 purified from lymphoid tissue (47kDa –thymus) (Barclay and Ward, 1982). This characteristic behaviour of OX-2 is paralleled in the Thy-1 protein purified from the same two sources. The differences are thought to be due to carbohydrate moieties since the OX-2 protein purified from these two tissues are antigenically indistinguishable and have a virtually identical amino acid content but differences are seen in carbohydrate content (Barclay and Ward, 1982).

1.6.2 Distribution of OX-2

The distribution of the OX-2 protein has been well characterised at the protein level in rats. The major site of expression are the nervous system and lymphoid compartments but a limited amount of expression was also observed in other tissues.

OX-2 tissue distribution	Reference
Lymphoid tissue	
Follicular dendritic cells	(Barclay, 1981)
Endothelium of post capillary venules	(Kroese et al., 1987)
Thymocytes	(Kroese et al., 1986)
Activated T-cells	
Re-circulating B lymphocytes	
Nervous system	
Central nervous system:	(Webb and Barclay, 1984)
Brain neurones (not glia, astrocytes or Purkinje cells)	(Morris and Beech, 1987)
and spinal cord	"
Blood vessels	"
Peripheral nervous system:	(Barclay, 1981)
Nerve bundles in peripheral tissues	"
Other tissues	
Kidney glomeruli	(Barclay, 1981)
Smooth muscle of gut	"
Female reproductive organs:	
basement membrane of large antral follicles	
Granulosa of degenerating (atretizing) antral follicles	(Bukovsky et al., 1983)
Ovarial germinal epithelium	"
Trophoblast	(Bukovsky et al., 1984)

Table 1-5. OX-2 spatial distribution in the rat.

Webb and Barclay (1984) noted that the levels of OX-2 expression in the postnatal developing nervous system increased from 95% of adult levels at birth to 150% at day 11 before declining to adult levels at around day 40, suggesting that OX-2 might have a role to play in neural tissue organisation. Indeed, Morris and Beech showed that the OX-2 antigen was expressed at the onset of axonogenesis on neurons undergoing dendrite outgrowth (Morris and Beech, 1987). Also, the levels of OX-2 expression were also found to be upregulated in the stratum granulosum of degenerating follicles in the rat ovary (Bukovsky et al., 1983).

A complementary part of this project to elucidate the function of the OX-2 glycoprotein has been a collaboration with Dr R. M. Hoek and Dr J. D. Sedgwick to generate an OX-2 knock out mouse. This necessitated the generation of an anti-mouse OX-2 mAb.

This was raised against recombinant purified mOX-2 protein obtained by cross-species PCR using cDNA generated from mouse splenocytes and oligonucleotides specific for rat OX-2. This mAb (MRC OX-90) has been used by our collaborators who have reported a distribution identical to that reported previously in rat (data not shown). Previously to the work presented in this thesis, the distribution of the human form of OX-2 had not been demonstrated at the protein level but had been identified at the nucleic acid level by southern blots from MAJA (a human B-cell lymphoma) and normal human brain but not thymocyte cell lines (McCaughan et al., 1987a). An aim of this thesis was to identify the expression of human OX-2 at the protein level and characterise its distribution by the generation of an anti-human OX-2 mAb.

1.6.3 Function of the OX-2 glycoprotein

The broad distribution of OX-2 makes prediction of its function difficult and the MRC OX-2 mAb had no functional effects, for example, in mixed leukocyte reaction cultures.

1.6.4 Viral OX-2 homologues

Herpes virus sequencing projects identified the presence of a close homologue of the OX-2 glycoprotein in the genomes of three β-herpes viruses (HHV-6A (Gompels et al., 1995), –6B (Dominguez et al., 1999; Isegawa et al., 1999) and HHV-7 (Singer and Frenkel, 1997)), a γ-herpes virus (HHV-8, the virus associated with Kaposi's sarcoma (KSHV) (Russo et al., 1996)) and also a pox virus (Yabba-like disease virus (H-J. Lee and Professor G. L. Smith unpublished data)). These viruses contain a large amount of genetic information (genome sizes often in excess of 120kbp) and are characterised by widespread and often

ubiquitous infection within a population. Indeed, HHV-6 is known to infect up to 80% of children by the age of two years (Okuno et al., 1989), usually asymptomatically, but can cause roseola infantum leading to the shocking statistic that HHV-6 infection is responsible for up to 20% of hospitalisations of children under the age of two (Hall et al., 1994). The genome of these viruses often contain genes which have been acquired from their host. These "hijacked" proteins are of great interest to immunologists since they are used by the virus against our own immune system in order to avoid detection and eradication (Smith et al., 1997; Spriggs, 1996). Thus, understanding how the virus uses the captured gene may provide insights into the role of the original host protein within the uninfected individual.

1.6.5 Previous work on OX-2 in this laboratory

Attempts to elucidate the function of OX-2 in our laboratory have adopted a more biochemical approach. An advantage of this reverse genetic approach as opposed to more classical forward genetics meant that no assumptions had to be made regarding the function of the protein. It was reasoned, from sequence homologies to other proteins of known function, that OX-2 was most likely to mediate a specific binding event with a receptor expressed on another cell type. A large step forward in understanding the function of OX-2 would be to characterise the molecular identity and distribution of this receptor.

The approach involved the expression of the two extracellular IgSF domains of the rat OX-2 glycoprotein as a recombinant soluble chimaeric protein by fusing rat CD4d3+4 to the OX-2 just prior to the transmembrane sequence (Fig. 1-7).

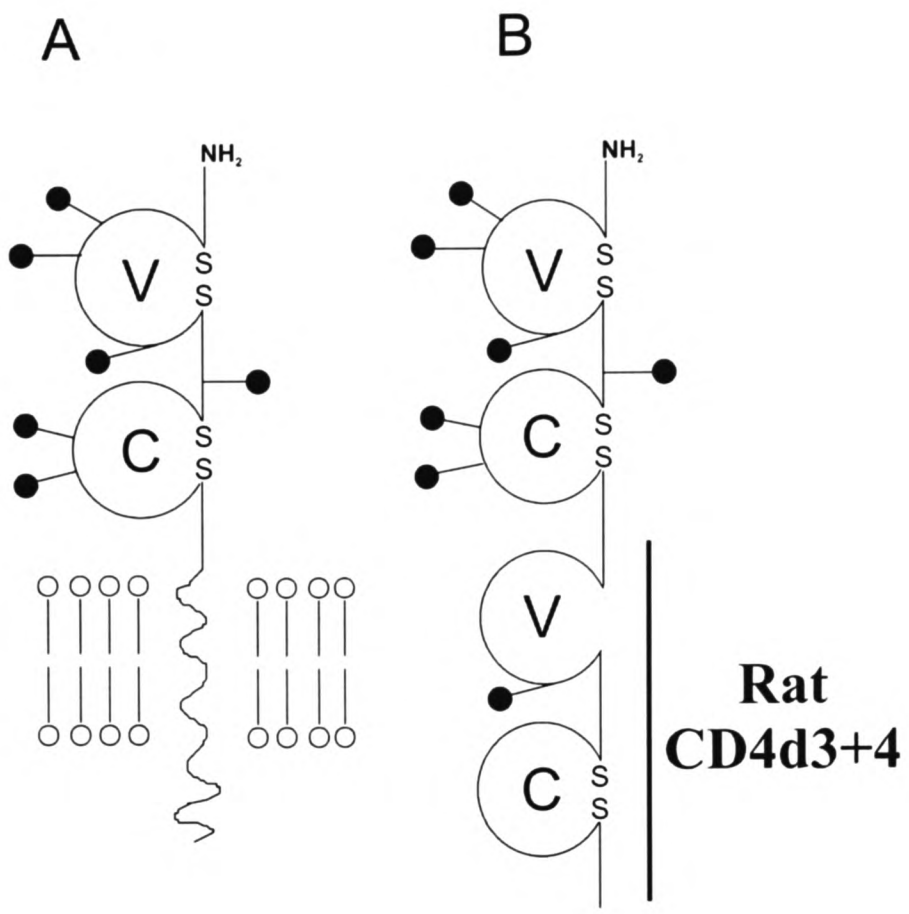

Figure 1-7. Schematic representation of the soluble recombinant OX-2 construct. (A) Schematic representation of the domain organisation of the OX-2 protein as it would appear at the cell surface and (B) the OX-2CD4d3+4 soluble construct. The filled lollipops represent the approximate sites of potential N-linked glycosylation, the IgSF set assignments are labelled and the C-terminal location of the CD4d3+4 antigenic tag is indicated.

Using the bead assay described in section 1.5.2.3, rat OX-2 coated beads specifically interacted with resident rat and mouse peritoneal exudate cells (PECs) (Fig. 1-8).

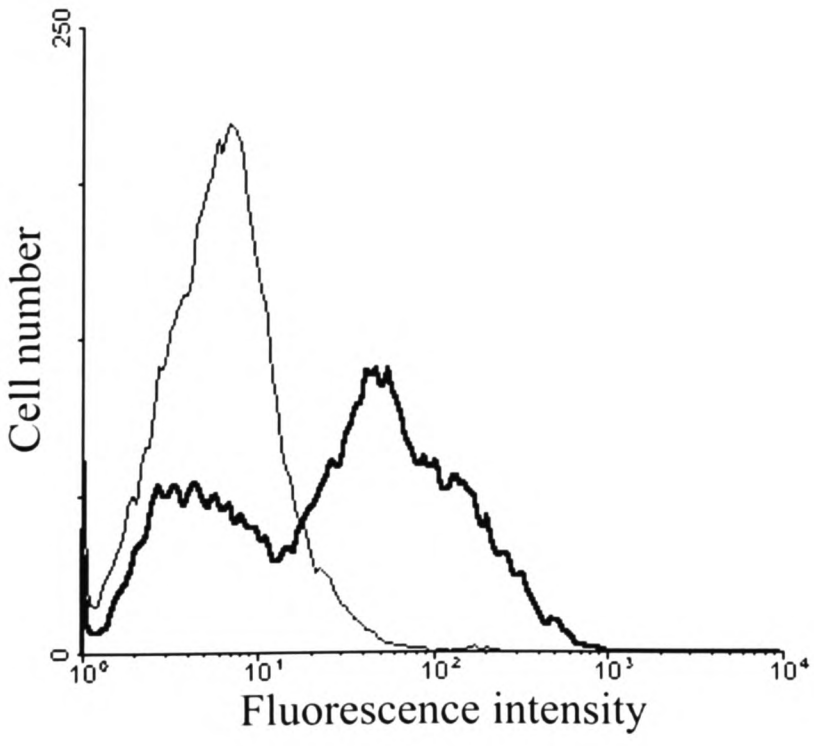

Figure 1-8. Rat OX-2 coated beads bind to rat PECs. Fluorescent beads coated with rat OX-2CD4d3+4 bind to rat macrophages (bold) compared to a negative control (CD4d3+4 coated beads).

The strategy initially used to identify the OX-2 receptor expressed on these cells was to raise panels of monoclonal antibodies to mouse PECs and screen for a mAb which blocked the binding of rat OX-2 coated beads. The mouse system was chosen since a greater number of macrophage expression libraries were available which would allow the receptor identification using the expression cloning technique. The first attempt yielded an IgM (MRC OX-88) which demonstrated that the mouse OX-2 receptor was restricted to resident macrophages in the peritoneal cavity but was unable to western blot or immunoprecipitate the protein (Preston et al., 1997).

1.6.6 Aims of this thesis

The primary aim of this thesis was to determine the molecular identity and distribution of the OX-2 receptor which would suggest further experiments to elucidate the functional role of the interaction *in vivo*. In an attempt to initiate the translation of this work done in rodent models to the human, a monoclonal antibody to the human form of OX-2 was to be generated to elucidate the distribution of the human OX-2 protein.

The organisation of this thesis is depicted schematically in Figure 1-9 and provides an outline of the whole OX-2 project.

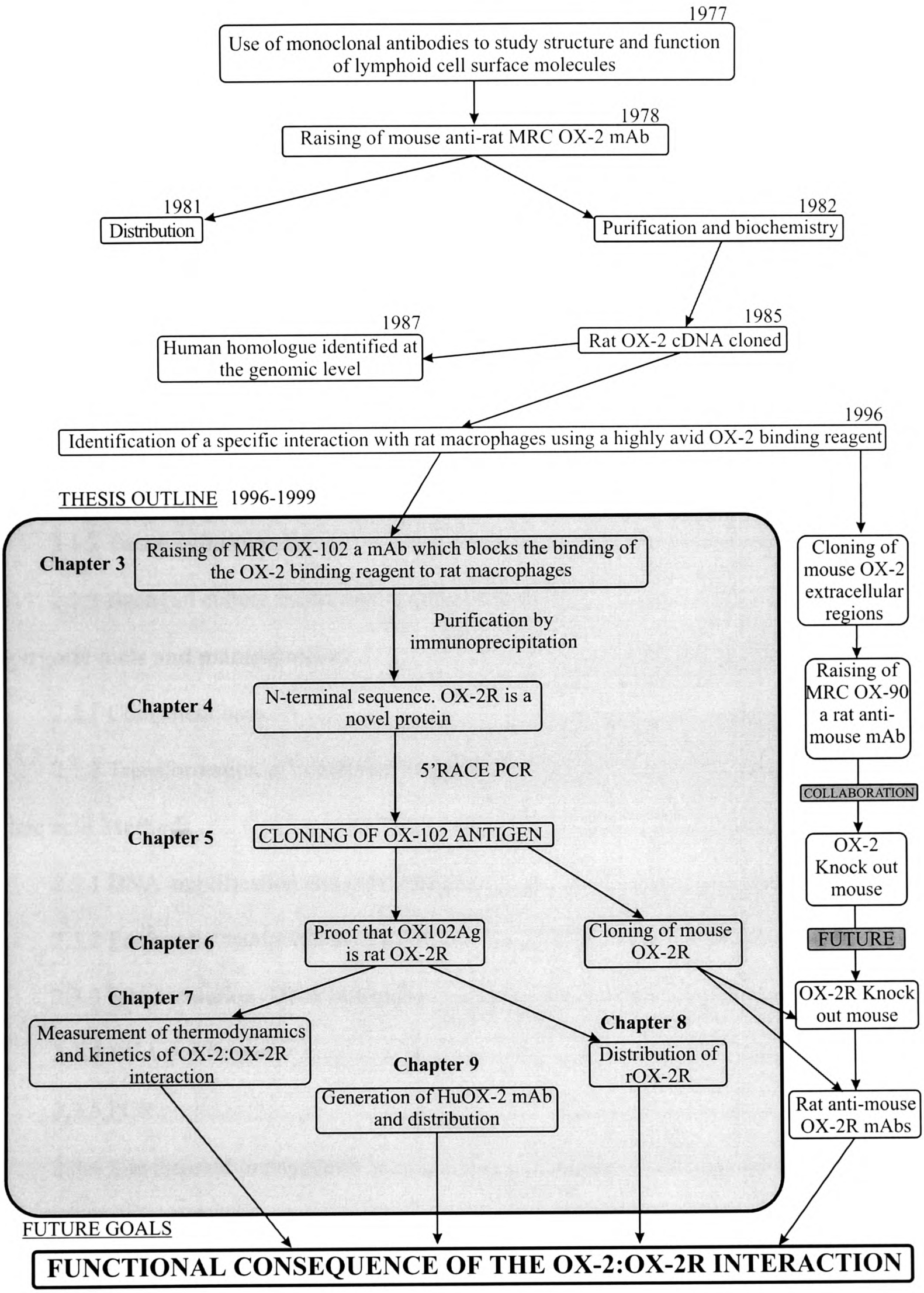

Figure 1-9. A schematic outline of the whole OX-2 project focussing on the contributions made by this thesis (shaded region).

Chapter Two

Materials and Methods

Note: Where concentrations of reaction constituents are given, they are the concentrations present in the final volume of the reaction. All pH measurements were performed at room temperature.

2.1 Reagents and solutions

All reagents were purchased from BDH chemicals unless directly specified.

All glassware and solutions were autoclaved before use.

2.1.1 Buffers

Phosphate buffered saline (PBS): 137mM NaCl, 2.7mM KCl, 8.1mM Na_2HPO_4, 1.5mM KH_2PO_4 pH 7.3 was made by dissolving tablets in dH_20 (Oxoid Ltd., Basingstoke, UK).

PBS/BSA: PBS containing 0.2% (v/v) bovine serum albumin (BSA) (Sigma-Aldrich Company, Poole, Dorset, UK) which was stored as a 10% stock solution in 25mM Tris:HCl (pH 7.4), 140mM NaCl at -20°C. 10mM NaN_3 was added to (PBS/BSA) to make PBS/BSA/N_3 where indicated.

Diethanolamine buffer: 10% diethanolamine (v/v), 0.5mM $MgCl_2$, 10mM NaN_3, pH 9.8. Stored at 4°C protected from light.

5x Tris Borate EDTA (5xTBE): 445mM Tris:HCl (pH 7.4), 445mM orthoboric acid, 10mM EDTA.

TE: 10mM Tris:HCl (pH 8.0), 1mM EDTA.

Tris-buffered ammonium chloride (TBAC): 17mM Tris:HCl (pH 7.2) supplemented with 140mM NH_4Cl. Erythrocytes were lysed by resuspending pelleted cells in 5ml TBAC followed by a two minute room temperature incubation before washing in PBS/BSA.

2.1.2 Tissue culture media

RPMI 1640 and DMEM (GibcoBRL, Irvine, UK) were supplemented with 2mM L-glutamine (GibcoBRL, UK), 20μM 2-mercaptoethanol, and antibiotics (Sigma) penicillin 50Uml^{-1}, streptomycin 50μgml^{-1} and neomycin 100μgml^{-1}. Heat inactivated foetal calf serum (Sigma or GibcoBRL) was added to a final concentration of 10% (v/v). All supplements were passed through 0.22μm filters (Millipore (UK) Ltd., Watford, Herts, UK).

X-VIVO-10 (Cat No. 04-380Q, BioWhittaker, Walkersville, Maryland) was used where indicated with the addition of L-glutamine and antibiotics as above.

2.1.3 Bacterial culture media and selective agents

Luria-Bertani (LB) broth: 171mM NaCl, 1.0% (w/v) bactotryptone and 0.5% (w/v) yeast extract pH 7.0.

2xTY broth: 85mM NaCl, 1.6% (w/v) bactotryptone, 1.0% (w/v) yeast extract pH 7.0.

Antibiotics: All antibiotics were stored and used as described (Sambrook, et al.,1989)

2.2 Prokaryotic tools and manipulations

The following *E. coli* strains were used:

MC1061: used for routine DNA amplification due to its rapid growth rate, maintenance of competency when stored at -70°C and sensitivity to standard antibiotics.

CJ236 (*dut*$^-$, *ung*$^-$): used to generate uracil containing templates for site directed mutagenesis.

GM48 (*dam*$^-$): used to produce unmethylated DNA to enable digestion with methylation sensitive restriction enzymes.

2.2.1 Competent bacteria

Competent bacteria were produced according to the method of Simmons (Simmons, 1993) and stored at -70°C.

2.2.2 Transformation of competent bacteria

Competent bacteria were thawed on ice, aliquoted (100µl) and then flick-mixed with 1 to 10ng purified plasmid or a ligation reaction in a total volume of 10µl. Transformations were carried out on ice for 15 to 30 minutes before heat shock at 37°C for 5 minutes followed by the addition of 100µl LB broth and a further incubation at 37°C for 30 minutes. Transformed bacteria were plated out on agar plates containing the appropriate selective agent and incubated for 16 hours at 37°C.

2.3 Nucleic acid Methods

All nucleic acid was stored at –20°C.

2.3.1 DNA amplification and purification

Plasmids were amplified by growing an isolated colony in the appropriate volume of LB broth at 37°C in a shaking incubator for a minimum of 16 hours. Extra genomic nucleic acid was routinely purified by using QIAGEN columns (as recommended by the manufacturer QIAGEN, Hilden, Germany.) or by the use of an automated robot (BIO-ROBOT 9600, QIAGEN.). Occasionally, nucleic acid was purified by phenol:chloroform extraction and ethanol precipitated as described (Sambrook et al., 1989). The DNA was

quantitated and the degree of purification assessed spectrophotometrically by measuring the absorbance of a diluted aliquot at 260 and 280nm.

2.3.2 Enzymatic manipulation of DNA

All enzymes with the exception of calf intestinal phosphatase (CIP) (4°C) were stored at –20°C.

2.3.2.1 Cloning vectors :PCRScript

PCRScript (Stratagene) (Fig. 2-1) was used to clone and sequence novel cDNAs. A SmaI digested, phosphatased vector was used for cloning PCR products generated using primers which did not contain restriction sites. 3'RACE PCR products produced using appropriate oligonucleotides were cloned using NotI/XhoI doubly digested PCRScript.

2.3.2.2 Restriction digests

Restriction enzymes were purchased from New England Biolabs (Beverly, MA) or Boehringer Mannheim (Lewes, East Sussex, UK) and used as instructed by the manufacturer. In general, two units of enzyme were used to cut 1μg DNA at the appropriate temperature in a one hour reaction which represented a two-fold excess of enzyme. Restriction enzymes used in double digests were assessed for compatibility at different salt concentrations and the appropriate protocol performed. Cut DNA was either repurified or enzymes heat inactivated before further manipulations performed.

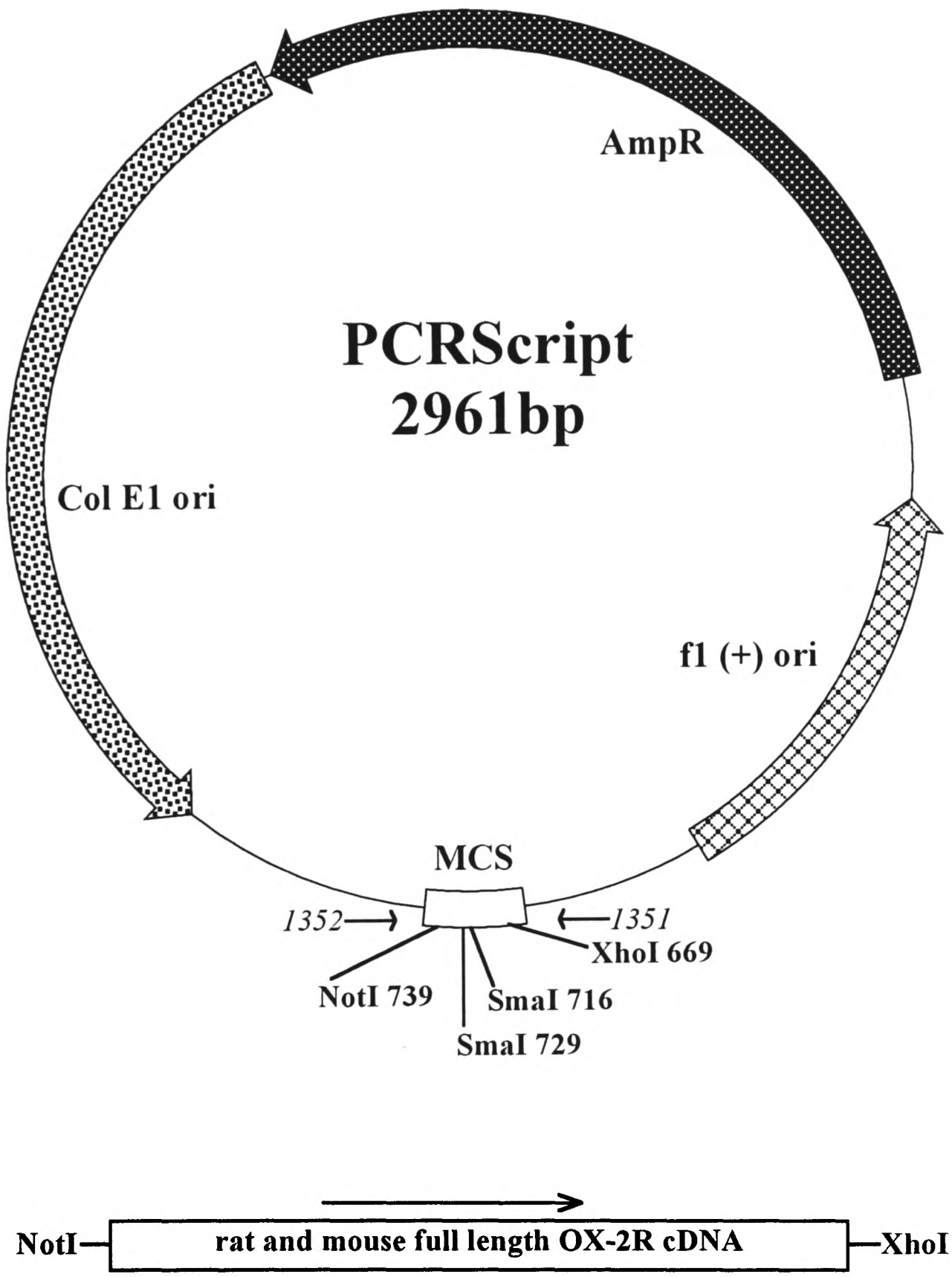

Figure 2-1. Schematic diagram of the cloning vector used in this thesis. PCRScript contains a bacterial replication origin site (ColE1 ori), an ampicillin resistance selectable marker (AmpR), the f1 filamentous phage origin of replication (f1 ori) and a multiple cloning site (MCS). Restriction enzyme sites relevant to this thesis are marked and the location of two oligonucleotides (*1351* and *1352*) used to detect cloned inserts are indicated. The orientation of the two contructs in this vector are shown.

2.3.2.3 Dephosphorylation of vectors

Blunt or vectors containing compatible 5' overhangs had their 5' terminal phosphates enzymatically removed with CIP (Boehringer Mannheim) to prevent religation. Approximately 5U of CIP per μg of vector was incubated in the supplied buffer (50mM Tris:HCl (pH 8.5), 0.1mM EDTA) in a final volume of 500μl for 1 hour at 37°C. DNA was re-purified before use in ligations.

2.3.2.4 Ligations

10 or 20 ng of appropriately digested vector was incubated in the presence of 1U T4 DNA ligase (Boehringer Mannheim) in the supplied buffer (66mM Tris:HCl (pH 7.5) 5mM $MgCl_2$, 1mM dithiotheitol (DTT) , 1mM ATP) and a molar vector:insert ratio of 1:3 was used (when the insert was abundant enough to be quantified) in a final volume of 10μl. Ligations were routinely incubated for 1 hour at room temperature (sticky-ended) or 24 hours at 16°C (blunt-ended). The ligation mix was then heat inactivated at 65°C for 20 minutes and either stored at –20°C or used immediately to transform competent MC1061.

2.3.2.5 Polishing of DNA ends

DNA terminating with incompatible single strand 5' overhangs which were to be ligated were made flush by generating fully double stranded DNA using the Klenow fragment (NEB) of *E. Coli* DNA polymerase I. 1U of polymerase per μg of DNA were incubated in the presence of 10mM Tris:HCl (pH 7.5), 5mM $MgCl_2$, 7.5mM DTT and 33μM dNTPs for 20 minutes at 25°C. The enzyme heat inactivated at 75°C for 10 minutes.

2.3.3 Size resolution -DNA minigels

DNA was routinely checked for purity, quantity and size by separation on 1% agarose minigels containing 0.5μgml^{-1} ethidium bromide in a 1x TBE buffer at 5Vcm^{-1}. Samples were mixed with a 6x DNA loading dye (0.025g bromophenol blue, 0.025g xylene cyanol FF and 1.5g Ficoll® 400 (Pharmacia, Uppsala, Sweden) were dissolved in 10ml ddH_20) before loading. DNA was visualised under ultra violet light and recorded using an Appligene Imager ™ (software version 2.02). DNA size standards used routinely were (19 to 1kbp) StyI cut phage lambda DNA (NEB) or (1kp-100bp) HinfI cut pATX vector.

2.3.4 RNA purification

RNAse contamination was kept to a minimum by using a dedicated bench space and solutions, wearing gloves and using RNAse free plastics or glassware washed with diethyl pyrocarbonate (DEPC) treated water.

Primary tissue was removed from rats or mice and disrupted to obtain a single cell suspension and erythrocytes lysed using TBAC. Cells were pelleted and between 5x10^7 and 2x10^8 cells (depending on their size) were homogenised by vigorous pipetting with 10ml ice cold RNAzolB (Biogenesis, Poole, England) and transferred to a Falcon 2059 tube (Becton Dickinson Labware, Le Pont De Claix, France) and 1ml chloroform was added before vortexing for 15 seconds. The upper aqueous layer containing solubilised RNA was removed after layering by centrifugation in a Beckman J2-HS centrifuge (Beckman Instruments, Palo Alto, CA) using a JA-17 rotor, at 8000rpm for 15 minutes (4°C) and an equal volume of isopropanol added before precipitating the RNA at –20°C overnight. If lower amounts of biological starting material were used 40μg prokaryotic rRNA (16S and 23S RNA - Boehringer Mannheim) was added to act as a carrier to aid precipitation. The pellet was

washed in 75% ethanol before drying and resuspension in RNAse free water. The integrity of the RNA was visualised on a formaldehyde gel and subsequent procedures only performed if three clear (28S, 18S and 5S) rRNA bands were visible. Often, poor $OD_{260/280}$ ratios were observed and thus the poly-A mRNA fraction was purified by the use of oligo-dT coated latex beads (OligoTex, QIAGEN.) as recommended by the manufacturer.

2.3.4.1 cDNA synthesis

Approximately 50ng poly-A RNA was mixed with 1μM oligonucleotide 1520 (contains oligo dT -see Table 2-1) heated to 72°C for 2 minutes before cooling on ice for 10 minutes. Then 200U of Superscript™ II (Cat. No. 18053-017, GibcoBRL) reverse transcriptase (contains a point mutation in the MMLTV RNAseH domain) was added in the presence of a supplied first strand synthesis buffer, (50mM Tris:HCl (pH 8.3), 75mM KCl, 3mM $MgCl_2$) and 2mM DTT and 1mM dNTPs added before incubation in an air incubator set at 42°C for 1 hour. The addition of the SMART oligonucleotide (1503) which tags the 5' end of the cDNAs to perform 5'RACE synthesis was carried out as above but in the presence of 1μM of this oligonucleotide added concomitantly with oligonucleotide 1520.

2.3.5 PCR

PCRs were routinely performed in a RoboCycler® Gradient 40 thermal cycler (Cat. No. 400860, Stratagene Ltd, Cambridge, England) which enabled the simultaneous use of eight different annealing temperatures in the same experiment. Where this feature has been used, the annealing temperature is labelled on the product analysis gel.

2.3.5.1 General PCR

PCR reactions were routinely performed using a master mix and autoclaved tubes/pipette tips/solutions. Typically, a PCR would contain the provided (Promega Corporation, Madison, WI.) thermophilic buffer (10mM Tris:HCl (pH 9.0), 50mM KCl, 0.1% Triton®X-100) supplemented with 2.5mM $MgCl_2$ (but see below), 0.2μM dNTPS, 0.2μM of each oligonucleotide and a thermophilic polymerase (see below). Purified templates were used at 1 to 10 ng per sample and cDNA templates were titrated until good signals were seen in positive controls.

Cycling conditions varied according to experiment but the following general guidelines were observed:

Template melting was performed at 93°C for 30 seconds to 1 minute, annealing temperatures calculated as described in the oligonucleotide section and were usually for 1 minute and a 72°C elongation period corresponding to 1 minute per kilobase of expected product. The number of cycles was generally 20 to 25 from a purified template or 30 cycles from cDNA. A final soak at 72°C for 8 to 12 minutes preceded a hold at 6°C until reactions were analysed. Diagnostic PCRs were performed using 0.2U Taq per 20μl sample (Cat. No. M1665, Promega) and cloning PCRs used either Vent® Taq polymerase (Cat. No. 254, NEB) at 0.1U per 50μl sample from purified templates or Advantage® thermophilic polymerase mix (Cat. No. 8417-1, Clontech, Palo Alto, CA) when cloning from a cDNA template as recommended by the manufacturer. In reactions using Vent®, the $MgCl_2$ concentration was optimised by diagnostic experiments and often found to be 4mM.

2.3.5.2 Colony PCR

Colony PCR was always used to detect the success of cloning. These reactions were performed as described above using 2.5mM $MgCl_2$ and 0.2U of Taq (Promega) per 20µl sample. The end of a bacterial stab (usually a sterile cocktail stick) was swirled into each sample as a template and normal PCR conditions were preceded by a 10 minute soak at 93°C.

2.3.5.3 Rapid amplification of cDNA ends (RACE) PCR

3'RACE was performed using the gene specific sense oligonucleotide and an oligonucleotide (No. 1536) matching the 3'RACE tag (cDNA synthesis priming oligonucleotide No. 1520). 5'RACE was performed using an antisense gene specific oligonucleotide and an oligonucleotide (No. 1501) matching the 5'RACE tag (oligonucleotide No. 1503). Further details of RACE procedures are detailed in the text. Degenerate oligonucleotides were used at double the concentration (0.4µM) of exact match oligonucleotides.

2.3.6 Site directed mutagenesis

Mutagenesis was performed using the Muta-Gene® Phagemid in vitro mutagenesis kit (version 2) (Bio-Rad, Richmond, CA). This protocol is based on a method developed by Kunkel (Kunkel et al., 1987; Kunkel et al., 1991).

2.3.6.1 Preparation of single stranded uracil containing DNA template

Uracil containing plasmids are made by transformation of the CJ236 (*dut*$^-$, *ung*$^-$) bacterial strain. The *dut* mutation inactivates the dUTPase enzymatic activity, resulting in higher intracellular concentrations of dUTP enabling uracil to substitute for thymine in the replicating plasmid. The *ung* mutation inactivates the uracil N-glycosylase activity which allows the incorporated uracil residues to remain in the plasmid. The pEF-BOS vector contains the M13 phage intergenic region (Fig. 2-2) which, upon infection with M13 helper phage, packages the "coding strand" (+) of pEF-BOS into phagemid particles (Mizushima and Nagata, 1990).

Briefly, 20ml 2xTY bacterial media containing 15μgml^{-1} of chloramphenicol was inoculated with a single colony of CJ236 containing the template for mutagenesis and grown with shaking overnight at 37°C. 1ml of this overnight culture was inoculated into 50ml 2xTY containing 50μgml^{-1} ampicillin and 15μgml^{-1} chloramphenicol and grown at 37°C to an OD_{600} of 0.3. M13KO7 helper phage was added at a multiplicity of infection of 20 phage cell^{-1}. Infection was allowed to proceed for an hour, kanamycin added to 70μgml^{-1} to prevent lysogeny and the incubation at 37°C continued overnight. The culture was then centrifuged at 13000rpm (JA-17 rotor) for 15 minutes to pellet debris, the supernatant harvested and respun. The supernatant containing the phagemid particles was transferred to a fresh tube and incubated with 150μg RNAseA at room temperature for 30 minutes. A 1/5th volume of 20% PEG6000, 2.5M NaCl was added, vortexed, and placed on ice for 30 minutes. Phagemids were pelleted by centrifugation at 13000rpm (JA-17 rotor) for 15 minutes, resuspended in 200μl of a salt buffer (100mM Tris:HCl (pH 8.0), 300mM NaCl, 1mM EDTA), incubated on ice for 30 minutes and debris removed by 2 minutes of microcentrifugation (13000rpm). The uracil containing single stranded DNA was extracted from the phagemids by phenol:chloroform extraction and ethanol precipitation.

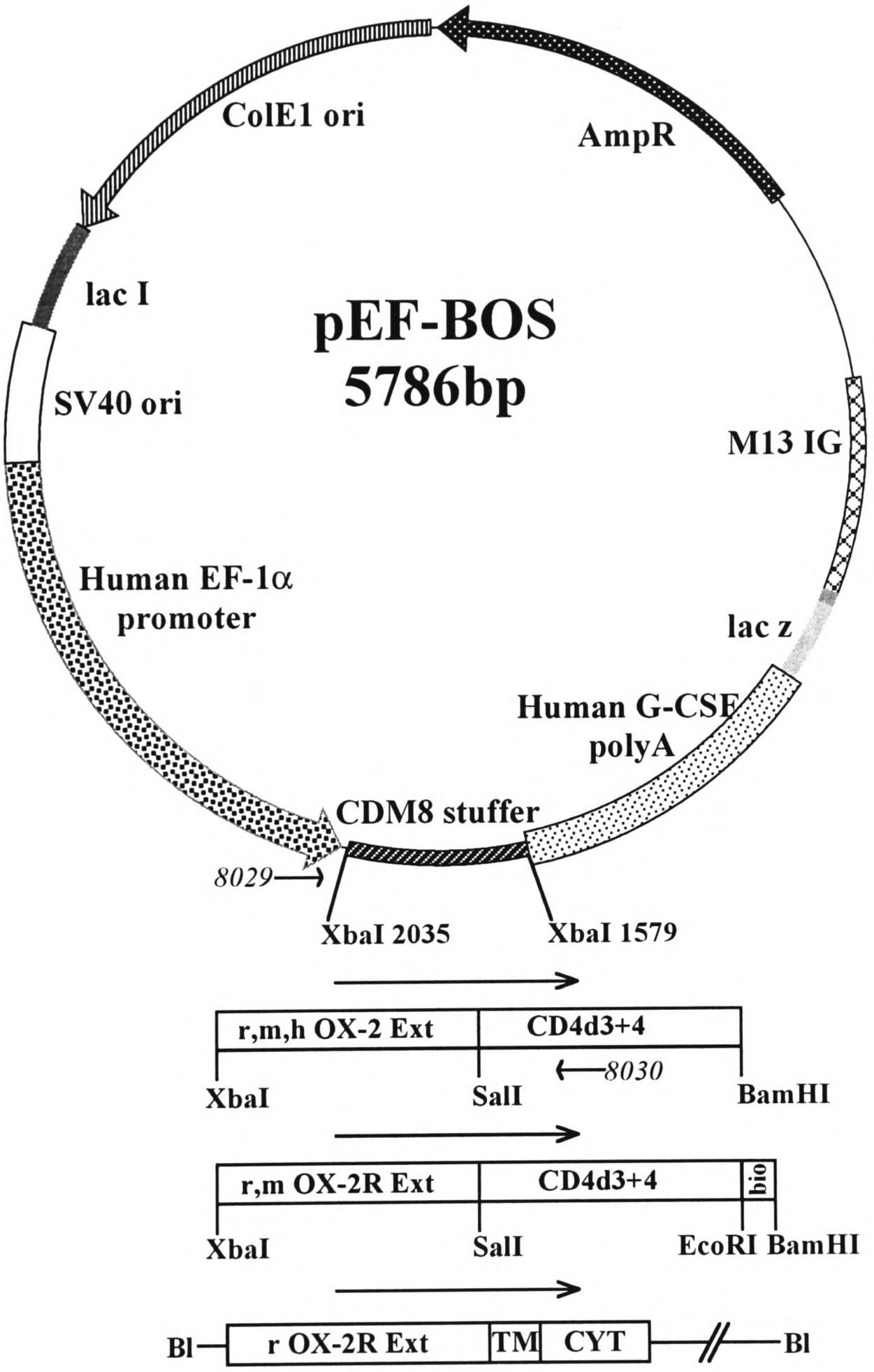

Figure 2-2. Schematic diagram of the transient expression vector used in this thesis. pEF-BOS, a derivative of pUC119, contains features enabling bacterial maintanance, selection on ampicillin and sense strand recovery by M13 phage (using the M13 intergenic region) for mutagenesis. The constructs in this vector and their orientation are indicated. Restriction enzyme sites relevant to this thesis are marked (Bl = blunt ended ligation) and the location of two oligonucleotides (*8029* and *8030*) used to detect cloned inserts are shown. The details of plasmid construction are described in Brown *et. al.*, 1998. The vector contains an SV40 origin of replication which allows high levels of plasmid replication in cells transformed with the large T antigen (293T cell line) enabling high levels of expression from the human elongation factor-1α promoter. The 3'UTR from the human G-CSF gene allows efficient polyadenylation.

2.3.6.2 Phosphorylation of the mutagenic oligonucleotide primer

5' phosphates were enzymatically added to enable ligation by incubating 200pmol of oligonucleotide with 4.5 units of T4 polynucleotide kinase (NEB) in 100mM Tris:HCl (pH 8.0), 10mM $MgCl_2$, 5mM DTT, 0.4mM ATP in a reaction volume of 30µl for 45 minutes at 37°C. The reaction was terminated by heat inactivation at 65°C for 10 minutes.

2.3.6.3 Synthesis of the mutant strand

6pmol 5' phosphorylated mutagenic oligonucleotide was annealed to 200ng of the uracil containing single stranded DNA template in a reaction volume of 10µl containing 20mM Tris:HCl (pH 7.4), 2mM $MgCl_2$, 50mM NaCl. The oligonucleotide was annealed to the template by cooling the mixture from 70°C to 30°C at a rate of one degree per minute, in a Perkin Elmer Thermal cycler and then placed on ice. 0.5U of T7 DNA polymerase (NEB), 3U of T4 DNA ligase (NEB) were added in the presence of 10mM Tris:HCl (pH 7.9), 0.5mM dNTPs, 1mM ATP, 5mM $MgCl_2$, 2mM DTT and the mixture incubated on ice for 5 minutes followed by 5 minutes at 25°C and finally at 37°C overnight. 90µl TE was added to terminate the reaction and 10µl of the hybrid double stranded plasmids products used to transform competent MC1061. The MC1061 strain (*ung*$^+$) degrade the uracil containing template strand thereby actively selecting for the mutant strand.

2.3.6.4 Mutant identification

Transformed MC1061 colonies were identified as mutants by amplifying the region of interest using colony PCR and using a diagnostic, transcriptionally silent restriction enzyme site present in the mutagenic oligonucleotide.

2.3.7 DNA sequencing

DNA sequencing was performed by A. Bhomra (Sir William Dunn School of Pathology) or the Biochemistry sequencing facility (Oxford University) using the BigDye ™ (ABI) Sanger dideoxynucleotide method. Chain terminating dideoxynucleotides were fluorescently labelled and products of single nucleotide incremental length produced by a PCR based method using a specific oligonucleotide 5' upstream of the region and strand of interest from a purified double stranded DNA template. Products were separated and analysed by gel electrophoresis on an ABI Prism 377 DNA sequencer (ABI). Raw chromatograms were analysed and assembled into contigs using the Staden Pregap4 and Gap4 software.

2.3.8 Oligonucleotides

Oligonucleotides were synthesised by Genosys (Genosys Biotechnologies Ltd., Pampisford, England.), desalted unless otherwise stated and shipped in a lysophilised form. All nucleotides used in this thesis are listed in Table 2-1.

Oligonucleotides were designed using the following guidelines:

1) Oligonucleotides were generally between 20 to 30 nucleotides long and matched the template exactly for the 3' 10 residues.

2) GC content was matched between primer pairs where possible and usually at approximately 55%. The resulting annealing temperature was estimated using the formula:

$$Tm = (\text{Number of G and C residues}) \times 4 + (\text{Number of A and T residues}) \times 2$$

Annealing temperatures for specific primer pairs were then optimised by experiment.

3) The 3' end of the oligonucleotide was terminated with G or C followed by A or T which has been shown to be optimal for priming oligonucleotide extension by thermophilic polymerases.

Table 2-1. Oligonucleotides used in this thesis. The oligonucleotides are arranged in sections according to their use. The orientation (Ori.) of each oligonucleotide is designated S (sense) or AS (antisense) and the presence of any restriction enzyme sites (R.E.) indicated and the relevant residues capitalised. Modifications indicated are 5'phosph=5'phosphate chemically added during synthesis, HPLC pur.= HPLC purified.

Oligo No.	Sequence (5' to 3')		Ori	R.E.	Modifications
Vector					
8029	gtttggatcttggttcattctc	EF-1α of pEF-BOS (Fig. 2-2)	S	-	-
8030	ccatctcaactctccctgc	CD4d3+4 (Fig. 2-2)	AS	-	-
1351	gtaaaacgacggccagtgagcgc	Primer binding sites each side of the MCS in PCRScript (Fig. 2-1)	S	-	-
1352	ggaaacagctatgaccatgat		AS	-	-
8387	tgacacgaagcttgggc	Primer binding sites each side of the MCS in PEE14 (Fig. 2-3)	S	-	-
8271	ctacaaatgtggtatggctg		AS	-	-
HuOX-2 cloning					
1287	cccgggggatTCTAGAcacaccatgggcagtccg		S	XbaI	-
1288	gggtcaccacttgcactTGCGCAgtgcacagcacc	Mutagenesis oligo.	AS	FspI	-
cDNA synthesis and RACE					
1520	gactcgagttgacatcgaggttttttttttttttttttv		-	-	HPLC pur.
1536	gaCTCGAGttgacatcgagg		AS	XhoI	-
1503	aagcagtggtaacaacgcagagtacgcggg		-	-	HPLC pur.
1501	aagcagtggtaacaacgcagagt		S	-	5' phosph
1522	gctgacctgctggattacat	Specific for mouse and human HPRT mRNA.	S	-	-
1523	ccagtttcactaatgacacaa		AS	-	-
5'β-actin	atgccatcctgcgtctggacctggc	Specific for rat beta-actin mRNA	S	-	-
3'β-actin	agcatttgcggtgcacgatggaggg		AS	-	-
rOX-2R cloning					
1500	tgcatngtytgrttyttrtc		AS	-	5'phosph
1502	ttrttytgcatngtytg		AS	-	5'phosph
1504	tcatgGCGGCCGCtgctcccctac		S	NotI	-
1505	gcaccgagtAAGCTTctgaaaaccag		S	HIII	-
1506	ctcacgtagcagtactcttg		S	-	-
rOX-2R sequencing					
1507	gcatgaagggcgttactcatg		S	-	-
1508	gccagatggggattgtgtc		S	-	-
1509	gttctcccacctacatatatag		AS	-	-
1510	cccaaagatatgaatccagttcc		AS	-	-
1514	cattcaatacatcatcccatc		S	-	-
1515	gcgtcacaaggcaaagtcaatggc		S	-	-
1516	gcgcattccaactgacagg		AS	-	-
1521	gcactgatctgaaggtcag		AS	-	5'phosph
1529	cagcatgaagggcgttactcatg		S	-	5'phosph
1530	acacaatccccatctggcgtcca		AS	-	5'phosph
1531	gtccggagcacatgccactgg		S	-	5'phosph
1532	tagctagcatacggctgcat		AS	-	5'phosph
1517	cataaatctggaacgccagtgag		AS	-	-
mOX-2R cloning					
1550	gagtgagcggcggaaaaccagaaaaccgaaatg		S	-	-
1551	gagcggcggGCGGCCGCaaaaccgaaatgttttgct		S	NotI	-
mOX-2R sequencing					
1534	gtggctgggtcaagttgtactg		S	-	-
1535	aaagctcagaggcctgccatc		S	-	-
1552	gtcctgaacttcagatcagtg		S	-	-
1553	ggcaagcctgctgcacagatc		S	-	-
1554	ctctgtccatagaactgggtag		S	-	-
1555	ctgtgactaaggtggaggca		S	-	-
1556	ctgcaggaggaacaatcatca		S	-	-
1557	gaatctctgctgctacctgt		S	-	-
1558	tgtggaggcccaggtgatgt		AS	-	-
Soluble, chimaeric OX-2R proteins					
1518	ccctacctgTCTAGAgaaagagcaccgagtgag		S	XbaI	-
1519	cctaataatGTCGACccccctctacccagttc		AS	SalI	-

2.4 Protein methods

Native proteins were generally stored at 4°C or –20°C for longer term storage. Purified chimaeric proteins, which often had a propensity to degrade, were snap frozen on dry ice before storage at –70°C. Crude tissue culture supernatants were stored at 4°C.

2.4.1 Analysis, detection and quantitation

Proteins were quantified by measuring their absorbance at 280nm and an extinction co-efficient of $5x10^5 M^{-1}cm^{-1}$ for an average protein (50kDa with normal aromatic amino acid content) was assumed if the true extinction co-efficient was unknown. The presence of aggregated protein was determined by a turbidity scattering measurement at 320nm.

2.4.1.1 One dimensional size resolution (SDS-PAGE)

Proteins were resolved according to their molecular mass using BIO-RAD protein mini-slab gels. Resolving gels were between 7.5 and 10% (v/v) acrylamide/bisacrylamide (30:0.8), 0.375M Tris:HCl (pH8.8), 0.1% (w/v) SDS, 0.05% (w/v) ammonium persulphate and 0.1% (v/v) TEMED. Samples were boiled for 10 minutes with an equal volume of a 2x non-reducing (0.5M Tris:HCl (pH 6.8), 5% (w/v) SDS, 20% (v/v) glycerol and 0.005% (w/v) bromophenol blue) or 2x reducing sample buffer (2x non-reducing containing 130mM DTT) before loading onto the gel apparatus. Where both reduced and non-reduced samples were run on the same gel samples were treated with over a two fold molar excess of 1M iodoacetamide (280mM) to prevent disulphide re-oxidisation. Gels were run at $30Vcm^{-1}$ in a running buffer (25mM Tris:HCl (pH 8.3), 192mM glycine, 0.1% (w/v) SDS).

2.4.1.2 SYPRO® stain

Proteins were stained using SYPRO® orange protein gel stain (Cat. No. S6650 Molecular Probes) by mixing 8µl of the 5000x concentrate with 40ml 7.5% (v/v) acetic acid and incubating with the gel at room temperature with rocking for 1 hour. The gel was then rinsed briefly in 7.5% acetic acid and the gel visualised using a STORM 840 transilluminator (Molecular Dynamics, Sunnyvale, CA).

2.4.1.3 Western blotting

Proteins resolved by SDS-PAGE were blotted onto Hybond™ C-super (Amersham International plc, Bucks, UK) nitrocellulose membranes overnight at 30v or for 1 hour at 100v in a methanol containing transfer buffer (25mM Tris:HCl (pH 8.3), 192mM Glycine and 20% (v/v) methanol at 4°C. 3 to 5 µl of rainbow molecular mass markers (Cat. No. RPN 756 Amersham) were run on gels that were blotted.

All subsequent procedures were performed with rocking at room temperature and washing was performed by two brief rinses in washing buffer, WB (20mM Tris:HCl (pH 7.6), 137mM NaCl, 0.2% (v/v) Tween 20 (Sigma) in dH_2O) before rocking the membranes for 15, 10 and finally 5 minutes in fresh changes of buffer.

Blotted membranes were blocked in 5% (w/v) Marvel (Premier Beverages, Stafford, England) in WB for 1 hour and rinsed in WB. 5ml primary antibody (usually as a tissue culture supernatant) diluted one part in five in 1% (w/v) Marvel in WB was incubated with a 7cm x 10cm membrane for 1 hour and then washed. The membrane was then incubated for 1 hour at room temperature with 5ml of a 1:2000 dilution of a horseradish peroxidase conjugated secondary (Cat. No. P161 rabbit anti-mouse, DAKO Immunoglobulins, Denmark or Cat. No. A-0545 goat anti-rabbit, Sigma), and washed before developing with ECL (Cat.

No. RPN 2109) or ECL-plus (Cat. No. RPN 2132) chemiluminescence detection system (both Amersham) and visualised using X-OMAT LS photographic imaging film (Kodak, UK Cat. No. 868 8681) and then developed in a RP X-OMAT processor (Kodak).

2.4.1.4 ELISAs: inhibition and direct

All incubations were performed at 4°C for 1 hour with shaking unless stated. The expression of CD4d3+4 soluble chimaeric proteins was quantified by inhibiting the binding of an anti-rat CD4d3+4 mAb (MRC OX-68) to purified, soluble rat CD4 (extracellular regions only) adsorbed onto a plastic ELISA plate by preincubating a titrated amount of MRC OX-68 with dilutions of crude TCS containing the chimaeric proteins. Briefly, 80µl of neat and serially diluted (in PBS/BSA/N_3) chimaeric protein TCS and CD4 standards were incubated in duplicate with 20µl of a 1:200 dilution (in PBS/BSA/N_3) of MRC OX-68 crude TCS. 50µl of these supernatants were transferred onto the ELISA target plate containing the adsorbed rat CD4 and incubated at 4°C for 1 hour. Rat CD4 was adsorbed to the plastic by addition of 50µl $well^{-1}$ of 50µgml^{-1} diluted in PBS/N_3 and incubated for 1 hour at room temperature and then blocked for 30 minutes (room temperature) with 0.5% BSA in PBS/N_3. Plates were washed 3 times with PBS/N_3 and incubated with 100µl of a 1:2000 dilution of anti-mouse alkaline phosphatase (Cat. No. A9316 Sigma) in PBS/BSA/N_3. Phosphatase activity in individual wells was assayed by spectrophotometrically measuring the development of a dye after addition of 100µl of a phosphatase substrate (104 phosphatase substrate Cat. No. 104-0 Sigma) during the linear phase.

Direct ELISAs were performed by adsorption of the purified target as above and addition of titrated sera, followed by an appropriate alkaline phosphatase conjugated secondary and finally the phosphatase substrate.

2.4.1.5 Amino Acid analysis

The amino acid content of purified protein was used to precisely calculate the extinction co-efficient enabling accurate protein quantification. Analysis was performed on triplicate samples by A.Willis (MRC Immunochemistry Unit, Oxford University) using an ABI 420A derivatiser/analyser (PE Applied Biosystems, Warrington, UK) linked to an HPLC system (Applied Biosystems 130A) for analysis. Data handling was performed using Gynkotek Chromeleon software (version 4.10 from Gynkotek UK Ltd, Macclesfield, UK).

2.4.1.6 N-terminal protein sequencing

N-terminal protein sequencing was performed by A.Willis (MRC Immunochemistry Unit) using an automated Edman degradation in an Applied Biosystems Procise 494A protein sequencer (Perkin-Elmer Ltd.,UK).

2.4.1.7 Removal of N-linked carbohydrates

Approximately 0.5µg purified OX-102 antigen was incubated at 37°C in the presence of 50mM sodium phosphate (pH 7.5) and 1% NP-40 without or with 10U of PNGase F (Cat. No. 704 NEB) without prior boiling and reduction in a total volume of 10µl. Aliquots were removed at various times and stored frozen before further analysis.

2.4.2 Protein purification

2.4.2.1 Purification of the OX-102 antigen from deoxycholate lysates

Chapter four describes the diagnostic steps taken to purify the OX-102 antigen but a brief description used routinely in further purifications is given here. 200 to 300µl MRC OX-102 mAb coupled Sepharose beads are added to approximately 250ml of a deoxycholate (DOC) solubilised rat splenic membrane preparation and rotated for at least 24 hours at 4°C. The Sepharose was pelleted by a gentle spin at 1000 rpm (GPR benchtop centrifuge, Beckman) and the supernatant removed by pipetting. The Sepharose was transferred to a 15ml 2095 (Falcon) tube and washed in 5ml 0.5%DOC, 10mM Tris (pH 8.0) and pelleted by centrifugation as above. The Sepharose was then washed sequentially with 5ml 0.5%DOC, 10mM Tris (pH 8.0), 150mM NaCl, 2ml 0.5%DOC, 0.05M Diethylamine:HCl (pH 11.5), 5ml 0.5%DOC, 10mM Tris (pH 8.0), 2ml 0.1% SDS before elution in 1ml 0.5% SDS at 55°C for 15 minutes. The eluted material was concentrated using spin concentrators to a volume of approximately 50µl.

2.4.2.2 Immunoaffinity chromatography

Soluble chimaeric proteins containing the CD4d3+4 antigenic tag were purified at 4°C by immunoaffinity chromatography using purified MRC OX-68 coupled to Sepharose (see section 2.5.4) made by Karen Starr. Large volumes (~1 litre) of spent tissue culture supernatant containing these proteins were first concentrated to a volume of 50ml using a Minitan ultrafiltration system (Millipore, Herts, England.) before passing over a pre-eluted and washed MRC OX-68 column. The column was then washed with 25 column volumes (CV) of a low salt buffer (25mM Tris:HCl (pH 7.5) 140mM NaCl, 10mM NaN_3), then 5 CVs of a high salt buffer (25mM Tris:HCl (pH 7.5) 500mM NaCl, 10mM NaN_3), and finally

5 CVs of the low salt buffer. The adsorbed protein was eluted in suitably sized fractions using 0.1M glycine:HCl (pH 2.5) and neutralised with 2.5M Tris:HCl (pH 7.5). The OD_{280} of each fraction was measured and positive fractions pooled and concentrated.

2.4.2.3 Gel filtration

Purified proteins which were to be used for BIAcore analysis were further resolved by FPLC (Pharmacia) using a Superdex S-200 column (Pharmacia) to exclude higher order aggregates from the preparation.

2.4.2.4 Immunoprecipitation

All procedures were performed at 4°C. Whole cell lysates were precleared with 50µl of a 20% slurry of GammaBind® G Sepharose® (Pharmacia Biotech, Uppsala, Sweden) by rotation overnight. Mabs coupled to Sepharose were added to the precleared lysate either covalently linked to Sepharose (section 2.5.4) or via protein G using GammaBind® G Sepharose®. To couple mAbs to protein G, 1.4ml of a crude mAb TCS were rotated overnight with 50µl of a 20% GammaBind® G Sepharose® slurry and washed twice in PBS/BSA. Immunoprecipitations were performed overnight and then washed 3 times before analysis.

2.4.2.5 Concentration and dialysis

Proteins were concentrated using appropriately sized spin concentrators (MWCO 10000Da) 15ml (Cat. No. 4305) or 500µl (Cat. No. 42403) (Amicon, Beverly, MA) and used according to the manufacturers instructions.

Proteins were dialysed at least twice against a large volume of buffer at 4°C with stirring using Slide-A-Lyzer dialysis cassettes (Pierce, Rockford, IL) as recommended by the manufacturer.

2.4.3 Solubilisation of cell surface proteins

2.4.3.1 Whole cell lysis

Whole cells were washed three times in PBS before being lysed at 10^8 per ml in an NP-40 lysis buffer (1% NP-40, 10mM Tris:HCl (pH 7.4), 150mM NaCl, 1mM EDTA to which 1mM PMSF (Sigma) and 10mM iodoacetamide (Sigma) were added immediately prior to cell lysis. Lysates were incubated on ice for 20 minutes before spinning at 13000rpm in a microfuge at 4°C to remove insoluble material and the supernatant stored -20°C.

2.4.3.2 Crude Tween 40 membrane purification

Cells were pelleted after washing and lysed in 5% Tween-40 lysis buffer (5% Tween-40 in 25mM Tris:HCl (pH 7.4), 140mM NaCl, 10mM NaN_3) containing 0.2mM PMSF and 2.5mM iodoacetamide by mixing for 1 hour at 4°C. The lysate was passed through a 25 gauge needle six times before pelleting the insoluble fraction (includes nuclei) by centrifugation at 1500xg 4°C. The supernatant was removed and the extraction repeated before the solubilised fractions were pooled and the detergent microsomes pelleted by spinning at 50000rpm in a TLA-100.3 rotor in a TL-100 Beckman Ultracentrifuge at 4°C for 1 hour. The microsome pellet containing membrane proteins was resuspended in 500µl 10mM Tris:HCl (pH 8.0) 10mM NaN_3 and stored at -20°C. The protein content of each measured using protein assay reagent (Cat. No. 23236 Pierce).

2.4.3.3 Deoxycholate solubilisation

Crude Tween 40 membrane preparations were solubilised in an equal volume of 4% sodium deoxycholate (which had been dialysed into Tris:HCl (pH 8.0) 10mM NaN_3 for 1 week) by passing through a 25 gauge needle six times and then stirring for 1 hour at 4°C. Deoxycholate insolubles were removed by ultracentrifugation at 70000xg for 1 hour and the supernatant used for immunoaffinity chromatography and immunoprecipitation.

2.5 Monoclonal antibodies (mAbs)

MAb Name	Isotype	Antigen	Notes	Ref.	Source
MRC OX-1	Mouse IgG_1	Rat CD45	-	1	MRC CIU
MRC OX-2	Mouse IgG_1	Rat OX-2	Blocks binding of OX-2R	2	MRC CIU
MRC OX-6	Mouse IgG_1	Rat MHC II	Non polymorphic	2	MRC CIU
MRC OX-21	Mouse IgG_1	Human iC3b	-	3	MRC CIU
MRC OX-33	Mouse IgG_1	Rat CD45	B-cell specific	4	MRC CIU
MRC OX-34	Mouse IgG_{2a}	Rat CD2	-	5	MRC CIU
MRC OX-39	Mouse IgG_1	Rat CD25	Activated T-cell marker	6	MRC CIU
MRC OX-41	Mouse IgG_1	Rat SIRP	-	7	MRC CIU
MRC OX-45	Mouse IgG_1	Rat CD48	Block binding of rCD2	8	MRC CIU
MRC OX-48	Mouse IgG_1	Unknown	Activated T and B cells	6	MRC CIU
MRC OX-62	Mouse IgG_1	Rat integrin	Rat DC marker	9	MRC CIU
MRC OX-68	Mouse IgG_{2b}	Rat CD4d3+4	-	10	MRC CIU
MRC OX-82	Mouse IgG_1	Unknown	Neutrophil marker	11	MRC CIU
MRC OX-88	Rat IgM	Mouse OX-2R	Blocks binding of rOX-2	12	MRC CIU
MRC OX-102	Mouse IgG_1	Rat OX-2R	Blocks binding of rOX-2	Thesis	MRC CIU
MRC OX-104	Mouse IgG_1	Hu OX-2	-	Thesis	MRC CIU
W6/32	Mouse IgG_{2a}	Human HLA	-	13	MRC CIU
M-A251	Mouse IgG_1	Human CD25	Purchased FITC conjugate	14	MCA1319F S
HIB19	Mouse IgG_1	Human CD19	Purchased biotinylated	15	30652X Ph
UCHT1	Mouse IgG_1	Human CD3	Purchased biotinylated	16	30102X Ph
4G10	Mouse IgG_{2b}	phospho-Y	-	17	05-321 TCS
RET-PE2	Mouse IgG	Rat CD147	-	18	Mr P. Kirk

Table 2-2. Monoclonal antibodies used in this thesis. Monoclonal antibodies used in this thesis are tabulated here. Source: MRC CIU -mAb made within the MRC Cellular Immunology Unit, S -Serotec, Oxford, UK; Ph -Pharmingen, San Diego, CA; TCS -TCS Biologicals, Buckingham, UK. References are: 1) Sunderland et al., 1979, 2) McMaster and Williams, 1979, 3) Hsiung et al., 1982, 4) Woollett et al., 1985, 5) Jefferies et al., 1985, 6) Paterson et al., 1987, 7) Adams et al., 1998, 8) Arvieux et al., 1986, 9) Brenan and Puklavec, 1992, 10) Brown and Barclay, 1994, 11) Highnam unpublished, 12) Preston et al., 1997, 13) Barnstable et al., 1978, 14) Serotech catalogue, 1999, 15) Nadler et al., 1983, 16) Beverley and Callard, 1981, 17) Cohen et al., 1990, 18) Finnemann et al., 1997.

Monoclonal antibodies were stored at 4°C whether purified or as a spent TCS. Table 2-2 lists the mAbs used in this thesis.

2.5.1 Generation of mAbs

2.5.1.1 Immunisations

The immunisation protocols for the generation of MRC OX-102 and MRC OX-104 are detailed in chapters three and nine respectively. Where adjuvants were used in immunisations the first immunisation was given in complete Freund's adjuvant (CFA) (sub-cutaneously) and subsequent immunisations given in incomplete Freund's adjuvant (IFA) (sub-cutaneously). The immunogen was vigorously mixed in a 1:1 (v/v) ratio with adjuvants to form an insoluble emulsion before injection.

2.5.1.2 Fusion procedure

The generation of hybridoma lines secreting antibodies of monospecificity by cellular fusion of the splenocytes of immunised mice or hamsters with the NS-1 myeloma was performed by Michael Puklavec according to a standard protocol. The fusion mix was plated out over 4x96well plates and selective HAT medium added 24 hours after fusion. After 10 days, the supernatants were harvested, screened and the positively selected wells grown and recloned three times.

2.5.2 Isotyping

The mAbs secreted from cloned hybridomas were isotyped using a sheep red blood cell agglutination assay kit (Cat. No. MMT RC1, Serotec, Oxon, England).

2.5.3 Mab purification by ammonium sulphate precipitation

Monoclonal antibodies were purified from concentrated hybridoma spent TCS by salting out using a saturated ammonium sulphate solution. Cellular debris was first removed by centrifugation before adding an equal volume of 25mM Tris:HCl (pH 7.4) and then an equal volume of ice cold ammonium sulphate added slowly whilst stirring and then stirred for a further 4 hours at 4°C. Precipitated mAb was pelleted by centrifugation in a JA-20 rotor (Beckman J2-HS centrifuge) at 12000rpm for 30 minutes at room temperature and finally resuspended in a suitable buffer.

2.5.4 Covalent coupling of purified mAbs to Sepharose 4B

Purified mAbs to be coupled were dissolved in or dialysed against 0.1M $NaHCO_3$ (pH 8.3), 0.5M NaCl at a concentration of $5mgml^{-1}$. 5ml purified mAb at $5mgml^{-1}$ was coupled to 3.5ml of reconstituted CNBr-4B Sepharose (Pharmacia Biotech) as recommended by the manufacturer. The mAb coupled Sepharose was finally resuspended as a 20% slurry in a tris/saline buffer (25mM Tris:HCl (pH 7.4), 140mM NaCl, 10mM NaN_3) and stored at 4°C.

2.5.5 Biotinylation of mAbs

The optimal biotin to mAb ratio was determined by diagnostic experiments before a bulk preparation was biotinylated. NHS-LC-Biotin (Cat. No. 12336, Pierce Chemical Company) was dissolved in dimethylsulphoxide and added to purified mAbs (dialysed into an amine free buffer -usually PBS) and biotinylation performed at room temperature for 50 minutes before the reaction was terminated by adding an excess of 2.5M Tris:HCl (pH 7.6). The free biotin was removed by dialysis against PBS/N_3.

2.5.6 Flow cytometry

All cells were freshly stained (unfixed) at 4°C in the presence of oxidative respiration inhibitors (10mM sodium azide) and wash steps performed using PBS/BSA/N_3. Cells for flow cytometry were aliquoted at 10^6 per well of a 96 well round bottomed plate and incubated in 50µl PBS/BSA/N_3 containing 5% heat inactivated serum from the same species to saturate Fc receptors for 10 minutes prior to the addition of 50µl mAb TCS. Cells were stained for an hour before washing twice and incubating for an hour with an appropriately titrated fluorescence-conjugated secondary mAb, (usually goat anti-mouse FITC adsorbed against rat immunoglobulins (Cat No. STAR 70, Serotec) for single colour or Donkey anti-mouse phycoerythrin (Cat. No. AO193E Chemicon, Temecula, CA) for multicolour staining). Cells in a single stain experiment were resuspended in 1ml PBS/BSA/N_3 before analysis on a FACScan (Beckton Dickinson, Palo Alto, CA). Cells for multicolour staining were then blocked with 50µl appropriate normal serum (usually mouse) for 10 minutes before addition of biotinylated and/or directly FITC conjugated mAbs for an hour. Each well was then washed twice and 50µl streptavidin-quantum red (Cat. No. S2899, Sigma) diluted 1:50 added for 30 minutes before cells were resuspended and analysed as described above.

2.5.7 Immunohistochemistry

Staining of unfixed frozen human tissue was performed by Professor David Y Mason's laboratory (Department of Clinical Biochemistry and Cellular Science, John Radcliffe Hospital, Oxford) using a standard indirect peroxidase technique. Sections were viewed on an orthoplan Leitz microscope (Leitz, Germany) and images viewed and stored using a digital camera (3-CCD. Cat. No. KY-F55B, JVC, Japan).

2.6 Biological material

All cell culture using human tissue was performed in a Class II laminar flow hood.

2.6.1 Primary biological tissue

Rats were obtained from a specific pathogen free unit (MRC Cellular Immunology Unit) and mice from the Mouse Breeding Unit (Sir William Dunn School of Pathology). Rats and mice were also obtained from the Pathology Support Building. Syrian hamsters were housed in the department of Physiology animal house (Oxford University). Animals were killed by CO_2 asphyxiation and neck dislocation before subsequent procedures were performed according to both institutional and Home Office regulations. Experiments revealed that the results of all OX-2 binding experiments were independent of both strain and sex. In general, PVG rats and BALB/c mice of either sex were used as sources of primary biological tissue.

2.6.1.1 Rat peripheral blood leukocytes (PBL)

Blood was removed from a dead rat by cardiac puncture in the presence of 5 units of heparin. Erythrocytes were lysed using TBAC (as described in section 2.1) and PBL washed twice in PBS/BSA/N_3.

2.6.1.2 Peritoneal exudate cells (PECs)

Resident PECs were obtained by injecting 20ml (rats) or 5ml (mice) of ice cold PBS/BSA/N_3 into the peritoneal cavity, the abdomen massaged and the fluid removed using a plastic pasteur pipette. Erythrocytes were lysed using TBAC (as described in section 2.1)

and PECs washed twice in PBS/BSA/N_3. Thioglycollate elicited PECs were obtained by injecting 7 ml Brewers thioglycollate broth into the peritoneal cavity and PECs harvested as above three or four days later.

2.6.1.3 Thymocytes and splenocytes

Thymi and/or spleens were removed from 12 week old rats or 6 week old mice and dispersed by teasing the tissue apart using tweezers in PBS/BSA/N_3 and a single cell suspension obtained by passing through a cell strainer (Falcon).

2.6.1.4 Alveolar macrophages

Plastic tubing attached to a needle was inserted into the severed trachea of a dead rat and secured in place using surgical suture. Alveolar lavage was performed by attaching a syringe to the needle and flushing the lungs numerous times with ice cold sterile PBS/BSA. The harvested cells were resuspended at $7x10^5$cells ml^{-1} in RPMI/10% FCS supplemented with $100Uml^{-1}$ of recombinant rat IFN-γ and stimulated overnight at 37°C before FACS analysis.

2.6.1.5 Human PBMC

Screened human buffy coats were collected from the National Blood Centre, John Radcliffe Hospital, Oxford the day after collection. Blood was diluted with an equal volume of RPMI 1640 (GibcoBRL) before 25ml was layered over 15ml Ficoll Hypaque (Cat. No. 17-1440-02, Pharmacia Biotech) and erythrocytes removed by centrifugation (no brake) at 2500rpm in a Beckman benchtop GPR centrifuge for 20 minutes. The leukocyte interface

was removed, remaining erythrocytes lysed using TBAC and then washed until the supernatant was clear (platelet free) before activation or direct use for cell surface staining.

2.6.2 Activation of biological tissue

2.6.2.1 ConA/LPS stimulation

Human PBL or rat splenocytes were activated for three days at $1.5x10^6$cellsml^{-1} in RPMI 1640/10%FCS in the presence of 5μgml^{-1} of concanavalin A (Cat. No. 17-0450-01, Pharmacia Biotech) or 25μgml^{-1} lipoylpolysaccharide (Cat. No. L4516, Sigma).

2.6.2.2 Pervanadate activation of rat PECs

Vanadium ions are potent inhibitors of protein tyrosine phosphatases but their potency is reduced when polymerised. Vanadate ions tend to polymerise in solutions >0.1mM at neutral pH and form a characteristic orange/yellow colour but can be depolymerised or activated by adjusting the pH of a 200mM sodium vanadate solution to 10.0 using either HCl or NaOH which turns the solution colourless. The solution is then repeatedly boiled and cooled until the solution remains colourless and the pH stabilises at pH 10.0 when it is aliquoted and stored at –20°C.

1mM sodium pervanadate was prepared by oxidising an activated 200mM sodium vanadate stock by dilution in PBS and incubation for 5 minutes at room temperature with a molar excess of a stabilised hydrogen peroxide solution (Cat. No. H1009, Sigma.) Unreduced hydrogen peroxide was enzymatically removed by the addition of 50μl bovine catalase covalently attached to Sepharose (Cat. No. C-9284, Sigma) and incubated at room

temperature for 5 minutes. Sepharose bound catalase was removed by centrifugation before pervanadate was added to cells.

$9x10^7$ rat PECs were harvested in PBS, subdivided into two 4.5ml aliquots and incubated with shaking at 37°C for 25 minutes before being either stimulated (500µl 1mM pervanadate in PBS) or left unstimulated (500µl PBS). Cells were then washed, pelleted and each aliquot lysed on ice for 1 hour using 1ml ice cold WOP-40 buffer (1%NP-40, 50mM Tris:HCl (pH 8.0), 150mM NaCl, 1mM EDTA, 10mM NaF, 10mM sodium pyrophosphate supplemented with 0.4mM activated sodium vanadate, 10mM iodoacetamide, 1mM PMSF, $10\mu gml^{-1}$ leupeptin and aprotinin). Insoluble material was removed by centrifugation and 50µl 20% mAb coupled Sepharose added and immunoprecipitated (see section 2.4.2.4)

2.6.3 Cell lines

The cell lines used in this study are listed in Table 2-3.

Cell line	Derived from:	Reference.
293T	Human kidney epithelium	(Cherington et al., 1986)
CHO.K1	Chinese hamster ovary	ATCC-CCL61
NS-1	Mouse B-cell lymphoma (non-immunoglobulin secreting)	(Kohler et al., 1976)
MAJA	Human B-cell lymphoma	(Spielman et al., 1984)

Table 2-3. Cell lines used in this thesis.

2.7 Recombinant protein construction and expression

All recombinant proteins were expressed in eukaryotic cells and therefore were presumed to contain eukaryotic post translational modifications including the formation of disulphide bonds and addition of carbohydrate.

2.7.1 Expression constructs used in this thesis

The constructs made or used in this study are diagrammatically represented in Figure 2-2 and Figure 2-3. In general, constructs were initially tested for their ability to generate antigenically active recombinant protein by transient expression in HEK 293T cells by the use of the pEF-BOS expression vector (Fig. 2-2) before subcloning into the pEE14 vector (a derivative of pEE6) (Stephens and Cockett, 1989) (Fig. 2-3) and generating stably transfected CHO-K1 lines.

2.7.2 $CaPO_4$ mediated transfection of CHO-K1 and HEK 293T cells

All solutions were sterilised by passing through a 0.22μm filter before use. The following protocol was used when transfecting an $80cm^2$ flask of 293T cells and was scaled up as required. 20μg DNA was added to 248μl 1M $CaCl_2$ solution and the volume made up to 1ml with dH_2O. This was then added dropwise over one minute to a 2x HBS solution (280mM NaCl, 50mM HEPES (Cat. No. H-9136, Sigma), 2.8mM Na_2HPO_4 pH 7.05) in a 2001 tube (Falcon) with gentle flicking. After a 20 minute incubation at room temperature the resulting translucent precipitate was added to the tissue culture flask (which had been seeded the previous day with $1x10^5$ $cellscm^{-2}$ (cell surface expression) or $5x10^5 cellscm^{-2}$ (secreted proteins)) in a dropwise fashion and left overnight. The next day, the precipitate was carefully washed from the cells and the media replaced with either the normal DMEM/10%FCS or, if the expressed proteins were to be biotinylated, with serum free X-VIVO-10. The transfected cells were then left for a further 3 days.

To ensure the correct level of precipitation, the pH of the 2xHBS solution was adjusted by the addition of 0, 5, 10, 15, or 20 μl 1M HCl in separate tubes before the addition of the $CaC1_2$ (with no DNA). After the 20 minute incubation with occasional flick

mixing the test precipitates were examined and the amount of HCl required to form a fine translucent precipitate determined.

The CHO.K1 cell line was transfected by Ruth Hatton with constructs subcloned into the pEE14 vector using the calcium phosphate method as described above. The selection of transfected clones is achieved by culturing the CHO.K1 cells without the addition of L-glutamine to the culture media and therefore cellular survival is dependent upon the amidation of glutamate by glutamine synthetase. This enzyme is competitively inhibited by L-methionine sulphoximine (MSX) which is therefore lethal when added to the culture media. The pEE14 vector contains the Chinese Hamster glutamine synthetase gene and thus is able to confer selection on clones containing enough copies of the vector via a gene dosage effect, which is also dependent on the concentration of MSX used. The concentration of MSX used was 25μM. Clones were assayed by MRC OX-68 inhibition ELISA and those secreting most highly were recloned and tested before being grown as bulk cultures to produce large amounts of protein.

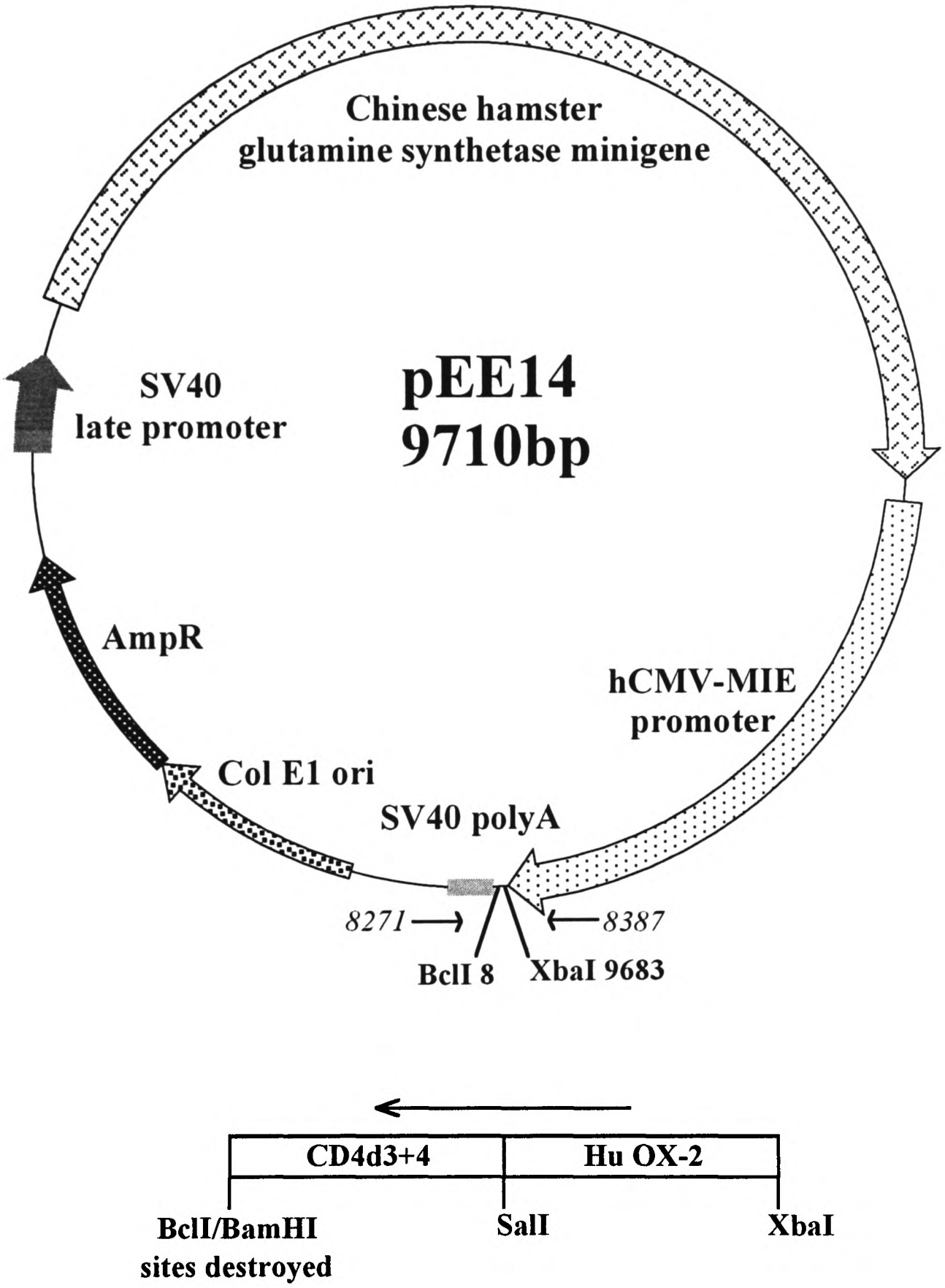

Figure 2-3. Schematic diagram of the vector used for generating stable lines in the chinese hamster ovary cell line. pEE14, also a derivative of pUC119, contains features enabling bacterial maintanance (Col E1 ori) and selection on ampicillin. Restriction enzyme sites relevent to this thesis are marked and the location of two oligonucleotides (*8271* and *8387*) used to detect cloned inserts are indicated. The glutamine sythetase gene used for selection is under the control of the SV40 late promoter and the expression of introduced genes driven by the human cytomegalovirus major immediate early promoter (hCMV-MIE).

2.7.3 Biotinylation of chimaeric proteins using BirA enzyme

Serum free spent tissue culture supernatant containing chimaeric proteins with the biotinylatable sequence were concentrated to approximately 500µl and concomitantly exchanged into 10mM Tris:HCl (pH 8.0). The concentrated TCS was then biotinylated as recommended by the manufacturer (Avidity, Denver) overnight at room temperature.

2.7.4 Generation of multivalent binding reagents

The generation of multivalent binding reagents has been described previously (Brown et al., 1995) and modifications (Brown et al., 1998). All steps were performed at 4°C unless stated and washes were performed by resuspending beads in PBS/BSA/N_3 using a waterbath sonicator (Heat Systems, Ultrasonic Processor, power setting of 20% for 1 minute) which had been pelleted by microcentrifugation. 20µl sample^{-1} of biotinylated, FITC-loaded plastic beads (Cat. No. TFP-0552-5, Spherotech Inc., Libertyville, IL 0.4 to 0.6µm diameter) were washed and coated in 4µg sample^{-1} of purified streptavidin (Cat. No. 21122, Pierce) by rotation in foil at room temperature. Beads were then washed three times and sonicated into 4µg sample^{-1} of biotinylated MRC OX-68 and incubated with rotation at 4°C for 1hour and washed twice. Beads were sonicated into 30µl sample^{-1} of chimaeric protein TCS and rotated for a further hour at 4°C before adding 30µl of the beads to a 20µl suspension of cells ($1x10^6$). Cells had generally been incubated in 50µl mAb TCS for 1 hour at 4°C and washed before addition of the beads. Cells and beads are then briefly shaken and spun for 20 minutes at 1000 rpm (GPR benchtop centrifuge, Beckman) and then incubated on ice for a further 40 minutes before resuspension in 1ml PBS/BSA/N_3 and analysis by cytofluorimetry as described in section 2.5.6.

2.8 Surface Plasmon Resonance (SPR) analysis

Protein interactions were analysed and quantitated using surface plasmon resonance technology. SPR analysis was performed on a BIAcore 2000 (BIAcore AB, St Albans, UK) using running buffer HBS (10mM HEPES (pH 7.4), 150mM NaCl, 3.4mM EDTA, and 0.005% surfactant P20) (BIAcore AB). Approximately 4000RU of streptavidin (Pierce) dissolved in 10mM sodium acetate (pH 5.5) was coupled using amine coupling to a CM5 research grade chip (BIAcore) at $0.2mgml^{-1}$. Biotinylated rOX-2RCD4d3+4 protein and CD4d3+4 (control) were immobilised at indicated levels in individual flow cells. Kd values were obtained both by non-linear curve-fitting of the Langmuir binding isotherm and Scatchard transformations of the binding data. Kinetic data were obtained at the maximum flow rate of $100\mu lmin^{-1}$ to minimise rebinding effects. K_{off} values were determined by fitting a first order exponential decay curve to normalised data using Origin (Microcal software version 5.0) obtained from individual flow cells containing rOX-2RCD4d3+4 after the subtraction of the negative control (CD4d3+4). K_{on} values were obtained by using this K_{off} value in BIAevaluation 3.0 (BIAcore AB) software over the association binding phase.

2.9 Computer programs

Most computational manipulations of sequence data were performed using the Wisconsin package via the Oxford University Bioinformatics Centre.

2.9.1 Sequence alignments and phylogeny

Multiple sequences were aligned using clustalW and then manually refined. The phylogenetic relationships of the sequences were determined using a neighbour-joining tree using clustalW and displayed using njplot.

2.9.2 Sequence data analysis

Sequence data was analysed using the pregap, Pregap4 and Gap4 software (Staden).

Chapter Three

Generation of MRC OX-102, a monoclonal antibody that binds rat macrophages and blocks the binding of OX-2 protein

3.1 Introduction

The observation that rat OX-2 coated beads could bind rat peritoneal exudate cells (PEC) (1.6.5) suggested the presence of a specific rat OX-2 receptor expressed on the surface of these cells (Preston et al., 1997). A major step forward in understanding the function of the OX-2 glycoprotein would be to characterise the molecular nature of this receptor.

The OX-2:PEC interaction was observed in both rat and mouse models, implying that the binding face of OX-2 and its receptor were conserved between these species (Preston et al., 1997). This cross species binding enabled the use of widely available mouse macrophage expression libraries in initial attempts to characterise the receptor. An attempt to clone the receptor by using fluorescent beads to sort cells transfected with these libraries by cytofluorimetry failed, possibly because the OX-2 coated beads were not sufficiently avid, the cDNA was poorly represented in the library or the receptor consisted of more than one gene product and wasn't suitable for cloning by this method (Preston, 1996). Therefore, efforts were concentrated on raising a monoclonal antibody which would bind the PEC cell surface and block the binding of the rat OX-2 binding reagent. This mAb could then be used to characterise the receptor by either expression cloning or biochemical methods. The first attempt generated MRC OX-88, a rat anti-mouse IgM, which did not immunoprecipitate or western blot making biochemical characterisation impossible (Preston, 1996). However, two colour cytofluorimetry using this mAb did suggest that the OX-2 receptor was restricted to macrophages in the mouse peritoneal cavity (Preston et al., 1997). An attempt to clone the MRC OX-88 antigen resulted in the cloning of a contaminant, the human poly Ig receptor, from a mouse macrophage expression library (Dr Marion H. Brown and G.J.W., unpublished data) and so further work using this mAb for cloning was abandoned.

The experimental starting point of this thesis was to raise panels of mAbs to rat peritoneal exudate cell surface molecules in mice. The species switch meant that mouse hybridomas would be generated, which, from experience within the laboratory generate more hybridomas per fusion and less IgM isotype monoclonal antibodies. In addition, the cellular composition of the resident peritoneal cavity differed between species, rats having up to 80% macrophages (10^7 total cells/animal) (Barclay, 1981) compared to 50% ($2x10^5$ total cells/animal) in mice (Padawar and Gordon, 1956). The higher percentage of receptor expressing cells generated a higher signal:noise ratio enabling clearer interpretation of blocking results and also, more receptor positive cells per animal could be harvested. This antibody would then be used not only to clone the OX-2 receptor but also for biochemical analysis, a detailed distribution study of the protein and functional studies.

In summary, (Fig. 3-1) this chapter describes the generation of a monoclonal antibody (MRC OX-102) which binds rat resident peritoneal exudate cells and blocks the binding of rat OX-2 coated beads when preincubated with the cells. Isotyping of the mAb revealed it was a mouse IgG_1 and a western blot of whole cell lysates showed that this antibody detected a protein of heterogeneous mass (60 to 100 kDa) and was thus very likely to be of high enough affinity to characterise the rat OX-2 receptor.

3.2 Production of panels of monoclonal antibodies

The generation of hybridomas was performed by Michael Puklavec using standard procedures (see section 2.5.1) and the fusion mix plated out over 4x96 well plates. After 10 days in selective media the hybridoma supernatants were removed and the 4x96 wells were pooled into 2x96 wells and tested for their ability to stain resident rat peritoneal exudate cells by cytofluorimetry. The two individual wells of the positive pools were then individually tested for the ability to block rOX-2 coated beads in a separate experiment.

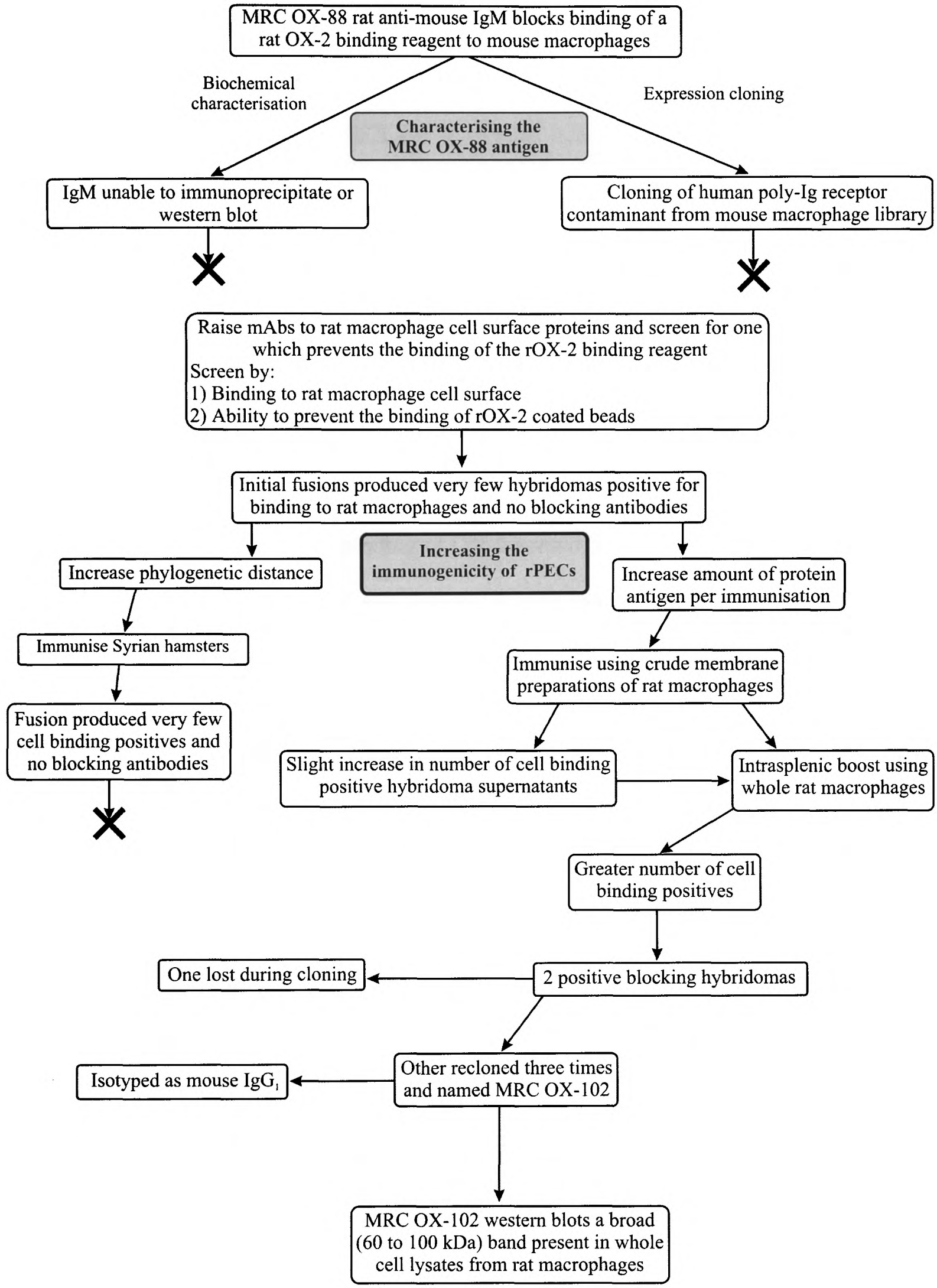

Figure 3-1. Diagram illustrating the strategies undertaken in chapter 3.

Initially, whole rat PECs were used as the immunogen, injected either intravenously (i.v.) or intraperitoneally (i.p.) and resulted in good responses as the sera from the immunised animals stained rat PECs (as shown by cytofluorimetry) when titrated out to dilutions of at least 1:10,000 when compared to an unimmunised control (data not shown). However, only very few hybridoma supernatants generated from these animals were able to bind the rPEC cell surface (Table 3-1, fusions 220 and 223).

3.3 Attempts to increase immunogenicity of rat peritoneal exudate cells

The success of the strategy to clone the OX-2 receptor by raising a monoclonal antibody which would block the binding of OX-2 coated beads depended upon raising large numbers of anti-rat PEC mAbs per fusion. It was therefore essential to increase the immunogenicity of the rat PEC immunogen. The factors affecting the degree of immunogenicity of a given immunogen are very poorly understood but is known to depend upon the host, route of delivery and amount injected.

3.3.1 Crude Tween-40 membrane preparations

Injecting both more protein and a greater percentage of membrane proteins per immunisation was achieved by preparing crude Tween-40 membrane preparations from thioglycollate elicited rat PECs. The use of elicited PECs (which bound the rat OX-2 coated beads at an equivalent level to resident PECs (data not shown)) enabled up to $6x10^7$ PECs to be collected per animal (a six-fold increase). Five membrane preparation batches were made and these are detailed below (Table 3-2). The crude membrane preparations were mixed with adjuvants and roughly 50 to 200 μg were injected sub-cutaneously (s.c.) per immunisation (Table 3-1). This schedule was successful in increasing the number of hybridomas able to

bind the PEC cell surface (Table 3-1 fusion 225) but did not result in the production of a blocking mAb.

Batch No.	Animals	Number of elicited PECs obtained.	[Protein] mg/ml	Protein injected per immunisation (μg)
1	15 female PVG	$6.5x10^8$	2.0	~ 200
2	20 female PVG	$6.5x10^8$	1.7	~ 200
3	16 female PVG	$1.0x10^9$	3.7	~ 400
4	16 female PVG	$4.0x10^8$	0.4	~ 50
5	16 female PVG	$5.0x10^8$	0.4	~ 50

Table 3-2. Details of membrane preparation batches. Each rat was injected with 7ml Brewers' thioglycollate broth four days before harvesting and the total number of cells obtained for the preparation of each batch is shown. The microsomes were prepared as described in section 2.4.3.2 and the protein concentration measured. Each batch was mixed 1:1 (v/v) with adjuvant and 200μl injected into each recipient as detailed in Table 3-1. An estimate of how much membrane protein per immunisation was present in each batch is also shown.

3.3.2 Increasing the phylogenetic distance

The immunogenicity of rat PEC membrane proteins might also be raised by increasing the phylogenetic distance between the immunogen and the host. The immune system is largely tolerant to self and therefore only *differences* in primary protein sequences between host and immunogen are immunogenic, thus, attempting to raise antibodies to proteins which are highly conserved is very difficult. Since rat OX-2 bound to the mouse OX-2 receptor, the function of the binding faces of these two proteins have been conserved across the rat and mouse species barrier (approximately 5 million years of evolution (Kumar and Hedges, 1998)). It was therefore a concern that there would be few or no antigenic sites to which a blocking mAb would bind.

In an attempt to increase the phylogenetic distance between the host and immunogen a series of immunisations were given to Syrian hamsters (*Mesocricetus auratus*). However,

this species switch proved unsuccessful (Table 3-1 fusion 226) possibly due to subtle species differences between hamsters and mice which disrupted the sensitive fusion procedure.

3.4 Intrasplenic injection

In another attempt to increase the number of PEC staining hybridomas per fusion, the final boost was delivered directly into the spleen. This procedure had been used with success in the past when immunising with limiting amounts of antigen (Dr Gordon MacPherson, personal communication). The intrasplenic injection was performed by Dr Gordon MacPherson. The resulting fusion produced a greater number of hybridomas secreting mAbs reactive with the rPEC cell surface and in addition, two of these hybridomas exhibited the ability to block the binding of rOX-2 coated beads. During subsequent cloning procedures, one of these hybridomas stopped secreting, a phenomenon which is sometimes observed (Williams et al., 1977) and (Michael Puklavec, personal communication) and is attributed to the unstable nature of fused cell hybridomas. However, one hybridoma continued to secrete a mAb able to stain rat PECs (Fig. 3-2) and was recloned three times and named MRC OX-102. An important control in the screening for a blocking antibody is to test the specificity of its blocking effects. MRC OX-102 was able to block the binding of the rat OX-2 coated beads back to a negative control (CD4d3+4 coated beads) but did not affect the binding of a control rat CD2:CD48 interaction, indicating that the blocking effects of the mAb were specific for the OX-2:OX-2R interaction (Fig. 3-3).

Fusion No.	H	Immunisation protocol												Bind	FE (%)	Block
		1	d	2	d	3	d	4	d	5	d	6	d	Boost			
220	M	$5x10^6$ rPECs i.v.	15	$3.3x10^6$ rPECs i.v.	14	$5x10^6$ rPECs i.v.	20	-	-	-	-	-	-	$5.2x10^6$ rPECs i.v.	7	1.8	0
223	M	$5x10^6$ rPECs i.v.	15	$3.3x10^6$ rPECs i.v.	14	$5x10^6$ rPECs i.v.	20	$5.2x10^6$ rPECs i.v.	32	-	-	-	-	μS^1 IFA s.c.	16	4.2	0
225	M	μS^1 CFA s.c.	15	μS^2 IFA s.c.	20	μS^3 IFA s.c.	15	μS^4 IFA s.c.	10	-	-	-	-	μS^5 IFA s.c.	34	8.9	0
226	S	μS^3 CFA s.c.	20	μS^4 IFA s.c.	20	-	-	-	-	-	-	-	-	μS^5 IFA s.c.	3	0.8	0
227	M	μS^1 CFA s.c.	15	μS^2 IFA s.c.	20	-	-	-	-	-	-	-	-	$1x10^7$ rPECs i.v.	16	4.2	0
230	M	μS^1 CFA s.c.	15	μS^2 IFA s.c.	20	μS^3 IFA s.c.	15	μS^4 IFA s.c.	63	$1x10^7$ rPECs i.v.	28	μS^5 IFA s.c.	49	$4x10^6$ rPECs Delivered intrasplenically	46	12	2

Table 3-1. Immunisations performed to generate MRC OX-102. Each fusion performed in the MRC Cellular Immunology Unit is numbered and this is noted in the first column. The immunised host (H) is indicated in the second column (M=mouse and S=Syrian hamster). Immunisations are indicated as either the number of cells immunised intra-venously (i.v.) or microsome membrane preparation (μS^x) injected sub cutaneously (s.c.) where the superscript number represents the membrane preparation batch (Table 3-2). The columns labelled "d" indicate the number of days the animal was left between successive immunisations and the boost column denotes the nature of the final immunisation delivered four days before the fusion procedure was performed. The number of hybridomas which stained the rat PEC surface in the first part of the fusion screen and the number which blocked the binding of the rat OX-2 coated beads are given in columns "bind" and "block" respectively. The fusion efficiency (FE) is the percentage of total hybridomas generated secreting immunogen specific mAbs. FEs were calculated by assuming a single hybridoma was present in each well (386 wells) and, since this is rarely observed, the FE value is probably an underestimate.

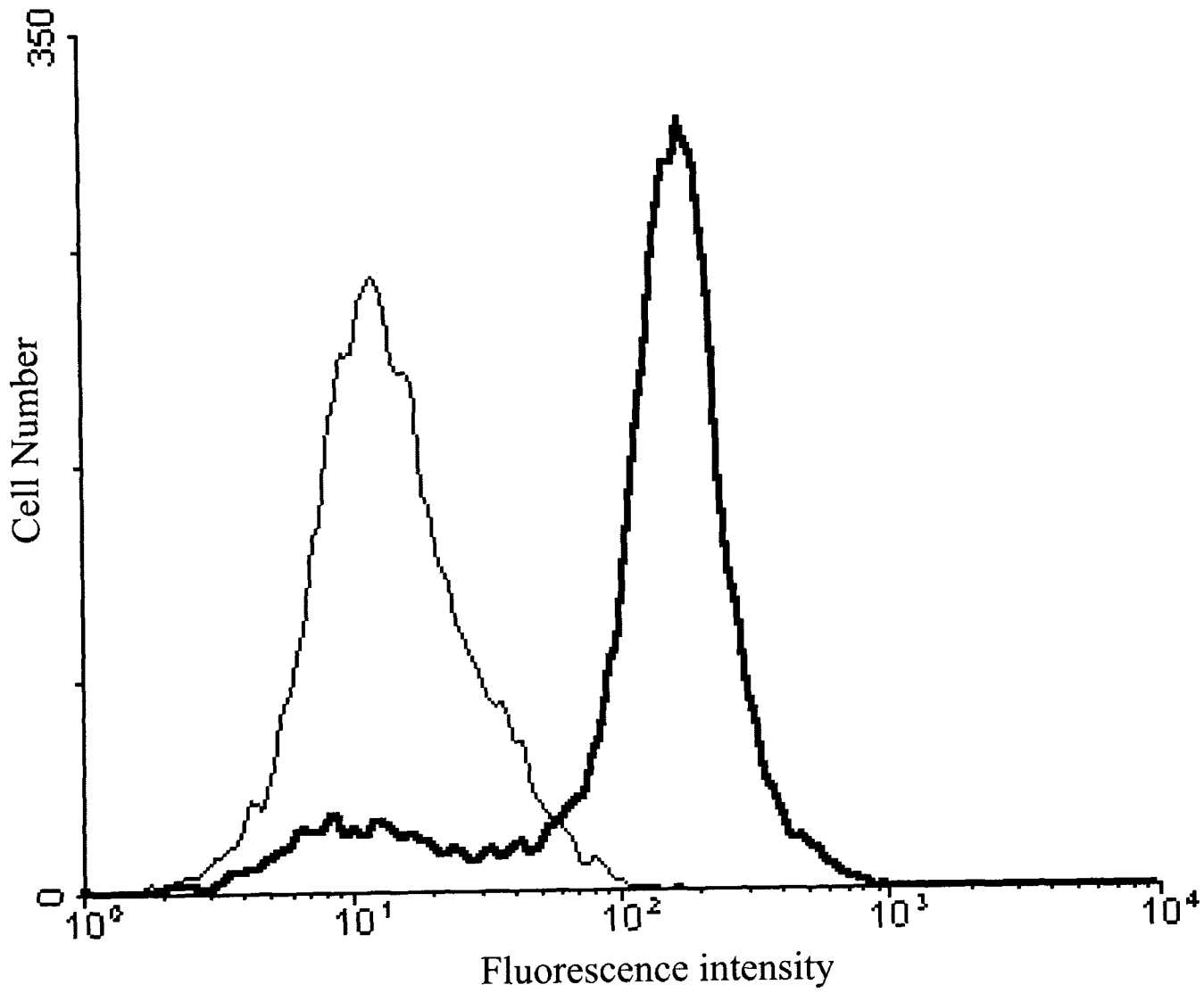

Figure 3-2. rPECs stained with MRC OX-102. Staining of rat PECs with MRC OX-102 (bold) and an isotype matched negative control (MRC OX-21). The MRC OX-102 mAb stained approximately 80% of PECs, a value suggesting that the positive cell type is the macrophage.

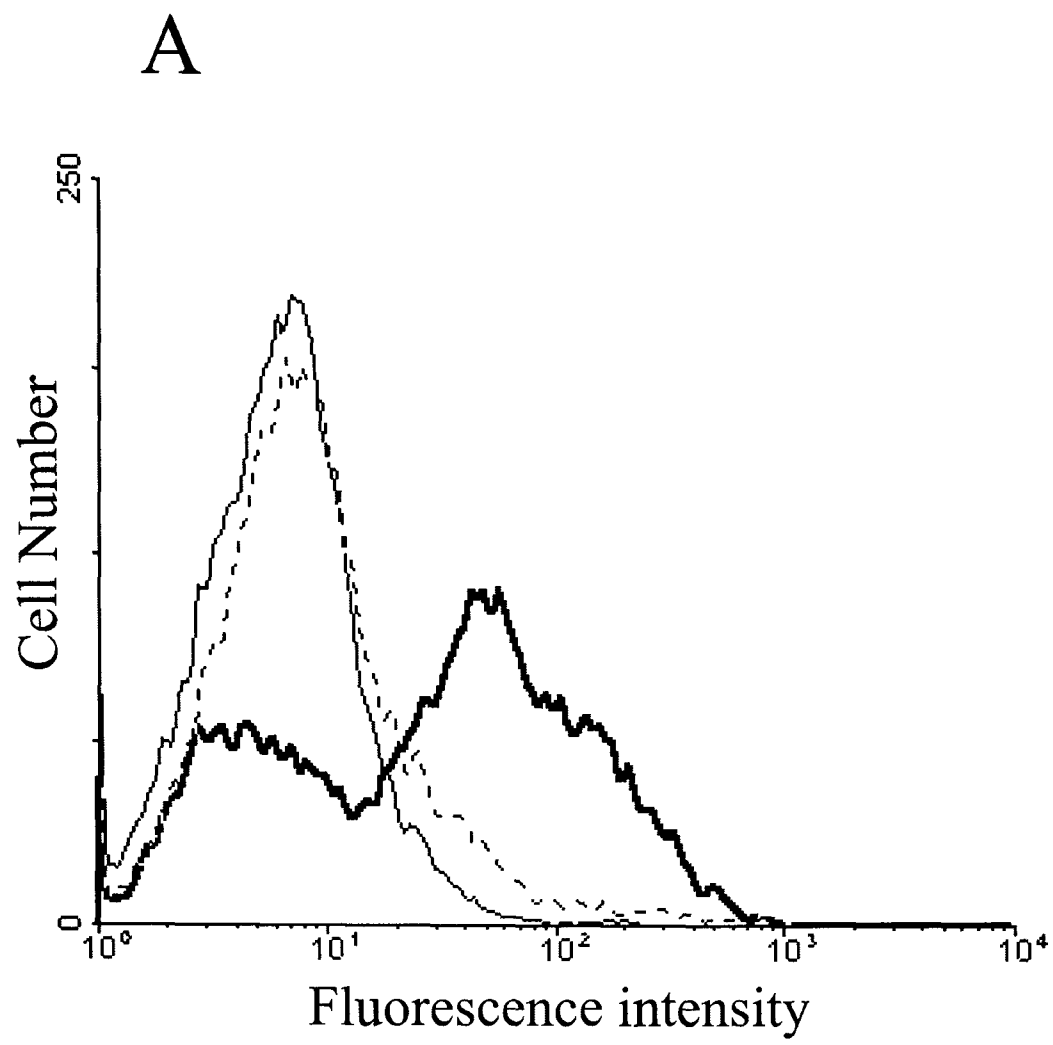

Figure 3-3. MRC OX-102 specifically blocks the OX-2:OX-2 receptor interaction. Rat PECs were pre-incubated with either (A) mAb MRC OX-45 (anti-rat CD48) or (B) mAb MRC OX-102 and tested for their ability to bind either rCD2CD4d3+4 (dotted line) or rOX-2CD4d3+4 (bold line) coated beads. MRC OX-45 allows rOX-2 binding but blocks rCD2, whereas MRC OX-102 specifically blocks the binding of rOX-2 but not rCD2 coated beads. The unbroken lines are CD4d3+4 coated beads (negative control).

3.5 MRC OX-102: isotyping and western blotting

MRC OX-102 was isotyped as a mouse IgG_1 by a red blood cell agglutination assay (data not shown). The antibody detected a broad band of 60 to 100 kDa in western blots of non-reduced whole rat PEC NP-40 lysates (Fig. 3-4). This indicated that the OX-102 antigen (OX-102 Ag) was soluble in the NP-40 detergent and that the MRC OX-102 mAb was probably of high enough affinity to allow useful biochemistry to be performed.

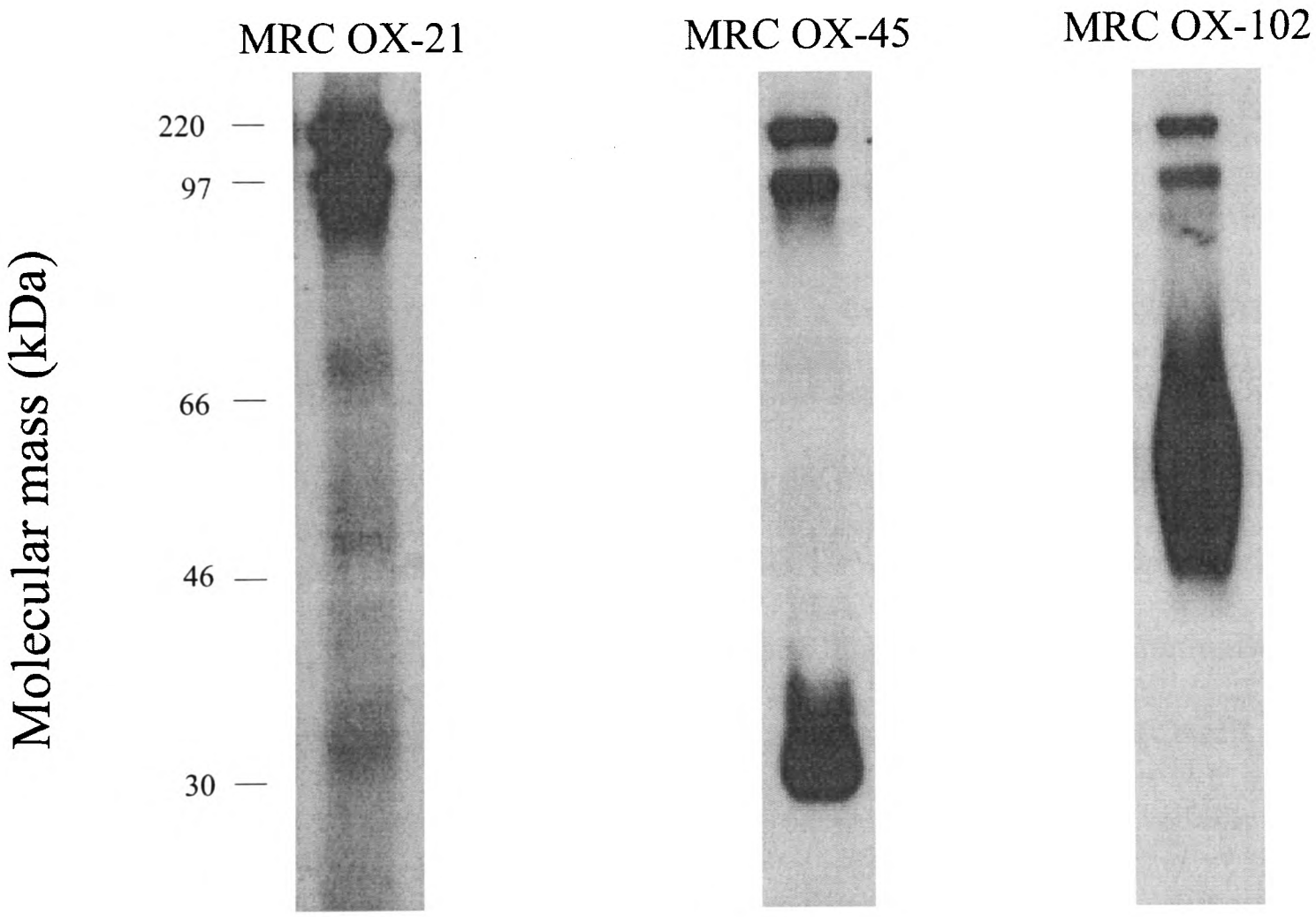

Figure 3-4. MRC OX-102 detects a broad band in western blots. 10^6 rat PECs were solubilised in a 1% NP-40 buffer and resolved under non-reducing conditions on a 7.5% acrylamide gel, transferred to nitrocellulose and probed with three isotype matched mouse mAbs. Notice that MRC OX-102 detects a broad smear, typical of a cell surface glycoprotein, from 60 to 100kDa which was not present in controls or in lysates run under reducing conditions. The positions of non-reduced molecular mass markers (in kDa) are indicated. Controls: MRC OX-21 (negative) MRC OX-45 (positive).

3.6 Discussion

The raising of monoclonal antibodies to cell surface proteins is now a well established technique and one which is in wide use today. However, despite the vast amount of experience, the ability to predict the success and appropriate protocol to raise a mAb of required specificity is limited by our relatively poor understanding of the mammalian immune system. Attempts to quantify and optimise the procedure have revealed the importance of several variables which will be discussed below.

Previous work had eliminated virtually all known mouse anti-rat macrophage mAbs as candidates for blocking the OX-2:OX-2R interaction and these probably represented the most immunogenic pool of antigens (Preston, 1996; Springer, 1981). Therefore, the success of the strategy taken to characterise the OX-2 receptor was dependent on the ability to produce large numbers of rat PEC specific mAbs to a broad range of antigens per fusion. Typically, fusion efficiencies (the ratio of hybridomas secreting immunogen specific mAbs to the total number of hybridomas generated) are in the order of 5 to 20% when using whole cells as the immunogen (Kohler and Shulman, 1978). However, initial attempts (fusions 220 and 223) were significantly lower than this despite the sera from the immunised mice indicating they were developing good immune responses to the rat PEC cell surface. Subsequent attempts to increase fusion efficiencies were based on altering variables known to influence the development of an immune response such as amount and route of antigen delivery and also the chosen immunised host species.

Immunising with membrane preparations of rat PECs delivered sub-cutaneously in adjuvants did increase the fusion efficiency significantly (fusion 225) although the precise immunological reason for this is unknown. Perhaps the disruption of the cellular nature increased its immunogenicity although particulate immunogens such as whole cells are known to be excellent at generating humoral immune responses.

Increasing the phylogenetic distance between the host and immunogen should lead to an increase in potentially immunogenic epitopes since the number of amino acid differences between homologous proteins in these species also increases. Proteins expressed in the nervous system are generally more highly conserved then those expressed in the immune system (G.J.W. unpublished observation) and it was thus a concern (since OX-2 itself was highly expressed in the nervous system, suggesting that the OX-2 receptor might have a similar distribution) that the OX-2 receptor would be highly conserved between rats and mice and therefore be poorly immunogenic. This was of particular relevance since rat OX-2 was known to interact with the mouse OX-2 receptor suggesting the binding face of these two molecules was indeed conserved. This poor immunogenicity of protein:protein binding sites had been previously reported in attempts to generate rat mAbs to mouse ALCAM with the ability to block the binding of CD6, all of which were unsuccessful, despite immunising with large quantities of purified protein (Bowen et al., 1997).

Hamsters, (family *cricetidae*) belong to a separate evolutionary family to rats and mice (subfamily *murinae*, family *muridae*) and thus rats are evolutionary less related to hamsters than to mice (Kumar and Hedges, 1998). This suggests that hamsters would generate a more diverse humoral response to most rat derived immunogens than mice. However, the ability to form stable hybridomas with the mouse NS-1 cell line varies greatly between species and attempts with rabbit, frog, gerbil, bovine and human lymphocytes usually fail, presumably due to the preferential loss of non-mouse chromosomes during hybridoma formation (Kohler and Shulman, 1978). There are two species of hamster, the Armenian (*Cricetulus migratorius*) and Syrian (*Mesocricetus auratus*) which do have the ability to form stable hybridomas with mouse cell lines and the former species are reported to fuse with a two fold greater efficiency (Sanchez-Madrid et al., 1983). The low fusion

efficiency of fusion 226 could possibly be attributed to the inherent instability of the hamster:mouse hybridoma caused by subtle species differences.

The final successful fusion differed by delivering the final boost of whole cells directly into the spleen and had the desired effect of increasing the fusion efficiency. However, the benefit of this procedure cannot be assessed due to the different number and types of immunisations the mouse used in fusion 230 received. It is possible that this immunisation protocol, due to the amount, site or nature of antigen delivery invoked an immune response to a broader range of epitopes since one might have expected, from statistical reasons, that fusion 225 should have yielded at least one blocking mAb.

It was important to show that the ability of MRC OX-102 to block the binding of OX-2 coated beads was specific for the OX-2:OX-2R interaction and did not influence other interactions (using reagents produced in an identical way) thereby excluding the possibility that the blocking effect was an artefact of the binding assay. MRC OX-102 did not influence any other interaction and thus presumably recognises the binding face of the OX-2 receptor at the cell surface. Isotyping revealed that MRC OX-102 was an IgG_1 and was therefore likely to have a relatively higher affinity for the OX-2 receptor than the MRC OX-88 (IgM) mAb and would probably be suitable for use in either expression cloning or biochemical characterisation.

The mAb recognised a broad and characteristic smear on non-reduced but not reduced western blots of whole rat PEC lysates suggesting that it was a cell surface protein with a large number of different glycoforms and that the epitope was dependent on the tertiary structure of the protein stabilised by one or more disulphide bonds. It was hoped to determine at this stage if the OX-102 antigen was a single or multiple polypeptide chain molecule by analysing the MRC OX-102 immunoprecipitates from biotinylated rPEC lysates but the results of these experiments were inconclusive.

Chapter Four

Purification and biochemical analysis of the OX-102 antigen

4.1 Introduction

The initial strategy to characterise the OX-102 antigen (OX-102 Ag) using the MRC OX-102 mAb was to use the technique of expression cloning which has proved to be both a quick and reliable method of cloning eukaryotic cell surface antigens (Seed and Aruffo, 1987; Simmons, 1993) and has the advantage that all cloned antigens are functionally expressed and usually of full length. The MRC OX-102 mAb was shown to stain IFN-γ stimulated alveolar rat macrophages (section 8.2) for which an expression library was available (Simmons, 1993). However, repeated attempts failed to show any encouraging results and so a biochemical approach was adopted, since N-terminal sequence from purified antigen would immediately identify the protein if it had been previously characterised or provide peptide sequence to enable cloning the protein from cDNA. In summary, this chapter describes the use of purified MRC OX-102 mAb immobilised on Sepharose beads to purify the OX-102 Ag from rat splenic lysates. The dissociation characteristics of the MRC OX-102 mAb:Ag complex were determined and found to be very unusual, requiring a 15 minute incubation at 55°C in 0.5% SDS to elute. Biochemical analysis subsequently showed that the OX-102 Ag was unusually highly glycosylated and N-terminal sequence obtained from the purified protein by Edman degradation showed no matches with any known protein in protein sequence databases. An outline of the strategy and experiments performed in this chapter are shown schematically in Figure 4-1.

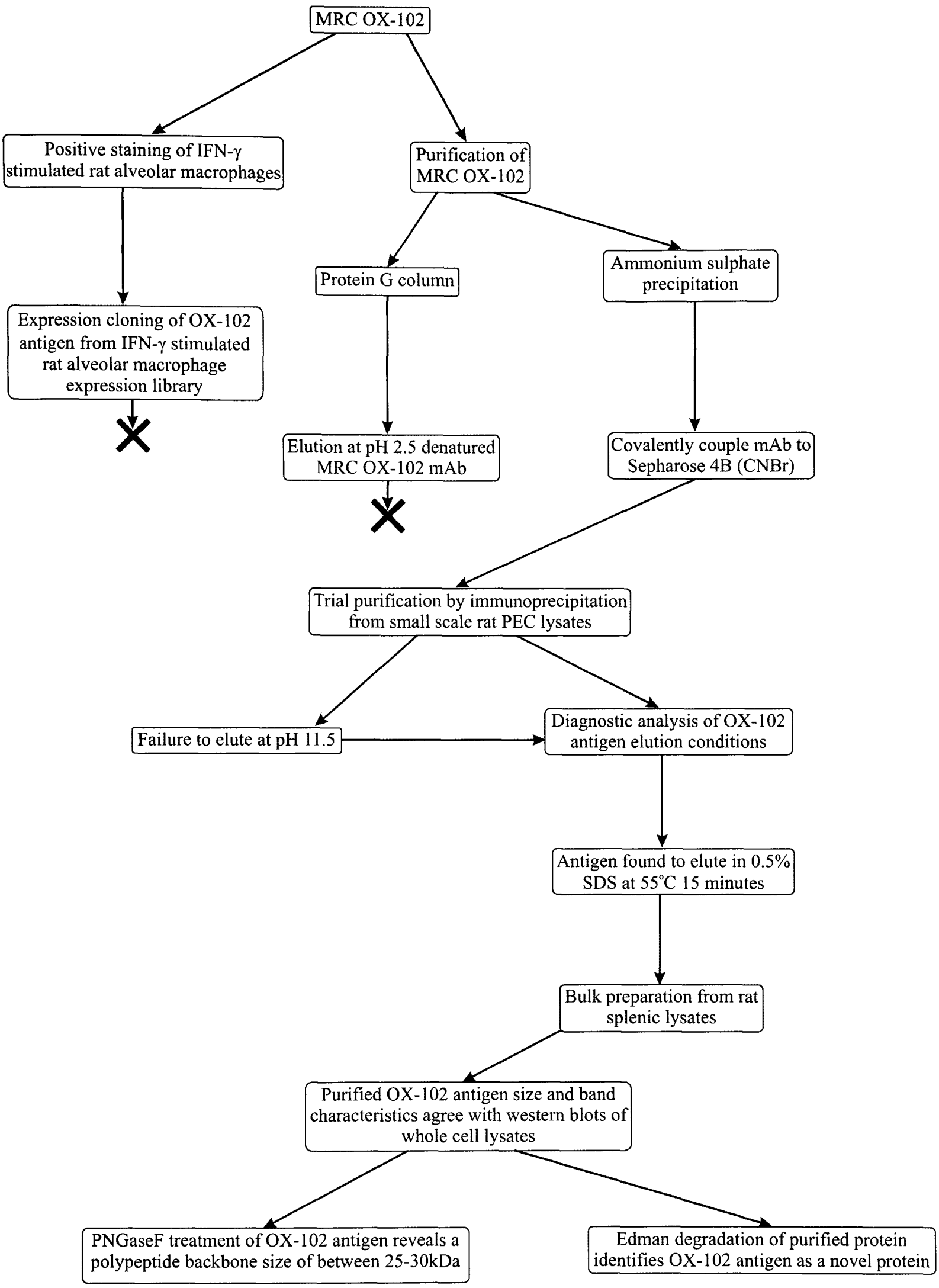

Figure 4-1. Flow diagram illustrating the strategies undertaken and results obtained and described in chapter 4.

4.2 Purification of the OX-102Ag

Purification of a protein restricted to a minority cell type is a challenging task since large amounts of biological material yield only small amounts of purified protein. However, the potent ability of the MRC OX-102 mAb to recognise antigen on western blots enabled nanograms of protein to be detected within complex mixtures aiding the purification procedure. Experience has shown that solubilisation and subsequent purification of membrane proteins is efficient in the deoxycholate detergent. The advantages of this detergent are a small micelle size enabling the removal of the detergent by dialysis and its ability to solubilise virtually all known membrane proteins (Williams and Barclay, 1986).

4.2.1 Purification of MRC OX-102 monoclonal antibody

In order to purify the OX-102 Ag, the MRC OX-102 mAb had to be purified to covalently attach it to a solid phase. Standard purification methods using protein G and elution at pH 2.5 were attempted but yielded inactive antibody. It was thought that elution of the mAb at this low pH led to the denaturation of the antibody. The mAb was subsequently purified by salting out using ammonium sulphate which produced antigenically active mAb (data not shown). Testing of the purified mAb revealed that it was able to maintain its antigenic activity after incubations at pH 11.5 (data not shown). The purified mAb was coupled to Sepharose 4B using the CNBr method for use in purification procedures.

4.2.2 Solubilisation of the OX-102 Antigen

Before purification, the OX-102 Ag had to be efficiently solubilised. A small scale diagnostic experiment was performed as outlined in Figure 4-2.

A crude Tween 40 membrane preparation from rat PECs was initially performed to separate the nuclei from the rest of the cellular components in an identical way used to prepare membrane microsomes used for immunisation in the raising of MRC OX-102. This crude preparation was then solubilised in deoxycholate (DOC) and insoluble material removed by centrifugation at 50000xg. Comparison of lanes E and F (Fig. 4-2) shows that all the OX-102 Ag remains in the DOC solubilised fraction. It was therefore clear that the OX-102 Ag was soluble in the DOC detergent.

4.2.3 Dissociation conditions for the OX-102 Ag:mAb complex

The deoxycholate solubilised rat PEC membrane glycoproteins (total volume 1ml) were passed over a 0.5ml MRC OX-102 column three times, washed, and eluted in 0.05M diethylamine:HCl pH 11.5 in nine 200µl fractions and neutralised directly in glycine. Western blotting (data not shown) revealed that the MRC OX-102 column had removed all OX102 Ag activity from the lysate and that remarkably, none of the eluted fractions contained OX-102 Ag activity. However, antigenic activity remained associated with the beads in the column suggesting that the OX-102 Ag was binding to the column but not eluting at pH 11.5 (data not shown).

This was confirmed by performing small scale immunoprecipitations of DOC solubilised rPEC antigens and assessing the elution conditions (Fig. 4-3) which showed that incubation at pH 11.5 did not remove OX-102 Ag from the MRC OX-102 Sepharose.

A larger scale purification of OX-102 Ag was attempted from 100 rat spleens but modified by eluting in 0.5% SDS and is shown in Figure 4-4.

Elution of antigen at pH 11.5 resulted in a small pulse of antigen being removed (fractions 3 to 7) which leaches into the wash buffer. However, elution at 0.5% SDS showed that more protein could be eluted at harsher conditions. It was thought that since the protein was still being eluted after 10 column volumes of 0.5% SDS a large proportion of the protein would still be left on the column. The 300µl column was resuspended in 0.5ml 0.5% SDS and stood at 4°C for 20mins before the supernatant was removed, pooled with fractions 4 to 15 and concentrated to 40µl. The rest of the MRC OX-102 Sepharose beads were incubated in a further 0.5ml 0.5% SDS, heated at 55°C for 15 minutes with agitation, removed and concentrated to 50µl. 5µl of each were resolved by SDS-PAGE (Fig. 4-5). The material eluted at 55°C in 0.5% SDS contained the characteristic broad smear at around 60 to 100kDa in agreement with western blots of whole cell lysates. Further purifications of the OX-102 Ag involved 0.1% SDS washes and pelleting of the MRC OX-102 Sepharose by centrifugation rather than the use of a column and is documented in section 2.4.2.1 of Materials and Methods.

Figure 4-2. The OX-102 antigen is soluble in deoxycholate. A small scale diagnostic purification from rat PECs was performed as shown and aliquots removed as indicated (**A** to **F**). These aliquots were resolved under non-reducing conditions and then subjected to western blotting with MRC OX-102 and an isotype matched negative control (MRC OX-21). The approximate cell equivalents (assuming 100% solubilisation efficiency) loaded in each lane are shown unless this is not applicable (N/A). The results show that the OX-102 antigen is present in both the Tween 40 crude membrane preparation and the deoxycholate solubilised fraction.

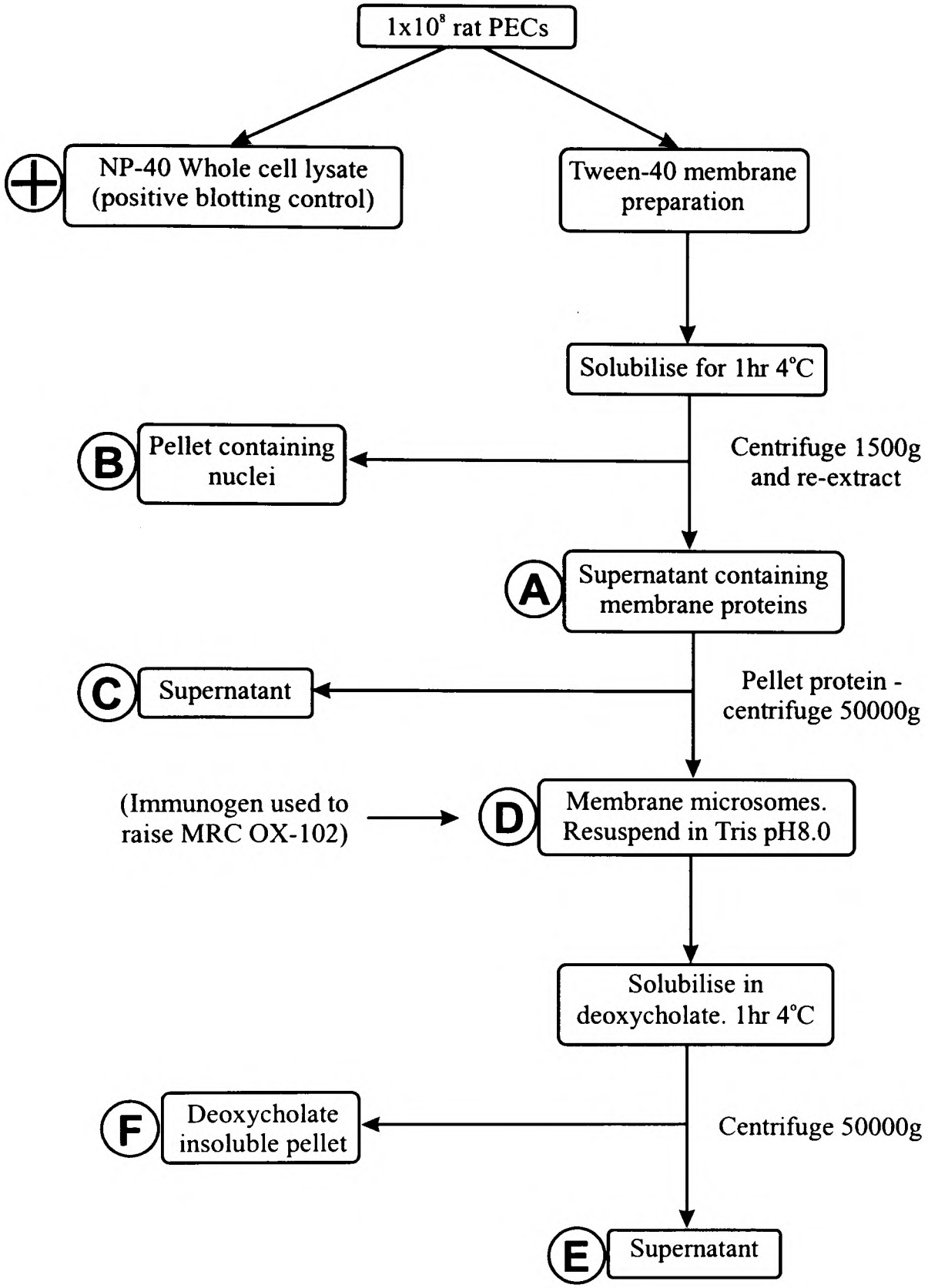
1x10^8 rat PECs
NP-40 Whole cell lysate (positive blotting control)
Tween-40 membrane preparation
Solubilise for 1hr 4°C
B
Pellet containing nuclei
Centrifuge 1500g and re-extract
A
Supernatant containing membrane proteins
C
Supernatant
Pellet protein - centrifuge 50000g
(Immunogen used to raise MRC OX-102)
D
Membrane microsomes. Resuspend in Tris pH8.0
Solubilise in deoxycholate. 1hr 4°C
F
Deoxycholate insoluble pellet
Centrifuge 50000g
E
Supernatant

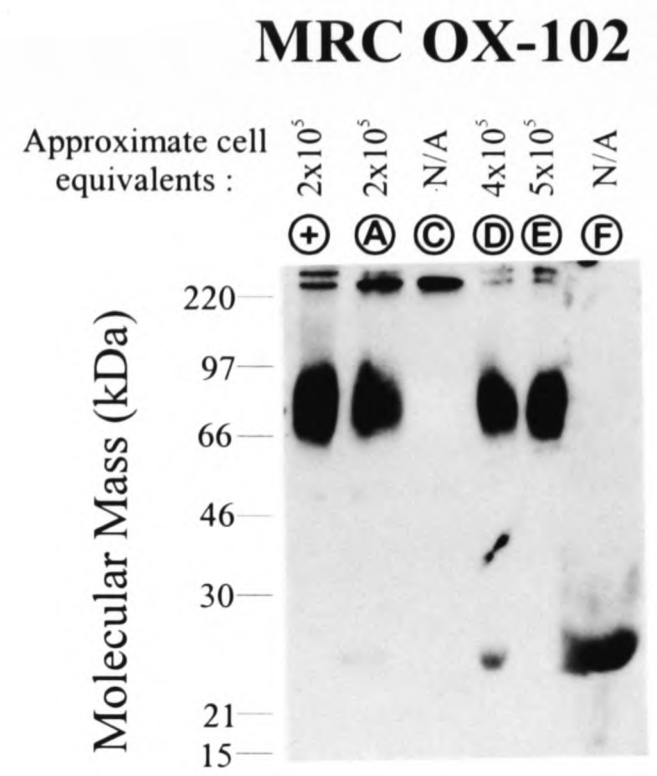
MRC OX-102
Approximate cell equivalents :
2x10^5
2x10^5
N/A
4x10^5
5x10^5
N/A
+ A C D E F
Molecular Mass (kDa)
220
97
66
46
30
21
15

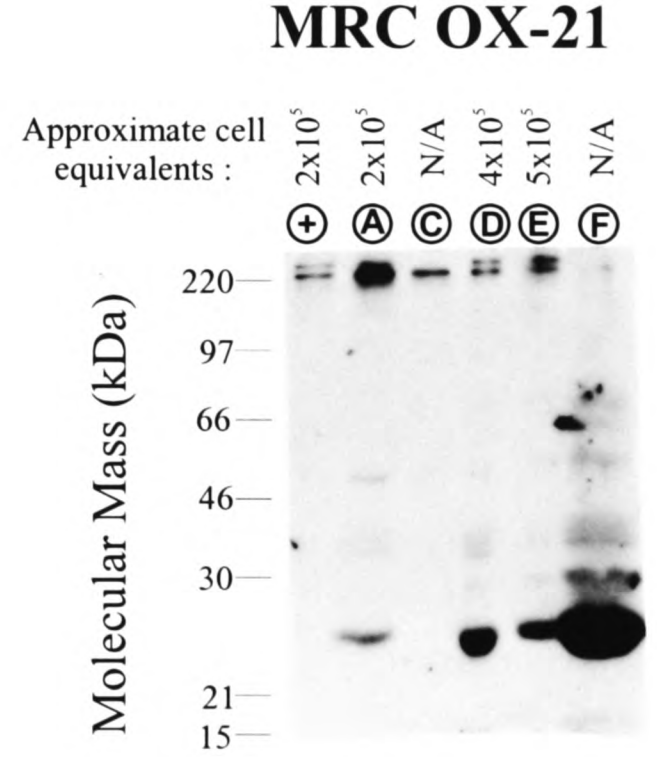
MRC OX-21
Approximate cell equivalents :
2x10^5
2x10^5
N/A
4x10^5
5x10^5
N/A
+ A C D E F
Molecular Mass (kDa)
220
97
66
46
30
21
15

Figure 4-3. The MRC OX-102mAb:Ag complex resists elution at pH 11.5. OX-102 Ag was purified by immunoprecipitation from deoxycholate solubilised rat PEC membrane proteins (**E**). The MRC OX-102 mAb:Ag complex was either eluted by boiling (**G**) or eluted at pH 11.5 (**H**) and then removing any remaining antigen by boiling (**I**). The strong double band present at 50kDa and the band at 25kDa and to a lesser extent bands at 150, 125, 100kDa present in both the query and control blot lanes are degraded fragments of the MRC OX-102 mAb which have been removed from the Sepharose beads present in that sample due to boiling before loading. These bands are detected due to the use of an anti-mouse peroxidase conjugated secondary antibody in the western blot and as controls, an equivalent amount of MRC OX-102 coupled Sepharose beads were boiled and also blotted (**Bds**).

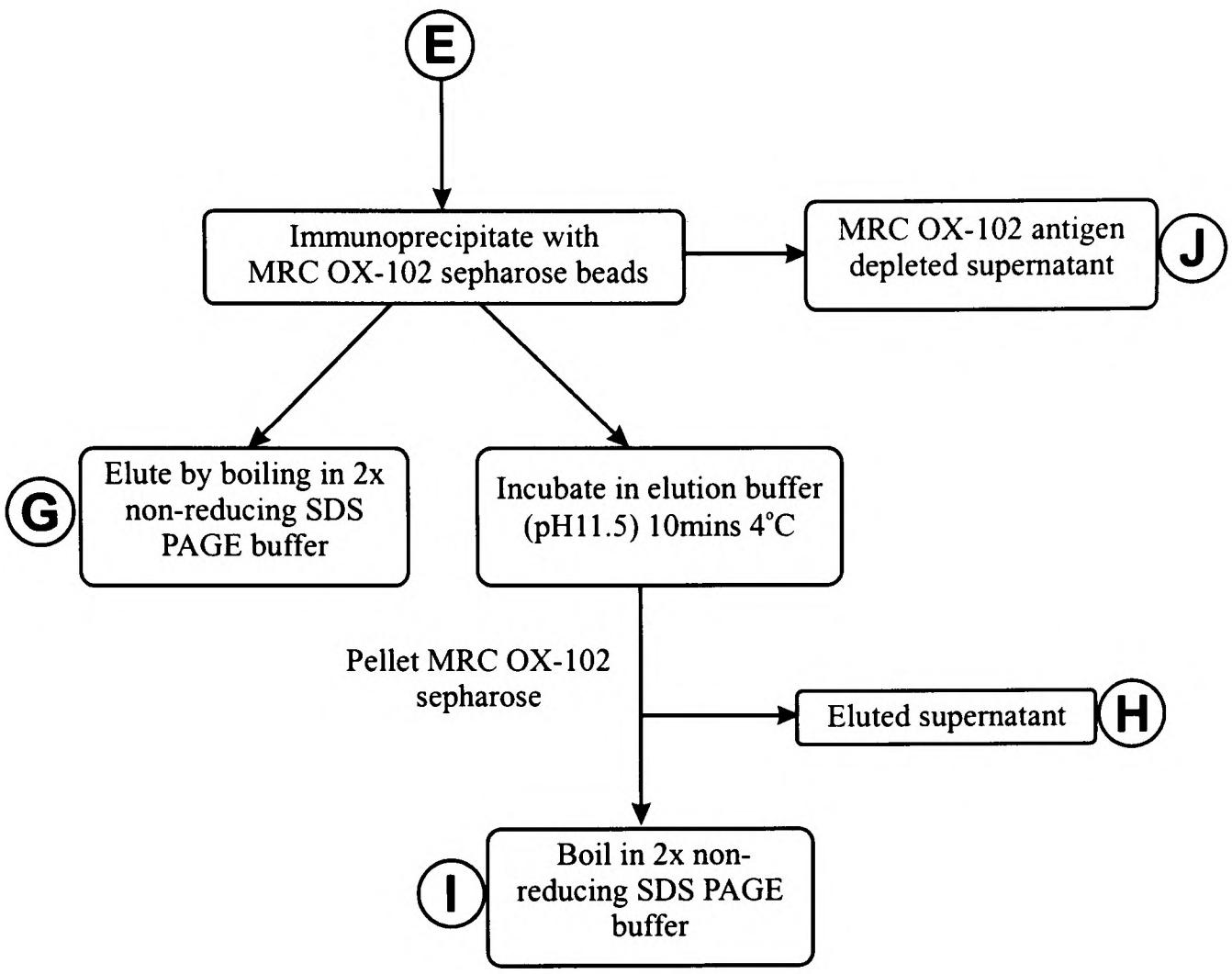
E
Immunoprecipitate with MRC OX-102 sepharose beads
MRC OX-102 antigen depleted supernatant
J
G
Elute by boiling in 2x non-reducing SDS PAGE buffer
Incubate in elution buffer (pH11.5) 10mins 4°C
Pellet MRC OX-102 sepharose
Eluted supernatant
H
I
Boil in 2x non-reducing SDS PAGE buffer

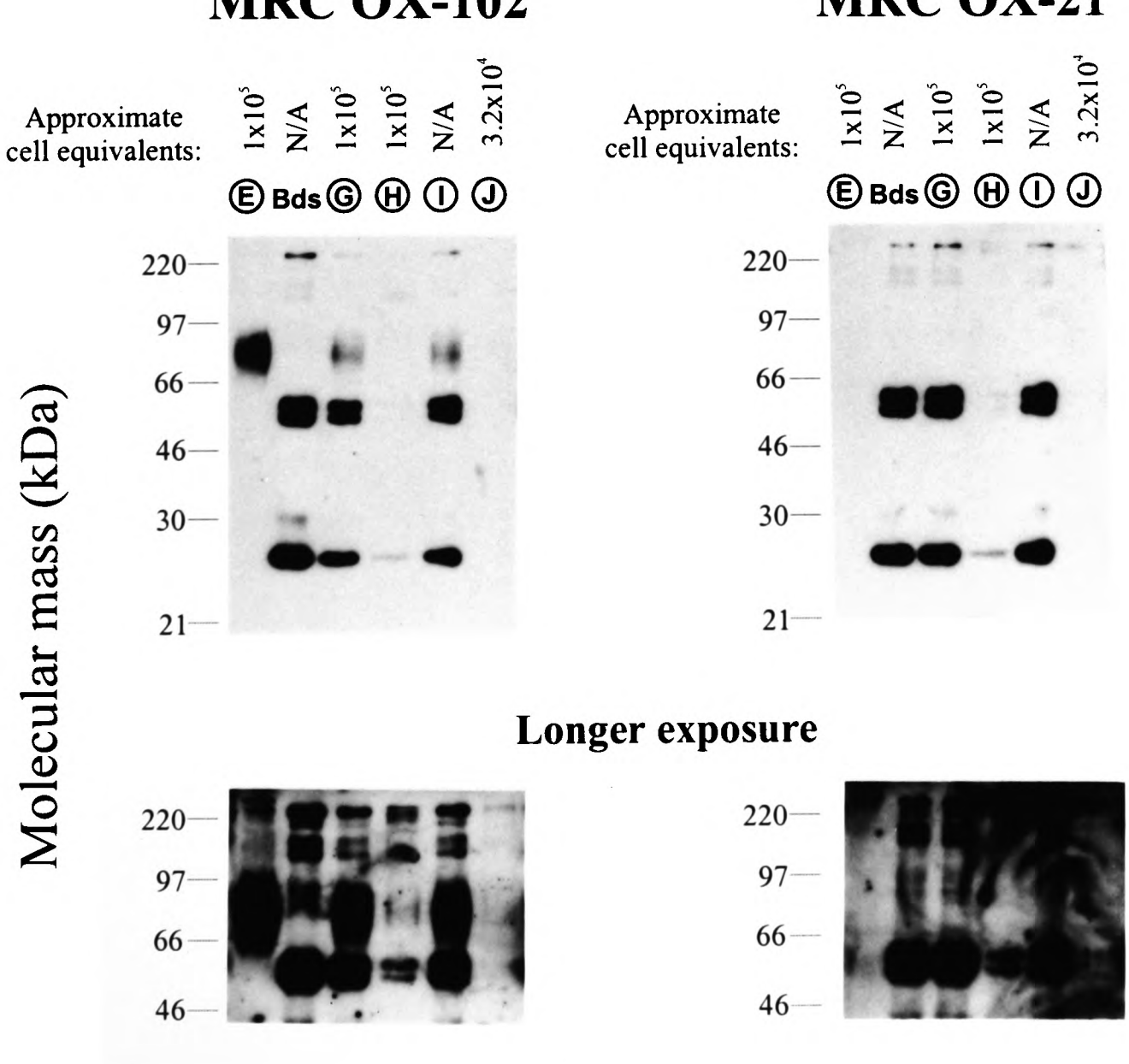
MRC OX-102
MRC OX-21
Approximate cell equivalents:
1x10^5
N/A
1x10^5
1x10^5
N/A
3.2x10^4
E Bds G H I J
Molecular mass (kDa)
220
97
66
46
30
21
Longer exposure

Figure 4-4. The MRC OX-102 mAb:Ag complex elutes using 0.5% SDS. OX-102 antigen was purified by immunoprecipitation from a bulk rat spleen membrane preparation using MRC OX-102 coupled Sepharose. The Sepharose was recovered from the lysate and packed into a small (300µl) column. The column was then washed as shown (steps 1 to 3) and then eluted using initially 0.5% DOC 0.05M diethylamine:HCl pH 11.5, then washed and then re-eluted in 0.5% SDS. 200µl fractions were collected during elution and 5µl of each fraction resolved under non-reducing conditions and western blotted with MRC OX-102 and an isotype matched negative control (MRC OX-21). The results show that elution at pH 11.5 led to a pulse of antigen which leached into the wash (fractions 3 to 7) but 0.5% SDS eluted far more protein (fractions 14 to 25). However, even 10 column volumes (CVs) of 0.5% SDS were not sufficient to remove all the bound antigen since the antigen is still being eluted in fraction 25. The bands present at 50 and 25kDa which are particularly visible in the control blot are the heavy and light chain (respectively) of the MRC OX-102mAb and are detected due to the reasons discussed in the Figure 4-3 legend.

100 Deoxycholate solubilised rat spleen membranes (250 mls)

350µl MRC OX-102 sepharose

Rotate 35 hours at 4°C

Pellet sepharose (1500g 10mins) and make a 300µl column

(One column volume (1CV) is 300µl)

1. Wash 5CV 0.5% DOC in Tris pH 8.0
2. Wash 5CV 0.5% DOC in 0.15M NaCl Tris pH 8.0
3. Wash 5CV 0.5% DOC in Tris pH 8.0

Start collecting 200µl fractions:

4. **Wash 2CV 0.5% DOC 0.05M diethylamine:HCl pH 11.5**
   (Fraction No.s 1 to 3 were neutralised with 20µl 2M glycine)
5. **Wash 5CV 0.5% DOC in Tris pH 8.0** *(Fraction No.s 4 to 10)*
6. **Elute 10CV 0.5% SDS in dH_2O** *(Fraction No.s 11 to 25)*

MRC OX-102

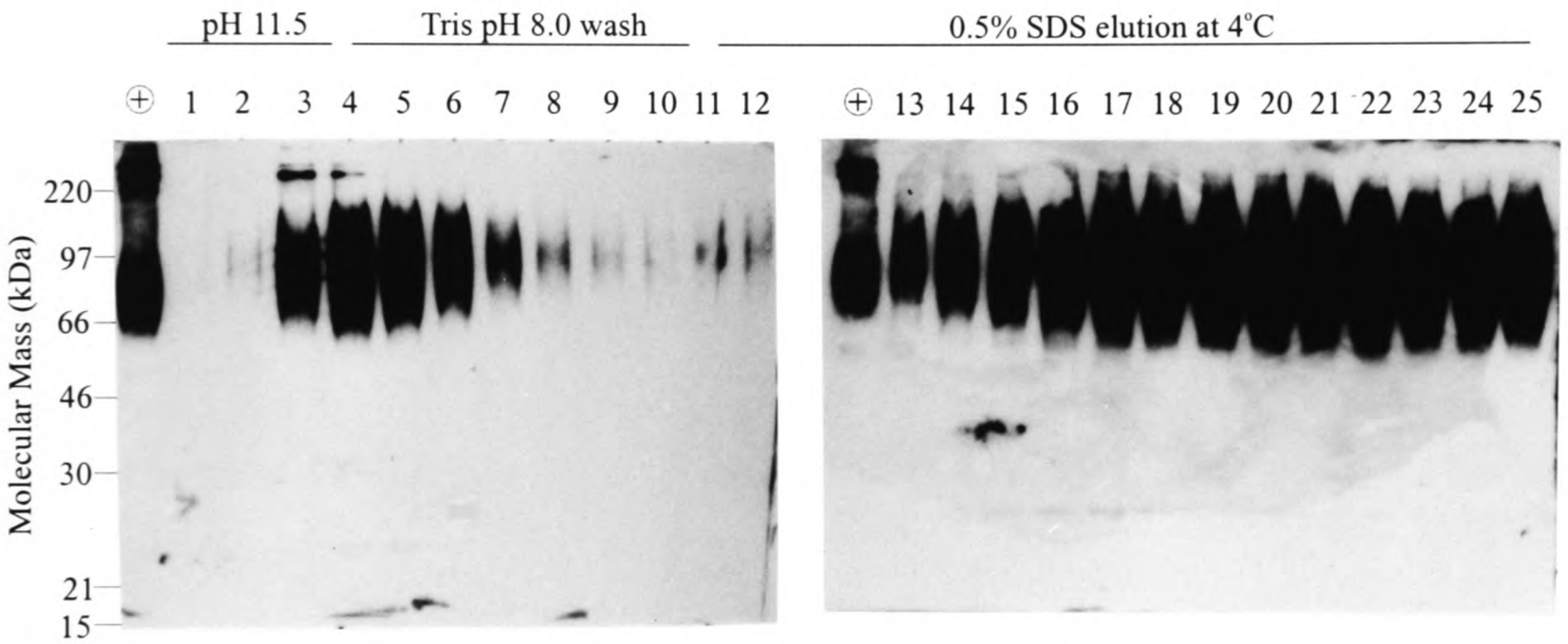

MRC OX-21

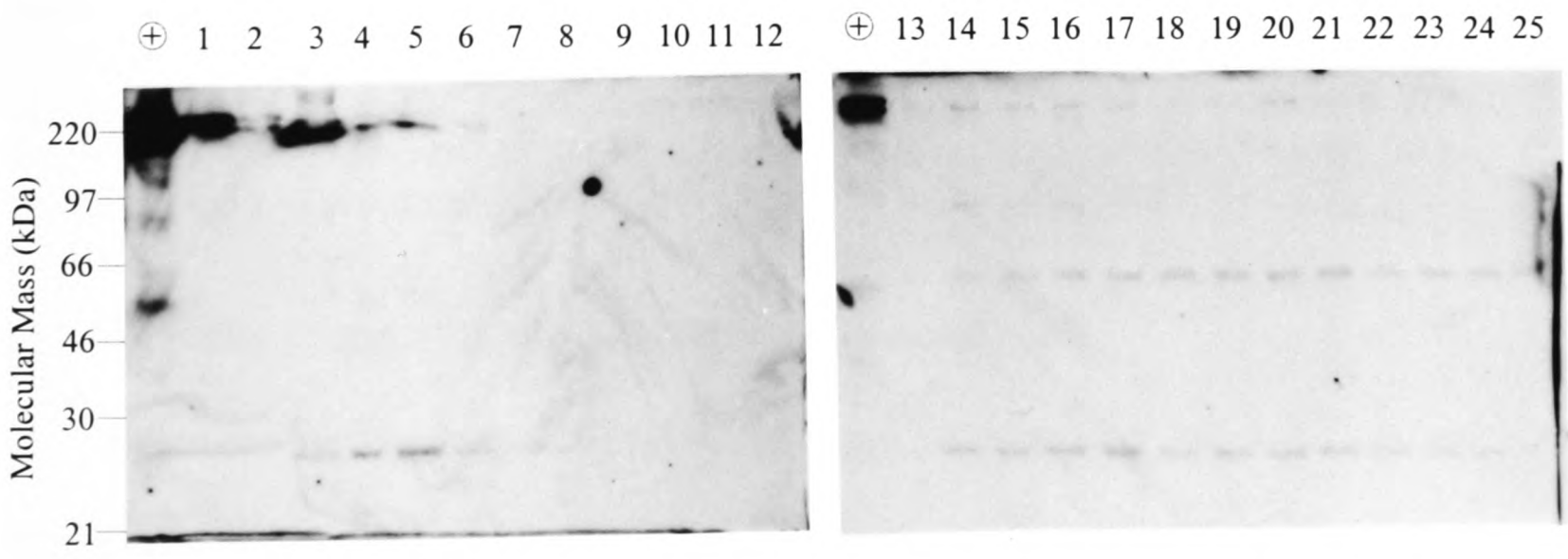

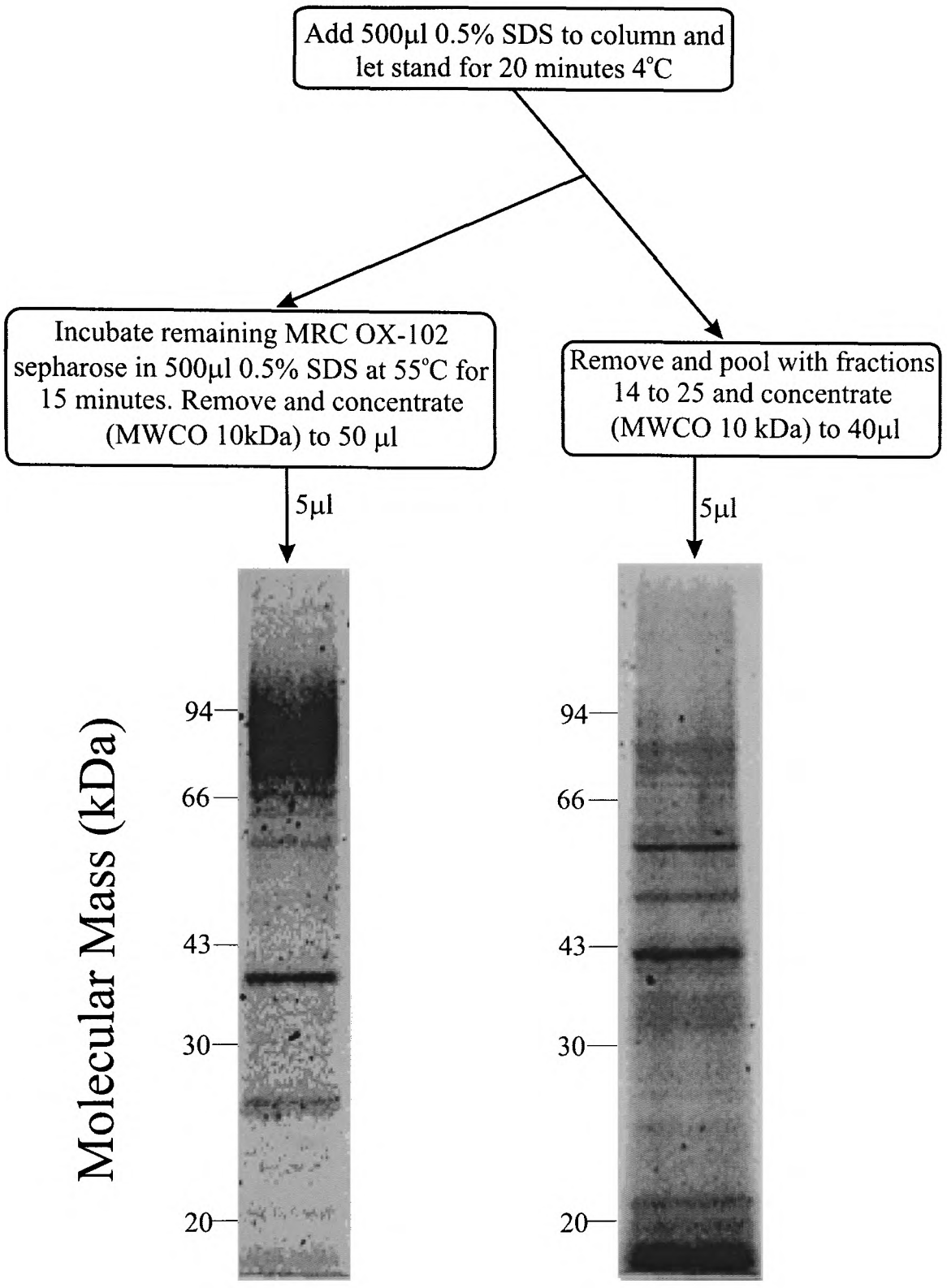

Figure 4-5. The OX-102 antigen is eluted at 55°C in 0.5% SDS. The column used in Figure 4-4 was further eluted using 0.5% SDS at 4°C, pooled with fractions 14 to 25 and concentrated to 40µl and a 5µl aliquot resolved under reducing conditions by SDS-PAGE (right gel track). Any remaining antigen was removed by a 15 minute incubation in 0.5% SDS at 55°C before concentrating to 50µl and a 5µl aliquot resolved as above (left gel track). Proteins were visualised using the SYPRO® orange fluorescent dye stain.

4.3 The size of the OX-102 antigen protein backbone

Both western blots of whole cell lysates and purified protein on SDS-PAGE showed that the OX-102 Ag ran as a characteristic broad smear ranging from 60-100kDa centred around 80kDa. This implied that a major component of the protein was carbohydrate and

that many different glycoforms might exist at the cell surface. N-linked carbohydrate moieties can be enzymatically removed from the protein polypeptide chain by treatment of the glycoprotein with PNGaseF. Incubation of the OX-102 Ag with PNGaseF reduced the mass of the OX-102 Ag to two major bands of ~23 and 25kDa and a minor band of ~21kDa as shown in Figure 4-6. This implied that 70 to 80% of the protein's mass was removed by PNGaseF treatment, and would need around 20 N-linked glycosylation sites on a 25kDa protein (assuming each N-linked glycan contributed an average of 3kDa of mass) to account for the protein's size. However, the size of highly glycosylated proteins cannot be reliably obtained by using SDS-PAGE, particularly under non-reducing conditions, and this is perhaps a more likely explanation for this observation.

Figure 4-6. Deglycosylation of OX-102 antigen reduces its apparent mass to approximately 25kDa. Purified OX-102 Ag was incubated with PNGaseF for the durations indicated, resolved under non-reducing conditions by SDS-PAGE, blotted onto nitrocellulose and probed with MRC OX-102 mAb or isotype matched negative control (MRC OX-21). Purified MRC OX-102 mAb was also deglycosylated as a control and could be detected directly by the anti-mouse peroxidase conjugated secondary.

Substrate	OX-102 antigen					MRC OX-102 mAb			None
PNGaseF	✗	✓	✓	✓	✓	✓	✓	✗	✓
Time	N/A	0	10m	1h	16h	0	16h	N/A	N/A

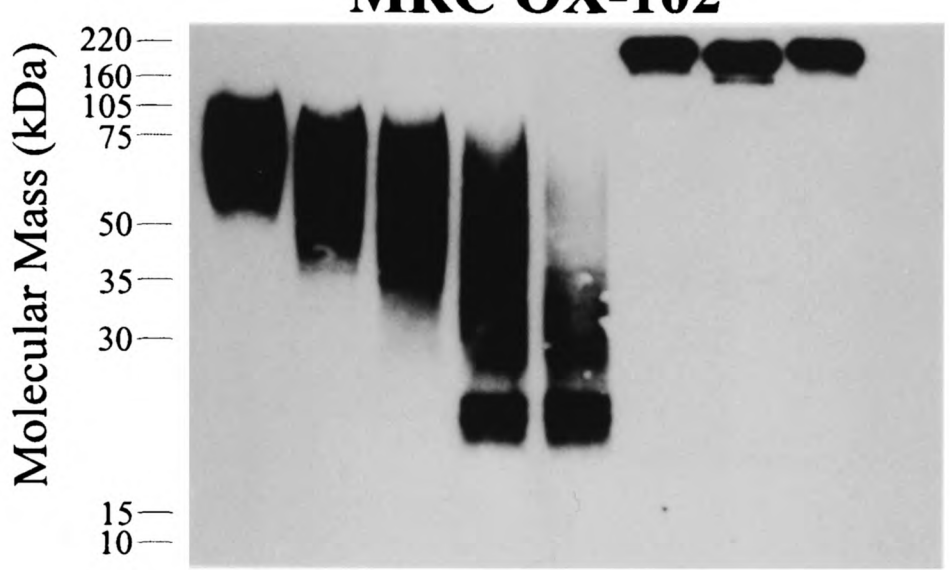

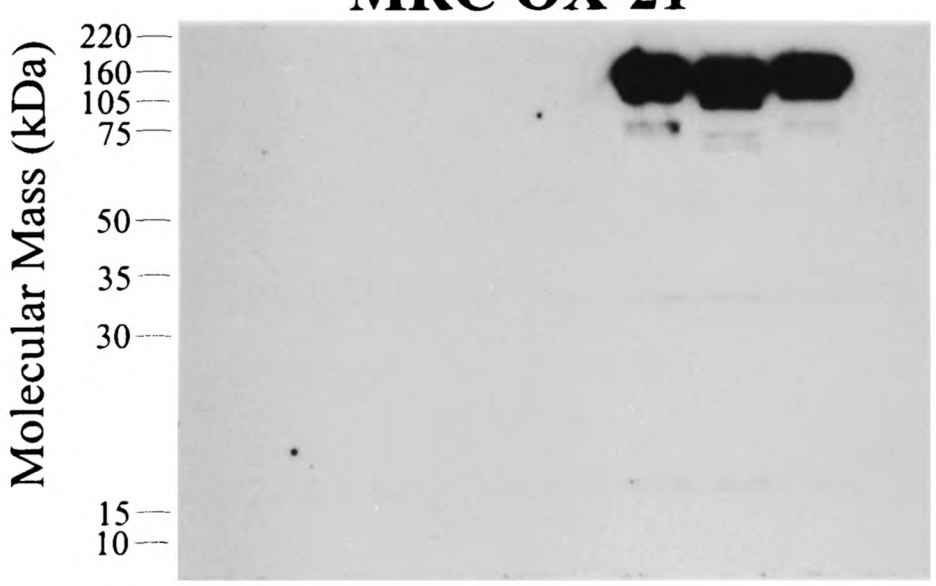

4.4 Protein sequencing of OX-102 Ag and contaminants

Five independent batches of OX-102 Ag were prepared as described in Materials and Methods for protein sequencing and all had the following characteristics: (a typical batch is shown in Fig. 4-7)

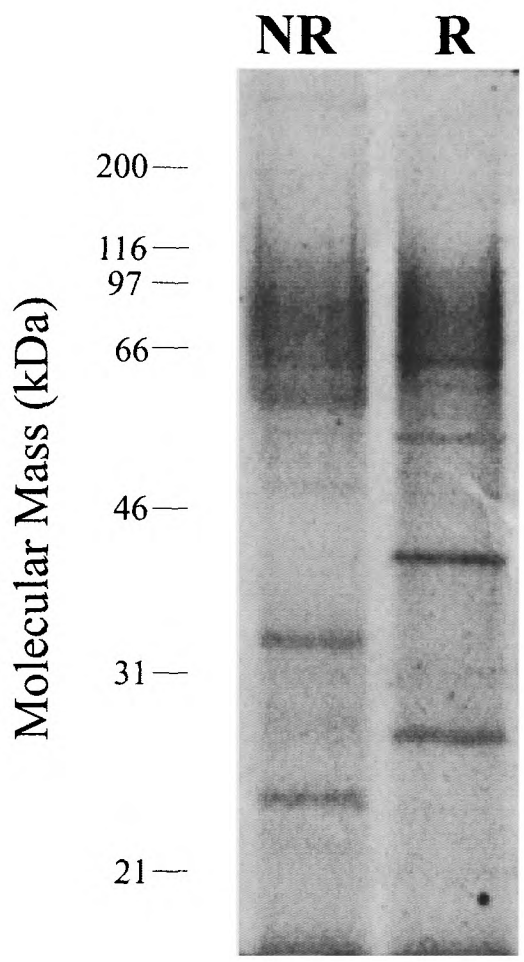

Figure 4-7. Purified OX-102 antigen. OX-102 antigen was purified from deoxycholate solubilised crude rat spleen Tween-40 membrane preparations by immunoprecipitation and further resolved under either reducing (R) and non-reducing (NR) conditions by SDS-PAGE and visualised using SYPRO® orange fluorescent dye stain.

1) A characteristic smear 50 to 100kDa which was completely removed by PNGase treatment indicating no major unglycosylated contaminants are present within this size range.
2) Presence of a band at 35kDa (non-reducing) which shifted to 40kDa upon reduction.

Both the 50 to 100kDa smear and the 40kDa band were subjected to 20 cycles of Edman degradation. This was performed by A. Willis at the MRC Immunochemistry Unit.

The smear produced good sequence whereas the 40kDa produced no sequence, possibly because the N-terminus did not contain a free amino group. The sequence obtained from the 50 to 100 kDa smear was: SCPDK_QTMQ_NSSTMTEVV. The blank cycles are assumed to be asparagine since they conform to N-linked glycosylation sequons and indicated that it was likely to be a membrane protein as was expected. Glycan modified asparagines are not detected by Edman degradation because the phenylthiohydantoin derivative produced from this cycle has a high and variable mass and thus cannot be identified by chromatography in the usual manner. However, it was observed that the asparagine signal at this position increased a little at both sites indicating some glycoforms were not modified at this site. The presence of two N-linked glycosylation sites so early in the protein were consistent with the observation that N-linked carbohydrate was a major feature of this protein. In addition, an asparagine is present in the sequence which conforms to an N-linked glycosylation sequon but, due to its proximity to a modified asparagine, is prevented from being glycosylated. Finally, screening of databases of known proteins yielded no matches indicating that this was a novel protein. Screening of EST databases with conceptual codons also yielded no significant matches.

4.5 Discussion

The purification of the OX-102 antigen by immunoaffinity chromatography /immunoprecipitation revealed that the MRC OX-102 mAb:antigen complex was unusually stable. The complex was able to withstand washes at pH 11.5 and 0.1% SDS and only poor elution was achieved with 0.5% SDS at 4°C. The antigen was finally eluted by heating to 55°C in 0.5% SDS. These characteristics have not been observed before in any other documented mAb indicating that the MRC OX-102 mAb:Ag interaction is highly unusual.

In five independent purifications, a band of 35kDa which migrated slower (40kDa) upon reduction indicated that it was likely to be a disulphide containing protein which is a feature of extracellular proteins. In addition, the size of this protein was not altered by an incubation with PNGaseF (data not shown). Several attempts were made to tryptically digest the band and obtain sequence from the resulting peptides but all failed (A. Willis -personal communication). The possibility that this band might be a protein associated with the 60 to 100kDa protein at the cell surface or simply a major contaminant is currently unclear. However, the association must be relatively stable since it is able to withstand washes with 0.5% SDS.

PNGaseF treatment of purified OX102 Ag suggested that 70 to 80% of the mass of the protein was asparagine-linked carbohydrate. This is an unprecedented amount of N-linked carbohydrate since the most highly glycosylated extracellular proteins known are the CEA antigens (CD66) which have ~60% of their mass contributed by N-linked carbohydrate (Benchimol et al., 1989). The amount of N-linked carbohydrate associated with the OX-102 antigen might not be quite so high since the MRC OX-102 mAb only bound non-reduced (globular) protein and therefore the size of the deglycosylated protein as visualised by western blot might be an underestimate. In addition, this calculation assumes an average mass of 3kDa for the average N-linked glycan which may also be an underestimate since the presence of poly-N-acetyllactosamines (which are known to decorate cell surface glycoproteins expressed by cells of myeloid origin (Rabinowitz and Gordon, 1991)) can be two to three times this mass (section 1.4.3). Another possibility is that the carbohydrate is O-linked which would not be removed by PNGaseF treatment. Nevertheless, N-linked carbohydrate moieties are clearly a major feature of this protein and might explain the failures to biotinylate and immunoprecipitate the molecule from the cell surface.

It is noteworthy that the PNGaseF treated protein was resolved as two major bands of approximately 23 and 25 kDa and a minor band of ~21kDa. These three bands could represent either incompletely deglycosylated glycoforms of the protein or distinct polypeptide chains containing the MRC OX-102 mAb epitope. Incomplete removal of N-linked glycans seems unlikely since these bands are roughly equally represented in aliquots removed after 1 hour and one taken after an overnight (16 hour) incubation, assuming that all N-linked glycans can be removed by the deglycosylating enzyme. However, because the OX-102 Ag was treated in its native, unreduced state it is feasible that all N-linked glycans could *not* be removed (due to steric considerations) and that the two bands represent different glycoforms present at a protected site or sites. An alternative suggestion is that the OX-102 Ag exists as at least two different polypeptide forms differing in approximately 2 kDa or ~20 amino acids. Cell surface proteins which exist as different forms have been widely reported and are generally due to alternative splicing. Alternative splicing has been shown to alter the addition of amino acids in the extracellular region (CD44 (Lesley et al., 1993), CD45 (Thomas, 1989)), the intracellular region (CD46 (Maisner et al., 1996) and several integrins CD29, CD49f, CD104 (Barclay et al., 1997)) and also altering the method of attachment to the membrane (CD58 (Dustin and Springer, 1991)). It is therefore feasible that the OX-102 antigen could be expressed as at least two discrete forms at the surface of a particular cell type or types present in the rat spleen. The answers to these questions might be answered once the gene encoding the OX-102 Ag has been cloned.

Chapter Five

Cloning of the OX-102 antigen

5.1 Introduction

The absence of any known protein matching the N-terminal sequence of the purified OX-102 antigen meant that the corresponding gene had to be cloned to allow further characterisation. Several attempts were made to obtain more peptide sequence from tryptic digests of the purified protein to aid cloning, but all these attempts failed. This failure was attributed to the fact that only small amounts of protein were obtained from large quantities of biological material and possibly the high level of variable glycosylation prevented the generation of homogenous molecular mass peptide fractions. Therefore, the N-terminal 20 amino acids were used to design degenerate oligonucleotides which corresponded to conceptual codons of the peptide sequence for use in cloning procedures (Fig. 5-1). Initial attempts to screen nitrocellulose filters representing a rat macrophage library by hybridisation of a radioactively labelled degenerate oligonucleotide failed and efforts were therefore directed into a PCR based approach. The first experiments employed a 3'RACE strategy using a degenerate (sense) oligonucleotide to amplify the cDNA. However, the observed products of the 3'RACE PCR were highly heterogeneous in both size and sequence (data not known) and this, coupled with the fact that the expected product size was between 2 to 3 kbp (close to the upper limit for conventional PCR) meant that this strategy met with little success. Therefore, a new 5'RACE PCR strategy was attempted using an antisense degenerate oligonucleotide to generate a much shorter PCR product consisting of the 5' end of the OX-102 Ag mRNA. In summary, this chapter describes the successful use of both 5' and 3' RACE PCR techniques to obtain the full length OX-102 antigen cDNA. The translation of the cDNA predicted a type I membrane glycoprotein belonging to the immunoglobulin superfamily and contained two IgSF domains in a V-C2 arrangement and thus is structurally similar to OX-2 itself. Furthermore, it had sequence similarities with OX-2 over and above those expected within the superfamily suggesting that the two proteins are

closely related in evolutionary history. It also contained a substantial (67 amino acid) cytoplasmic region which contained no known signalling motifs. A mouse homologue of the receptor was also cloned by a nested 3'RACE strategy. The experimental strategies and results described in this chapter are depicted schematically in Figure 5-1.

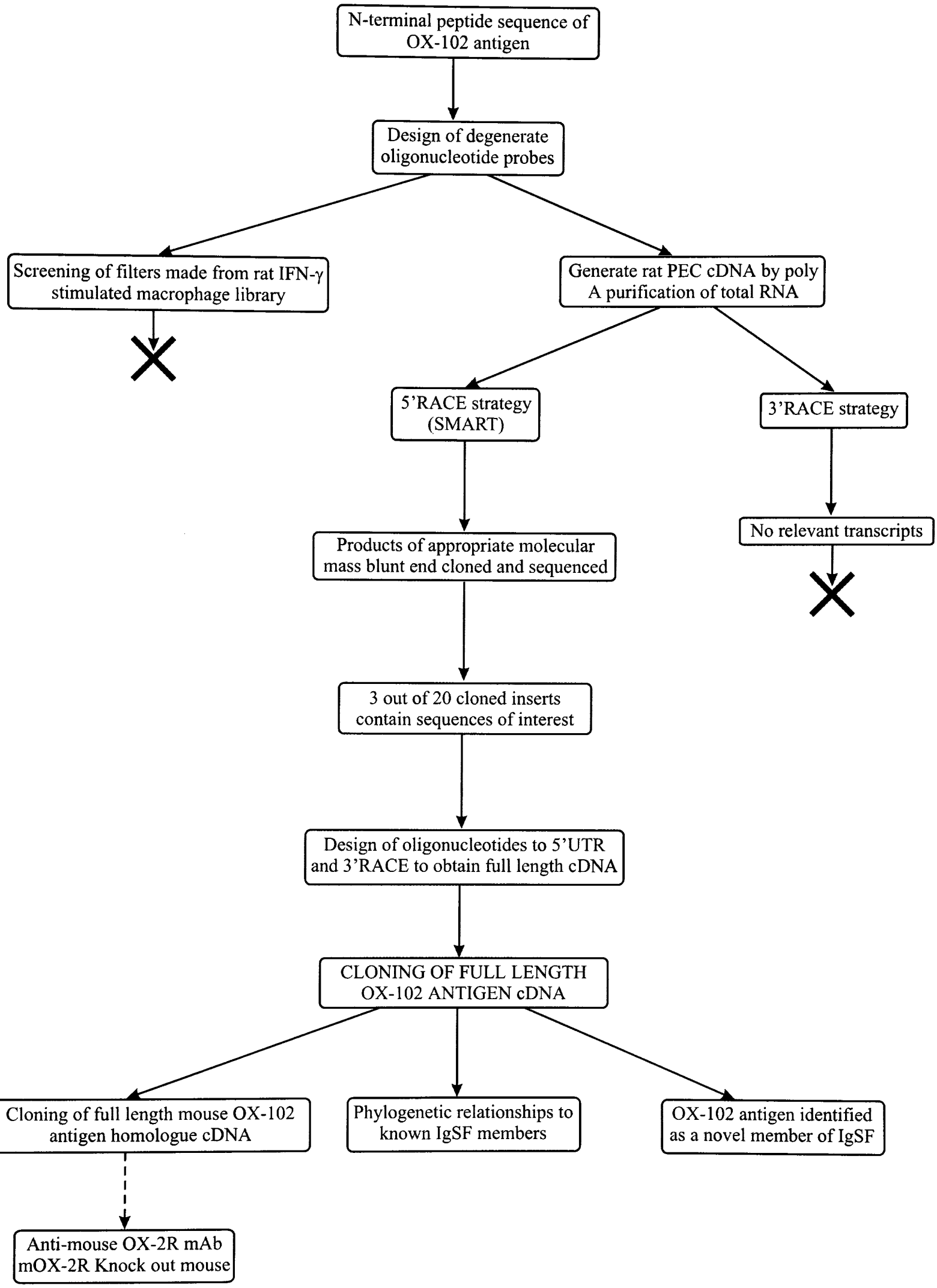

Figure 5-1. An outline of the strategies taken and results obtained from the experiments described in chapter 5.

5.2 Cloning of the OX-102 antigen using a 5'RACE strategy

The 5' end of the OX-102 Ag cDNA was amplified by 5'RACE PCR. This was made possible by the modification of a new technique developed by Clontech known as SMART™ (Switching Mechanism At the 5' end of the RNA Transcript). The use of this technique and RACE procedures are described in Figure 5-2. Briefly, this involves tagging cDNAs produced in a standard reverse transcription reaction at both the 3' and the 5' end. The cDNA is tagged at the 3' end by priming the reverse transcriptase using oligonucleotide 1520 (Table 2-1) which contains a known 20 residue sequence followed by a stretch of 20 deoxythymidylate residues which anneals to the polyA tail of the mRNA. 1520 is anchored to the very start of the poly-A tail by ending the poly-T stretch with any other nucleotide residue except T (A, C or G = V) and therefore prevents 3'RACE products containing variable lengths of the polyA tail. Once the reverse transcriptase reaches the 5' end of the mRNA it pauses and the enzymes intrinsic terminal transferase activity adds a few additional nucleotides, primarily deoxycytidylate 5'-triphosphates, to the 3' end of the cDNA. The SMART™ oligonucleotide (1503) which contains three deoxyguanylate residues at its 3' end, hybridises with the non template deoxycytidine nucleotides and thereby creates an extended template. The reverse transcriptase is able to switch templates and adds a complementary copy of the 1503 oligonucleotide to the 5' end of the cDNA and thus creates a "tag" at the 5' end of the cDNA. Both 5' and 3' RACE PCR can then be performed by using an oligonucleotide complementary to the 5' (1501) or 3' (1536) tag and a gene specific antisense or sense oligonucleotide respectively. Control experiments using both rat β-actin and rat CD48 exact match antisense oligonucleotides indicated that the technique was working (data not shown).

5.2.1 Antisense degenerate oligonucleotide design

All possible codons corresponding to the 20 N-terminal peptide residues and two degenerate oligonucleotides that were used are shown in Figure 5-3.

It was quite likely that the products of a RACE reaction using degenerate oligonucleotides would be heterogeneous and the product of interest may only comprise a small percentage of the total products observed. In order to achieve a high level of cloning efficiency to enable the cloning of rare PCR products, the oligonucleotides used in the reaction were chemically 5'phosphorylated at synthesis. Products were blunt end ligated into a SmaI cut and phosphatase treated PCRScript vector which gave very low background transformation levels.

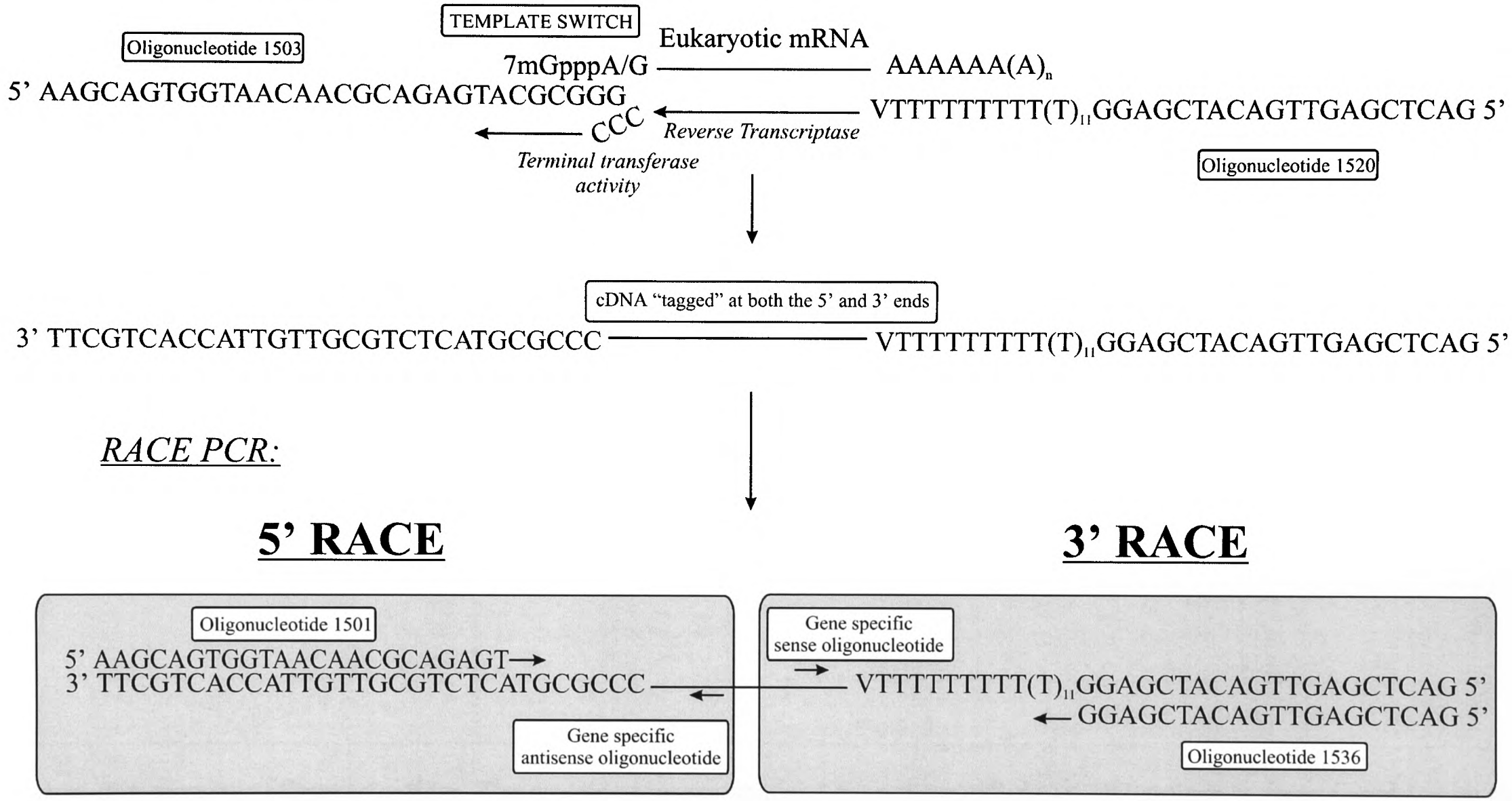

Figure 5-2. Generation of cDNA tagged at the 5' and 3' ends and its use in RACE PCR. A typical eukaryotic mRNA containing both a 5' methylated cap and a polyadenylated tail is shown being transcribed into cDNA containing "tags" at both the 3' and 5' ends as described in the main text (section 5.2).

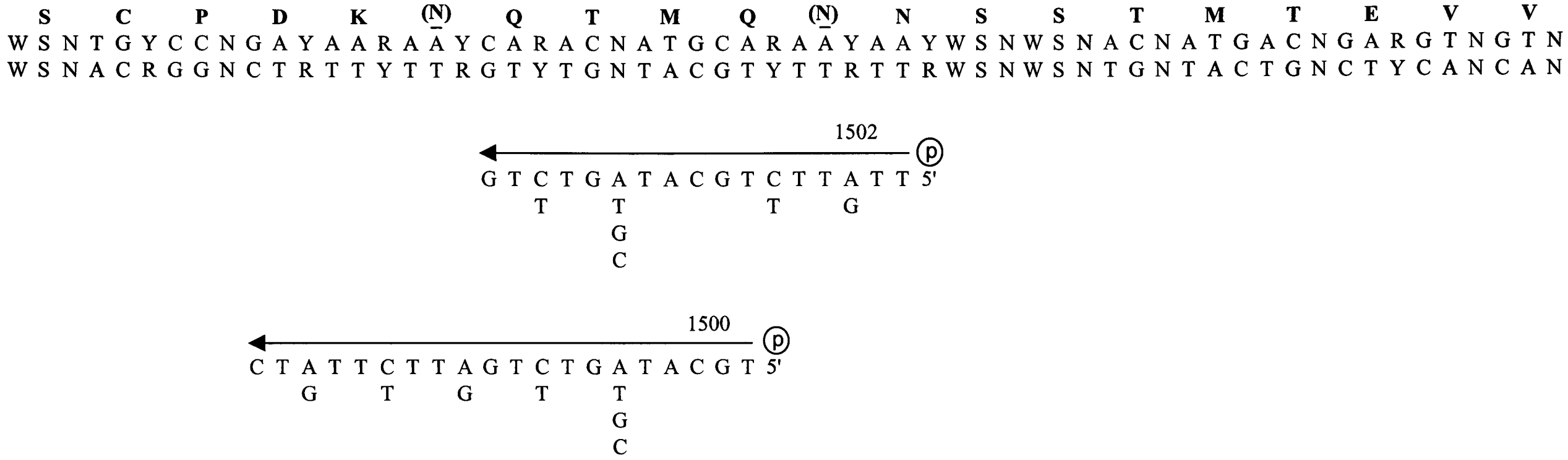

Figure 5-3. Design of degenerate oligonucleotides. The protein sequence obtained from the purified OX-102 antigen is given in bold (with the blank cycles assumed to be asparagine). All the possible codons for each amino acid are given underneath using the standard convention where W=A or T, S=G or C, R=A or G, Y=C or T and N= A,G,C or T. Two antisense oligonucleotides, 1500 and 1502 are shown. Both oligonucleotides are 20 residues long and have a 64-fold degeneracy and each oligonucleotide was chemically 5' phosphorylated at synthesis to aid cloning.

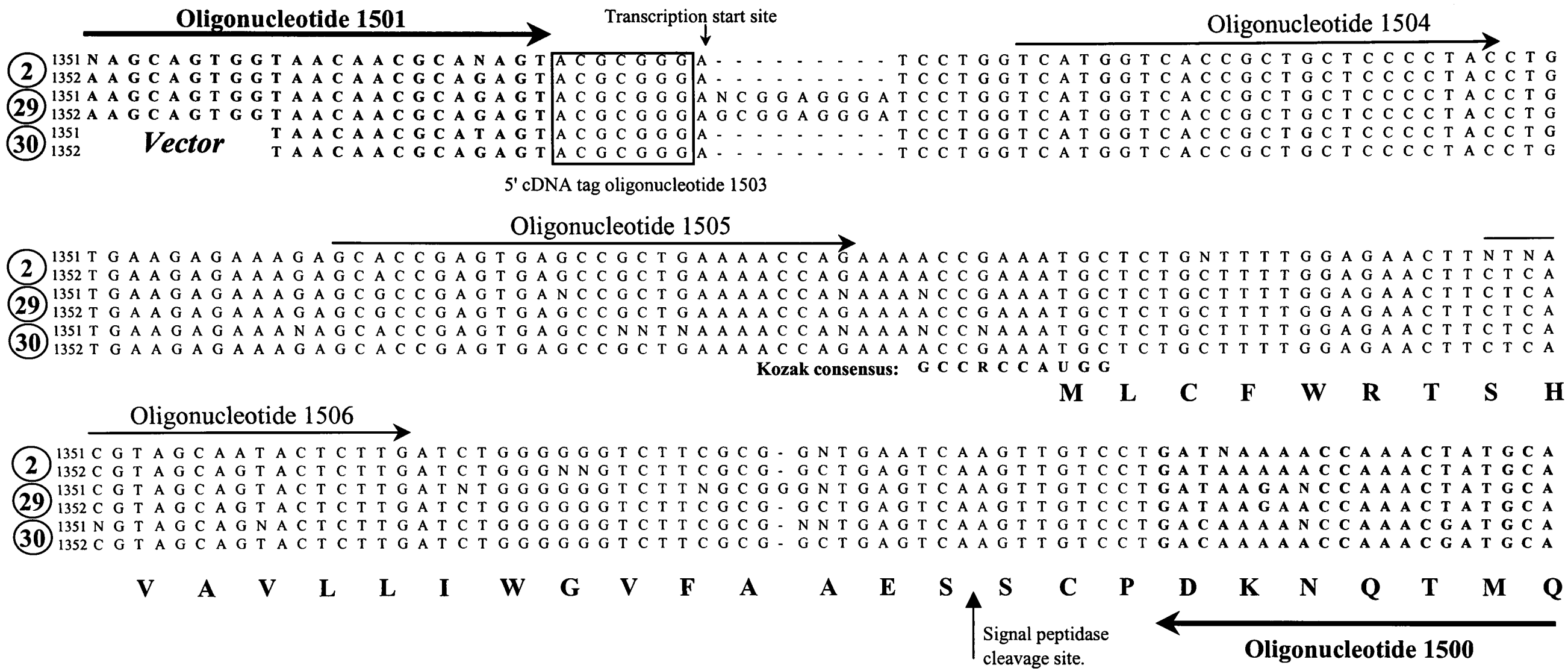

Figure 5-6. The sequences and features of the cloned inserts of interest. Inserts from colonies 2, 29 and 30 were sequenced on both strands using oligonucleotides 1351 and 1352 as shown. The degenerate oligonucleotide (1500) and 5' RACE oligonucleotide (1501) are indicted in bold and the rest of the SMART™ oligonucleotide (1503) which tagged the 5' end of the cDNA transcript is boxed. The inserts have been translated using the reading frame taken from the design of oligonucleotide 1500 and reveals the SCP sequence and a 23 amino acid leader sequence. The regions used to generate the exact match oligonucleotides for 3'RACE (1504, 1505 and 1506) have been indicated as have the predicted start site for transcription and the site of signal peptidase cleavage. The Kozak translation initiation consensus sequence is also shown.

5.2.2 5'RACE PCR

The optimal annealing temperature of the gene specific oligonucleotide within a degenerate mix is difficult to predict since the template is unknown. The use of a Stratagene Robocycler® enabled eight different annealing temperatures to be tested in the same PCR. The size of the expected product was estimated by comparison to mRNAs of other type I cell surface glycoproteins.

5'UTR	~ 100bp
5'RACE oligonucleotides	30bp
Degenerate oligonucleotide	20bp
Leader (20 to 30 amino acids)	60-90bp
Expected size of 5'RACE PCR product:	200-250bp

Products of this size were observed in the low annealing temperatures (44°C +/- 2°C) using the 1500 degenerate oligonucleotide (Fig. 5-4). These products were excised, purified, and ligated into vector. 37 out of 100 transformants were screened for both the presence and size of inserts by colony PCR (Fig. 5-5). 20 colonies were picked because they contained inserts of variable size and were amplified, plasmids purified and sequenced on both strands using vector specific oligonucleotides. Sequence analysis of these twenty clones identified three colonies containing almost identical sequences (Fig. 5-6) and were of further interest since:

1) The OX102 antigen N-terminal peptide sequence "SCP" which was not encoded by the degenerate oligonucleotide (Fig. 5-3) was present in frame, on the same strand and 5' to the degenerate oligonucleotide as would be predicted.

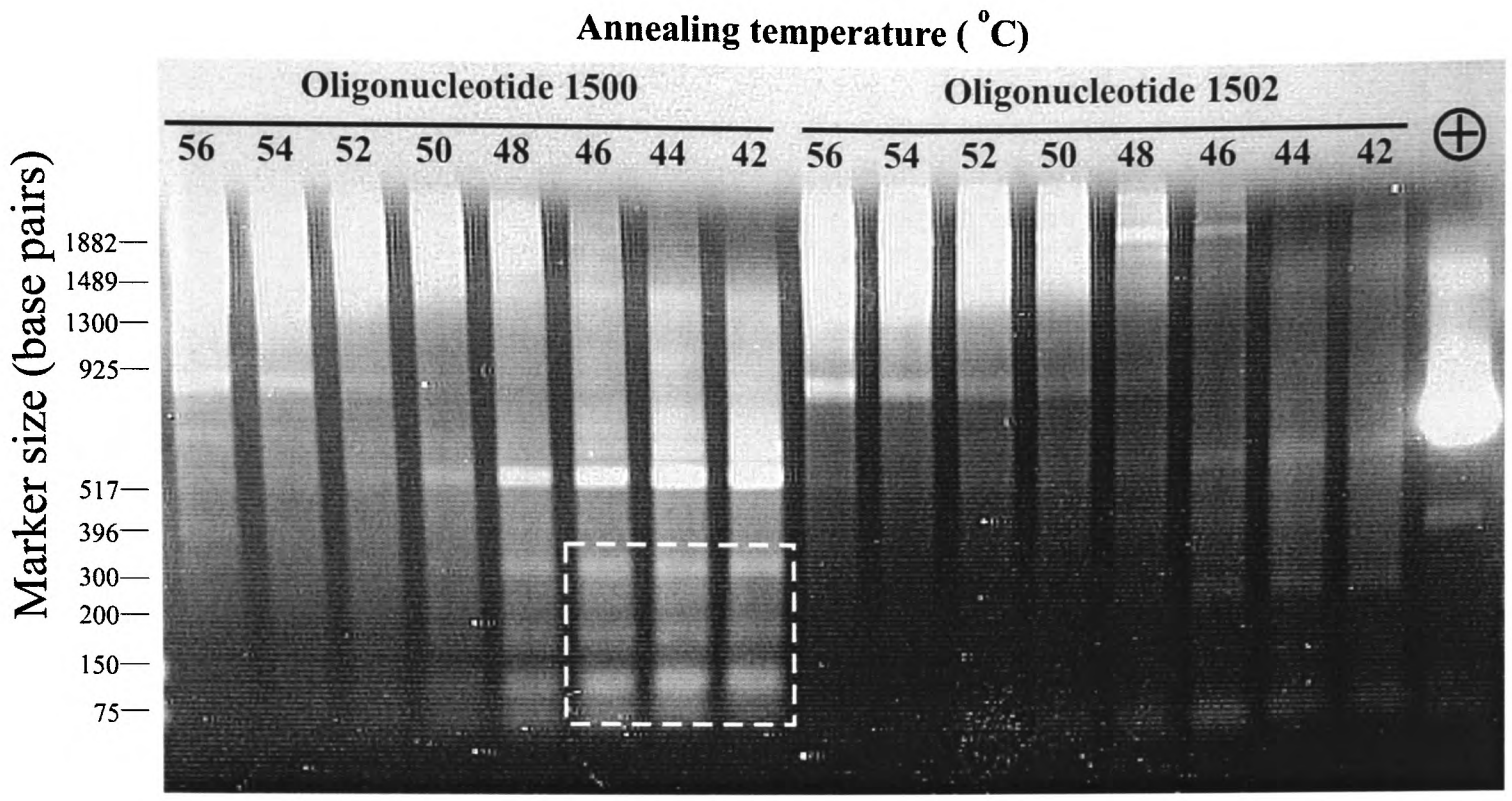

Figure 5-4. Products of low molecular mass were observed in a 5'RACE PCR using oligonucleotide 1500. The products of a 5'RACE reaction using both oligonucleotides 1500 and 1502 were resolved on a 1% agarose gel. The annealing temperature used in each reaction is indicated above the lanes, except for + which is a PCR positive control. The region outlined on the gel was excised and the products purified and ligated as described in the text.

2) 5' upstream on the same strand and in frame, there was a 23 amino acid sequence which contained all the features expected of a typical type I membrane glycoprotein leader.

3) The predicted initiator methionine was surrounded by a sequence which showed features of a Kozak eukaryotic translation initiation sequence.

4) The 1503 SMART™ oligonucleotide was identified 90bp 5' to the predicted transcription initiation site, a typical size for a eukaryotic 5'UTR.

5) Each transcript would have been initiated with a deoxyadenylate residue, consistent with the fact that all eukaryotic transcripts begin with a purine.

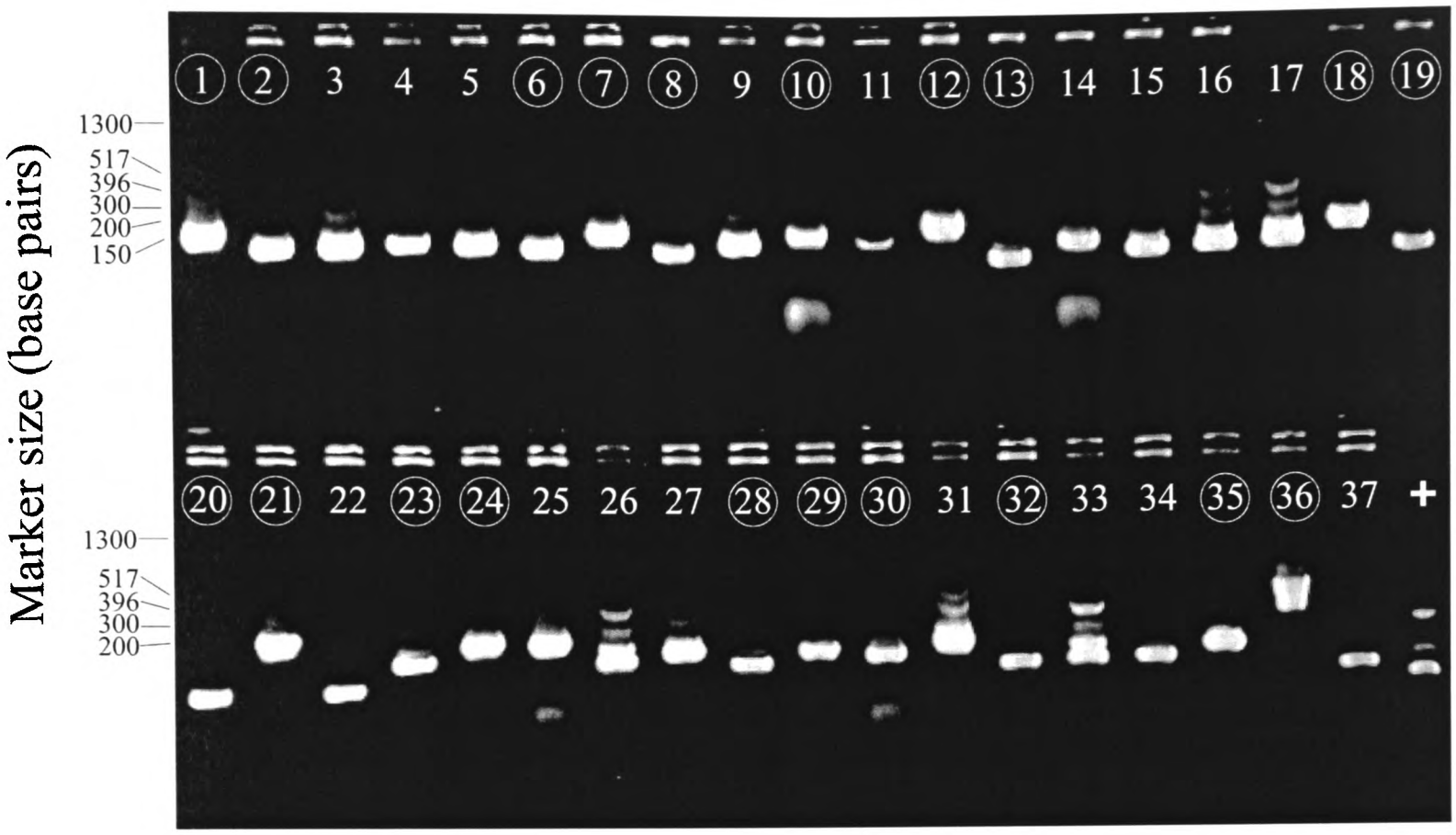

Figure 5-5. Transformed colonies contain inserts of variable size. The presence and size of cloned inserts from 37 randomly selected transformants were determined by colony PCR using oligonucleotides 1351 and 1352 which anneal approximately 100bp either side of the multiple cloning side of the PCRScript vector. The cloning efficiency was very high since all colonies contained an insert, except number 20 which was undigested PCRScript vector. Twenty colonies containing a range of insert sizes were selected, amplified, purified and sequenced on both strands. The selected colonies are indicated by being circled. The positive PCR control template was uncut PCRScript.

5.2.3 Obtaining the full length OX-102Ag cDNA by 3'RACE PCR

The full length OX-102 Ag cDNA was obtained by 3'RACE PCR by designing three different oligonucleotides (1504, 1505 and 1506) (Fig. 5-6) to the 5'UTR and using each in a separate PCR reaction. Strong common bands of approximately 2.3kbp were identified using all three oligonucleotides (Fig. 5-7). These bands were purified and cloned into appropriately digested PCRScript vector and sequenced.

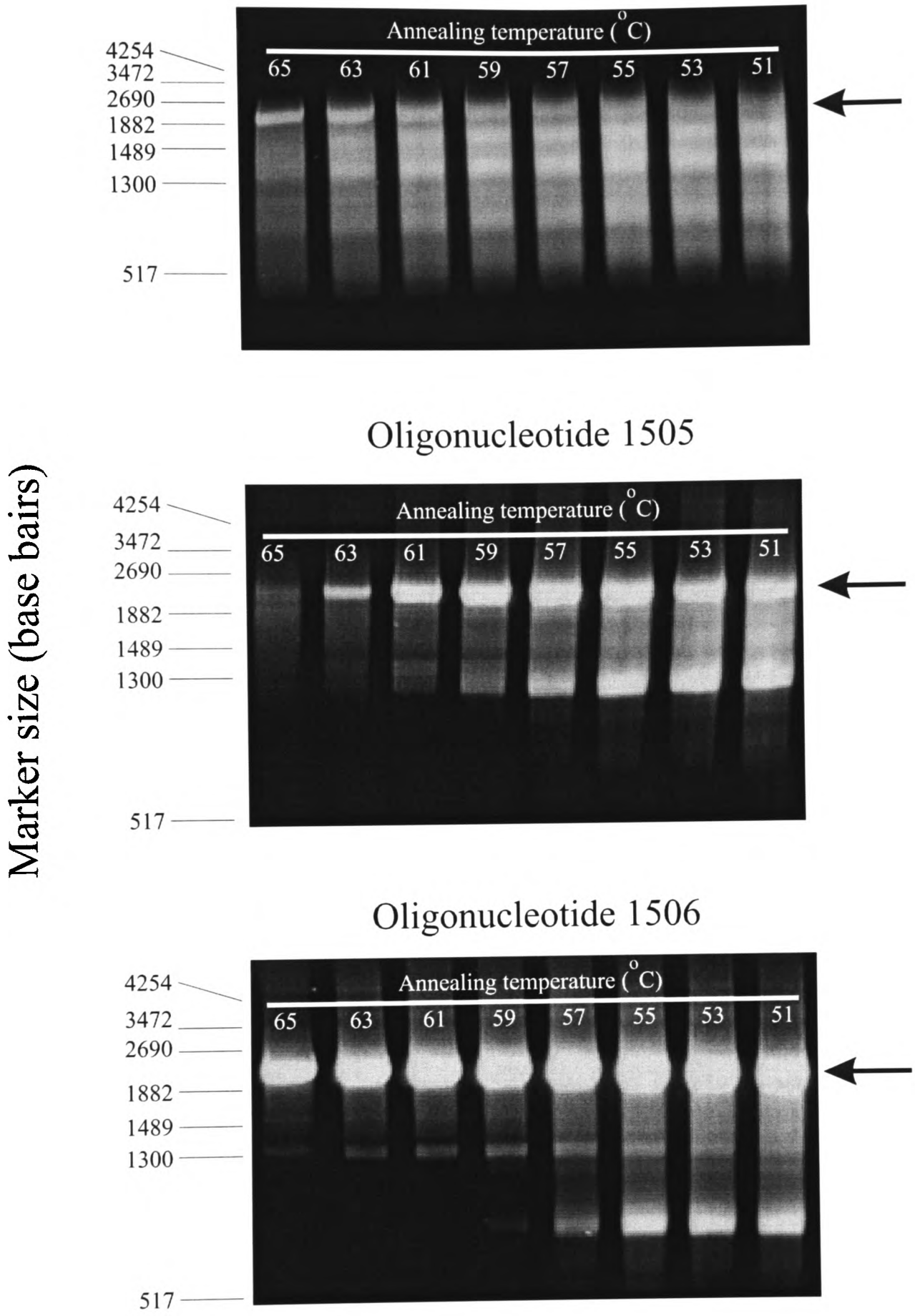

Figure 5-7. Oligonucleotides 1504, 1505 and 1506 produce a common 2.3kbp product in a 3'RACE reaction. Each oligonucleotide described in Figure 5-6 was used in a 3'RACE PCR at different annealing temperatures in order to amplify the full length OX-102 antigen cDNA. Each oligonucleotide produced a common product of approximately 2.3kbp (arrow).

5.3 Sequence analysis of the OX-102 Ag cDNA

Four independent clones were sequenced and all contained similar sequences. One clone contained the whole cDNA with no PCR errors as assessed by comparison to the sequences in other clones. The cDNA (Fig. 5-8) contains a 80bp 5'UTR and the initiator methionine is surrounded by a Kozak sequence (Kozak, 1987) as shown (Fig. 5-6). There is a 23 amino acid sequence which conforms to the features of a typical type I eukaryotic leader peptide (Nielsen et al., 1997) followed by nineteen out of the twenty residues obtained by direct protein sequencing from the purified protein. The twentieth amino acid (valine) obtained by protein sequencing was not predicted in the cDNA (which coded for an asparagine conforming to an N-linked glycosylation site and should therefore have been a blank cycle) presumably because the limiting amount of protein left after 20 cycles reduces the confidence of residue assignment. The mature form of the protein is predicted to consist of 304 amino acids of which 215 are located extracellularly, 22 span the lipid bilayer and 67 constitute the intracellular portion. The coding region is followed by a 1.3kbp 3'UTR which contains polyadenylation signals upstream of the polyA tail (Manley et al., 1985).

The extracellular region of the molecule is predicted to contain V and C2-set immunoglobulin like domains, a structural organisation highly typical of leukocyte cell surface antigens. However, the sequence does contain several unusual features:

1) It has 8 potential N-linked glycosylation sites, explaining the characteristic smear of the purified protein when resolved on gels. However, one side of the V-domain, the GFCC'C" face, appears carbohydrate free and is therefore likely to be the location of the OX-2 and MRC OX-102 mAb binding sites.

2) It has an unusually long sequence before the start of the predicted A strand suggesting the presence of another β-strand preceding the usual A-strand or an usually long A strand itself.

3) There are 6 noncanonical extracellular cysteines, suggesting additional constraints in the Ig fold by further intrachain disulphides in addition to the normal intersheet disulphide bond which usually covalently links strands B and F (Fig. 5-9).

4) The extracellular region shows sequence similarities to OX-2 over and above those expected within members of the IgSF indicating that the two proteins might have relatively recently diverged from the same ancestral precursor (Fig. 5-9)

Figure 5-8. The OX-102 antigen cDNA. The nucleotide sequence of the OX-102 antigen is divided into separate functional or structural regions and nucleotides numbered in italics. The protein translation is given and numbered in bold. The first nineteen of the twenty amino acid residues obtained from N-terminal protein sequencing of the purified antigen predict the N-terminus of the mature protein and are boxed. The polyadenylation sequence AAUAAA is shaded.

5'UTR

```
                                                                                                                  8
ATCCTGGTCATGGTCACCGCTGCTCCCCTACCTGTGAAGAGAAAGAGCACCGAGTGAGCCGCTGAAAACCAGAAAACCGAA
```

Leader

```
                                                                                                    150
ATGCTCTGCTTTTGGAGAACTTCTCACGTAGCAGTACTCTTGATCTGGGGGGTCTTCGCGGCTGAGTCA
 M  L  C  F  W  R  T  S  H  V  A  V  L  L  I  W  G  V  F  A  A  E  S
```

V-domain

```
1                                   10                                  20                                   2.
AGTTGTCCTGATAAGAATCAAACAATGCAGAACAATTCATCAACTATGACAGAAGTTAACACTACAGTGTTTGTACAGATG
S  C  P  D  K  N  Q  T  M  Q  N  N  S  S  T  M  T  E  V  N  T  T  V  F  V  Q  M

          30                                  40                                  50                                   3.
GGTAAAAAGGCTCTGCTCTGCTGCCCTTCTATTTCACTGACAAAAGTAATATTAATAACATGGACAATAACCCTCAGAGGA
 G  K  K  A  L  L  C  C  P  S  I  S  L  T  K  V  I  L  I  T  W  T  I  T  L  R  G

                60                                  70                                  80                                   3!
CAGCCTTCCTGCATAATATCCTACAAAGCAGACACAAGGGAGACCCATGAAAGCAACTGCTCGGACAGAAGCATCACCTGG
 Q  P  S  C  I  I  S  Y  K  A  D  T  R  E  T  H  E  S  N  C  S  D  R  S  I  T  W

                      90                                 100                                                      47
GCCTCCACACCTGACCTCGCTCCTGACCTTCAGATCAGTGCAGTGGCCCTCCAGCATGAAGGGCGTTACTCATGTGATATA
 A  S  T  P  D  L  A  P  D  L  Q  I  S  A  V  A  L  Q  H  E  G  R  Y  S  C  D  I

          110                                 120                                 531
GCAGTACCTGACGGGAATTTCCAAAACATCTATGACCTCCAAGTGCTGGTGCCCCCT
 A  V  P  D  G  N  F  Q  N  I  Y  D  L  Q  V  L  V  P  P
```

C2-domain

```
          130                                 140                                 150                                  61
GAAGTAACCCACTTTCCAGGGGAAAATAGAACTGCAGTTTGTGAGGCGATTGCAGGCAAACCTGCTGCGCAGATCTCTTGG
 E  V  T  H  F  P  G  E  N  R  T  A  V  C  E  A  I  A  G  K  P  A  A  Q  I  S  W

                160                                 170                                 180                                  69
ACGCCAGATGGGGATTGTGTCGCTAAGAATGAATCACACAGCAATGGCACCGTGACTGTCCGGAGCACATGCCACTGGGAG
 T  P  D  G  D  C  V  A  K  N  E  S  H  S  N  G  T  V  T  V  R  S  T  C  H  W  E

                      190                                 200                                                      77.
CAGAGCCACGTGTCTGTCGTGTTCTGTGTTGTCTCTCACTTGACAACTGGTAACCAGTCTCTGTCTATAGAACTGGGTAGA
 Q  S  H  V  S  V  V  F  C  V  V  S  H  L  T  T  G  N  Q  S  L  S  I  E  L  G  R

          210                 795
GGGGGTGACCAATTATTAGGA
 G  G  D  Q  L  L  G
```

Transmembrane

```
                220                                 230                                 861
TCATACATTCAATACATCATCCCATCTATTATTATTTTGATCATCATAGGATGCATTTGTCTTTTG
 S  Y  I  Q  Y  I  I  P  S  I  I  I  L  I  I  I  G  C  I  C  L  L
```

Cytoplasmic region

```
          240                                 250                                 260                                  94
AAAATCAGTGGCTGCAGAAAATGTAAATTGCCAAAATCGGGAGCTACTCCAGATATTGAGGAGGATGAAATGCAGCCGTAT
 K  I  S  G  C  R  K  C  K  L  P  K  S  G  A  T  P  D  I  E  E  D  E  M  Q  P  Y

                270                                 280                                 290                  10
GCTAGCTACACAGAGAAGAGCAATCCACTCTATGATACTGTGACCACGACGGAGGCACACCCAGCGTCACAAGGCAAAGTC
 A  S  Y  T  E  K  S  N  P  L  Y  D  T  V  T  T  T  E  A  H  P  A  S  Q  G  K  V

                      300                 304   1065
AATGGCACAGACTGTCTTACTTTGTCAGCCATGGGAATCTAG
 N  G  T  D  C  L  T  L  S  A  M  G  I  *
```

3'UTR

```
                                                                                                                  11
AACCAAGGAAAAGAAGTCAAGAGACATCATAATTACTGCTTTTCTTTCTTTAAACTTCTCCAATGGAGGGAAATTAGCTCT
TCTGAAGTTCTTAGAAAGCACAAATGTTCTAATGGATTTGCCTTTAAGTTCTTCTATCATTGGAAGTTTGGAATCTTTGCT
GCTACCTGTTAATTCTAGGAAGAACTGATTTAATTATTACAAAGAAAGCACATTGTTATGGTAAAATATCAAATTGTGCAA
TACAATGATGAAAACTGAGTTTCCTCAAGAAATAACTGCAGAAGGAACAATCATTACTAAAGCATTTCATGTGAGTTCTTC
CAAAAAAGAAAATCCCTGTGTATACGACATGATTATGGTATGTGTGTGCCTTTATATGTTTGTTTACAAATGTGTATATAT
GCACACATCTGATTATCAAGACATCTCTGTCAAAAACTCACTGGCGTTCCAGATTTATGAAAGCTAATAAAGTGAGTATTG
GAGATGTTTTTATATCTGTATATGTAAAACTACCTCATTCTTTTTAATGGCTACATAAAATTCATGGTCCTTGGATGGGCA
TTTAGACTTTGTGTTGTATGTGGTATTAAATGATACCATGTGGAATGTTTCTTGTGGTGAATCTCCGCATTATTTGAGTGC
ACCTGTGAGATAATTTCTGTGAGTGTAATGGTCCTGTCAGTTGGAATGCGCTTTTATGATCAATAGATTAGTCAAACTGTG
TCAGTTTACATTTTCTCTAATTGTGTTTAATGTGACTTTCTCCATATTCTTATTCTTATGTTTTTAATATCTTCACTTTCA
CCTTTTATACTTTCCATCTTTAATTAACCAGTTGGGTGATGTGTCTTAAGGTTGTGATATTAACTTTATTATTTAATGGAA
CTGGATTCATATCTTTGGGTTTCATGTCCACAAAAGAGATAGAAAGCATTTGTAAAGACAGTATTTTCAACTCCTTGTATT
ACTACAAAAATGTTGACATCTGATGCACAACAGTTTTATGGATGTTATGAATTGTGTGTTTTTAACATTCTATTCTGATGT
ACTTATAAGAGAGCAACTGTCTTTGAACTATATATGTAGGTGGGAGAACTTGGAGTACTTTATGTGCTAATAGGATGGTAA
TGGGATGATATAACTTTTCCCTCCAGTTTTTTGGAGGGAAATATTAGGAATACATGTATTGATAATTTTTAGCATATATTT
TTTAATTGTTAAAAATAAACCTGTTCCCTTTATATCAGGAAAGATATTAAAAATGGATTTATTCATCTCAAAAAAAAAAAA
                                                                                  2349
```

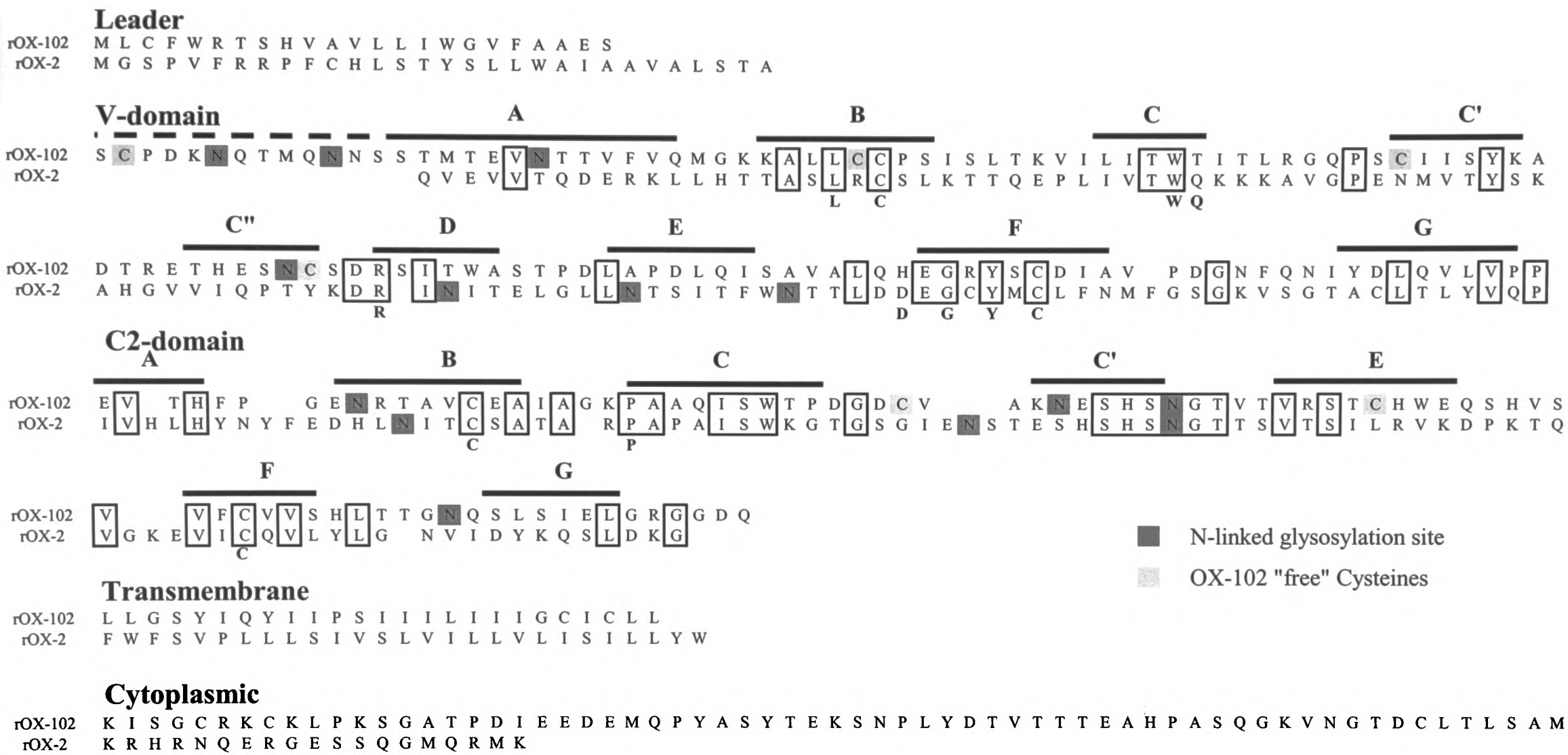

Figure 5-9. An alignment of the OX-102 antigen with rat OX-2. The protein sequences of the OX-102 antigen and OX-2 were aligned and separated according to the predicted domain organisation and topology. The superscripted bars in the extracellular regions predict the extent of the beta-sheets characteristic of the immunoglobulin fold by comparison to solved structures. In addition, the position of the IgSF signature residues are indicated in bold beneath both sequences. Asparagines conforming to N-linked glycosylation sequons have been darkly shaded and the six non-canonical cysteines present in the OX-102 Ag extracellular region shaded lightly.

Interestingly, the OX-102 Ag extracellular region showed greatest sequence similarity to a group of proteins whose only known function is that they are receptors for α-herpes viruses (Geraghty et al., 1998). An alignment of the extracellular N-terminal two domains (data not shown) was used to generate a neighbour joining tree showing the phylogenetic relationships of these proteins which is shown in Figure 5-10.

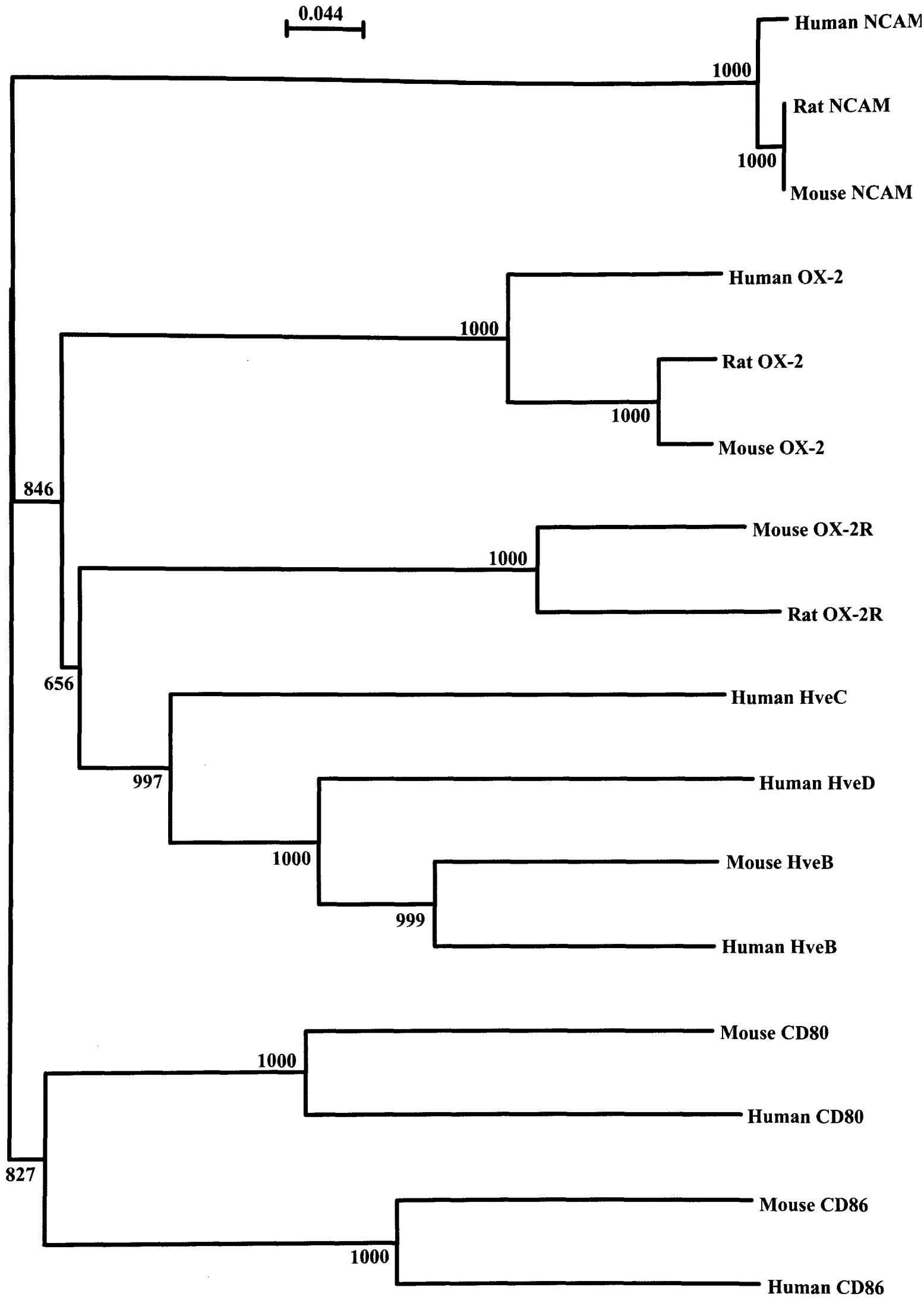

Figure 5-10. Phylogenetic relationship of the rat and mouse OX-102 Ag extracellular regions to other members of the immunglobulin superfamily. The N-terminal V and C2 set domains of the indicated sequences were aligned using ClustalW and then manually refined before the construction of a neighbour-joining tree with 1000 bootstrap trials.

The cytoplasmic region of the molecule shows no significant matches to any other previously characterised membrane protein cytoplasmic region and has no defined signalling motifs. However, it does contain three tyrosine residues and an interesting patch of acidic amino acids (DIEEDE) which suggest the possibility of initiating signal transduction via intracellular interactions. The highly acidic patch and the distance between two (residues 267 and 275) of the three tyrosines are conserved in the δ isoform of the human HveB (Eberle et al., 1995) indicating that these features may be used to initiate signal transduction cytoplasmically (Fig. 5-11).

Figure 5-11. OX-102 antigen and the δ isoform of human Hve B have sequence similarities in their cytoplasmic regions. The cytoplasmic regions of human Hve B (TrEMBL accession number Q92692) and rat OX-102 antigen have been aligned and regions of similarity boxed. Notice the acidic patch and that the spacing between the two tyrosines in bold is conserved in the two proteins.

5.4 Cloning of the mouse homologue of the OX-102Ag

Due to the biological phenomenon of homologous recombination in mouse embryonic stem cells and the consequent ability to ablate targeted genes has meant mice are now the preferred model for immunological functional studies. In order to generate both monoclonal antibodies and knockout mice for functional studies it is essential to characterise the mouse homologue of the protein.

5.4.1 Use of cross-species PCR

Probing of the publicly accessible mouse EST databases revealed two significant matches with the rat cDNA sequence, suggesting a mouse homologue did exist. However, neither of the ESTs were complete and did not contain the useful 5' end and thus prevented the simple amplification of the full coding sequence by PCR. Oligonucleotides (1518 and 1519) designed to amplify the extracellular regions of the rat OX102-Ag were used in a PCR using cDNA prepared from mouse PEC cDNA. A band of appropriate size was observed (Fig. 5-12A) which was cloned and sequenced, revealing it did indeed encode a protein closely related to the rat OX-102 Ag. The sequence obtained from this construct was used to generate two nested oligonucleotides (1550 and 1551) to clone the full length mouse OX-102 Ag by 3'RACE (Fig. 5-12B). The PCRs produced products of 1.7kbp, 1.5kbp and 1.1kbp (Fig. 5-12 C and D) which were purified (the shorter products were pooled) and the 1.7kbp and 1.1kbp products cloned and four completely independent clones sequenced.

Figure 5-12. Cloning of the mouse OX-102 Ag homologue. The mouse OX-102 Ag homologue was cloned by cross-species PCR and the full length cDNA obtained using a 3'RACE strategy in an analogous way used to clone the rat form. A) oligonucleotides used to amplify the extracellular regions of the rat OX-102 Ag sequence (1518 and 1519) were used on mouse PEC cDNA as a template. A product of expected size (775bp-arrow) was observed at low annealing temperatures, cloned and sequenced. B) the sequence of the 5' end of the mouse OX-102 Ag homologue and the two oligonucleotides (1550 and 1551) designed to amplify the full length mouse form by 3'RACE are shown. C) The use of oligonucleotide 1550 in a 3'RACE PCR reaction using cDNA prepared from mouse PECs as a template produced a band of approximately 1.7kbp (arrow) using annealing temperatures of 60 and 65 °C. The products of these PCRs (numbered 1 and 2 respectively) were used in a nested 3'RACE reaction with oligonucleotide 1551 at the same two annealing temperatures. D) The products of the nested 3'RACE PCR were a major band of 1.7kbp (arrow) and two minor ones of 1.5 and 1.1kbp (which were pooled). The products were purified and the 1.7kbp and 1.1kbp products cloned and sequenced.

A

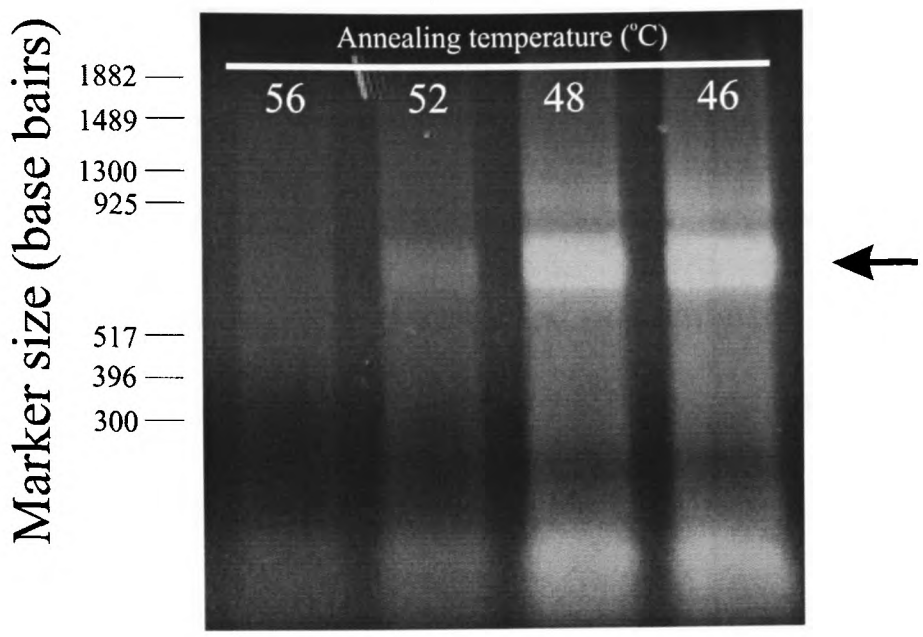

B

Mouse OX-102 antigen homologue sequence

Oligonucleotide 1518

TCTAGAGAAAGAGCACCGAGTGAGCGGCGGAAAACCAGAAAACCGAAATGTTTTGCTTT.....*etc*

XbaI

M F C F

Oligonucleotide 1550 GAGTGAGCGGCGGAAAACCAGAAAACCGAAATG

Oligonucleotide 1551 GAGCGGCGGGCGGCCGCAAAACCGAAATGTTTTGCT

NotI

3'RACE PCR to obtain full length mouse OX-102 antigen homologue

C Oligonucleotide 1550

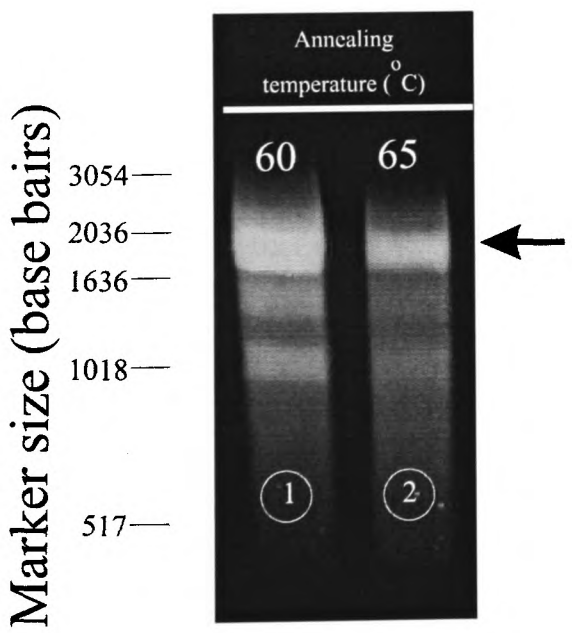

D Oligonucleotide 1551

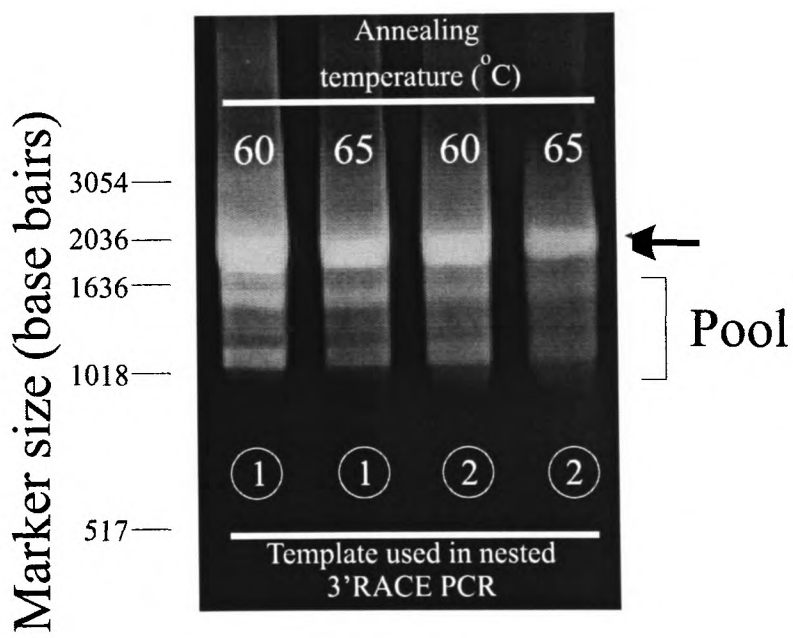

5.4.2 Sequence analysis of the mouse homologue of the OX-102 antigen

All four clones contained similar sequences and one clone contained the whole cDNA with no PCR errors (as assessed by comparison to the sequences in other clones) and is shown in Figure 5-13. The 1.1kbp PCR product encoded an inframe deletion which corresponded to almost the entire V-domain and is indicated in Figure 5-13. The translation of the mouse homologue predicted it would be one amino acid shorter than the rat in the extracellular domains but otherwise contained all the features of the rat sequence including the 6 non-canonical cysteines and the cytoplasmic tyrosines which were all perfectly conserved. The mouse protein was predicted to contain two additional N-linked glycosylation sequons (totalling 10 for the mouse homologue) and is shown aligned to the rat species in Figure 5-14.

Figure 5-13. The cDNA sequence of the mouse homologue of the OX-102 antigen. The nucleotide sequence of the OX-102 antigen is divided into separate functional or structural regions and nucleotides numbered in italics. The protein translation is given and numbered in bold. The 1.1kbp 3'RACE product contained a deletion which would remove most of the V-domain of the protein and the extent of this deletion is marked by brackets. The precise intron/exon boundary cannot be determined since the deletion occurs between two identical codons but the final product is inframe and contains the sequence LTQVPP.

5'UTR

....CGGCGGAAAACCAGAAAACCGAA *23*

Leader

ATGTTTTGCTTTTGGAGAACTTCTGCCCTAGCAGTGCTCTTAATATGGGGGGTCTTTGTGGCTGGGTCA *92*

M F C F W R T S A L A V L L I W G V F V A G S

V-domain

extent of deleted region.....

1 10 20 *173*

AGTTGTACTGATAAGAATCAAACAACACAGAACAACAGTTCATCTCCTCTGACACAAGTGAACACTACAGTGTCTGTACAG

S C T D K N Q T T Q N N S S S P L T Q V N T T V S V Q

30 40 50 *254*

ATAGGTACAAAGGCTCTGCTCTGCTGCTTTTCTATTCCACTGACAAAAGCAGTATTAATCACATGGATAATAAAGCTCAGA

I G T K A L L C C F S I P L T K A V L I T W I I K L R

60 70 80 *335*

GGCCTGCCATCCTGCACAATAGCATACAAAGTAGATACAAAGACCAATGAAACCAGCTGCTTGGGCAGGAACATCACCTGG

G L P S C T I A Y K V D T K T N E T S C L G R N I T W

90 100 *416*

GCCTCCACACCTGACCACAGTCCTGAACTTCAGATCAGTGCAGTGACCCTCCAGCATGAGGGGACTTACACATGTGAGACA

A S T P D H S P E L Q I S A V T L Q H E G T Y T C E T

110 120 *473*

GTAACACCTGAAGGGAATTTTGAAAAAAACTATGACCTCCAAGTGCTGGTGCCCCCT

V T P E G N F E K N Y D L Q V L V P P

C2-domain

130 140 150 *554*

GAAGTAACCTACTTTCCAGAGAAAAACAGATCTGCAGTCTGTGAGGCAATGGCAGGCAAGCCTGCTGCACAGATCTCTTGG

E V T Y F P E K N R S A V C E A M A G K P A A Q I S W

160 170 180 *635*

TCTCCAGATGGGGACTGTGTCACTACGAGTGAATCACACAGCAATGGCACTGTGACTGTCAGGAGCACATGCCACTGGGAG

S P D G D C V T T S E S H S N G T V T V R S T C H W E

190 200 *716*

CAGAACAATGTGTCTGATGTGTCCTGCATTGTCTCTCATTTGACTGGTAACCAATCTCTGTCCATAGAACTGAGTAGAGGT

Q N N V S D V S C I V S H L T G N Q S L S I E L S R G

210 *734*

GGTAACCAATCATTACGA

G N Q S L R

Transmembrane

220 230 *800*

CCATATATTCCATACATCATACCATCAATTATCATTTTGATCATCATAGGATGCATTTGTCTTTTG

P Y I P Y I I P S I I I L I I I G C I C L L

Cytoplasmic region

240 250 260 *881*

AAAATCAGTGGCTTCAGAAAATGCAAATTGCCAAAATTAGAAGCTACTTCAGCTATTGAGGAGGATGAAATGCAGCCTTAT

K I S G F R K C K L P K L E A T S A I E E D E M Q P Y *962*

270 280 290

GCTAGCTATACAGAGAAGAGCAATCCACTCTATGATACTGTGACTAAGGTGGAGGCATTTCCAGTATCACAAGGCGAAGTC

A S Y T E K S N P L Y D T V T K V E A F P V S Q G E V

300 303 *1004*

AATGGCACAGACTGCCTTACTTTGTCGGCCATTGGAATCTAG

N G T D C L T L S A I G I *

3'UTR *1085*

AACCAAGAAAAAAGAAGTCAAGAGACATCATAATTACTGCTTTGCTTTCTTTAAAATTCGACAATGGAAGGACTACTTGGA

AATTAGCTCTTCCAAAGCTATTAAAAAGCACAAATGTTCTAATGAAATTGCATTTAAATTCTATCATTGGAAGTTTGGAAT

CTCTGCTGCTACCTGTTAATTTTAGGAAGAACTGATTTAATTATTACAAAGAAAGCACATGGTTATGGTGAAATATCAAGT

TGTGCAATAAAGTATGATGAAAACTGAGTTTCCTCAAGAAATAACTGCAGGAGGAACAATCATCACTAAAGAATTTCATGT

GAGTTCTTACAAAAAAATTCCTATGTATACATGACTATGGTATGTGCGTCCAATTACATGTTTATTTACAAATGTGTATAT

ATGCACACATTTGCTTTTCAGGACATCTCCTTGTAAAAAACACACTGGAGTTTTGGATTTATAAAAGCTTATAAAGTGAGC

ATTGGAGATATTTTTATATCAGCATAAGTAAATCTACCTCATTCTTTTTAATGGCTACATAGAATTCTCCTGTATGATTAC

ATTGTAATTTAATTAATCATGGCCCTTGGATTTTGTGTTGTGTGTGGTATTAAACAAAACCATGTAGAATAAAAAAAAAAA

1641

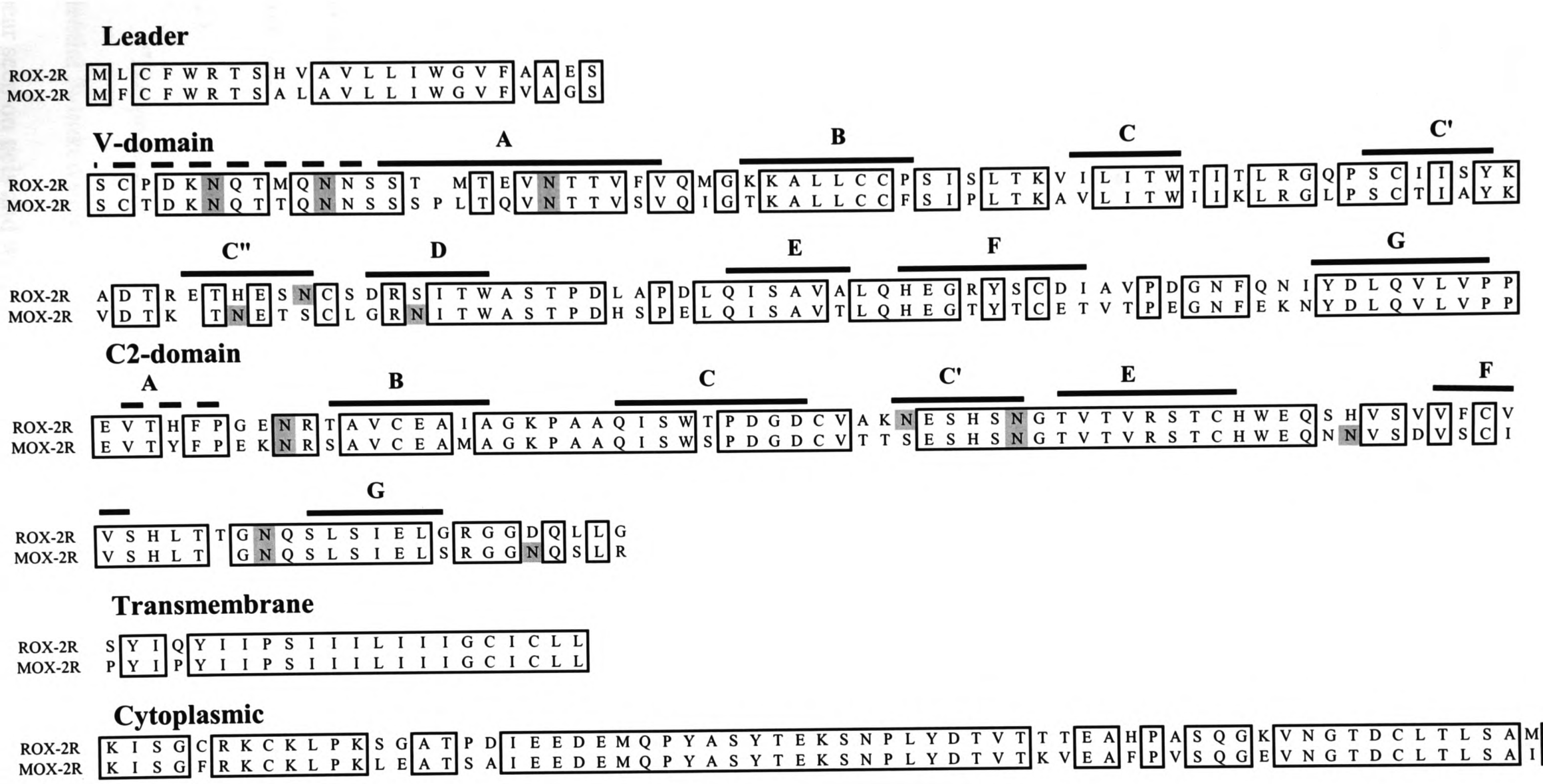

Figure 5-14. An alignment of the rat and mouse OX-102 Ag amino acid sequences. The two sequences have been split according to predicted domain organisation and topology. The superscripted bars in the extracellular regions predict the extent of the beta-sheets characteristic of the immunoglobulin fold by comparison to solved structures. Asparagines conforming to N-linked glycosylation sequons have been lightly shaded.

5.5 Discussion

The cloning of the OX-102 Ag and its mouse homologue revealed that the protein was a member of the IgSF containing two domains. This structural organisation accounts for 15% of all known leukocyte cell surface proteins (Brown et al., 1998) and appears to have evolved to mediate protein:protein interactions, supporting the possibility that this protein could be the OX-2 receptor. In addition, the protein sequence of the extracellular regions of the OX-102 Ag showed sequence similarities over and above those expected between members of the IgSF indicating that OX-2 and the OX-102 Ag had recently evolved from the same ancestral precursor. A close evolutionary relationship between receptor:ligand pairs have been observed before (Brown et al., 1998; Davis and van der Merwe, 1996) and this also supported the possibility that these two proteins would interact. This relationship implies that these individual receptor:ligand pairs have evolved from a single gene product which was presumably able to mediate a homophilic interaction. The evolutionary pressure driving the divergence of a single gene product which interacts in a homophilic manner is easy to understand because the gene product will be expressed in an identical spatio-temporal manner and thus have limited communicative potential. However, this potential is dramatically increased after gene duplication, since two genes could be expressed in different developmental patterns, allowing adhesion between cell types of different lineages or developmental state. The subsequent evolution of differing signalling roles of the interacting proteins allows the initiation of a complex dialogue via the interacting proteins which will eventually become discrete genes (this is discussed in more detail in section 10.2).

The protein sequence of the rat and mouse OX-102 antigen contained eight and ten potential N-linked glycosylation sites respectively which would account for the characteristic smear seen on gels and western blots. This is not as many sites as would have been predicted

from the deglycosylation experiment shown in Figure 4-6 which suggested around 70% of the protein would be contributed by N-linked carbohydrate. However, this calculation was based on an apparent molecular mass of 25kDa for the non-reduced, PNGaseF treated protein and an average of 3kDa contributed by each N-linked glycosylation site. Analysis of the cDNA suggests the protein backbone should have a theoretical mass of approximately 34kDa. It is possible that the non-reduced protein would have a compact globular structure (especially if stabilised by several disulphide bonds) and this would explain the lower apparent molecular mass measured by western blot. It is also possible that the average mass of the carbohydrate moieties at each site is greater than 3kDa (see section 4.5).

The protein sequence of the OX-102 antigen was interesting from a structural point of view since it contained several non-canonical cysteines which might form extra inter- or intra- domain disulphide bonds in addition to the usual F to B β-strand disulphide. Also, when compared to other IgSF V-domains, the OX-102 Ag contains an unusually long and glycosylated β-strand A, which may extend around the back of the BED face of the Ig fold and be potentially stabilised by a disulphide formed between cysteines at positions 2 and 34. This extended A strand may have evolved from a long leader sequence which became incorporated into the mature protein structure due to the switching of the signal peptidase cleavage site. Evidence that this may have happened comes from the cloning of what is likely to be a mis-spliced form of the mouse OX-102 Ag which was missing the majority of the V-domain. The deletion begins after the extended A-strand and joins inframe to the end of the V-domain suggesting that the start of the A strand is encoded on a separate exon to the rest of the V-domain. The fact that this is an inframe deletion indicates that the intron position with respect to the reading frame is in phase which supports the suggestion that this is a genuine mis-splice since most domain boundaries coincide with introns with identical splice phases. The actual phase of the splice site cannot be determined since splicing occurs between identical codons but is likely to be phase 1 (Sharp, 1981) by comparison to the

genomic structure of other IgSF domain containing proteins (Barclay et al., 1997). Examination of the intron boundaries once the genomic sequence is available will allow further speculation and future structural work including disulphide bond mapping of recombinant forms of the protein will reveal more structural details.

The proteins showing the greatest sequence similarity to the OX-102 antigen in the extracellular region were a small family of three (Hve -B,-C and -D) IgSF proteins which contain 3-domains (V-C2-C2) which were identified due to their ability to mediate the entry of α-herpes viruses and are thus known as Hve's (Herpes Virus Entry) (Geraghty et al., 1998) and are shown aligned to the OX-102 antigen in Figure 5-14. This family of host proteins is functionally poorly characterised except for their ability to interact with glycoprotein D from numerous alpha herpes (Cocchi et al., 1998a; Warner et al., 1998). The suggestion that the OX-102 antigen may bind glycoprotein D from herpes viruses is one which should be investigated. These proteins are widely expressed (Geraghty et al., 1998; Lopez et al., 1998) and have been identified in cells of haematopoietic and neural origin as well as various epithelia. One feature of these proteins is that they can exist in different forms at the cell surface, differing only in their transmembrane and cytoplasmic regions as a result of alternative splicing (Eberle et al., 1995; Cocchi et al., 1998b; Koike et al., 1990). The functional relevance of this is not known, but different cytoplasmic regions could clearly lead to the generation of different intracellular signals. Interestingly, one of the mouse EST matches to the OX-102 Ag cDNA contained a divergent sequence close to the start of the predicted transmembrane region indicating that the OX-102 Ag might also contain alternative transcripts differing in their transmembrane and intracellular portion (section 10.3.1). It should be noted that the 3'RACE reactions from macrophage cDNA did produce several products but none of a consistent size between different gene specific oligonucleotides but these alternative transcripts may be exclusively expressed in other tissues besides macrophages. It is feasible that the non-glycosylated 40kDa band consistently

present during OX-102 Ag purifications from rat splenic lysates may be associated with one of these alternative forms. This also raises the possibility that the OX-102 Ag itself may not be necessary or sufficient to confer OX-2 binding and that OX-102 Ag associated proteins are required.

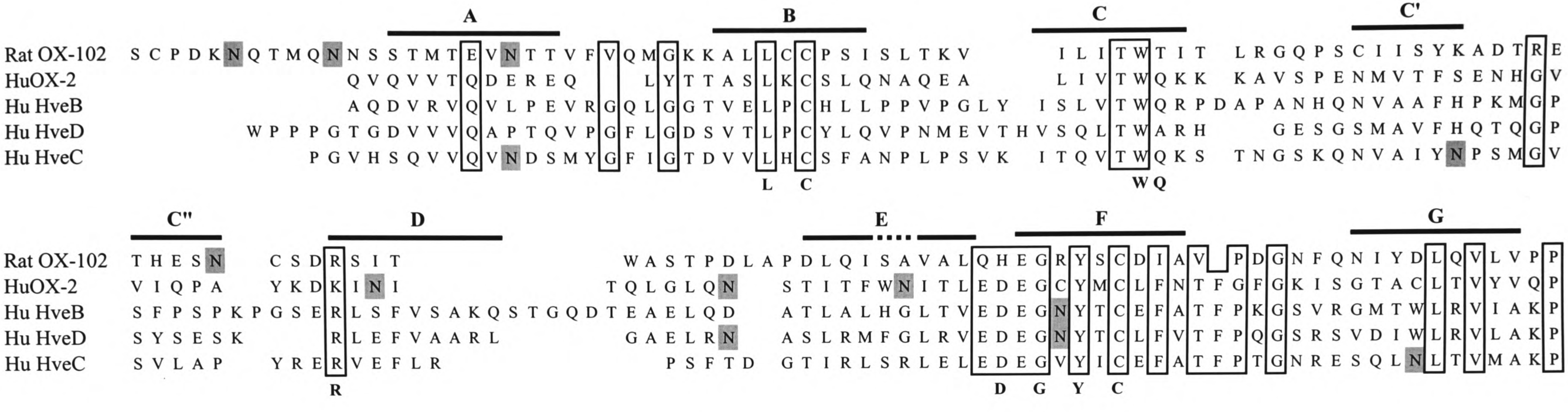

Figure 5-14. An alignment of the predicted immunoglobulin-like V-domains of rat OX-102 and other related proteins. The amino acid sequences of the predicted V-domains of rat OX-102, human OX-2 and human Hve B, C and D were aligned to highlight regions of similarity. The superscripted bars in the extracellular regions predict the extent of the beta-sheets characteristic of the immunoglobulin fold by comparison to solved structures. In addition, the position of the IgSF signature residues are indicated in bold beneath the sequences. Asparagines conforming to N-linked glycosylation sequons have been darkly shaded and four out of five identical residues in equivalent positions boxed.

Chapter Six

The OX-102 antigen is the rat OX-2 receptor

6.1 Introduction

It was important to show that the OX-102 antigen was both necessary and sufficient to confer the ability to bind OX-2. This was particularly important due to the consistent presence of the 40kDa band in immunoprecipitations which suggested the possibility that the OX-102 Ag was a two chain molecule. This chapter describes experiments which prove that the OX-102 Ag contained the MRC OX-102 epitope and also the rat OX-2 binding site by transfecting the OX-102 Ag cDNA into cells and generating both these properties at the cell surface of a human cell line. The OX-102 antigen was therefore renamed the rat OX-2 receptor (rOX-2R). In addition, the rOX-2R was found to be solely sufficient to confer OX-2 binding properties since purified recombinant forms of both proteins were shown to interact, as determined by surface plasmon resonance technology. The recombinant form of the rOX-2R was shown to bind native OX-2 expressed on the rat thymocyte cell surface since the observed interaction could be completely prevented by preincubating the cells with the MRC OX-2 mAb. This also suggested that OX-2 was the only ligand for the rOX-2R expressed on the rat thymocyte cell surface. The recombinant mouse OX-2R behaved in a similar fashion, as predicted from the ability of rat OX-2 coated beads to bind mouse PECs (section 1.6.5). In summary, this chapter describes the conclusive proof that the OX-102 Ag is the rat OX-2R using three independent methods.

6.2 HEK 293T cells transfected with the OX-102 Ag cDNA bind MRC OX-102 mAb and rOX-2 coated beads

In order to demonstrate that the OX-102 Ag cDNA was able to generate both the MRC OX-102 epitope and the ability to bind rOX-2 coated beads, the full length cDNA was transfected into human endothelium kidney (HEK) 293T cells. The full length OX-102 Ag

cDNA was excised and blunt end ligated into the pEF-BOS vector and transfected into HEK 293T cells by the $CaPO_4$ method. Previous experience has shown that this transient expression system will usually result in around 30% transfection efficiency and that the transfected cells will express a broad range of expression levels after 48 hours.

Cytofluorimetry showed that a significant proportion of the transfected but not the mock transfected controls were able to bind the MRC OX-102 mAb (Fig. 6-1) indicating that the reactivity of the mAb had been cloned and the OX-102 Ag cDNA encoded a protein which was functionally expressed at the cell surface.

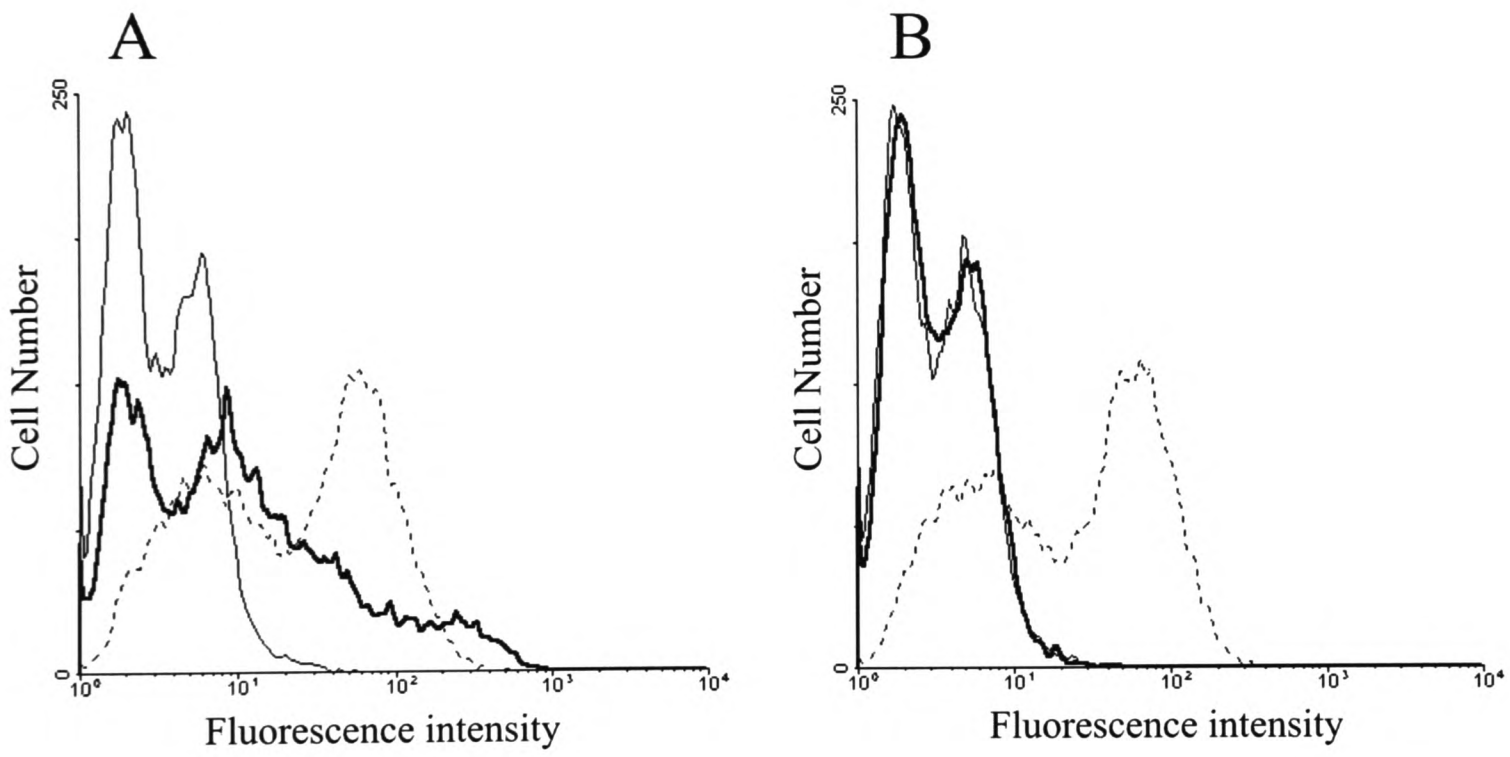

Figure 6-1. The MRC OX-102 mAb stains cells transfected with the OX-102 Ag cDNA. (A) HEK 293T cells were transfected with rOX-102Ag cDNA and stained with MRC OX-102 (bold line), the endogenous human MHC Class I with mAb W6/32 (dotted line) and a negative control (MRC OX-21). Mock transfected cells stained with MRC OX-102 showed no staining greater than the negative control (B).

In addition, the transfected (but not control) cells were able to bind rat OX-2 coated beads (Fig. 6-2 A/B) and this binding could be blocked back to a negative control by preincubating the transfected cells with the MRC OX-102 mAb (but not control mAb) (Fig. 6-2 C/D).

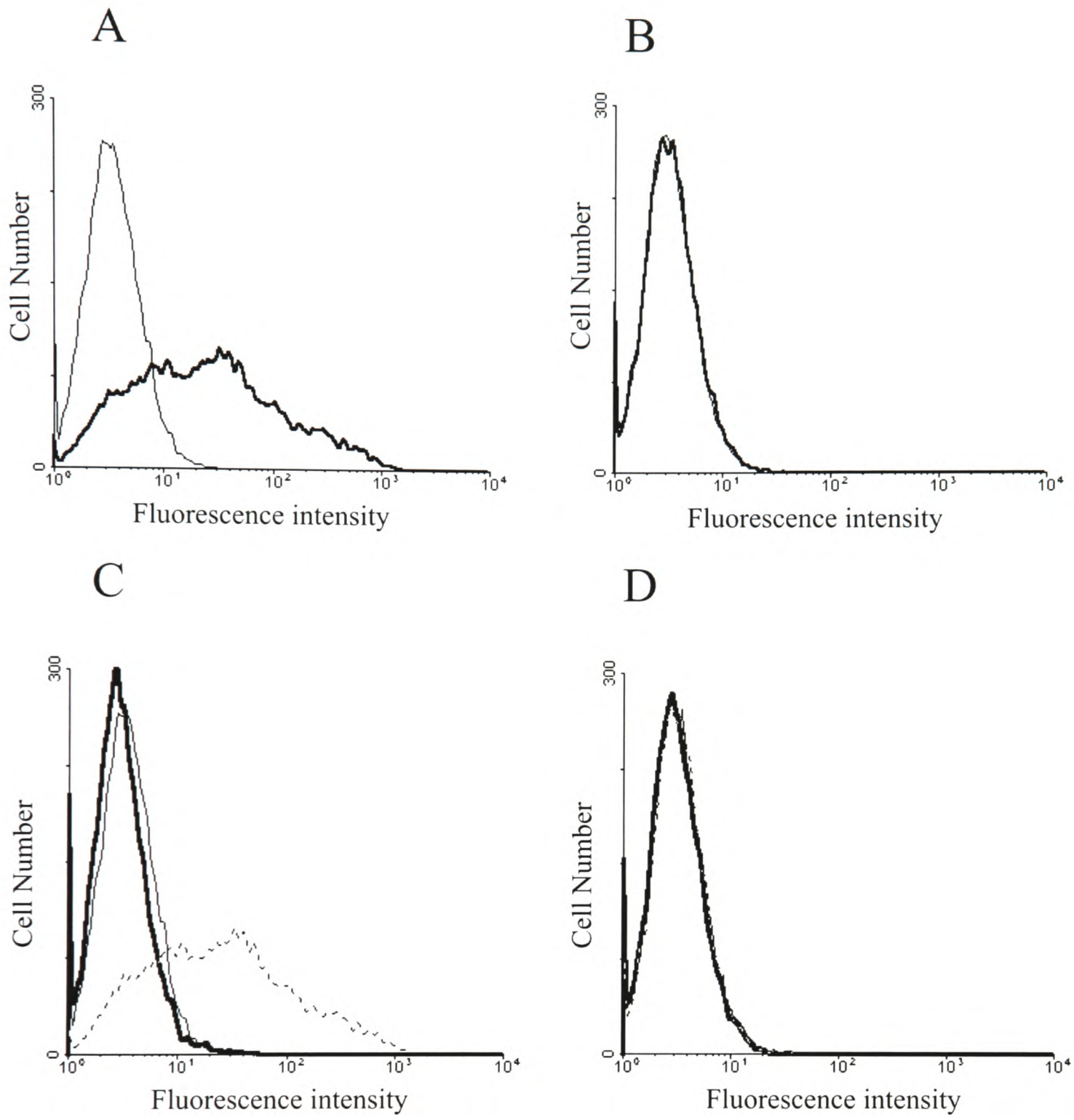

Figure 6-2. The MRC OX-102 Ag is able to bind rOX-2 coated beads at the cell surface. (A) HEK 293T cells transfected with the OX-102 Ag cDNA were able to bind rOX-2 coated beads (bold line) compared to a negative control (CD4d3+4 coated beads –thin line). Mock transfected cells (B) showed no staining greater than the negative control. (C) OX-102 Ag cDNA transfected 293T cells pre-incubated with MRC OX-102 (bold) but not W6/32 (dotted) were able to block binding of rOX-2 coated beads back to a negative control (CD4d3+4 coated beads-cells preincubated with W6/32). Mock transfected cells (D) did not bind rOX-2 coated beads.

These results indicate that the OX-102 Ag cDNA encodes the MRC OX-102 epitope and is necessary for the gain of antibody and ligand binding functions. The OX-102 Ag was

thus renamed the rat OX-2 receptor (OX-2R). However, this experiment did not preclude the possibility that more than one gene product was responsible for the ability to bind OX-2.

6.3 Generation of a recombinant soluble form of rOX-2R

In an analogous manner to that used to generate a soluble OX-2 protein, the extracellular regions of rOX-2R were recombinantly fused to rat CD4d3+4 (Fig. 6-3). This construct differed from the one used in the OX-2 proteins in that it contained a 19 amino acid sequence at the C-terminus of the protein which could be enzymatically biotinylated on a specific lysine residue using the *E.Coli* BirA enzyme (Brown et al., 1998).

Oligonucleotides (1518 and 1519) were designed so that the OX-2R and CD4d3+4 junction was inframe and contained the sequence IELGRGGSTSIT. The construct was expressed as shown by inhibition ELISA (data not shown), and biotinylated as described in section 2.7.3. Using the same oligonucleotides and cDNA prepared from mouse PECs the mouse homologue of the rOX-2R was amplified (as described in section 5.4.1) and biotinylated protein produced in an identical manner. The mouse OX-2RCD4d3+4-bio construct contained the amino acid change S206G because oligonucleotide 1519 was based on the rat sequence.

The rOX-2RCD4d3+4-bio protein bound streptavidin and the mAbs MRC OX-102 and MRC OX-68 as assessed by surface plasmon resonance (data not shown) indicating that the protein was antigenically active (and therefore likely to be correctly folded) and the biotin tag had been successfully added to a significant proportion of the expressed material.

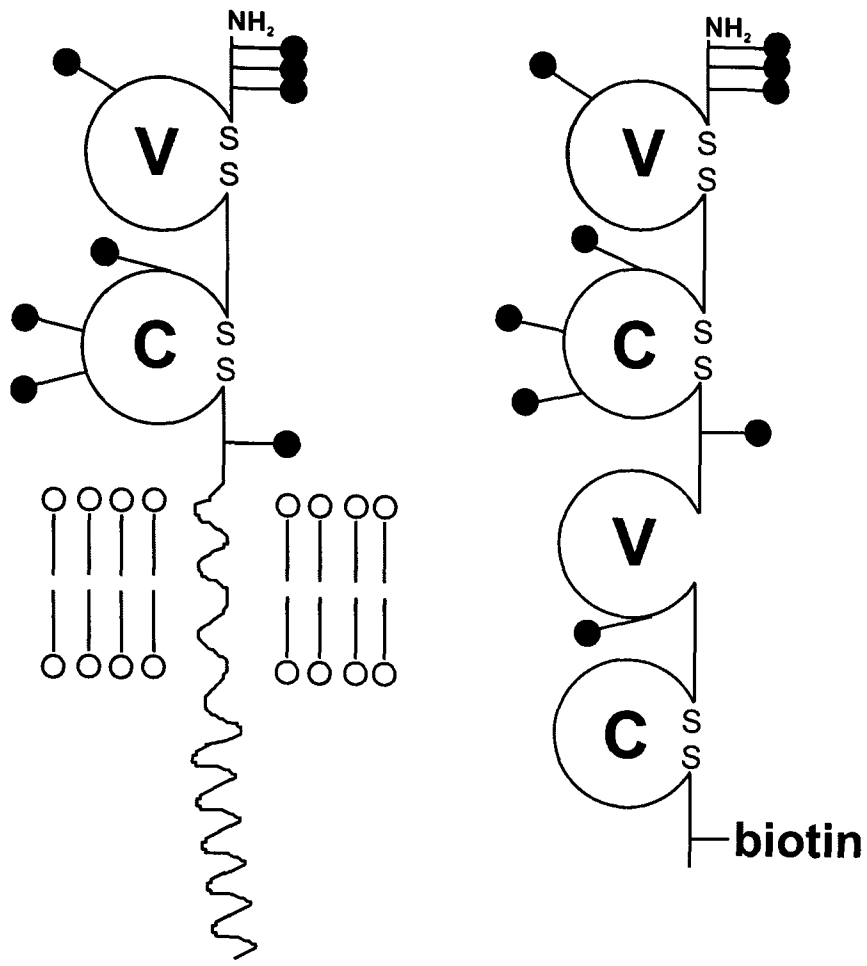

Figure 6-3. Schematic representation of the soluble recombinant OX-2R construct containing a biotinylatable tag.

Schematic representation of the domain organisation of rat OX-2R as it would appear at the cell surface and rOX-2RCD4d3+4-bio soluble construct. The filled lollipops represent the approximate sites of potential N-linked glycosylation, the IgSF set assignments are labelled and the C-terminal location of the enzymatically added biotin tag is indicated.

6.4 Rat and mouse OX-2R bind OX-2 on rat thymocytes

Producing a recombinant form of the rat OX-2R allowed the demonstration that just the extracellular domains were sufficient for OX-2 binding. The biotinylated rat and mouse OX-2RCD4d3+4 (Fig. 6-3) could be attached directly to avidin coated fluorescent beads via their biotin tag and presented to OX-2 expressing cells. Rat thymocytes express high levels of OX-2 (Fig. 6-4A) and were able to bind both rat and mouse OX-2R coated beads (Fig. 6-4B). Fab fragments of the MRC OX-2 mAb, incubated with rOX-2 coated beads before presentation to cells had been shown to prevent the beads binding to rat PECs (Preston et al., 1997). This blocking activity could be reproduced since preincubation of cells with MRC OX-2 (whole IgG) but not MRC OX-1 was able to prevent the binding of both rat (Fig. 6-4C) and mouse (Fig. 6-4D) OX-2R coated beads to rat thymocytes. This demonstrated that the native OX-2 expressed on rat thymocytes was wholly responsible for the observed binding and suggests that OX-2 was the only ligand for rat and mouse OX-2R on this cell type.

The observation that the mouse OX-2 receptor, when immobilised on beads, was able to bind to rat thymocytes and that this binding could be specifically blocked by pre-incubating the cells with MRC OX-2 mAb demonstrated that it was correctly folded and antigenically active.

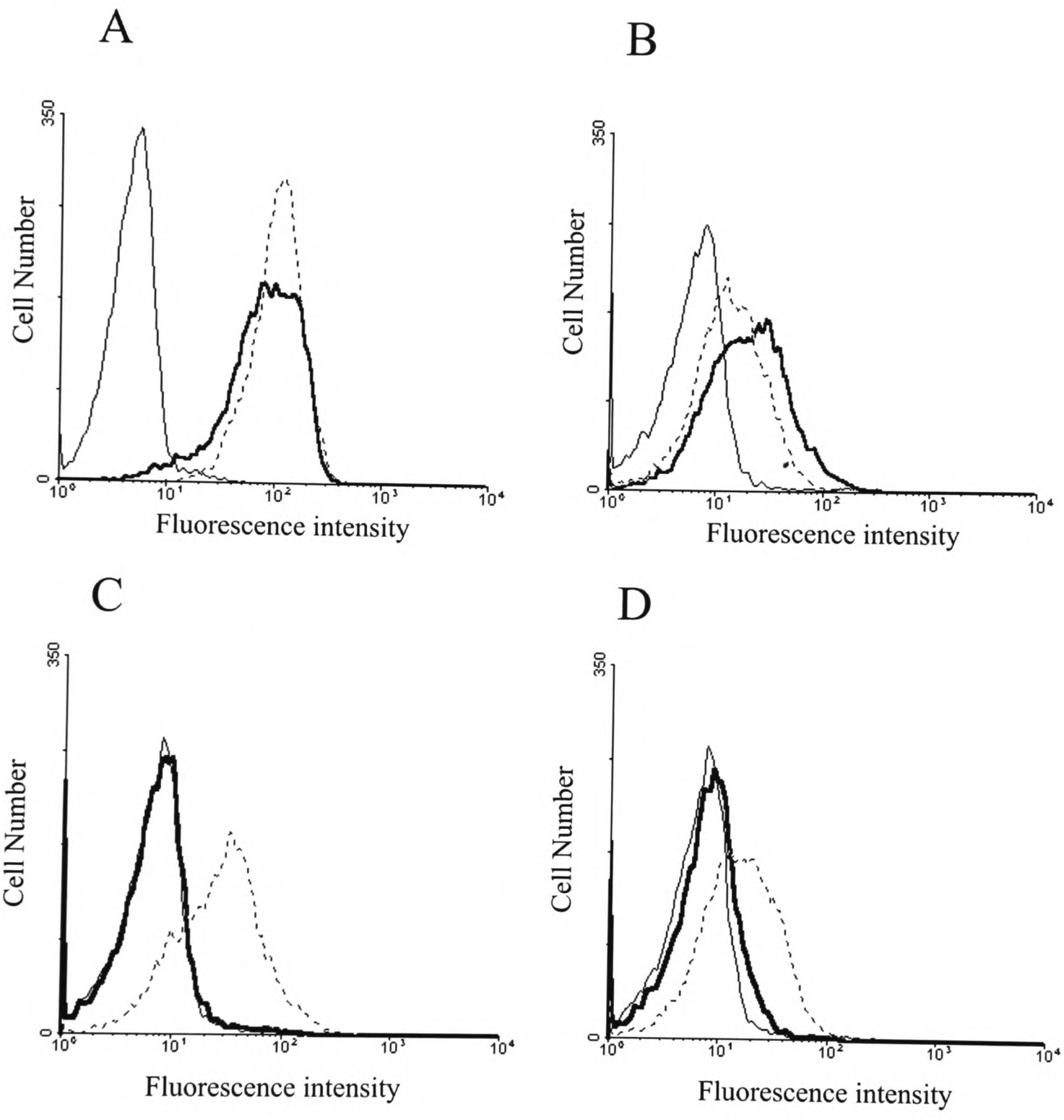

Figure 6-4. Rat and mouse OX-2R coated beads bind native OX-2 antigen on rat thymocytes. (A) Staining of rat thymocytes with MRC OX-1 (dotted line), MRC OX-2 (bold line) and an isotype matched negative control mAb MRC OX-21. (B) Rat thymocytes preincubated with MRC OX-21 bound rat (bold) and mouse (dotted) OX-2RCD4d3+4 coated beads compared to a negative control (CD4d3+4). Rat thymocytes pre-incubated with MRC OX-2 (bold) but not MRC OX-1 (dotted) were able to block the binding of rat OX-2RCD4d3+4 coated beads (C) and mouse OX-2RCD4d3+4 coated beads (D) back to the negative control (CD4d3+4 coated beads -cells preincubated with MRC OX-1).

6.5 Recombinant soluble OX-2 and OX-2R proteins interact *in vitro*

The definitive proof that a direct interaction has been identified is to show that the interaction can be demonstrated using purified components. This was demonstrated for OX-2 and its receptor using surface plasmon resonance, a technique which allows the measuring of protein:protein interactions in real time and which is discussed in detail in section 7-2. The experiment is shown diagrammatically in Figure 6-5. Purified, monomeric rat OX-2CD4d3+4 was injected over three flow cells containing biotinylated recombinant forms of the rat and mouse OX-2Rs and a negative control (biotinylated CD4d3+4) connected in series. All the biotinylated constructs were immobilised via their biotin tag onto a streptavidin coated chip and the relative amount of binding in each flow cell measured.

The results (Fig. 6-6) demonstrate that both the rat and mouse OX-2R were able to bind purified rOX-2CD4d3+4 indicating all components necessary for the interaction have been identified. In addition, the MRC OX-102 mAb binds rOX-2R and if this binding is allowed to reach saturation, the mAb prevents any further binding of rat OX-2 as expected. Both purified and crude TCS of the mAb MRC OX-88 (IgM) failed to bind mouse OX-2R (data not shown) indicating that the blocking observed using this mAb on mouse macrophages was not due to the mAb binding this protein. It is possible that the large IgM isotype might be able to exhibit blocking effects by binding to an associated protein at the macrophage cell surface or recognise a carbohydrate epitope present on mouse macrophages but not on recombinantly expressed material.

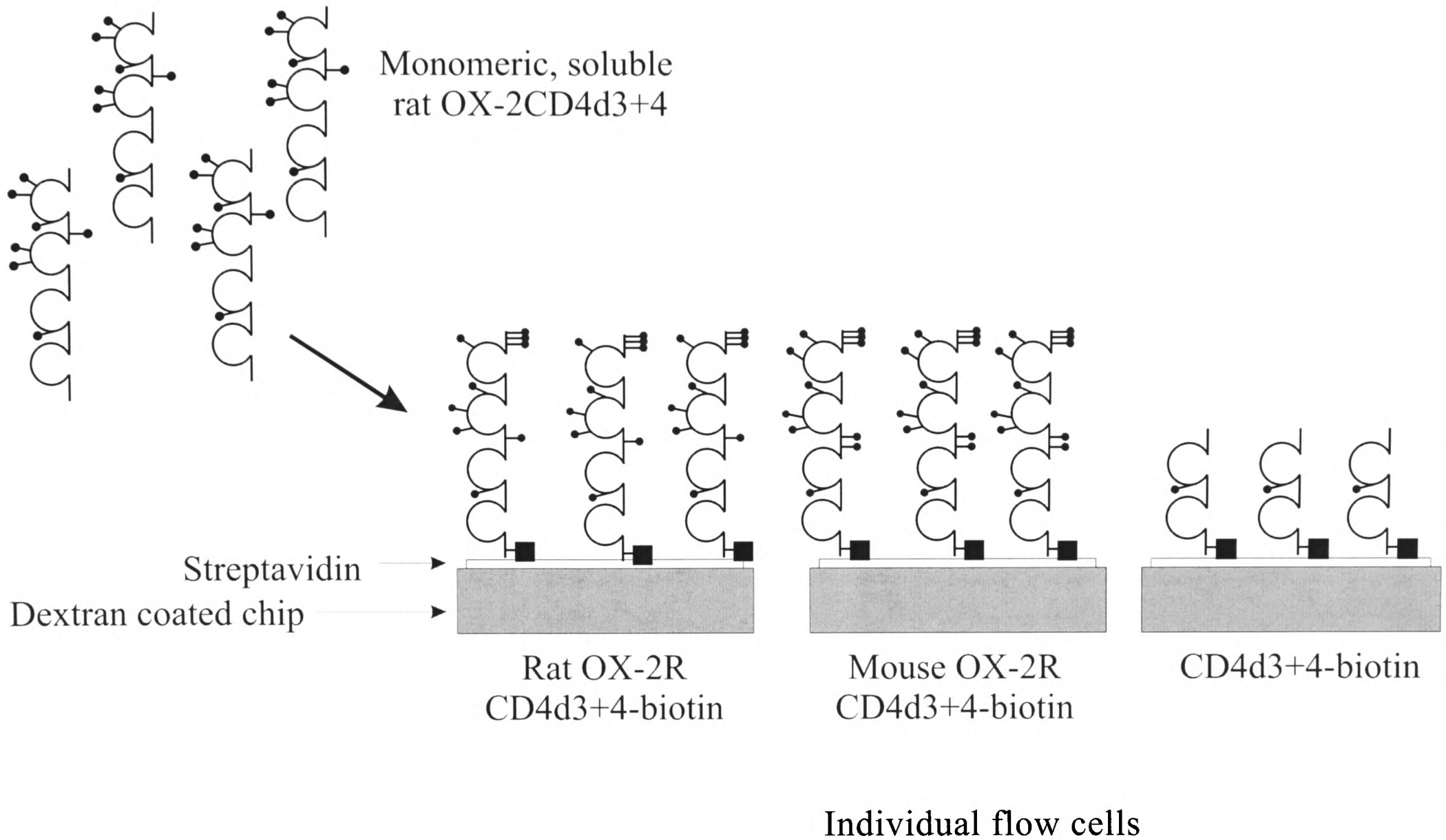

Figure 6-5. Protein:protein interactions were quantitated by surface plasmon resonance. A typical experiment is shown schematically. Streptavidin was covalently coupled to the dextran matrix of the chip, washed and then the biotinylated OX-2Rs and control constructs were immobilised in individual flow cells. Purified, soluble monomeric rat OX-2CD4d3+4 was then injected through all flow cells which are connected in series. The extent of binding is determined by the subtracting the response observed in the control flow cell (CD4d3+4) from that in the query flow cells.

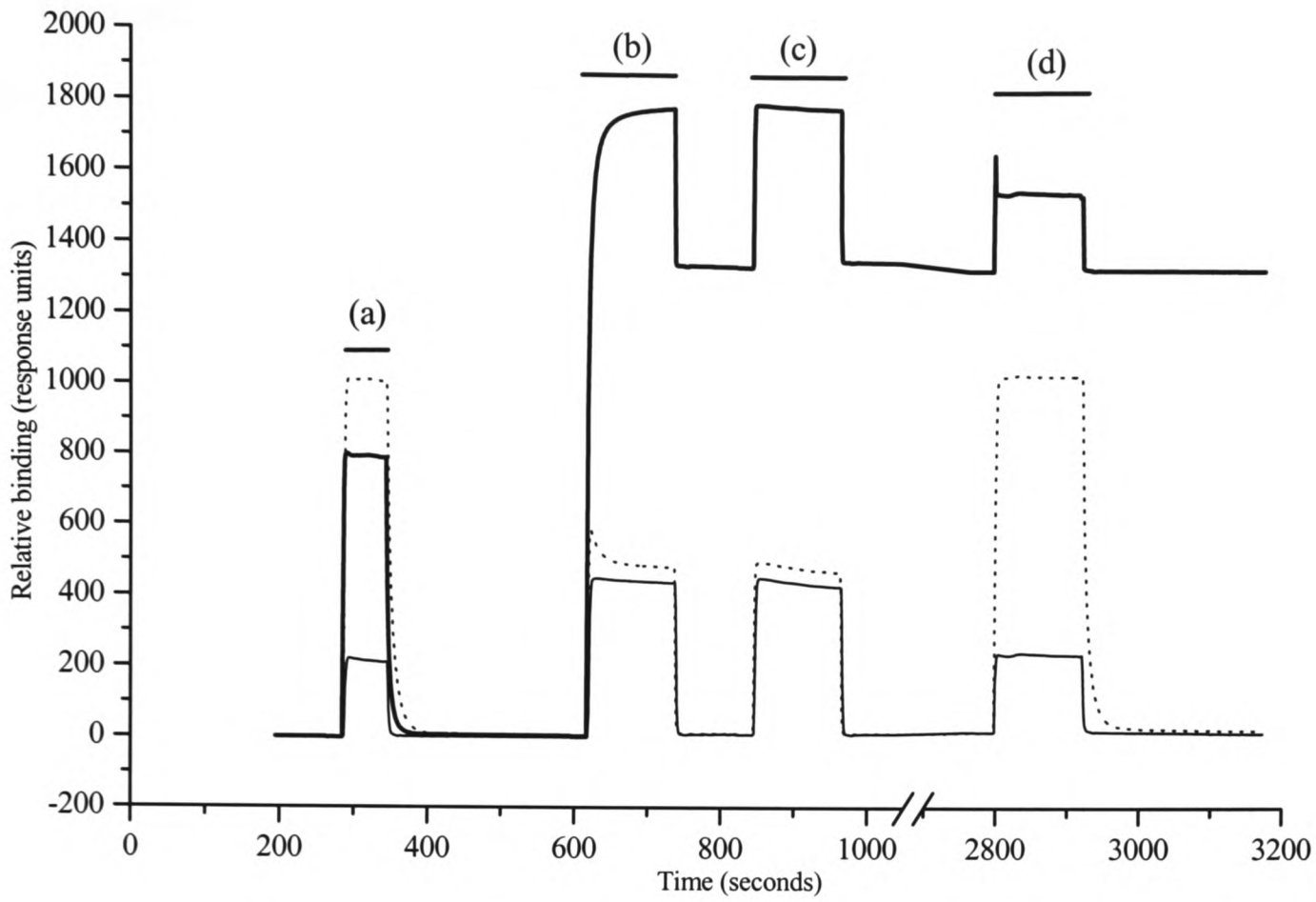

Figure 6-6. Recombinant rOX-2R and rOX-2 interact and this interaction can be blocked by MRC OX-102 mAb. 1030RU of rat (bold), 1415RU of mouse (dashed) OX-2RCD4d3+4-bio and 1839RU of CD4d3+4-bio (negative control) were immobilised on a streptavidin coated chip in separate flow cells as depicted in Figure 6-5. (a) represents the injection of 9.5μM purified rat OX-2CD4d3+4 for the duration indicated by the bar and the responses in each flow cell have been normalised to allow ease of comparison. Notice that both rat and mouse OX-2R flow cells showed binding above that seen in the negative control. Also, the observed binding is highly transient, reaching equilibrium very quickly and returning to base line almost immediately after the termination of the injection suggestive of very fast interaction kinetics. The bar labelled (b) represents the duration of the injection of purified MRC OX-102 mAb at 0.5mgml^{-1}. Notice that the MRC OX-102 mAb bound only the rat OX-2RCD4d3+4 significantly above the negative control and that the binding characteristics differ from the OX-2 in that a plateau is reached slower and upon washing, the antibody remained bound and dissociated slowly. This is typical of a high affinity interaction with a slow dissociation rate. The rOX-2RCD4d3+4-bio constructs were shown to be saturated with mAb since a further injection of MRC OX-102 mAb (c) led to no further increase in binding (the changes in RU upon mAb injection were due to the high concentration of protein within the flowcell and is no different to that observed in the control flow cells –compare with injection (b)). Each flow cell was then reinjected with rOX-2CD4d3+4 (d). The mOX-2R was still able to bind the injected OX-2 but the rOX-2R is now blocked, demonstrating the ability of the MRC OX-102 mAb to block the binding of rat OX-2 to the rat OX-2R.

6.6 Discussion

The experiments described in this chapter have shown that the OX-102 Ag was the sole gene product both necessary and sufficient to confer the ability to bind OX-2 and was thus renamed the rat OX-2 receptor (rOX-2R). In addition, the mouse homologue of the OX-102 Ag (mOX-2R) has also been demonstrated to specifically bind to rat OX-2 indicating it too is an OX-2 receptor. The ability of the MRC OX-2 mAb when preincubated with rat thymocytes to block the binding of rat OX-2R coated beads back to a negative control indicated the presence of no other ligand for OX-2R on rat thymocytes. The observation that the MRC OX-88 mAb did not bind the mOX-2R suggests that the mOX-2R is not responsible for binding rat OX-2 coated beads to mouse PECs and that multiple OX-2 ligands may exist on these cells. It is also possible that the IgM isotype was able to prevent the binding of rat OX-2 coated beads to mouse macrophages by binding to a closely associated protein to the mOX-2R or possibly a carbohydrate determinant expressed by mouse macrophages but not by the HEK 293T cell line. The latter suggestion might explain the low affinity since many antibodies recognising carbohydrate are of the IgM isotype since these antigens are usually T-cell independent. However, mAbs raised to glycans are only rarely observed between mice and rats since carbohydrate structures are highly conserved between these species. It is worth noting that MRC OX-102 blocks rOX-2 binding to rat PECs back to a negative control (Fig. 3-3B) suggesting that multiple ligands don't exist on these cell types in this species.

Several two domain IgSF containing CAMs expressed by leukocytes have been shown to bind multiple ligands e.g. CD80 and CD86 bind both CTLA-4 and CD28 (Greene et al., 1996; van der Merwe et al., 1997) and more recently CD48 has been shown to interact with both CD2 and 2B4 (Brown et al., 1998). Thus, although these results suggest that there are no further ligands for either OX-2 or the OX-2R this cannot be completely excluded. Further ligands may exist but may be expressed on the cell surface of rare cells or cells in a

specific developmental state or expressed at levels below the threshold of detection using the bead assay.

Chapter Seven

Kinetic analysis of the rat OX-2:OX-2R interaction

7.1 Introduction

Leukocytes interact reversibly and transiently with the cells of other tissues enabling them to continue their migratory passage throughout the blood and lymphatics in search of pathogens (van der Merwe and Barclay, 1994). These transient interactions are mediated by cell surface molecules whose interaction characteristics are typically of low affinity and have half-lives which are fractions of a second, providing a biochemical explanation for their ability to freely migrate. OX-2, due to its expression pattern, was thought to contribute to the regulatory messages delivered to migratory cells in their passage throughout the body and was consequently predicted to interact in a transient manner.

The characterisation of a new ligand receptor pair enables the interaction characteristics to be analysed in more detail using surface plasmon resonance and then compared to other measured interactions. The characteristics of an interaction have evolved over millions of years to perform a certain function and therefore precise measurements of protein:protein interaction characteristics may allow us to predict function from analysis of the way in which the two proteins interact.

Therefore, this chapter describes the use of surface plasmon resonance to characterise the details of the rat OX-2:OX-2R interaction. The two proteins were found to interact with a low affinity (2.5μM) which was due to very fast off rate kinetics ($k_{off} = 0.8s^{-1}$, interaction half life of 0.9s), values comparable to other measured leukocyte CAM interactions.

7.2 Use of surface plasmon resonance: the BIAcore instrument

The BIAcore instrument combines miniaturised fluid delivery with an optical sensor and is well suited to the study of low affinity interactions (Jonsson et al., 1991). Binding is measured in real time (up to 10 Hz resolution) and therefore thermodynamic and kinetic data

from even very low affinity and highly transient interactions can be obtained. Each flow cell has a volume of 60nl and one side is bounded by a disposable sensor chip containing a hydrophilic dextran matrix to which a ligand can be covalently coupled (Johnsson et al., 1991). Small volumes (μl) of crude or purified samples containing ligands are then injected through the flow cells which are usually all connected in series. If the macromolecule in the injected sample binds to the immobilised ligand, the resultant increase in mass within the matrix leads to an increase in the refractive index near the sensor surface. This increase is detected by the BIAcore instrument using a sensitive optical technique based on surface plasmon resonance. The binding response is measured in response units (RU) and an increase of 100RU is approximately equivalent to an increase of a protein concentration of $1mgml^{-1}$ within the dextran matrix (Jonsson et al., 1991).

7.2.1 Using SPR to measure low affinity interactions

SPR is now a popular technique used to measure low affinity interactions and experience has shown it to be a reliable method of obtaining both thermodynamic and kinetic measurements provided certain artefacts can be accounted for and excluded (van der Merwe and Barclay, 1996; Davis et al., 1998b).

The first use of this technique to measure the kinetics of low affinity interactions highlighted the problem of protein aggregates (van der Merwe et al., 1993) which influenced the observed association and dissociation binding phases of an interaction. It is critical that the measured interaction be monovalent since increasing the binding valency leads to dramatic, but unpredictable, increases in the avidity of the interaction. These low abundance (often <2% of the analyte) multimeric protein aggregates have a tendency to form in purified protein stored at concentrations of greater than $1mgml^{-1}$. The presence of aggregates results

in the measurement of very slow on and off rates and it is thus very important to exclude these effects when obtaining kinetic data, indeed, when the measured k_{on} is < $x10^4 M^{-1}$ s^{-1} then the presence of aggregates should be excluded (Davis et al., 1998b).

An additional source of error is that part of the response signal represents background due to the injection of concentrated protein solutions over the chip. This background signal, which is measured in a control flow cell, must be subtracted from the signal in the query flow cell and the difference represents the true level of binding. A second potential source of error is that the association and dissociation of two interacting proteins can be limited by the rate at which the injected protein becomes accessible to the immobilised protein in the matrix. The problems associated with this mass-transport effect can usually be identified by observing increases in K_{off} measurements when the level of immobilised ligand is decreased and usually adequately addressed by using high ($100\mu l min^{-1}$) flow rates. Lastly, it is possible that the dissociated protein will rebind to the immobilised protein during the washout (dissociation) phase which also leads to an underestimate of the dissociation rate. Again, a high flow rate will minimise this effect and the amount of rebinding can be assessed by comparing the dissociation rate calculated from two flow cells containing a high and a low level of immobilised ligand.

7.3 Purification and analysis of rat OX-2CD4d3+4

Soluble rat OX-2CD4d3+4 was purified from spent tissue culture supernatant of a stably transfected CHO.K1 line by immunoaffinity chromatography using a MRC OX-68 column. Positive fractions were pooled and dialysed into PBS/10mM sodium azide at 4°C and then concentrated to 0.6mls using Centricon spin concentrators. The purified protein ran as a single band of expected mass on SDS-PAGE (data not shown). A preliminary analysis

of this preparation by SPR showed that it contained rOX-2R binding activity which had two phase association and dissociation characteristics indicating the presence of higher order multivalent aggregates (data not shown). The purified protein was further resolved by gel filtration and the protein eluted as a single peak (data not shown). The amino acid composition of a known quantity of protein (as measured by optical density at 280nm) was determined using amino acid analysis by A.Willis, MRC Immunochemistry Unit, Oxford University and used to calculate the extinction coefficient of the protein ($44439 M^{-1}cm^{-1}$). The bulk of the purified protein was shown to be antigenically active since at least 90% of the protein could be immunoprecipitated by MRC OX-2 mAb (data not shown).

7.4 Equilibrium binding affinity constant of the rat OX-2:rOX-2R interaction

BIAcore experiments were conducted by covalently coupling streptavidin to the dextran matrix of all four flow cells within a research grade CM5 sensor chip via free amino groups. After washing, different levels of either biotinylated rat OX-2RCD4d3+4 (rOX-2RCD4d3+4) and a negative control (CD4d3+4-bio) were attached to the streptavidin within individual flow cells. The affinity of the rOX-2:rOX-2R interaction was calculated by injecting varying levels of purified, monomeric rOX-2CD4d3+4 through the flow cells and measuring the amount of binding achieved once equilibrium had been reached. Binding is represented by the difference in response units (RU) observed between the flow cells containing the rOX-2R and the background response in the control flow cell -a typical experiment is shown in Figure 7-1A. The data are plotted as a conventional binding curve (Fig. 7-1B) and as a Scatchard transformation (Fig. 7-1B-inset) and the Kd of the interaction calculated by both non-linear curve fitting and Scatchard transformation. The results of several experiments are shown in Table 7-1.

Temperature (°C)	Level of rOX-2R immobilised (RU)	K_d (μM)	
		Scatchard analysis	Non-linear curve fitting
37	1010	2.08	2.45
37	220	2.03	2.45
37	80	2.62	3.33
25	1155	1.70	1.77

Table 7-1. Equilibrium binding affinity of the rat OX-2:OX-2R interaction. The Kd of the rat OX-2:OX-2R interaction were determined at different levels of receptor immobilisation and at two different temperatures. The Kd values obtained at a receptor immobilisation level of only 80RU are probably not as accurate as the values obtained from higher levels of receptor immobilisation since the level of binding achieved at equilibrium was low and varied between experiments. The increase in equilibrium affinity (decreased K_d) as temperature is decreased is due to the fact that the binding reaction is exothermic.

7.5 Kinetic analysis of the interaction

Kinetic analysis of the interaction was performed at a flow rate of 100μlmin^{-1} to minimise mass transport and rebinding effects. Two different concentrations of rOX-2CD4d3+4 were injected over flow cells containing different levels of immobilised rOX-2RCD4d3+4-bio and a control (CD4d3+4-bio). The response in the control flow cell was subtracted from each of the query sensorgrams after alignment using the BIAevaluation (version 3.0) software. The resulting dissociation curves were then normalised, plotted and then a first order exponential decay curve fitted to the data and the K_{off} value determined (Table 7-2). The dissociation curves obtained using injected 14.5μM rOX-2CD4d3+4 are shown in Figure 7-2.

Figure 7-1. Rat OX-2 interacts with its receptor with an affinity of 2.5μM. (A) 5μl of increasing (as shown) then decreasing (data not shown) concentrations of Rat OX-2CD4d3+4 were injected (bars) at 20μl/min through flow cells with 1,010RU of rOX-2RCD4d3+4-biotin (solid trace) or 1444RU of CD4d3+4-biotin (dotted trace) immobilised. The amount of rOX-2 that bound rOX-2R at each concentration was calculated as the average difference between the response at equilibrium in the rOX-2R and control flow cell during the increasing and decreasing phases and is plotted in (B).
(B) The solid line in the main plot represents a non-linear fit of the Langmuir binding isotherm to the data, yielding a K_d of 2.45μM. Shown inset is a Scatchard plot of the same data, which by linear regression yields a K_d of 2.1 μM.

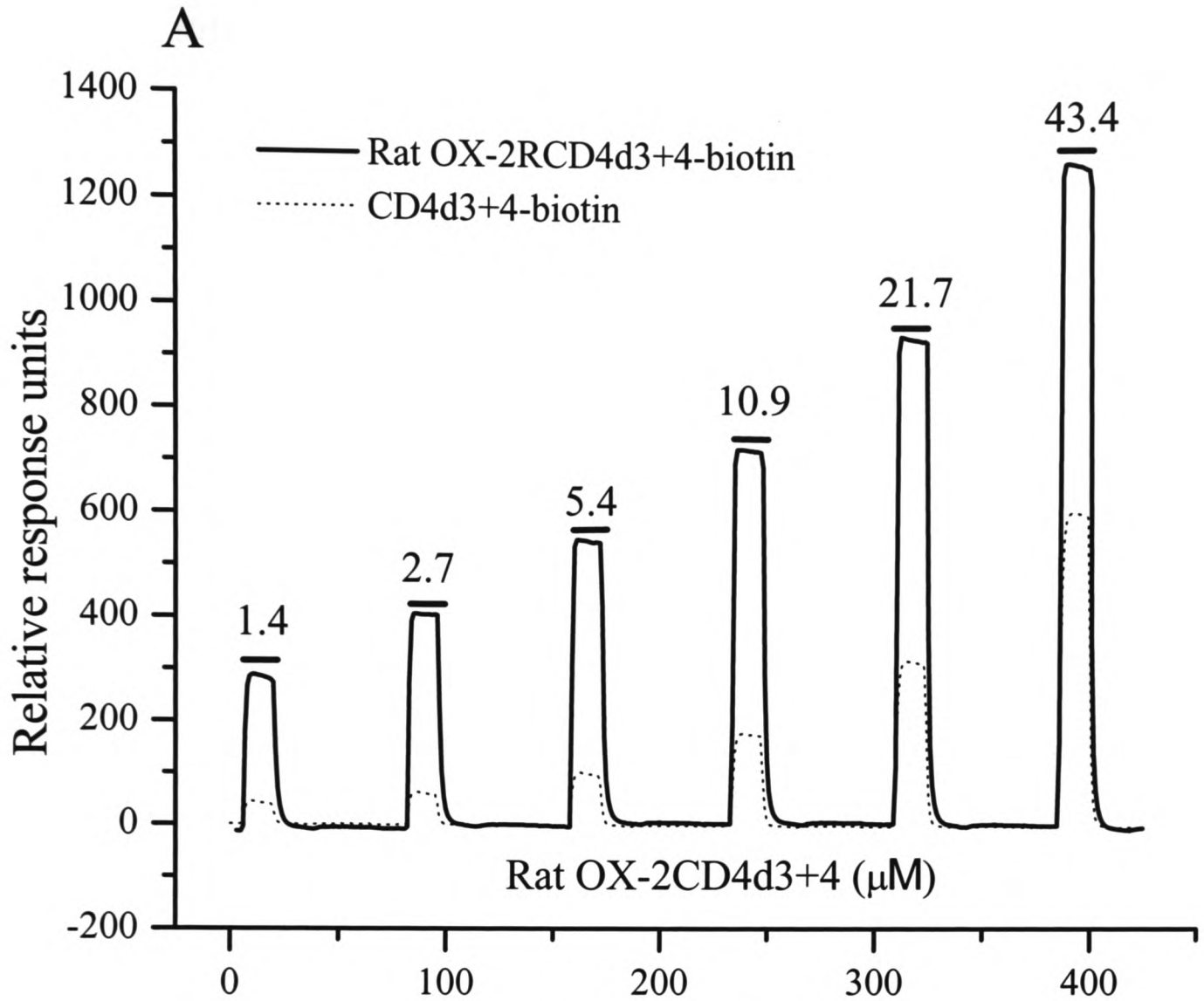
A
Rat OX-2RCD4d3+4-biotin
CD4d3+4-biotin
Relative response units
1400
1200
1000
800
600
400
200
0
-200
1.4
2.7
5.4
10.9
21.7
43.4
Rat OX-2CD4d3+4 (μM)
0
100
200
300
400
Time (seconds)

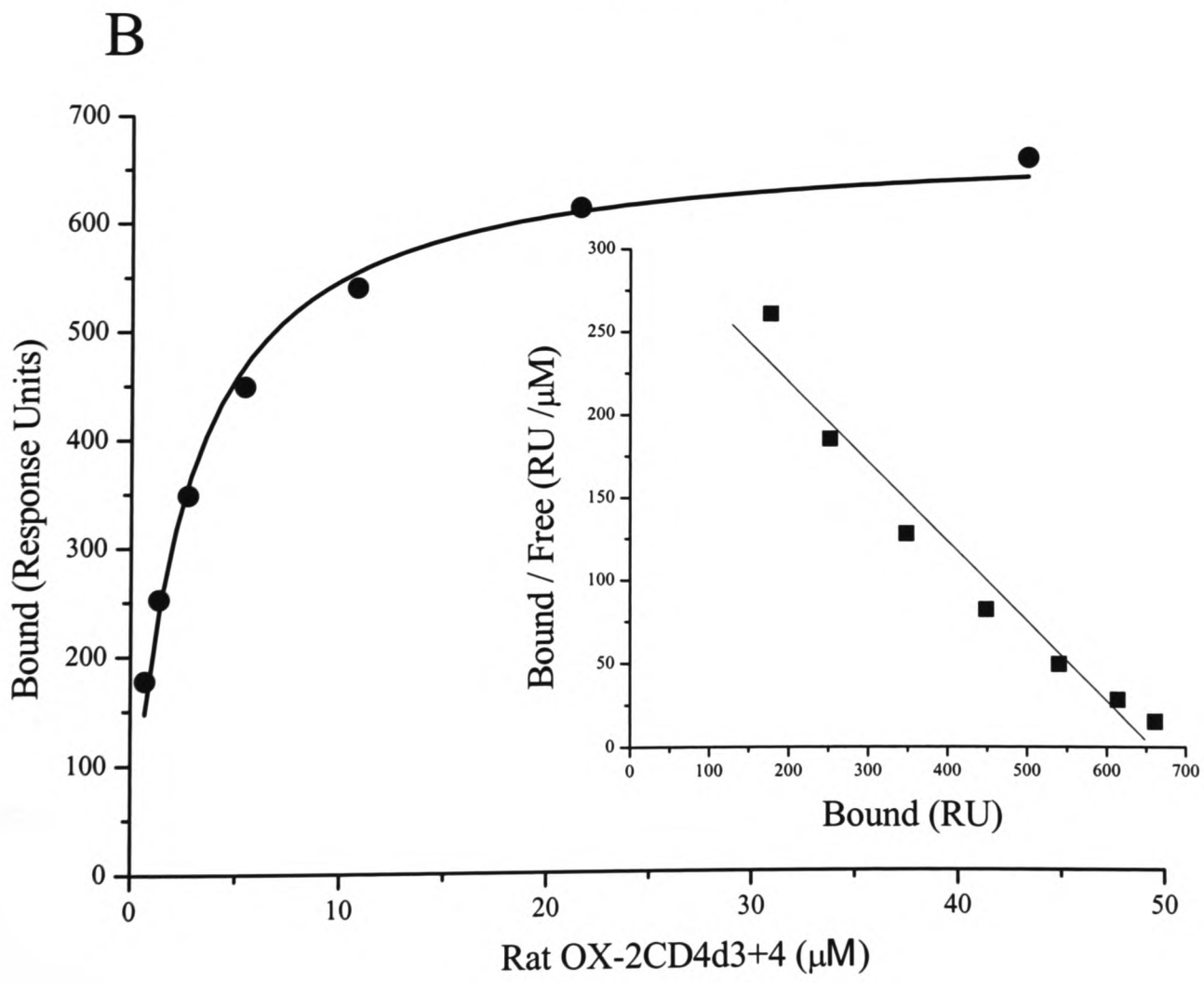
B
Bound (Response Units)
700
600
500
400
300
200
100
0
0
10
20
30
40
50
Rat OX-2CD4d3+4 (μM)
Bound / Free (RU /μM)
300
250
200
150
100
50
0
0
100
200
300
400
500
600
700
Bound (RU)

Amount of rOX-2R immobilised (RU)	Concentration of injected rOX-2CD4d3+4 (μM)	Calculated K_{off} (s^{-1})
1013	14.5	0.84
1013	1.6	0.72
605	14.5	0.89
605	1.6	0.76

Table 7-2. Kinetic analysis of the rat OX-2:OX-2R interaction. The K_{off} values of the rat OX-2:OX-2R interaction were obtained using two different rat OX-2 concentrations and receptor immobilisation levels.

The difference in the calculated K_{off} value when using either 14.5 or 1.6μM rat OX-2CD4d3+4 are probably due to pipetting errors when the rat OX-2 was diluted to each separate concentration. The slight increases in K_{off} upon decreasing the immobilised ligand level at each concentration of injected OX-2 indicates that some mass transport/rebinding effects are influencing the K_{off} measurement. However, these are relatively insignificant and the two dissociation curves are basically super-imposable upon each other (Fig. 7-2).

The K_{on} values for each experiment were calculated (Table 7-3) using the BIAevaluation (version 3.0) software (using the K_{off} values calculated for each above) over a fit of the association phase using a simple 1:1 binding model. The data fitted the model well, indicated by the low residual errors and suggests that the two proteins bound with a 1:1 stoichiometry. In all cases, the K_{on} value was unremarkable for a protein:protein interaction and was always greater than $3x10^5 M^{-1}s^{-1}$, excluding the possibility that higher order aggregates were dominating the measured binding. The accuracy of these rate constants were assessed by comparing their ratio (K_{off} / K_{on}) which represents a calculated Kd or Kd_{calc}. The Kd_{calc} for each set of data was in good agreement with the Kd values obtained directly from equilibrium binding (~ 2.5μM) indicating consistency between equilibrium and kinetic measurements.

Amount of rOX-2R immobilised (RU)	Concentration of injected rOX-2 (μM)	K_{on} ($M^{-1}s^{-1}$)	Residuals (RU)	K_{off} (s^{-1})	Kd_{calc} (μM)
1013	14.5	$3.5x10^5$	+/- 4.0	0.84	2.4
1013	1.6	$4.8x10^5$	+/- 1.0	0.72	1.5
605	14.5	$4.6x10^5$	+/- 1.0	0.89	1.9
605	1.6	$8.6x10^5$	+/- 0.5	0.76	0.9

Table 7-3. Summary of kinetic measurements of the rat OX-2:OX-2R interaction. The table shows the K_{on} values calculated by fitting the association data to a simple 1:1 binding model using the K_{off} values obtained as described above. The quality of the fit to the model is indicated by the residual errors and each set of kinetic data was used to calculate a theoretical affinity constant (Kd_{calc}).

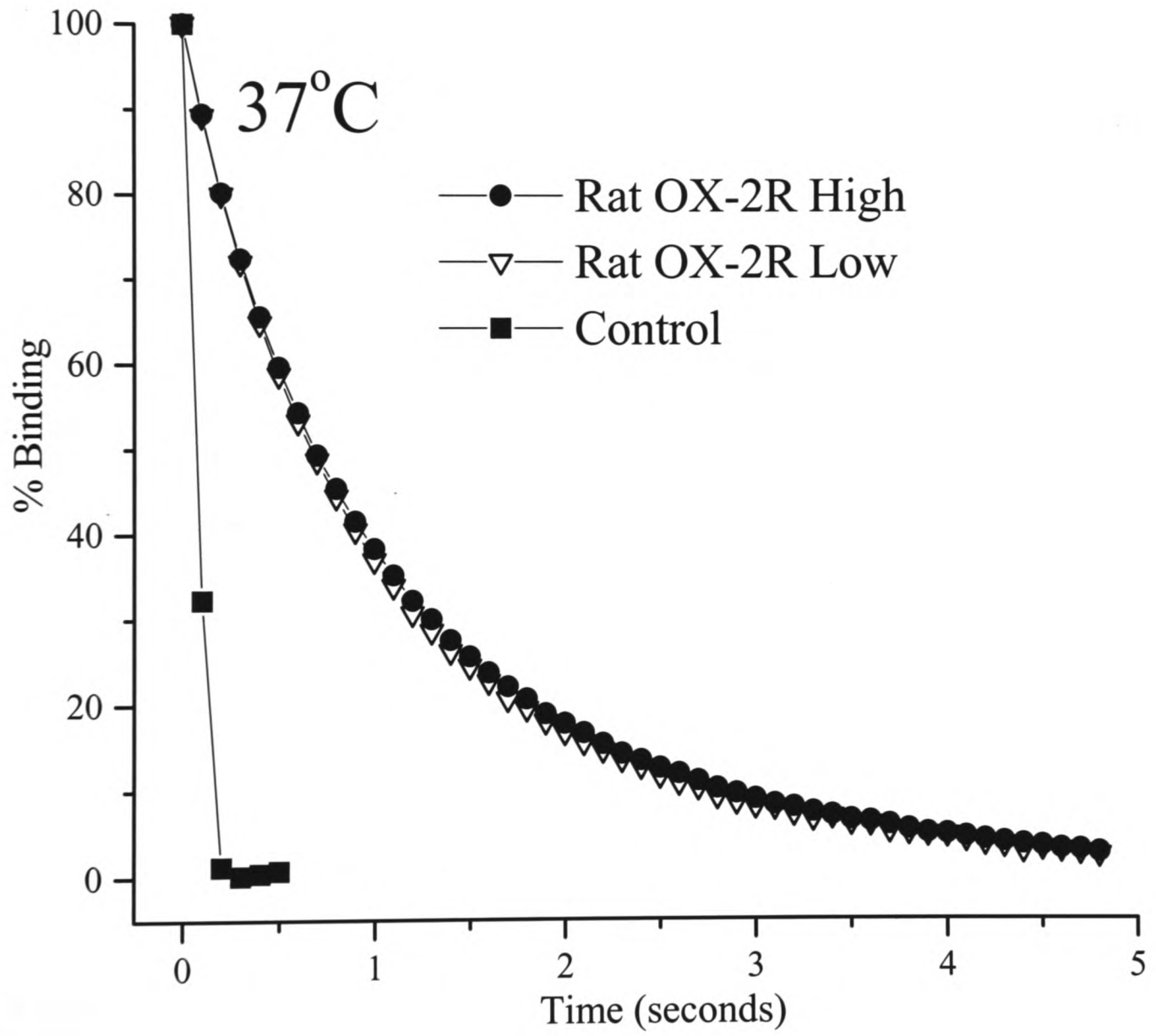

Figure 7-2. Kinetics of the rOX-2:rOX-2R interaction. 5μl of soluble rOX-2CD4d3+4 (14.5μM) was injected at 100μl/min over immobilised rOX-2RCD4d3+4-biotin at high (1,013RU) and low (604RU) and also a negative control CD4d3+4-biotin (1,100RU) and data collected at 10Hz. The response in the control flow cell was subtracted from the rOX-2R flow cells and the data normalised (100% at the start of the dissociation phase) and first order exponential decay curves fitted to the data which yielded K_{off} values of 0.80 s^{-1}.

7.6 Discussion

The use of SPR to measure the thermodynamic and kinetic characteristics of an interaction necessitates the need to account for several artefacts which could influence the parameters measured. The data presented in this chapter are able to account for these artefacts which include the exclusion of protein aggregates and an assessment of the effects of mass transport and rebinding on the determination of kinetic constants providing strong evidence that the results presented here are accurate.

The thermodynamic and kinetic characteristics of the rat OX-2:OX-2R interaction correlate well with other values obtained from similar analyses of known leukocyte cell surface protein interactions (Fig. 7-3). This confirms the prediction that OX-2 does interact with its receptor in a transient fashion ($t_{1/2}$ =0.9seconds) and explains the need to use a highly avid multivalent binding reagent to identify the interaction.

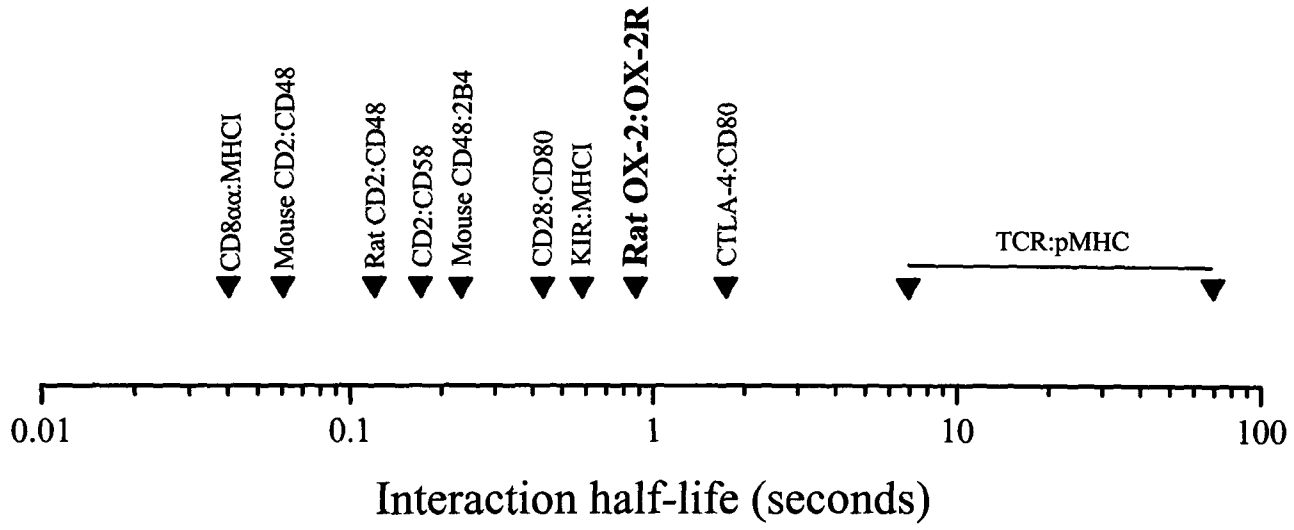

Figure 7-3. Comparison of the interaction half-lives of measured leukocyte cell surface interactions. The interaction half-lives were calculated from the off rate constants taken from (Maenaka et al., 1999). Note that the interactions mediated by antigen receptors (TCR/BCR) are not thought to be rigid body association but require conformational adjustments upon binding and therefore can be considered as a special class of low affinity interaction (Willcox et al., 1999; Maenaka et al., 1999).

The off rate constant or half-life of the interaction is considered important since it is this value which ultimately is responsible for the interaction affinity since the on rates of most protein:protein (macromolecular) interactions tend to vary much less and are usually in the order of $10^5/10^6$ M^{-1} s^{-1}.

The limited number of interactions for which kinetic data are available, coupled with our relatively poor knowledge regarding the biological outcome of these interactions, makes a correlation between the two difficult to suggest. However, the thermodynamic and kinetic properties of an interaction have been determined by millions of years of evolution and presumably are therefore directly related to the biological role of the proteins. Whilst the limiting amount of available data makes conclusive corollaries inappropriate, (Fig. 7-3) Davis and van der Merwe (personal communication) have suggested that slightly higher affinity interactions may be a feature of proteins delivering an inhibitory signal. They suggest that protein interactions between cell surface molecules with a slightly higher affinity may hinder the free diffusion of stimulatory adhesion pairs into the contact zone formed between two opposing membranes (Grakoui et al., 1999). Both CTLA-4:CD80 and the KIR:MHCI are reported as delivering an inhibitory signal (Oosterwegel et al., 1999; Lanier, 1998) and have slightly higher affinities than those implicated in a stimulatory role. The OX-2:OX-2R interaction has an affinity between that reported for these two interactions (Fig. 7-3) suggesting that the interaction may deliver an inhibitory signal.

The nature of these low affinity interactions have been well studied in the rat CD2:CD48 interaction (Davis et al., 1998a) and now supported by the recent structure of the CD2:CD58 heterophilic adhesion complex (Wang et al., 1999). These studies show that the binding faces of the two interacting proteins are flat and have virtually no surface-shape complementarity, in contrast to high affinity interactions such as those mediated by antibodies and proteases (Davis et al., 1998a). In addition, the binding faces are highly

charged and binding involves the formation of many hydrogen bonds and salt links between complementary charges on each binding face (Wang et al., 1999). These charged residues do not contribute to the binding energy of the interaction (the equilibrium binding affinity of the rat CD2:CD48 interaction did not alter when ionic strength was varied) but enable the proteins to maintain their binding specificity without any additional increases in affinity (Davis et al., 1998a).

The good fit of the association phase data with a 1:1 binding model is good evidence that the two glycoproteins interact with a 1:1 stoichiometry. In addition, it is likely that the two molecules associate in a rigid body fashion and will not require conformational adjustments since the equilibrium affinity is only slightly increased upon performing equilibrium binding at 25°C compared to 37°C (Table 7-1). This is in contrast to the interactions mediated by the TCR which shows a dramatic temperature dependence due to loss of flexibility upon ligand binding (Willcox et al., 1999).

Chapter Eight

Functional aspects of the OX-2 receptor:

Distribution and signalling

8.1 Introduction

A huge step forward in understanding the function of the OX-2 glycoprotein has been achieved by the molecular characterisation of the OX-2 receptor. It is now possible to address functional questions in the context of knowing which two proteins are interacting. One of the most important issues when considering the function of the two proteins is an appreciation of their spatio-temporal distribution within an organism and thus identifying where and when they are able to initiate communication. Section 1.6.2 described the detailed distribution data available for OX-2 and a preliminary analysis for the distribution of the OX-2R is described in this chapter. Unfortunately, all attempts to use the MRC OX-102 mAb for immunohistochemistry of unfixed and fixed tissue sections failed and so distribution studies have so far been restricted to the isolation of cell type and analysis by two-colour cytofluorimetry.

In contrast to OX-2, the OX-2R has a substantial cytoplasmic region, which despite the absence of any well characterised signalling motif, contains three tyrosine residues perfectly conserved between rat and mouse. These tyrosine residues, if they have the ability to be phosphorylated, suggest a biochemical mechanism for regulating intracellular signals by the recruitment of SH2 domain containing molecules.

In summary, this chapter describes preliminary data which suggests that the OX-2R can be detected on the cell surfaces of macrophages isolated from different anatomical locations, dendritic cells, granulocytes and monocytes and that the rOX-2R can be phosphorylated on tyrosine residues after pervanadate activation, indicating it has the potential to generate intracellular signals.

8.2 rOX-2R is expressed by cells of myeloid origin

Single stain cytofluorimetry using the MRC OX-102 mAb determined that the OX-2R was present on IFN-γ stimulated alveolar macrophages (Fig. 8-1A) and dendritic cells (Fig. 8-1B/C). Rat lymph dendritic cells were estimated to be 30% pure by morphology and therefore it is difficult to prove that the MRC OX-102$^+$ population are indeed dendritic cells. However, the size (side scatter) of the MRC OX-62$^+$ population (a rat dendritic cell marker) correlated very well with the size of the MRC OX-102$^+$ population, suggesting that the OX-2R$^+$ population are indeed dendritic cells (Fig. 8-1C). Thymocytes, ConA and LPS activated and unactivated splenocytes did not show any staining of MRC OX-102 above negative controls (data not shown).

The use of multicolour cytofluorimetry would allow the phenotype of the OX-2R$^+$ cell types to be analysed in more detail and greater confidence and therefore the MRC OX-102 mAb was biotinylated. Purified MRC OX-102 was biotinylated at molar 40:1 (biotin :mAb), a ratio which gives the best signal:noise ratio for FACS analysis as determined by experiment (data not shown).

Rat PECs and PBMCs were doubly stained with biotinylated MRC OX-102 and a range of other mAbs (MRC OX-2, 6, 33, 34, 39, 41, 48, 62, 82) (Table 2-2). MRC OX-102 stained ~80% of the cells from the peritoneal cavity (Fig. 8-2A/B), consistent with the positive cell type being the macrophage. MRC OX-102$^+$ cells were predominantly brightly stained, although there was a small population of cells which were MRC OX-102^{dull}. Both the MRC OX-102$^+$ populations were MRC OX-41$^+$, however, the MRC OX-102^{dull} but not ^{bright} were MRC OX-34$^+$ (rat CD2) (Fig. 8-2B). The nature of these MRC OX-41$^+$, MRC OX-34$^+$ cells is not clear. They could be a subpopulation of T-cells or NK cells which are known to express CD2 but the low levels of OX-2R expression questions its biological role in these cells.

Rat PBMCs which had not been fractionated by size or density contained a significant population of MRC OX-102^{dull} and a very small MRC OX-102^{bright} population. Both populations of MRC OX-102^{+} cells were again MRC OX-41^{+} suggesting that the positively staining population was the monocyte, granulocyte or dendritic cell. Further distribution studies are required to distinguish between these possibilities. Interestingly, the MRC OX-102^{+} cells were not positive for MRC OX-2, 33, 34, 39, 48, 62 or 82 (Table 2-2) but did show some MRC OX-6 (MHC II) staining (data not shown).

The presence of MRC OX-102 on a minor cell type in the spleen can be inferred due the ability to purify the OX-102 antigen from rat splenic lysates.

The presence (or absence) of the OX-2R in the nervous system is an important question which must be addressed due to the high levels of OX-2 expression in this tissue. However, repeated attempts to stain rat brain sections with the MRC OX-102 mAb did not yield any interpretable results. The neonatal rat cerebellum expresses large amounts of OX-2 and this tissue was homogenised and subjected to western blotting with the MRC OX-102 mAb. No bands of the expected size were seen suggesting that it is not an abundantly expressed protein in this tissue (data not shown).

Figure 8-1. OX-2R is expressed on rat IFN-γ stimulated alveolar macrophages and dendritic cells. (A) Rat alveolar macrophages were harvested and stimulated as described in section 2.6.1.4 before FACS analysis. The cells were stained with mAbs MRC OX-102 (bold) and an isotype matched negative control MRC OX-21. (B) Rat lymph dendritic cells were a gift of Dr Gordon MacPherson and were estimated to be 30% pure by morphology and stained with a rat dendritic cell marker MRC OX-62 (dotted line), MRC OX-102 (bold) and an isotype matched negative control MRC OX-21. (C) The same data collected in (B) is plotted as a dot plot comparing the side scatter with stained fluorescence (i) MRC OX-21, (ii) MRC OX-62, (iii) MRC OX-102.

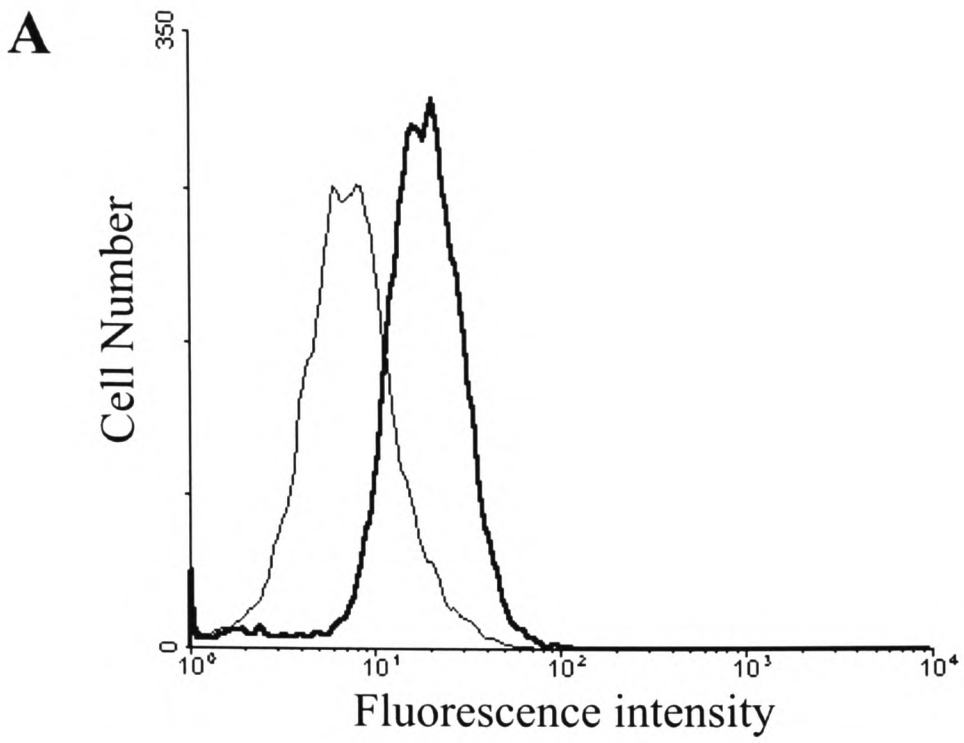
A
350
0
Cell Number
10⁰
10¹
10²
10³
10⁴
Fluorescence intensity

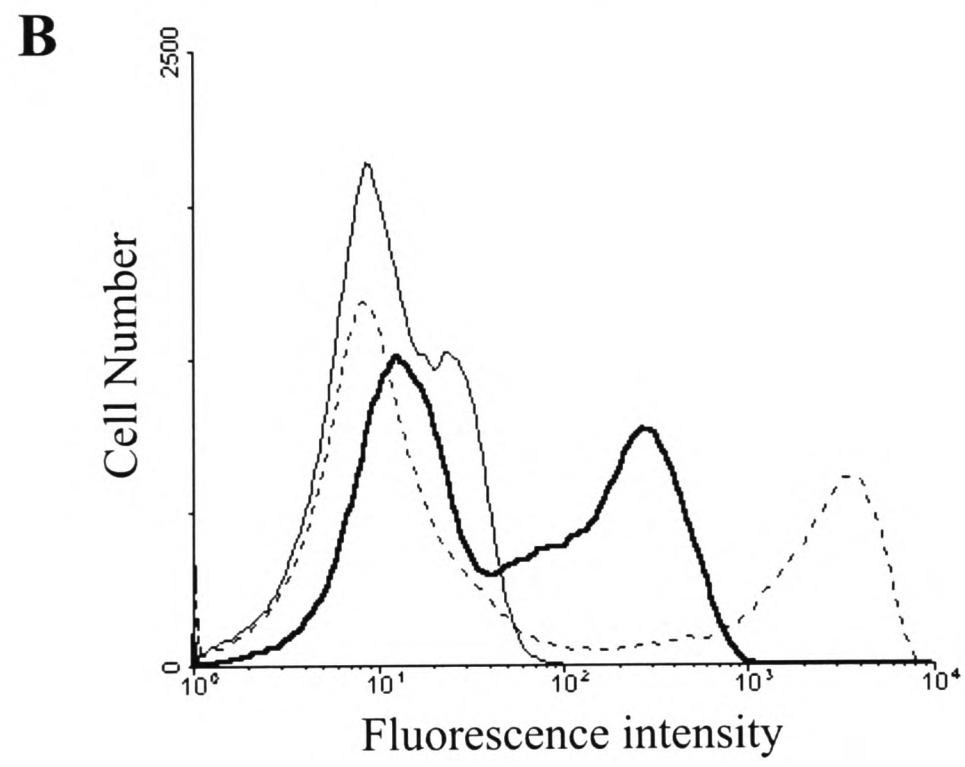
B
2500
0
Cell Number
10⁰
10¹
10²
10³
10⁴
Fluorescence intensity

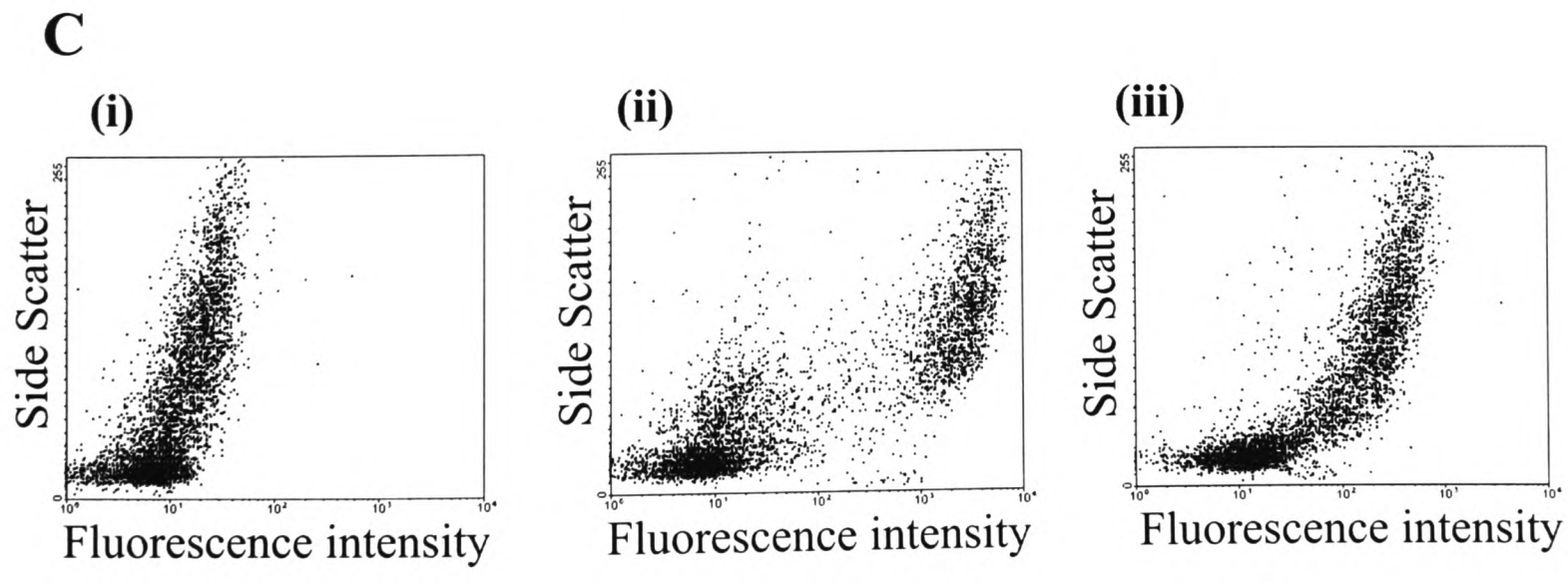
C
(i)
(ii)
(iii)
Side Scatter
255
0
10⁰
10¹
10²
10³
10⁴
Fluorescence intensity

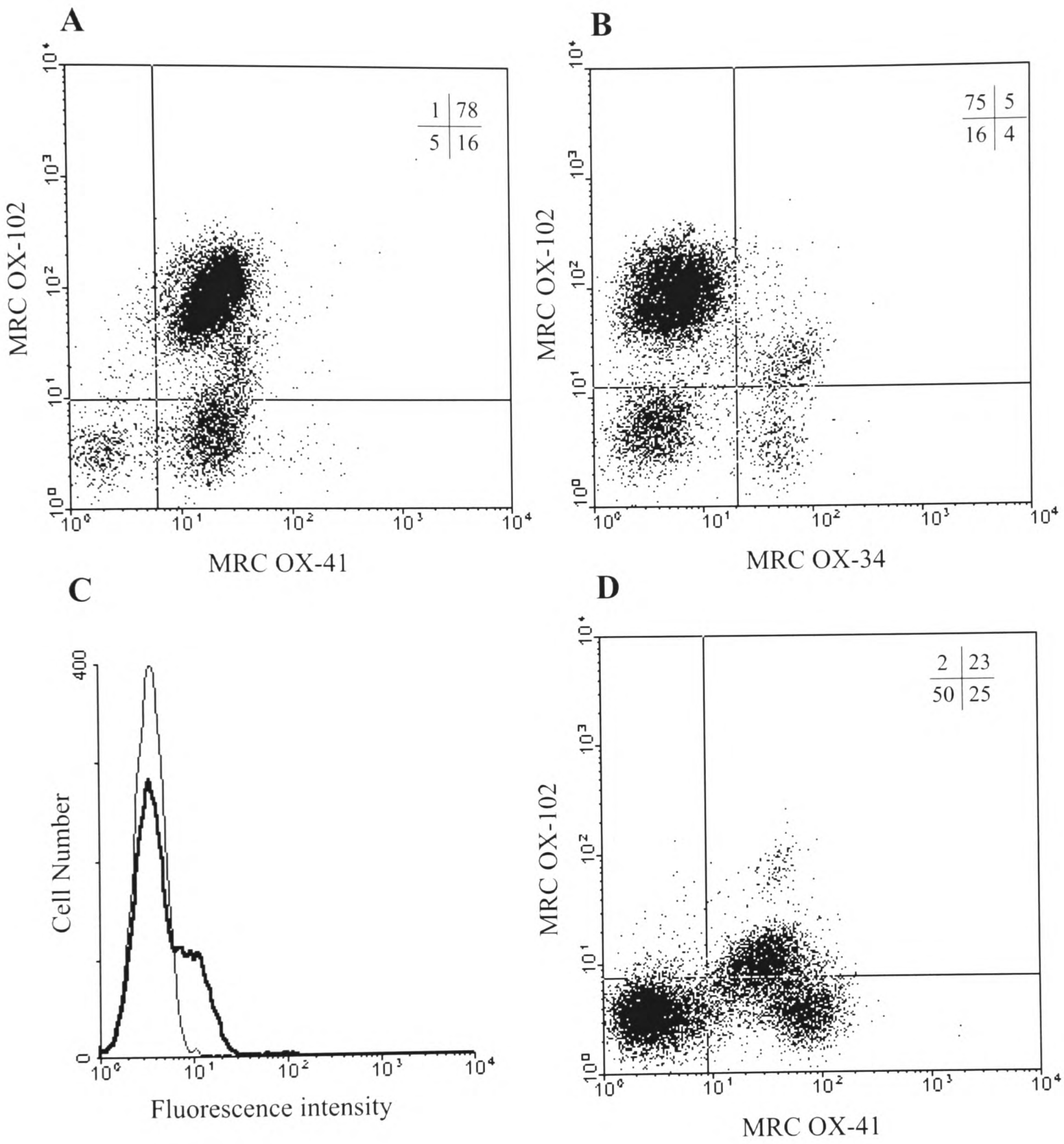

Figure 8-2. OX-2R is expressed on MRC OX-41$^+$ cells in both the peritoneal cavity and peripheral blood. Rat PECs (A) and (B) were stained with MRC OX-102 and MRC OX-41 (A) and MRC OX-34 (B). (C) Total rat PBMCs were stained with biotinylated MRC OX-102 (bold) and a biotinylated isotype matched negative control (MRC OX-21). (D) Double staining of rat PBMCs with MRC OX-102 and MRC OX-41. The numbers represent the percentage of events in that quadrant.

8.3 rOX-2R is tyrosine phosphorylated upon pervanadate activation

A mechanism of intracellular signal initiation is the reversible phosphorylation of tyrosine residues present in the cytoplasmic portion of the cell surface molecule. The overall phosphorylation state of the tyrosine substrates is determined by the sum of the tyrosine kinase and phosphatase activities in the appropriate localisation. The use of tyrosine phosphatase inhibitors such as pervanadate allows a gratuitous phosphorylation state of the molecule to be visualised, usually by western blotting immunoprecipitated proteins with mAbs specific to phosphotyrosine.

Resident rat PECs were activated with 1mM pervanadate as described in section 2.6.2.2, lysed and immunoprecipitated using MRC OX-102 coupled Sepharose beads or control beads. The immunoprecipitates were resolved by SDS-PAGE, blotted onto nitrocellulose and probed with an anti-phosphotyrosine mAb or control (Fig. 8-3). A strong band of appropriate size is seen in stimulated but not unstimulated cells indicating the potential of the tyrosines to be phosphorylated and thereby recruit SH2 domain containing molecules to regulate intracellular signals.

Figure 8-3. Rat OX-2R is phosphorylated on tyrosine residues upon pervanadate activation. Rat PECs were stimulated with pervanadate (P+) or left unstimulated (P-), lysed and the OX-2R immunoprecipitated with MRC OX-102 mAb coupled Sepharose beads or control beads (RET-PE2 mAb coupled Sepharose was a kind gift of Mr Peter Kirk). The immunoprecipitates were resolved under reducing conditions on a 10% acrylamide gel, blotted and probed with an anti-phosphotyrosine (α-PY) mAb 4G10 or a negative control (MRC OX-21).

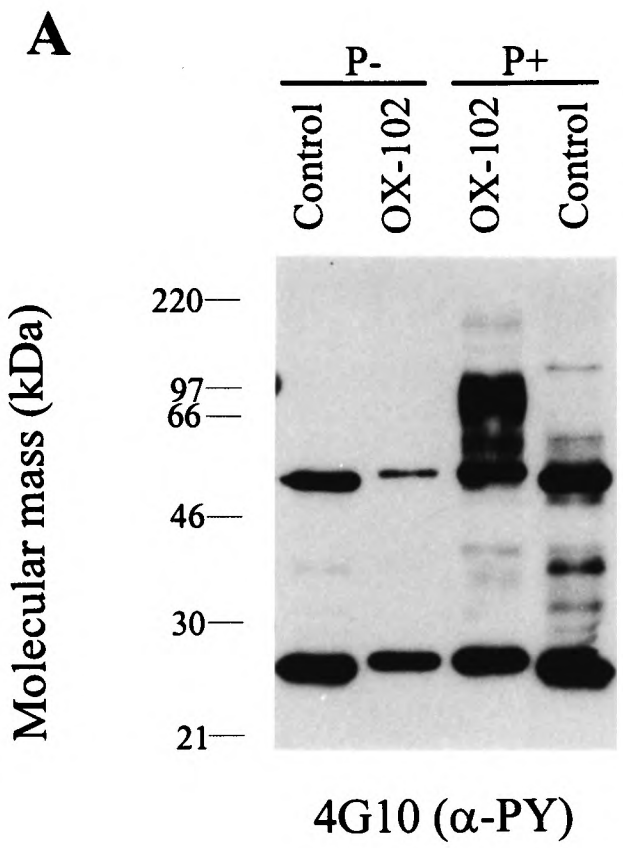
A
P-
P+
Control
OX-102
OX-102
Control
Molecular mass (kDa)
220
97
66
46
30
21
4G10 (α-PY)
B
P-
P+
Control
OX-102
OX-102
Control
Molecular mass (kDa)
220
97
66
46
30
21
MRC OX-21

8.4 Discussion

The distribution of the OX-2R appears to be restricted to haematopoietic cell types and in particular, cells of myeloid origin. In contrast, OX-2 is expressed on the cell surfaces of a diverse range of tissues, which, arguably will not share the need for a recently evolved signal delivered through the OX-2 protein. Thus, the expression of the OX-2R on a more restricted and functionally analogous cell type suggests that the main signalling events would be propagated within OX-2R$^+$ cells. This hypothesis is supported by the fact that the OX-2R has a substantial (67 amino acid) cytoplasmic tail which can be phosphorylated and the OX-2 cytoplasmic tail is short and contains no known signalling motifs. This would suggest that the role of OX-2 is simply to "mark" certain tissues which regulate myeloid cellular function and that the OX-2R is the protein through which these regulatory signals are delivered. A consequence of this hypothesis is that the diverse range of tissues which express OX-2 have a common need to regulate myeloid cellular function. However, this shared regulatory requirement is not immediately obvious given our current understanding of myeloid cellular function.

The high levels of OX-2 expression on neural tissue suggests the presence of a ligand within the nervous system. The most obvious candidates are the macrophages which reside in neural tissue, which are termed microglia. These cells were found to be weakly MRC OX-102 positive (Dr J.D. Sedgwick, personal communication) after isolation. The meningial macrophage population which co-purify expressed high levels of MRC OX-102. Microglia are mature tissue macrophages whose functions (such as phagocytosis) are "downregulated" (Perry and Gordon, 1991). The mechanism by which various macrophage functions are repressed is not known and the OX-2:OX-2R interaction would be an excellent candidate to account for these observations (see Chapter 10).

A very interesting tissue where OX-2:OX-2R communication could be important is the mammalian ovary. OX-2 is expressed by ovarian tissue which does not develop further such as the stratum granulosum of degenerating follicles (Bukovsky et al., 1983). It is known that follicular degeneration is accompanied by macrophages which invade follicles during the advanced stages of atresia (Takaya et al., 1997; Bukovsky et al., 1995) and this event coincides with the appearance of OX-2 on the surface of the stratum granulosum (Bukovsky et al., 1983). Macrophages are known to mediate many events in the biology of luteogenesis and luteolysis such as follicle development and atresia, ovulation, corpus luteum formation and regression (Gaytan et al., 1998) and thus estimating the function of the OX-2:OX-2R interaction in this tissue is difficult. It is possible that the appearance of OX-2 on degenerating follicular tissue prevents further phagocytosis or proliferation by the invading macrophages.

Chapter Nine

Distribution of the human homologue of OX-2

9.1 Introduction

In order to test the suitability of the rodent model for studying the OX-2:OX-2R interaction with regard to humans, it was necessary to show that the spatio-temporal distribution of the protein of interest is conserved between these species. A highly conserved distribution across species implies that this distribution is important for function. Often, leukocyte cell surface antigens show subtle differences in both the levels of expression and distribution suggesting different non-conserved functions of the proteins between these species. Since it is the protein product which performs function, a study of distribution is best performed at the protein level rather than that of RNA message. The use of monoclonal antibodies would allow cellular and even sub-cellular localisation of the HuOX-2 protein. Prior to these studies, the HuOX-2 homologue had been characterised at the genomic level and message detected in two B-cell lymphomas (MAJA and WI-L2) and "normal" brain but not the thymocyte lines MOLT-4, JURKAT and HSB2 by northern blot (McCaughan et al., 1987a).

Previous work had attempted to generate a HuOX-2CD4d3+4 chimaera by PCR amplification of the extracellular domains of HuOX-2 using oligonucleotides designed from the known genomic sequence and human splenocyte cDNA as a template (K.Starr unpublished data). However, all efforts to express this recombinant protein in COS-7 cells failed. In an attempt to express recombinant HuOX-2, this study transfected a human thymocyte line (Jurkat) and also created a construct where the 2 IgSF domains of HuOX-2 were fused to the rat OX-2 leader sequence but without success. These failures were explained when the HuOX-2 construct was re-sequenced and several cloning artefacts identified.

In summary, this chapter describes the "correction" of a HuOX-2CD4d3+4 clone by site directed mutagenesis, its subsequent expression and the construction of a stably

transfected cell line secreting protein which was correctly folded as assessed by specific binding to rat macrophages. A monoclonal antibody, MRC OX-104 was raised and preliminary distribution studies using both cytofluorimetry and immunohistochemistry show that OX-2 is highly conserved in terms of its spatial distribution and exhibited similar patterns of staining on equivalent cell types between human and rat.

9.2 Correction of cloning errors by site directed mutagenesis

The inability to express the HuOX-2CD4d3+4 chimaeric protein in both COS and Jurkat lines was explained by the identification of cloning artefacts in the originally selected clone. Analysis of other clones revealed that one contained the HuOX-2CD4d3+4 construct in the pBluescript® (Stratagene) cloning vector but encoded a single amino acid substitution (Q3R) attributed to a PCR error by comparison to the genomic sequence (McCaughan et al., 1987a). This clone was used as a template for a PCR reaction using oligonucleotides which allowed cloning inframe to CD4d3+4 into the pEF-BOS expression system via the use of XbaI/SalI digestion. Single stranded, uracil containing mutant HuOX-2(Q3R)CD4d3+4 in pEF-BOS was packaged into phage M13, extracted and an oligonucleotide containing the wild type coding sequence and a diagnostic silent (FspI) restriction site annealed before transformation and wild type revertants selected (section 2.3.6 for detailed methods).

9.3 Production of antigenically active recombinant HuOX-2CD4d3+4

The construct containing the wild type HuOX-2 protein sequence was expressed at levels comparable to both rat and mouse soluble OX-2CD4d3+4 constructs as determined by MRC OX-68 inhibition ELISA (data not shown).

The secreted protein was shown to be antigenically active by immobilising it as a multivalent array around fluorescent beads and presenting it to rat PECs. Rat PECs pre-incubated with MRC OX-45 but not MRC OX-102 were able to bind these HuOX-2 coated beads indicating that the HuOX-2 protein was correctly folded and antigenically active (Fig. 9-1). In addition, this also demonstrated that HuOX-2 was able to bind the rat OX-2R indicating that the binding sites of the two proteins were still capable of interacting despite ~ 40 million years of evolutionary separation.

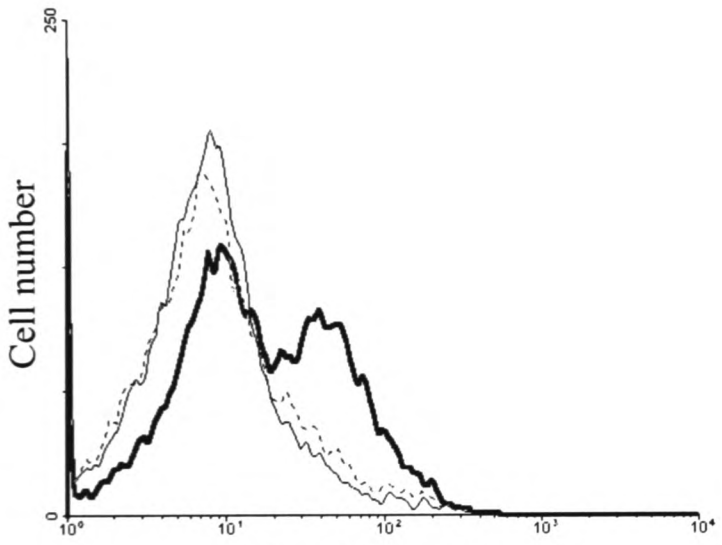

Figure 9-1. Expression of antigenically active HuOX-2CD4d3+4.

HuOX-2CD4d3+4 coated beads were able to bind rat PECs preincubated with MRC OX-45 (bold) but MRC OX-102 (dotted) blocked binding back to a negative control (CD4d3+4 coated beads -cells preincubated with MRC OX-45).

The HuOX-2CD4d3+4 construct was sub-cloned into the plasmid pEE14 allowing the generation of a stable CHO.K1 cell line secreting the construct. A highly secreting stable clone was selected by inhibition ELISA and used to generate large (milligram) quantities of soluble protein. HuOX-2CD4d3+4 was purified from 1 litre of a bulk culture and analysed by SDS-PAGE (Fig. 9-2).

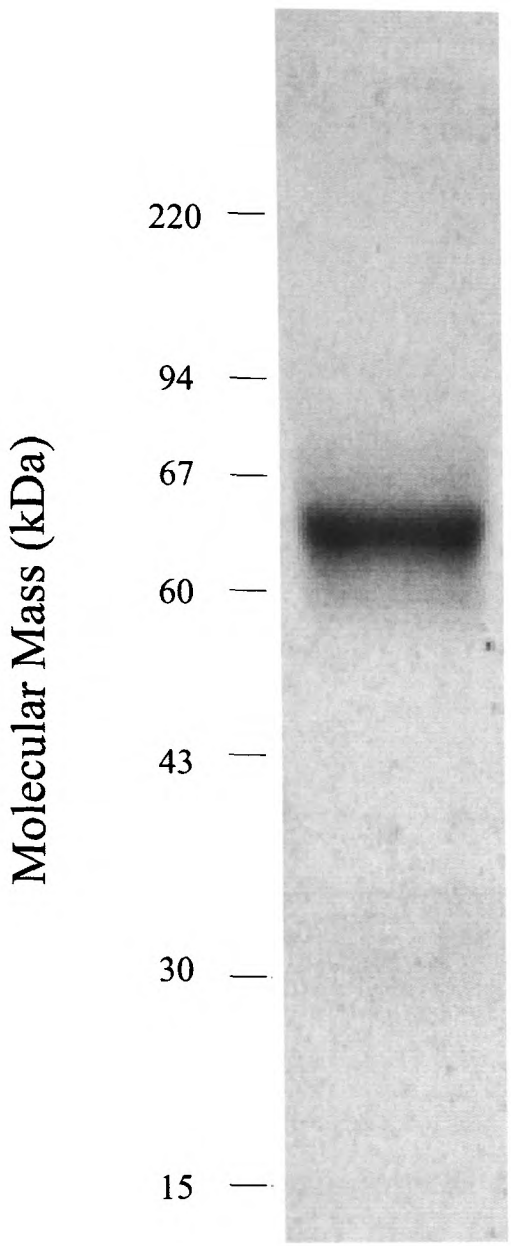

Figure 9-2. Purified HuOX-2CD4d3+4.

2μg of purified HuOX-2CD4d3+4 was resolved under reducing conditions by SDS-PAGE on a 10% gel. The protein was stained and visualised by using a fluorescent SYPRO® -orange dye.

9.4 MRC OX-104, a mouse anti human OX-2 mAb

The purified protein was used to immunise mice according to the schedule in Table 9-1 and the sera of the animals analysed for their responses to the immunogen by direct ELISA (Fig. 9-3).

Procedure:
10μg s.c. in CFA (rest 20 days)
20μg in IFA (equally between two sites) (rest 24 days)
20μg in IFA (equally between two sites) (rest 11 days)
test sera (wait 4 days)
Boost 70μg i.p. (wait 4 days)
Fusion performed

Table 9-1 Immunisation schedule for the production of MRC OX-104.

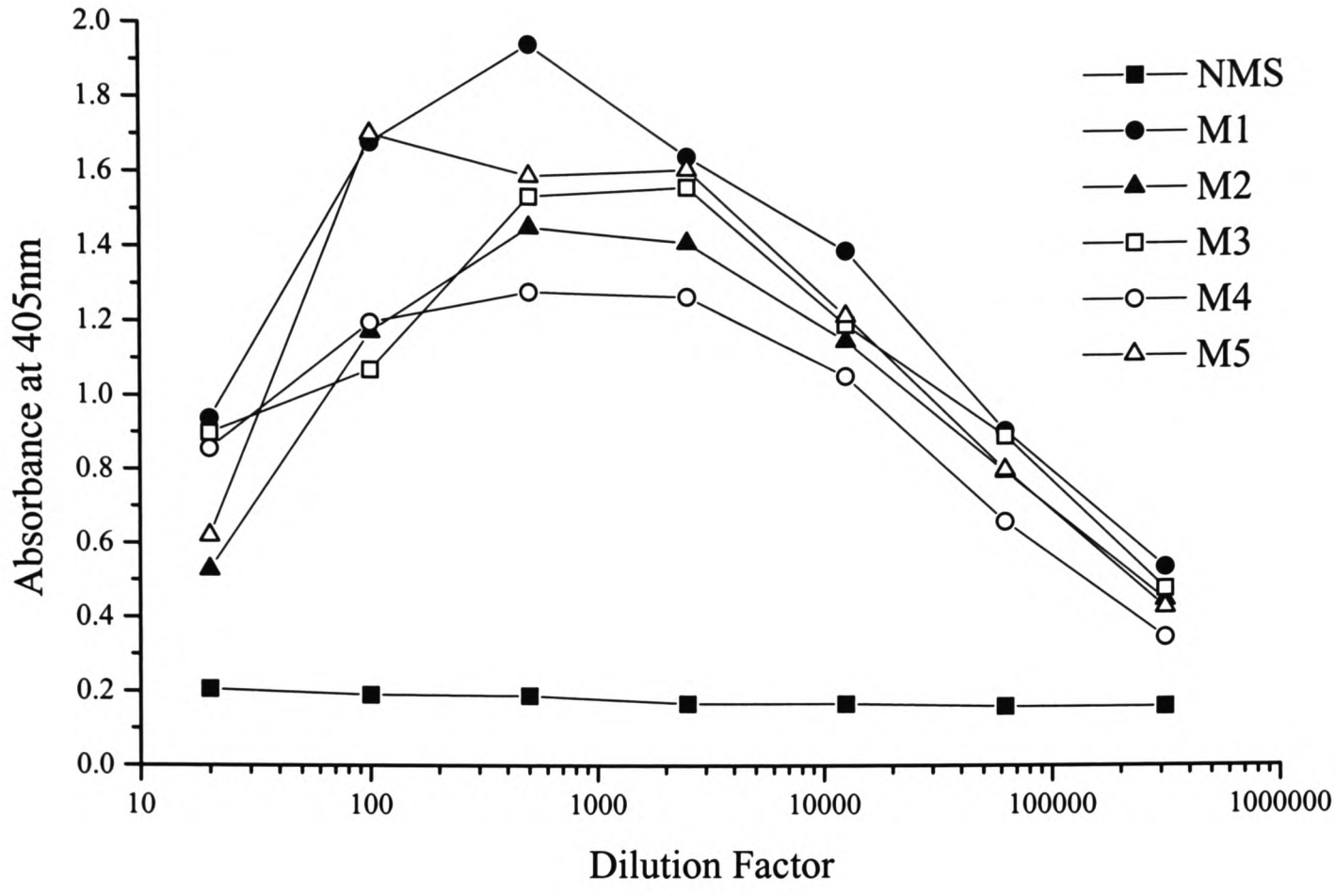

Figure 9-3. Immunological response to the HuOX-2CD4d3+4 protein. The sera from five separate immunised mice (M1 to 5) and an unimmunised control (NMS) were serially diluted and tested for their response to the HuOX-2CD4d3+4 by direct ELISA.

The mice were shown to be generating very good responses (half maximal response at ~1:50,000 dilution) to the immunogen. Interestingly, mice boosted (4th immunisation) with 35μg of protein i.v. died (2 attempts) from apparent cardiovascular collapse, suffering from acute cyanosis and panting. These symptoms have been observed in hyper-immune mice before (Garnett, 1993) and is thought to be due to the formation of large immune complexes causing thrombosis. The final boost was therefore delivered intraperitoneally.

Four days after the boost, the spleen was removed and fused by standard procedures to the NS-1 myeloma by M. Puklavec. 4x96 hybridoma supernatants were initially screened by direct ELISA using purified HuOX-2CD4d3+4 as a target and then whole rat CD4. Surprisingly, all 384 wells were positive for HuOX-2CD4d3+4 indicating both the immunisation schedule and fusion protocol had worked optimally and 25% of these were

found to react strongly with the rat CD4 portion of the immunogen. The top 94 hybridomas giving the best response were tested for binding to the MAJA cell line (data not shown) by cytofluorimetry. 40% of the hybridoma supernatants positive for binding to the HuOX-2 portion of the recombinant molecule in ELISA were able to bind the native protein at the cell surface. One hybridoma was recloned three times and named MRC OX-104 and isotyping revealed it was a mouse IgG_1.

9.5 Distribution of HuOX-2

The MRC OX-104 mAb gave good staining of MAJA cells in flow cytometry (see above) demonstrating the expression of human OX-2 at the cell surface of human tissue for the first time. To characterise the distribution in more detail, human peripheral blood mononuclear cells (PBMC) were stained using three colour flow cytometry and frozen human tissue sections were stained in a collaborative study with Professor D.Y. Mason (Department of Clinical Biochemistry and Cellular Science, John Radcliffe Hospital, Oxford.)

9.5.1 Three colour cytofluorimetry of human PBMC

Human blood was collected from the National Blood Centre, Oxford and PBMCs purified over Ficoll as described in section 2.6.1.5. Approximately 20% of the total PBMCs are MRC OX-104^+ and these can be split into both $CD19^+$ and $CD3^+$ subpopulations (Fig. 9-4). All $CD19^+$ cells are MRC OX-104^+ and approximately a fifth of $CD3^+$ cells are MRC OX-104^+ indicating HuOX-2 is expressed by all re-circulating B cells and at slightly lower levels by a subpopulation of re-circulating T cells. Activation of PBMCs by ConA generated T-blasts, as assessed by an increase in both size and granularity of cells (data not shown) and

CD25 staining (Fig. 9-5). 60% of $CD25^{+}CD3^{+}$ cells express MRC OX-104 at high levels, closely paralleling the situation in rat (data not shown).

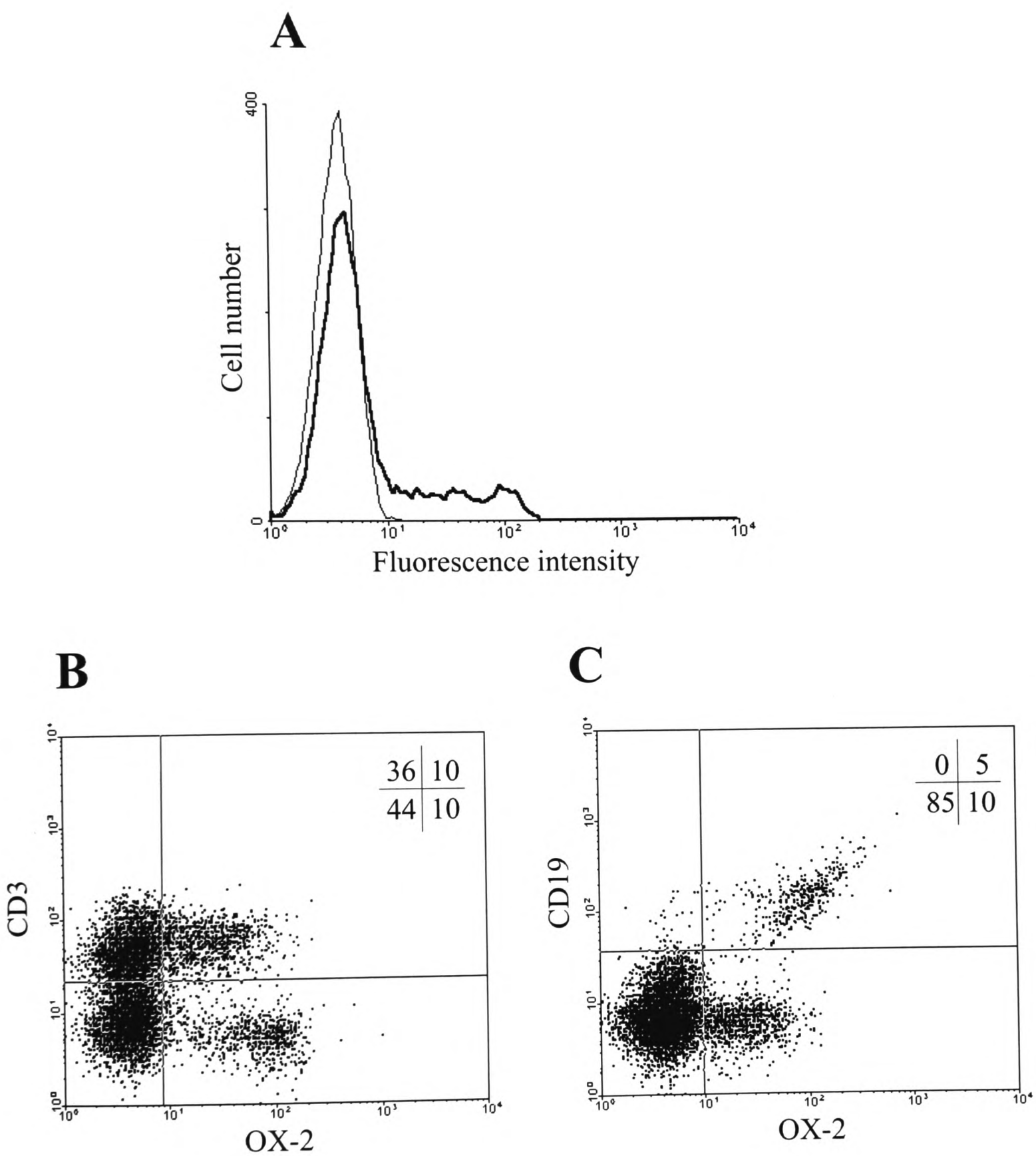

Figure 9-4. OX-2 is expressed on all B-cells and a sub-population of T-cells in human. (A) MRC OX-104 (bold) stained ~20% of total PBMCs when compared to an isotype matched negative control (MRC OX-1). Approximately 20% of all $CD3^{+}$ cells (B) and all $CD19^{+}$ cells (C) were MRC $OX\text{-}104^{+}$. The number of events in each quadrant are expressed as a percentage of the total.

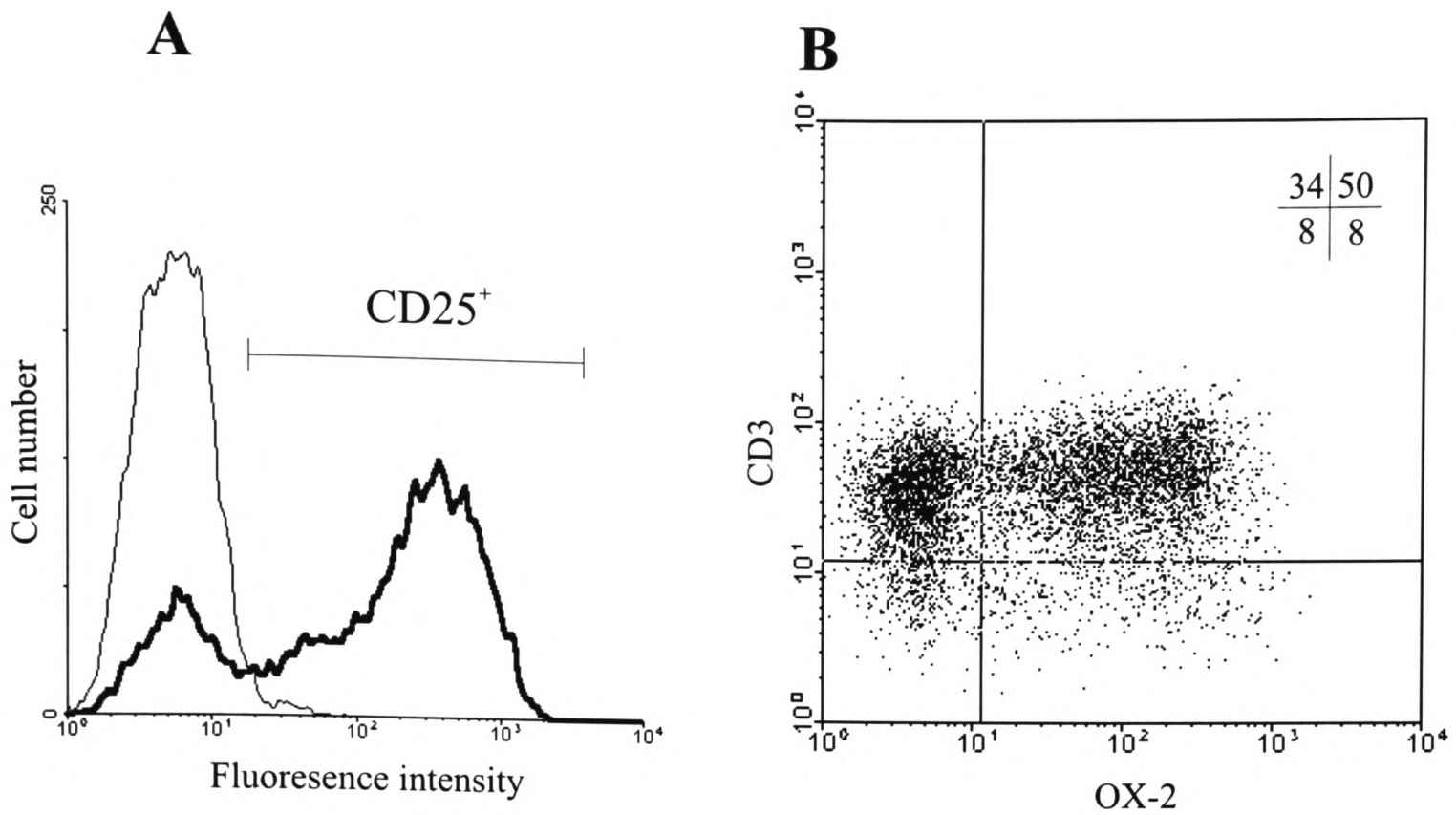

Figure 9-5. OX-2 is expressed by 60% of $CD3^+$,$CD25^+$ T-cells. (A) 3-day ConA-stimulated human PBMCs were stained for the activation marker CD25 (bold) and these activated cells were gated as shown. Approximately 60% of the $CD25^+CD3^+$ cells were MRC $OX\text{-}104^+$. The number of events in each quadrant are expressed as a percentage of the total gated.

9.5.2 Immunohistochemistry

Frozen human tissue sections were stained and visualised as described in section 2.5.7 and sections are shown in Figure 9-6. In all cases, the staining pattern agreed remarkably well with the distribution documented in the rat. The MRC OX-104 mAb gave strong staining in the cerebellum but did not stain the Purkinje cells or glia (Fig. 9-6A) and strongly stained the thymus (data not shown). The follicles of the tonsil were strongly stained (Fig. 9-6B) and this is probably due to the staining of follicular dendritic cells. A consistent feature of the distribution was the staining of vascular endothelium (Fig. 9-6D) in several tissues including the liver, lung, large bowel and extra-follicular regions of the tonsil. The glomeruli of the kidney were characteristically and diffusely stained which could be attributed to the endothelium (Fig. 9-6C). The MRC OX-104 mAb did not stain paraffin fixed sections (D. Mason, personal communication).

9.6 Discussion

The generation of an anti-human OX-2 mAb has allowed the visualisation of HuOX-2 at the protein level for the first time. Studies using this mAb show that the patterns of OX-2 expression are highly conserved between rodents and humans particularly regarding its spatial distribution and possibly the levels at which it is expressed at the cell surface. The levels of expression were found to be high on ConA activated T-cells but slightly lower on re-circulating lymphocytes, a pattern also observed in the rodent model. These conserved features imply that they are important regarding the function of the OX-2 protein. Indeed, the suggestion that OX-2 is expressed by tissues which deliver a regulatory signal to OX-2R$^+$ cell types would require the need for tight control of OX-2 distribution and expression levels to prevent inappropriate regulation. The cellular distribution of other leukocyte cell surface proteins across the same species barrier is often less well conserved, for example, the expression of the Thy-1 (CD90) glycoprotein varies considerably among different species. It is expressed in neural tissue of most vertebrate species and is one of the most abundant glycoproteins present on rat and mouse thymocytes and yet is absent from human thymocytes. In addition, Thy-1 is used as a T-cell marker in mice, but most rat T-cells lack its expression (Campbell et al., 1981).

Interestingly, it was shown that HuOX-2 was able to interact with rat OX-2R at the cell surface indicating that the binding faces of both molecules have been relatively well conserved during evolution. This is not an unusual finding and has been observed in many other systems, for example, mouse CTLA-4 has been reported to interact with both human, bovine and even chicken CD80. However, other, presumably more recently evolved interactions, do not show this behaviour and human CD2/CD48 is unable to interact with either rat or mouse CD48/CD2 respectively (Davis et al., 1998).

The presence of OX-2 homologues in several human herpes viruses raises the possibility that both OX-2 itself and a viral form might be expressed at cell surfaces within an infected individual. Thus, any biological data relating to the viral OX-2 protein can be interpreted with an appreciation of the host OX-2 protein distribution. Experiments to determine whether virally encoded OX-2 proteins are able to interact with the human OX-2R have been initiated and are discussed further in section 10.4.2.

Finally, attempts to western blot and immunoprecipitate with MRC OX-104 failed which prevented a comparison of the biochemical properties (e.g. different glycosylation patterns observed in lymphoid and neural tissue) of the human OX-2 with the rat.

Figure 9-6. Frozen human tissue stained with MRC OX-104. (A) Cerebellum. MRC OX-104 mAb gives strong staining of the molecular layer (M) with patches of staining in the granular layer (G). The Purkinje cells (P) are unstained. (B) Tonsil. The follicles (F) are stained (main picture) and some extra-follicular staining of vascular endothelium (e) is visible. The inset frame is a magnification which suggests that the MRC OX-104 positive cell type is the follicular dendritic cell. (C) Kidney. The glomeruli (G) give strong staining. (D) Vascular endothelium in the follicles. High magnification of the extra-follicular staining shows reveals endothelial structures.

A

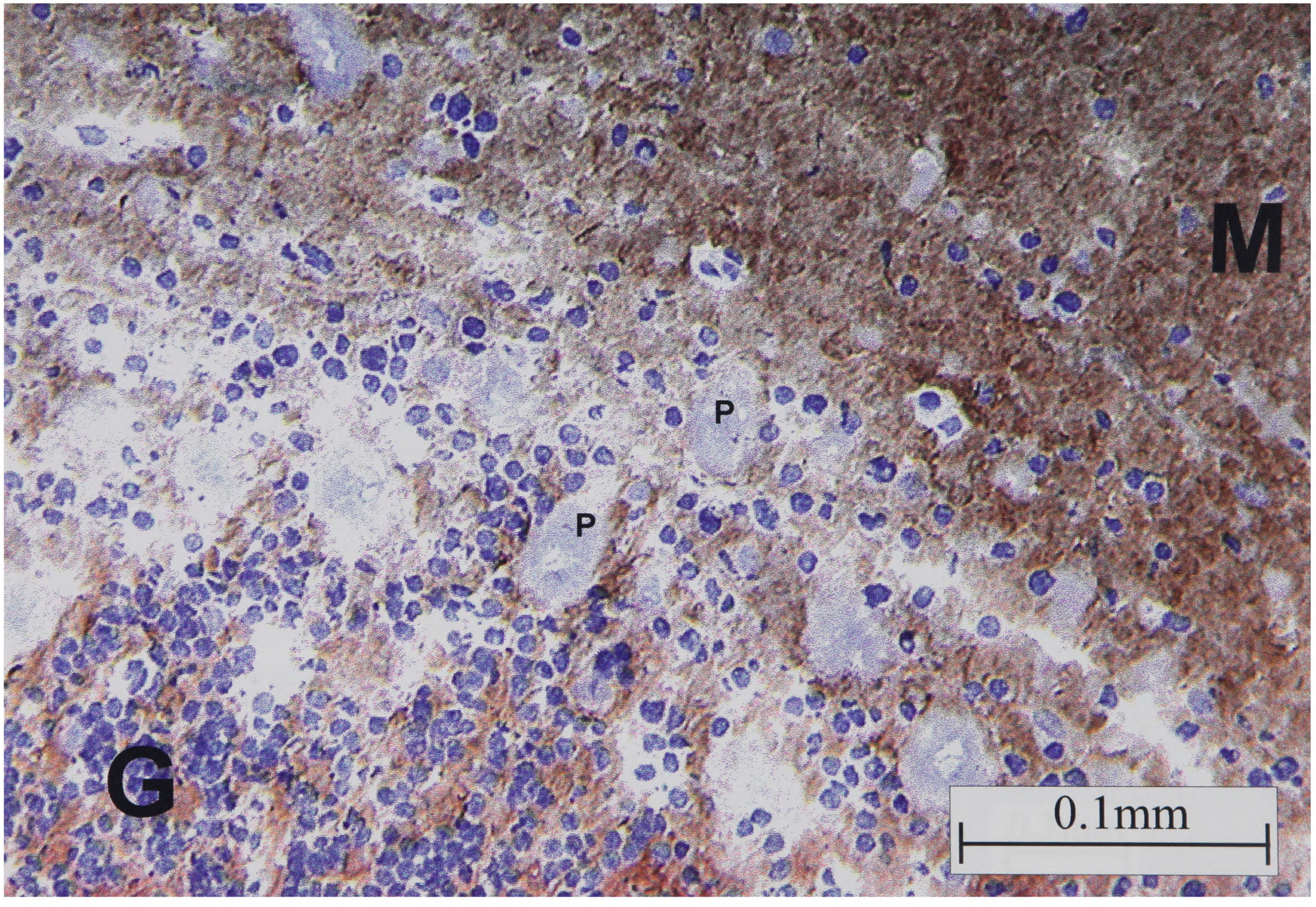

B

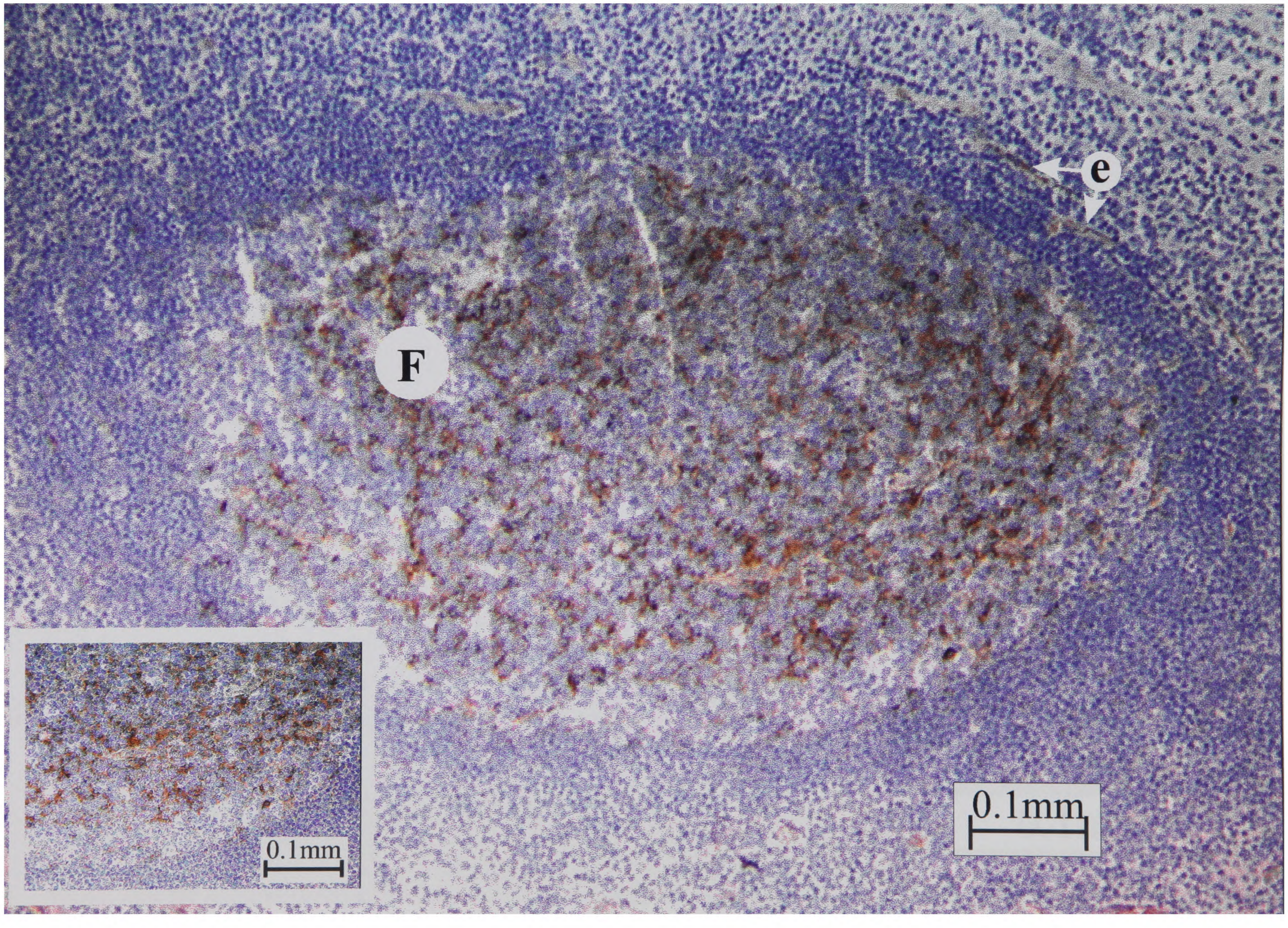

C

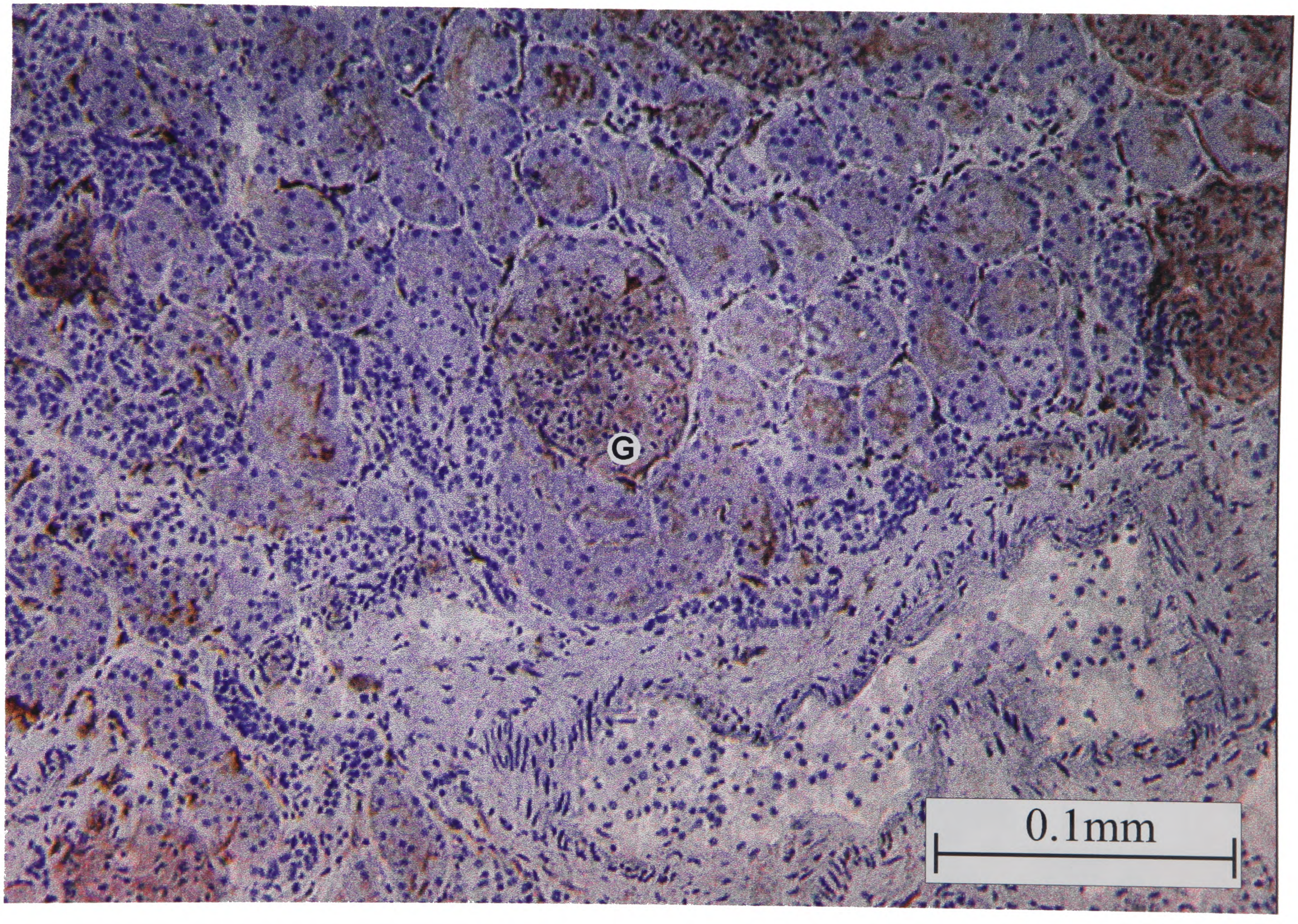

D

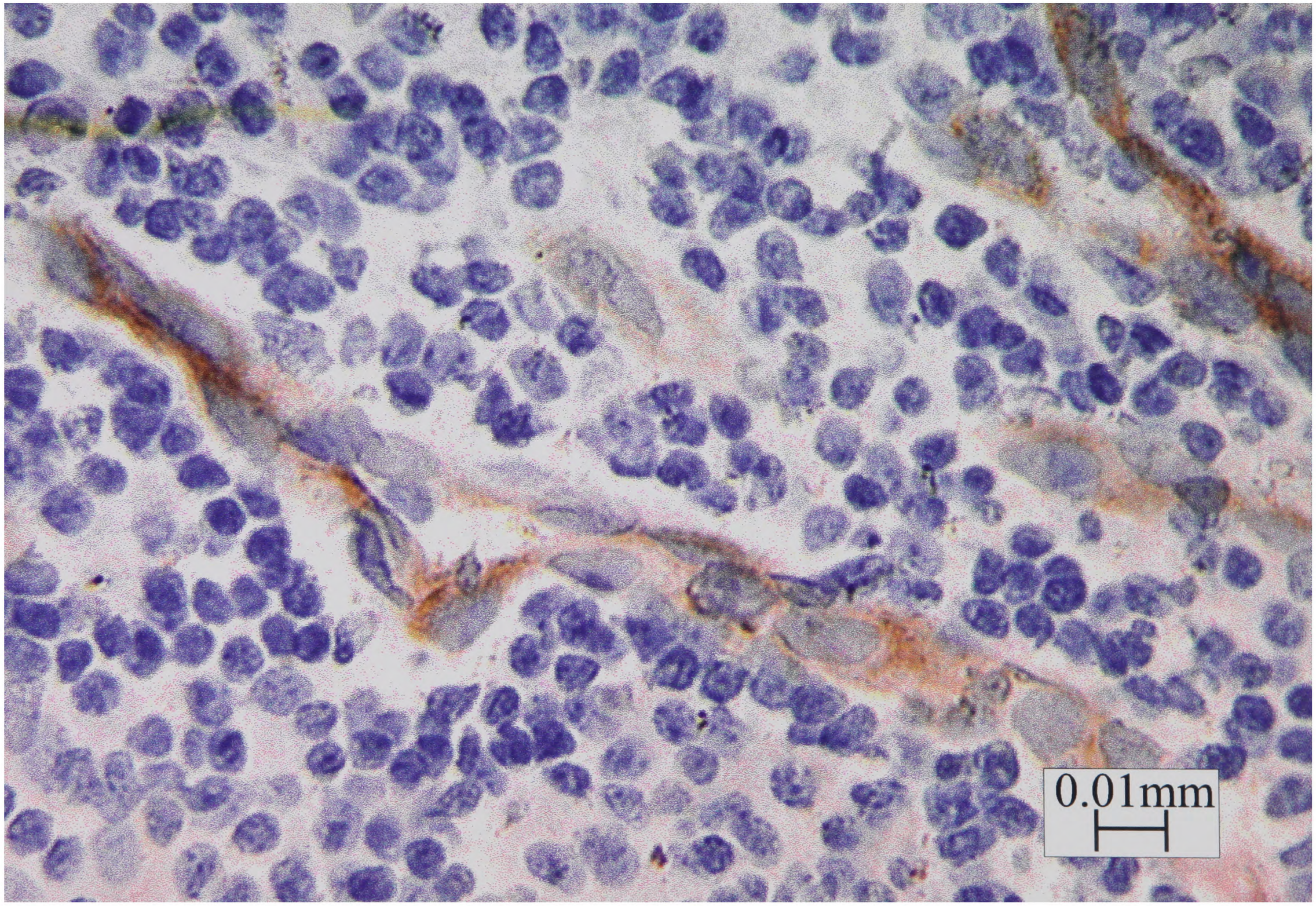

Chapter Ten

General Discussion

10.1 Introduction

Our understanding of the mammalian immune system is limited by knowing the function of only half of the 200+ characterised proteins at the cell surface of leukocytes. It has been argued that the majority of these proteins of unknown function are involved in specific intercellular recognition events at the cell surface and that further characterisation of these proteins has been technically challenging since these interactions are typified by extremely low affinities and are of a highly transient nature.

This thesis has presented the use of techniques which address these difficulties to identify the receptor for a glycoprotein, OX-2 expressed in both the lymphoid and neuronal compartments. This chapter is divided into two broad sections. Initially, I will discuss the confirmation and broadening of the general principles of membrane proteins and their interactions. Then I will discuss the biological role of the OX-2:OX-2R interaction in the context of our current understanding of the mammalian immune and nervous systems.

10.2 Evolution of receptor-ligand pairs

The observation that the extracellular region of OX-2 and its receptor were not only structurally related (containing two IgSF domains in a V/C2 arrangement) but also showed evidence of a common evolutionary ancestor was consistent with previous observations. Sequence analysis of several characterised receptor-ligand pairs within the immunoglobulin superfamily reveals that these pairs show evidence of a common evolutionary ancestor and are also genetically linked (Fig. 10-1). Notice that each interacting pair is more closely related to each other than the other members of the IgSF and that CD2, CD48, CD58 and 2B4 are more related to each other (and form the CD2 sub-family (Davis and van der Merwe, 1996; Brown et al., 1998)) than to OX-2 and its receptor. These observations

strongly imply that discrete receptor ligand pairs have evolved, relatively recently, due to gene duplication from a single gene able to mediate homophilic interactions.

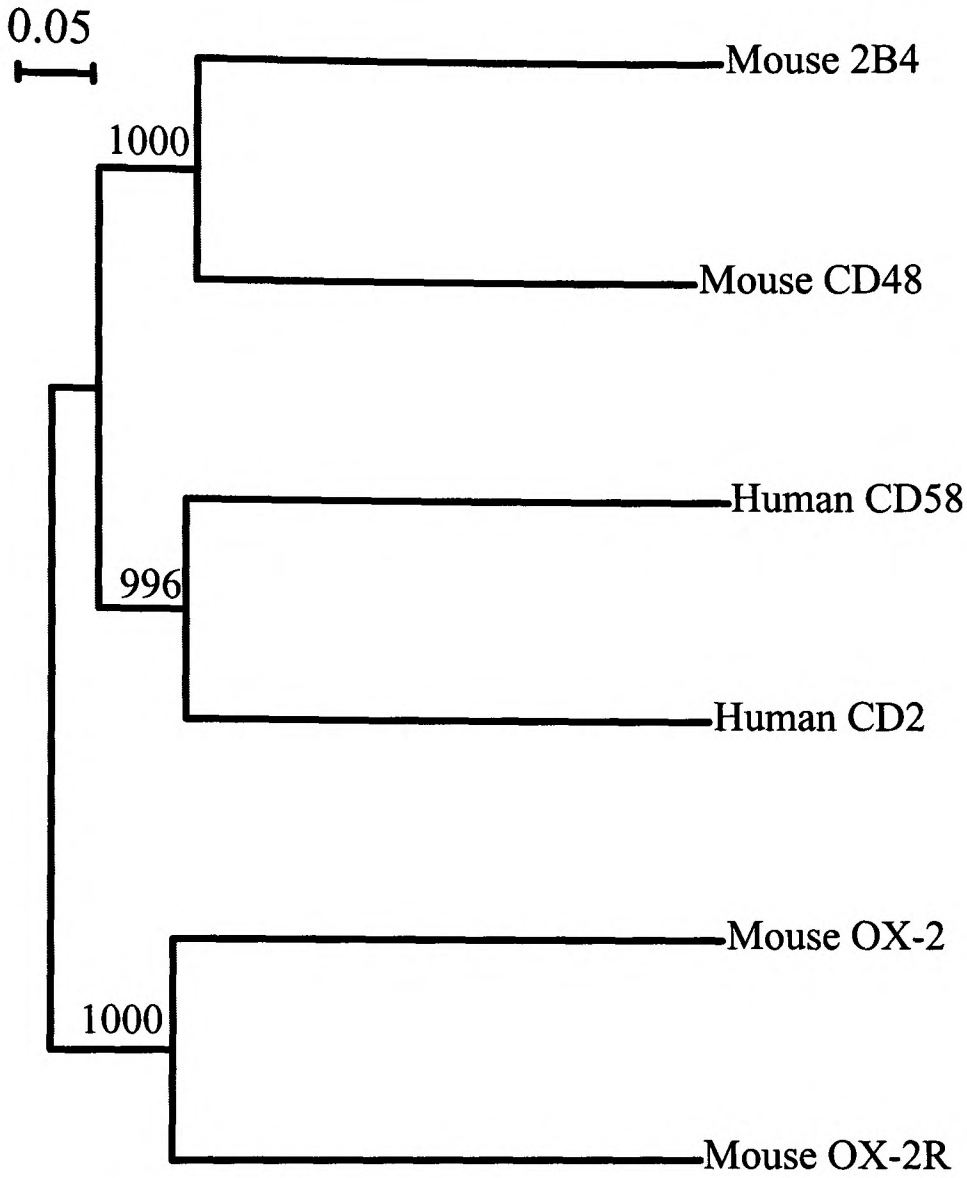

Chromosomal location	Interacting heterophilic pair		Chromosomal location
1p13.1	hCD2	hCD58	1p13.1
mouse 1q21-q23	mCD48	m2B4	mouse 1
unknown	OX-2R	mOX-2	mouse 16

Figure 10-1. Phylogenetic relationship between three characterised receptor:ligand pairs within the IgSF and their chromosomal location. The extracellular regions of the indicated molecules were aligned using clustalW, manually refined and then a neighbour joining tree constructed with 1000 bootstrap trials. The table shows the genomic localisation of the genes and are referenced: human CD2, Brown et al., 1987; mouse CD48, Wong et al., 1990; human CD58, Sewell et al., 1988; mouse 2B4, Mathew et al., 1993; mouse OX-2, Borriello et al., 1998.

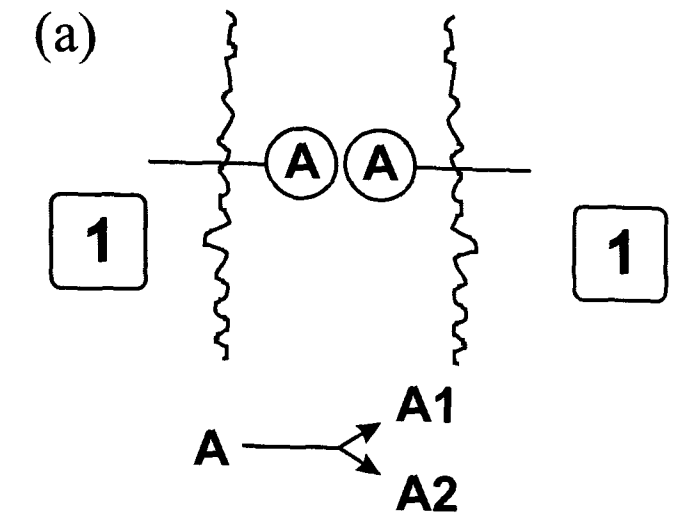

A gene, A, expressed by cell type 1 whose product is capable of homophilic interactions duplicates into A1 and A2 by gene duplication.

Both gene products retain the ability to interact in a homophilic manner but are limited to a single cell type.

The mutability of genomic DNA might allow additional expression of one of these genes, A2 by a separate differentiated cell type, 2, which vastly increases the communicative potential of the system.

The loss of expression of A2 from cell type 1 and further mutations in the regions initiating signal transduction (cytoplasmic regions) form the basis of heterophilic cell:cell interactions.

Figure 10-2. A mechanism suggesting how heterophilic interactions may have evolved from a primordial homophilic interaction.

A mechanism suggesting how this might occur is presented in Figure 10-2. Gene duplication is followed by further mutation which could lead to alterations in tissue distribution of one of the duplicated genes. The expression of the protein on different tissues

will vastly increase the potential of the proteins to communicate and therefore evolve. The selection of further mutations which alter the type of signal propagated by the proteins form the basis for creating evolutionary related heterophilic ligand:receptor pairs.

It is conceivable that once genomic data are readily available, a less labour intensive method of identifying novel receptor:ligand pairs would be the identification of predicted cell surface molecules which show both sequence similarities and genetic linkage. These pairs would then be expressed and tested for their ability to interact at the biochemical level.

10.3 Biochemical features of the OX-2R

10.3.1 Multiple forms of the OX-2R

During this work, there were several indications that the OX-2R might exist as multiple forms at the cell surface. This evidence is detailed below:

1) Two bands on PNGaseF treated protein purified from spleen (Fig. 4-6 –section 4.5).
2) Homologies with the herpes viral entry proteins which are known to exhibit alternative splicing of their transmembrane and cytoplasmic regions (section 5.5).
3) The consistent presence of a 40kDa (reducing) 35kDa (nonreducing) protein upon purification of mOX-2R from spleen, the identity of which, despite several efforts, has yet to be identified (Fig. 4-7).
4) The identification of mouse EST matches which, when translated and aligned to the cloned OX-2R showed sequence divergence immediately prior to the transmembrane region (Fig. 10-3).

mOX-2R	GNQSLSIELSRGGNQSLR	Membrane proximal region
EST	GNQSLSIELSRGTTSTT	
mOX-2R	PYIPYIIPSIIILIIIGCICLL	Transmembrane
EST	PSLLTILYVKMVLLGIILL	
mOX-2R	KISGFRKCKLPKLEAT *etc...*	Cytoplasmic
EST	KVGFAFFQKRNVTRT *	

Figure 10-3. An alignment of the mouse OX-2R cloned in this thesis (mOX-2R) and the translation of an EST match at the predicted transmembrane and cytoplasmic regions. These data were provided by Dr J.D. Sedgwick and colleagues. Identical residues have been boxed and the lysine predicted to lie within the transmembrane region has been underlined.

It is impossible to assess the quality of the EST sequence data. However the differences in translated protein are not due to a simple frame shift in the EST sequence since the two sequences bore no resemblance to each other at the nucleic acid level. It is feasible that, if these represented true alternative forms of the receptor, then it is quite likely that the lysine present in the transmembrane region will associate with an oppositely charged residue in a closely associated protein within the membrane. The suggestion that this may be the 35/40kDa band is provocative, but should be explored since proteins which exhibit this property are known (section 1.3.2.3) and presumably would initiate a distinct signal from the form which lacks this feature. It is possible that any alternative form could be expressed by different cell types other than the macrophage, since no common band was seen in the 3'RACE reactions performed on macrophage cDNA (for rat see Fig. 5-7 and for mouse see Fig. 5-12).

10.3.2 Interaction characteristics

A kinetic analysis of the OX-2:OX-2R interaction showed that the two glycoproteins interacted with low affinity due to fast off rate kinetics. These interaction characteristics are very similar to those measured for other cell surface interactions. It was argued in section 7.6

that interactions characteristics may have evolved to fulfil a particular function at the cell surface and that a corollary was emerging which suggested that cell surface interactions which had a slightly higher affinity (those with a longer half life than 0.6/0.7 seconds) might be involved in the transduction of an inhibitory signal. The OX-2:OX-2R interaction is certainly within this range and other evidence (see below) suggests that the interaction may deliver an inhibitory signal, supporting the hypothesis.

10.4 Functional Aspects

The identification of a new receptor:ligand pair immediately raises the question regarding the biological outcome of the dialogue between two cell types expressing these proteins. An indication of their biological roles can be obtained by a consideration of their respective distributions.

OX-2	OX-2R
Central and peripheral nervous systems	Microglia
Resting B-cells	Macrophages
Activated T-cells	Granulocytes
Follicular dendritic cells	Monocytes
Endothelium	Dendritic cells
Degenerating ovarian follicles	

Table 10-2. The major sites of expression of OX-2 and its receptor.

The fact that OX-2 is expressed on a diverse range of tissues and the OX-2R on a more restricted and functionally analogous cell type suggests that the role of the interaction is to regulate myeloid cellular function. The function of OX-2 would therefore be to simply

"mark" certain tissues which need to regulate myeloid function and this regulatory signal would be delivered through the OX-2R.

The distribution of OX-2 and its receptor quite clearly suggest a role in neuronal/myeloid interactions and these two tissues are known to interact. Macrophages are ubiquitously distributed cell types, migrating and differentiating from blood monocytes to reside in the tissues where they display a multitude of morphologies and functional potentials which are determined by the surrounding tissue (Gordon, 1995). The central nervous system also contains resident macrophages termed microglia which express several macrophage specific markers. The functions of microglia are still controversial (Matyszak et al., 1999) but have been implied in tissue remodelling roles (Perry and Gordon, 1991) and are capable of limited antigen presentation (they are often described as non-professional antigen presenting cells) which can be increased upon microglial activation (Matyszak et al., 1999). However, microglia are often described as having a "quiescent" or "downregulated" phenotype which led Perry and Gordon to propose:

> "the presence of ligand/s within the CNS to which some receptor(s) on the macrophage cell surface will bind. It is the presence of such ligand(s) that is responsible for the unique morphology of this type of macrophage, and associated with this morphology is a general downregulation of many macrophage functions." (Perry and Gordon, 1991).

The OX-2:OX2-R interaction would seem an ideal candidate to explain this biology and experiments to manipulate macrophage function via OX-2R ligation with OX-2 are planned.

Macrophages are not the sole leukocyte which can cross the blood brain barrier and enter the CNS. The pathology of a neural inflammation autoimmune disease model in rodents known as experimental allergic encephalomyelitis (EAE -a model for multiple sclerosis) is characterised by perivascular infiltrates of activated $CD4^+$ T-cells and

macrophages. The disease can be prevented by administration of an anti-CD4 mAb at the time of disease onset (Brostoff and Mason, 1984). This protection is thought to be due to the skewing of the CD4+ T-cells to a Th2 phenotype (Stumbles and Mason, 1995). Administration of MRC OX-102 in this model both increased the severity and onset time of the disease suggesting that the OX-2:OX-2R interaction has a role to play in regulating macrophage function in disease states, although MRC OX-2 administration had no effect (A.N. Barclay, unpublished results).

Ovarian tissue which expresses OX-2 also has the potential to regulate myeloid cellular function. However, due to the huge variety of implicated functions of macrophages in ovarian biology it is difficult to predict with confidence what the role of the OX-2:OX-2R interaction in this tissue might be (section 8.4).

10.4.1 Genetic approaches: The OX-2 knock out mouse

A complementary approach to determine the function of OX-2 was to generate an OX-2 deficient mouse in a collaboration with Drs R.M. Hoek and Dr J.D. Sedgwick at the DNAX Research Institute, Palo Alto, CA. The mice were viable and had an interesting phenotype:

1) Mesenteric lymph nodes had fused into a "tube" containing a macrophage infiltrate.
2) The cellularity of the spleen in young mice differed from the wild type, containing twice as many macrophages and the metallophilic marginal macrophages appeared to be an expanding population.
3) Microglia in the CNS appeared to be in a "more activated" state and were present in higher numbers compared to the wildtype.

4) A neural damage model which involves intracranial transection of the facial nerve showed a quicker repair response of the microglia.

5) No evidence for a co-stimulatory role of OX-2 in proliferation assays was found.

The phenotype of these mice is consistent with the finding that a specific OX-2 receptor is expressed on cells of myeloid origin and that the OX-2:OX-2R interaction has a role to play in macrophage regulation. The phenotype also suggests that the type of signal delivered by the OX-2 to the receptor is in some way "inhibitory" and thus might prevent macrophage proliferation and/or activation.

10.4.2 Viral OX-2 homologues

Viral sequencing projects have identified the presence of OX-2 homologues in the genomes of several human viruses. Understanding the role of these viral OX-2 homologues in the lifecycle of the virus may suggest the functional role for the OX-2:OX-2R interaction in the healthy individual. Work on one of these viral homologues has been initiated. Before starting to work on these viral homologues it was important to show that they were true homologues of OX-2 and not just an unrelated members of the IgSF. An alignment of these viral homologues is shown in Figure 10-4. It is clear that these viral proteins are members of the IgSF but also contain the cysteines which are predicted to form an addition disulphide bond in the F and G β-strands, a feature which is unique to OX-2. In addition, a statistical assessment of the phylogenetic relationships between the proteins is shown in Figure 10-5 which shows that it is likely that the K14 orf, the viral homologue from KSHV (HHV-8), is indeed a true OX-2 homologue. It is more difficult to determine whether the other viral proteins are genuine OX-2 homologues but the conserved pattern of cysteine residues suggests they are at least structurally related.

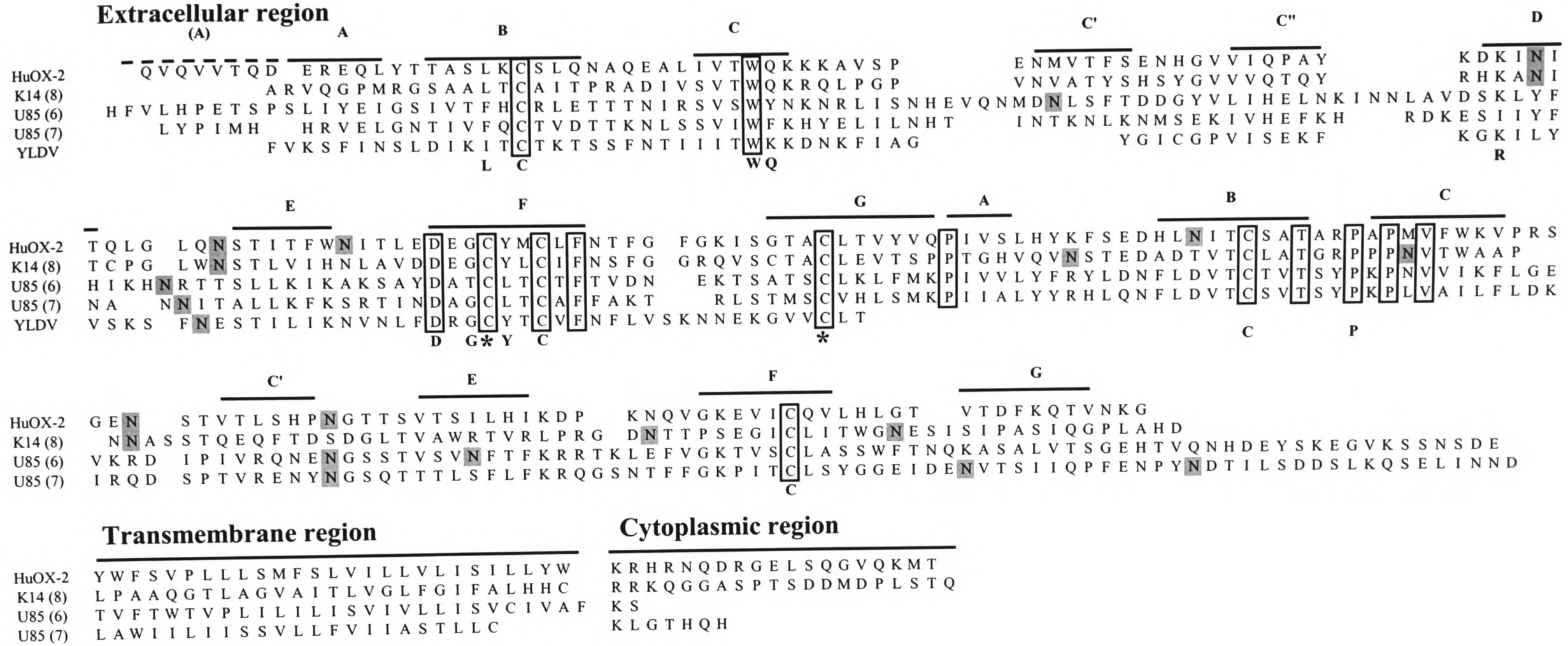

Figure 10-4. An alignment of human OX-2 and viral OX-2 homologues. The five sequences have been split according to their predicted domain organisation and topology. The OX-2 viral homologues are K14 (from HHV-8 (KSHV)), U85 from HHV-6 and –7 (indicated in parentheses) and Yabba like disease virus (YLDV). The superscripted bars in the extracellular regions predict the extent of the β-strands characteristic of the immunoglobulin fold by comparison to solved structures and the position of IgSF signature residues are indicated in bold beneath the sequences. Asparagines conforming to N-linked glycosylation sequons have been lightly shaded and residues common to all five sequences boxed. Notice the position of the unusual cysteines (*), which are a characteristic feature of OX-2, and are conserved across all five sequences.

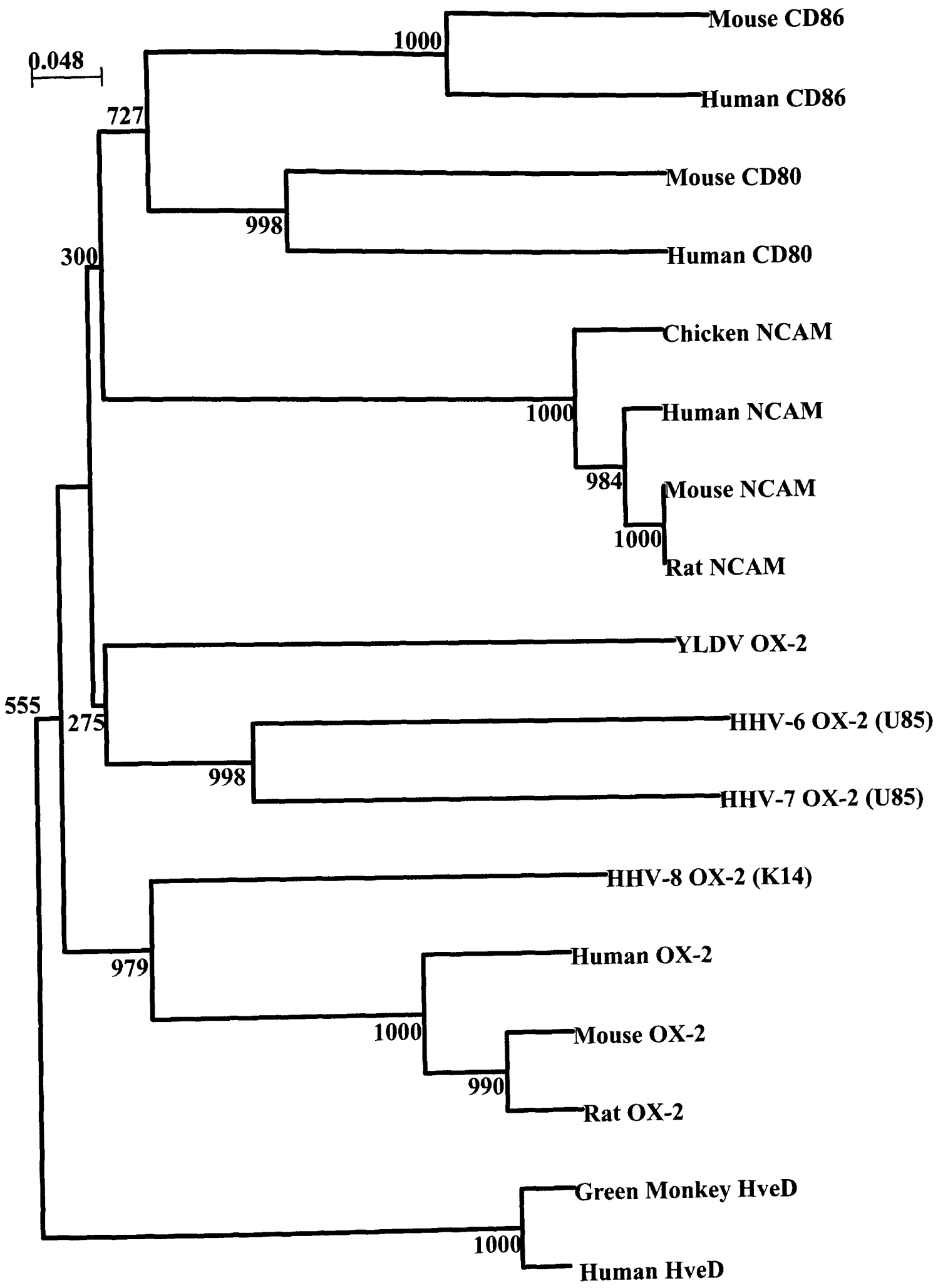

Figure 10-5. Neighbour joining tree showing the phylogenetic relationship between OX-2 proteins, their viral homologues and other members of the IgSF. The V-domains of the indicated proteins were aligned using clustalW, manually refined, and then a neighbour joining tree was constructed with 1000 bootstrap trials.

There is evidence that the acquisition of OX-2 by these viruses was not a single, isolated event but had occurred individually within each virus (with the exception of the two highly related viruses HHV-6 and HHV-7). Firstly, the viruses belong to highly diverged evolutionary groups. The Yabba-like disease virus (YLDV) is a poxvirus (*poxviridae, yatapoxvirus*) whereas the others are herpesviruses but belong to separate evolutionary groups; HHV-6 and HHV-7 belong to the subfamily *betaherpesvirinae*, whereas HHV-8 is a *gammaherpesvirinae*. These two herpesvirus subfamilies diverged approximately 200 million years ago, predating the major mammalian radiation of 60 to 80 million years ago (McGeoch et al., 1995). In addition, the viral OX-2 orfs are present in unrelated regions of the viral genome (Gompels et al., 1995; Russo et al., 1996; Singer and Frenkel, 1997). The fact that the three groups of viruses acquired and retained the OX-2 protein in separate events suggests that a significant evolutionary advantage was accrued by OX-2 acquisition. It is implied from the presented sequence analysis that they might bind the human homologue of the OX-2 receptor but the functional consequence of this is not known. It could be that the viral OX-2 proteins bind the HuOX-2R to target viral entry into cells of myeloid origin and indeed these cell types are known to be targets for infection (Kondo et al., 1991; Yasukawa et al., 1997; Rettig et al., 1997) although infection is by no means restricted to these cell types. Also, the K14 orf is known to be upregulated during the early lytic stage of the viral lifecycle (Kirshner et al., 1999) and thus would be present in the plasma membrane during viral replication suggesting this protein would be located within the outer membrane of the virion. However, the presence of a soluble homologue in YLDV suggests that this is not the case for this virus. Alternatively, the expression or secretion of these viral OX-2 proteins from infected cells could control or manipulate the immune system and thereby prevent the mounting of an effective immune response against the virus. The molecular mechanism of this manipulation could feasibly involve binding the HuOX-2R and

thereby negatively modulating macrophage function (see below). A soluble K14CD4d3+4 chimaera has been made but did not bind rat PECs when presented on beads (data not shown) and several attempts to observe binding to human tissue including monocyte derived macrophages also failed to show binding above the negative control. In addition, a monoclonal antibody, MRC OX-105, was raised to the K14 portion of the chimaera. However, data (not shown) suggest that this mAb might not recognise native material and thus further work is required, possibly making a new mAb, before interpretable results regarding the distribution of the viral protein can be obtained.

10.5 The function of the OX-2:OX-2R interaction

The work presented in this thesis represents a significant step forward in the functional understanding of the OX-2 glycoprotein, but the precise biological role of OX-2 and its receptor remain to be elucidated. In this section, I attempt to estimate the function of this novel interaction using both the presented data and the reports relating to OX-2 function published by groups which have recently started to work on OX-2.

Despite the fact that both the MRC OX-2 mAb and antigen presenting cells derived from OX-2 deficient mice had no reported effect in proliferation assays, it has recently been suggested that OX-2 plays a costimulatory role in T-cell activation. This is primarily due to both close structural and genetic links of OX-2 with CD80/CD86 and Borriello *et. al.* have mapped the mouse OX-2 genetic locus to within a few cM (~5 to 7 Mbp) of the co-stimulatory molecules CD80/CD86 (Borriello et al., 1998; Reeves et al., 1997) and report a proliferative response made by mouse and human $CD4^+$ T-cells using CHO-cells co-transfected with $I\text{-}A^d$ and rat OX-2 as antigen presenting cells (Borriello et al., 1997). The supernatants of these proliferative cultures did not contain IL-2 or IL-4 which led to the proposal that OX-2 defined a novel co-stimulatory pathway and implied that the OX-2

receptor is expressed on T-cells. Further work by Gorzynski *et. al.* have proposed that OX-2 is upregulated on dendritic cells upon immunological stimulation (Gorczynski et al., 1998) and is then primarily responsible for the delivery of a tolerogenic rather than immunogenic signal to antigen specific T-cells which again suggests the OX-2 receptor is expressed by T-cells (Gorczynski et al., 1999a; Gorczynski et al., 1999c; Gorczynski et al., 1999b). Remarkably, they report that the tolerance of mice to a renal allograft can be broken by the administration of the *mouse* anti-*rat* MRC OX-2 mAb (Gorczynski et al., 1998). These data are difficult to reconcile with both basic immunological principles and the observation that MRC OX-2 does not bind mouse OX-2 (N. Hutchings, unpublished data). The functions reported for OX-2 by other groups are centred around the expression of OX-2 by antigen presenting cells and the presence of the receptor on T-cells and thus are rather difficult to reconcile with the data presented in this thesis. In particular, no binding above negative controls was observed when OX-2 coated beads were presented to thymocytes, resting lymphocytes or activated lymphocytes (Preston et al., 1997).

The observations presented in this thesis coupled with the phenotype of the OX-2 knock-out mouse suggests that the OX-2 glycoprotein might deliver an inhibitory signal to OX-2R expressing cells, i.e. primarily those of myeloid origin. These data have come primarily from the phenotype of the OX-2 deficient mouse but is supported by circumstantial evidence based on the tissue distributions of the two glycoproteins, the manner in which they interact and the discovery of OX-2 homologues in several viruses.

The suggestion that OX-2 might be responsible for the down regulation of some macrophage functions in the CNS leading to the microglial phenotype is consistent with these data. However, the nature of these inhibitory signals and the functions that they effect are not clear at present. It is possible that the signal delivered via the receptor prevents macrophage functions such as phagocytosis which might explain the presence of OX-2

homologues in viruses during the lytic phase of their life cycle. Interestingly, the viruses which contain OX-2 homologues, when compared to other related viruses, are generally slow at virion production after infection (Table 10-3). It should be noted that these times are approximate and are measured *in vitro* using various stimuli to break latency.

Virus	Approximate replication time	Reference
Herpesviridae		
(α) HHV-1/HHV-2	18 to 20 hours	(Roizman and Seers, 1995)
(α) HHV-3	8 to 16 hours	(Cohen and Straus, 1995)
(γ) HHV-4	2 to 3 days	(Kief, 1995)
(β) HHV-5	2 to 3 days	(Mocarski, 1995)
(β) **HHV-6**	4 to 5 days	(Black et al., 1989)
(β) **HHV-7**	5 days	(Yasukawa et al., 1997)
(γ) **HHV-8**	2 to 3 days	(Renne et al., 1996)
Poxviridae		
Vaccinia	24 hours	(McIntosh and Smith, 1996)
YLDV	3 days	H. Lee. Personal comm.

Table 10-3. The approximate time taken to produce progeny virus after infection is indicated for several herpes and pox viruses. The herpes viruses are given their formal classification and the subfamily to which they belong is indicated in parentheses. Viruses containing an OX-2 homologue are indicated in bold.

The protection of an infected cell undergoing viral replication from the immune system by virally encoded proteins at the cell surface would clearly be advantageous. The inhibition of macrophage phagocytosis would fulfil this role.

In conclusion, the function of the OX-2:OX-2R interaction is currently thought to be the delivery of a negative regulatory signal inhibiting myeloid cellular functions. The functions which are inhibited by this interaction are not known and could potentially affect phagocytosis, proliferation, differentiation or migratory behaviour. It is not yet clear what the biological role of the OX-2:OX-2R interaction between myeloid cells and activated T-cells, resting B-cells or endothelium might be and it is possible that new myeloid biology could be discovered should the role of the interaction be elucidated.

10.6 Future experiments

There is much scope for further experiments which will primarily focus on elucidating the precise biological role of the OX-2:OX-2R interaction. It is important to perform a detailed study of the OX-2R distribution with particular attention to the distribution within the adult and developing nervous system. In addition, the cloning of the mouse form of the receptor has initiated the generation of an OX-2R knock-out mouse which will be performed in further collaborations with Dr J.D. Sedgwick in DNAX. An integral part of this work will be the characterisation of the mOX-2R gene at the genomic level which is probably the best method of assessing the potential of the gene to generate different forms by alternative splicing. Should there be a form of the receptor which has a charge in the transmembrane region as predicted from EST matches, then the co-purifying 40kDa band from splenic lysates is a good candidate.

The ability of the viral OX-2 homologues to bind to the human form of the OX-2R will be tested using surface plasmon resonance once it has been cloned. Should the viral OX-2 homologues bind, it will be interesting to contrast their binding kinetics with that of the native HuOX-2 protein. One might predict that the soluble viral OX-2 would bind with a higher affinity than membrane associated forms.

Further molecular characteristics of the two interacting proteins are currently being determined which includes mapping the disulphide bonds in OX-2 and its receptor and a mutational analysis of the predicted binding faces on the two molecules.

It is perhaps too early to speculate on any potential clinical applications of these discoveries but quite clearly the ability to negatively regulate a component of the immune system would be a powerful medical tool. Conditions such as allergies, autoimmune diseases and the rejection of transplanted organs which are all the result of an inappropriate or misdirected immune response are potential areas where this control would be desired.

References

Adams, S., van der Laan, L.J., Vernon-Wilson, E., Renardel de Lavalette, C., Dopp, E.A., Dijkstra, C.D., Simmons, D.L. and van den Berg, T.K. (1998) Signal-regulatory protein is selectively expressed by myeloid and neuronal cells. J Immunol 161, 1853-9.

Arvieux, J., Willis, A.C. and Williams, A.F. (1986) MRC OX-45 antigen: a leucocyte/endothelium rat membrane glycoprotein of 45,000 molecular weight. Mol Immunol 23, 983-90.

Barclay, A.N. (1981) Different reticular elements in rat lymphoid tissue identified by localization of Ia, Thy-1 and MRC OX 2 antigens. Immunology 44, 727-36.

Barclay, A.N. (1981) The localization of populations of lymphocytes defined by monoclonal antibodies in rat lymphoid tissues. Immunology 42, 593-600.

Barclay, A.N. (1986) Alternative processing of RNA in lymphoid cells. Immunol Today 7, 168-169.

Barclay, A.N. and Ward, H.A. (1982) Purification and chemical characterisation of membrane glycoproteins from rat thymocytes and brain, recognised by monoclonal antibody MRC OX 2. Eur J Biochem 129, 447-58.

Barclay, A.N., Brown, M.H., Law, S.K.A., McKnight, A.J., Tomlinson, M.G. and van der Merwe, P.A. (1997) Leucocyte Antigens Factsbook - second edition. Academic Press, London.

Barnstable, C.J., Bodmer, W.F., Brown, G., Galfre, G., Milstein, C., Williams, A.F. and Ziegler, A. (1978) Production of monoclonal antibodies to group A erythrocytes, HLA and other human cell surface antigens-new tools for genetic analysis. Cell 14, 9-20.

Benchimol, S., Fuks, A., Jothy, S., Beauchemin, N., Shirota, K. and Stanners, C.P. (1989) Carcinoembryonic antigen, a human tumor marker, functions as an intercellular adhesion molecule. Cell 57, 327-34.

Beverley, P.C. and Callard, R.E. (1981) Distinctive functional characteristics of human "T" lymphocytes defined by E rosetting or a monoclonal anti-T cell antibody. Eur J Immunol 11, 329-34.

Black, J.B., Sanderlin, K.C., Goldsmith, C.S., Gary, H.E., Lopez, C. and Pellett, P.E. (1989) Growth properties of human herpesvirus-6 strain Z29. J Virol Methods 26, 133-45.

Blattner, F.R., Plunkett, G., 3rd, Bloch, C.A., Perna, N.T., Burland, V., Riley, M., Collado-Vides, J., Glasner, J.D., Rode, C.K., Mayhew, G.F., Gregor, J., Davis, N.W., Kirkpatrick, H.A., Goeden, M.A., Rose, D.J., Mau, B. and Shao, Y. (1997) The complete genome sequence of Escherichia coli K-12 [comment] [see comments]. Science 277, 1453-74.

Bockaert, J. and Pin, J.P. (1999) Molecular tinkering of G protein-coupled receptors: an evolutionary success. Embo J 18, 1723-9.

Bodian, D.L., Jones, E.Y., Harlos, K., Stuart, D.I. and Davis, S.J. (1994) Crystal structure of the extracellular region of the human cell adhesion molecule CD2 at 2.5 A resolution. Structure 2, 755-66.

Boniface, J.J., Rabinowitz, J.D., Wulfing, C., Hampl, J., Reich, Z., Altman, J.D., Kantor, R.M., Beeson, C., McConnell, H.M. and Davis, M.M. (1998) Initiation of signal transduction through the T cell receptor requires the multivalent engagement of peptide/MHC ligands [corrected] [published erratum appears in Immunity 1998 Dec;9(6):891]. Immunity 9, 459-66.

Bork, P., Holm, L. and Sander, C. (1994) The immunoglobulin fold. Structural classification, sequence patterns and common core. J Mol Biol 242, 309-20.

Borriello, F., Lederer, J., Scott, S. and Sharpe, A.H. (1997) MRC OX-2 defines a novel T cell costimulatory pathway. J Immunol 158, 4548-54.

Borriello, F., Tizard, R., Rue, E. and Reeves, R. (1998) Characterization and localization of Mox2, the gene encoding the murine homolog of the rat MRC OX-2 membrane glycoprotein. Mamm Genome 9, 114-8.

Bowen, M.A., Bajorath, J., D'Egidio, M., Whitney, G.S., Palmer, D., Kobarg, J., Starling, G.C., Siadak, A.W. and Aruffo, A. (1997) Characterization of mouse ALCAM (CD166): the CD6-binding domain is conserved in different homologs and mediates cross-species binding. Eur J Immunol 27, 1469-78.

Bowen, M.A., Patel, D.D., Li, X., Modrell, B., Malacko, A.R., Wang, W.C., Marquardt, H., Neubauer, M., Pesando, J.M., Francke, U. and et al. (1995) Cloning, mapping, and characterization of activated leukocyte-cell adhesion molecule (ALCAM), a CD6 ligand. J Exp Med 181, 2213-20.

Brady, R.L., Dodson, E.J., Dodson, G.G., Lange, G., Davis, S.J., Williams, A.F. and Barclay, A.N. (1993) Crystal structure of domains 3 and 4 of rat CD4: relation to the NH2- terminal domains. Science 260, 979-83.

Brenan, M. and Puklavec, M. (1992) The MRC OX-62 antigen: a useful marker in the purification of rat veiled cells with the biochemical properties of an integrin. J Exp Med 175, 1457-65.

Brostoff, S.W. and Mason, D.W. (1984) Experimental allergic encephalomyelitis: successful treatment in vivo with a monoclonal antibody that recognizes T helper cells. J Immunol 133, 1938-42.

Brown, M.H. and Barclay, A.N. (1994) Expression of immunoglobulin and scavenger receptor superfamily domains as chimeric proteins with domains 3 and 4 of CD4 for ligand analysis. Protein Eng 7, 515-21.

Brown, M.H., Boles, K., van der Merwe, P.A., Kumar, V., Mathew, P.A. and Barclay, A.N. (1998) 2B4, the NK and T cell immunoglobulin superfamily surface protein is a ligand for CD48. J. Exp. Med 188, 2083-90.

Brown, M.H., Gorman, P.A., Sewell, W.A., Spurr, N.K., Sheer, D. and Crumpton, M.J. (1987) The gene coding for the human T-lymphocyte CD2 antigen is located on chromosome 1p. Hum Genet 76, 191-5.

Brown, M.H., Preston, S. and Barclay, A.N. (1995) A sensitive assay for detecting low-affinity interactions at the cell surface reveals no additional ligands for the adhesion pair rat CD2 and CD48. Eur J Immunol 25, 3222-8.

Bruno, L., Scheffold, A., Radbruch, A. and Owen, M.J. (1999) Threshold of pre-T-cell-receptor surface expression is associated with alphabeta T-cell lineage commitment. Curr Biol 9, 559-68.

Bukovsky, A., Caudle, M.R., Keenan, J.A., Wimalasena, J., Upadhyaya, N.B. and Van Meter, S.E. (1995) Is corpus luteum regression an immune-mediated event? Localization of immune system components and luteinizing hormone receptor in human corpora lutea. Biol Reprod 53, 1373-84.

Bukovsky, A., Presl, J. and Zidovsky, J. (1984) Association of some cell surface antigens of lymphoid cells and cell surface differentiation antigens with early rat pregnancy. Immunology 52, 631-40.

Bukovsky, A., Presl, J., Zidovsky, J. and Mancal, P. (1983) The localization of Thy-1.1, MRC OX 2 and Ia antigens in the rat ovary and fallopian tube. Immunology 48, 587-96.

Cambier, J.C. (1995) Antigen and Fc receptor signaling. The awesome power of the immunoreceptor tyrosine-based activation motif (ITAM). J Immunol 155, 3281-5.

Campbell, D.G., Gagnon, J., Reid, K.B. and Williams, A.F. (1981) Rat brain Thy-1 glycoprotein. The amino acid sequence, disulphide bonds and an unusual hydrophobic region. Biochem J 195, 15-30.

Cherington, V., Morgan, B., Spiegelman, B.M. and Roberts, T.M. (1986) Recombinant retroviruses that transduce individual polyoma tumor antigens: effects on growth and differentiation. Proc Natl Acad Sci U S A 83, 4307-11.

Choe, S., Kreusch, A. and Pfaffinger, P.J. (1999) Towards the three-dimensional structure of voltage-gated potassium channels. Trends Biochem Sci 24, 345-9.

Clark, M.J. (1986) MRC OX-2 lymphoid brain glycoprotein: S1 mapping suggests higher levels of abnormal RNA in the thymus than in the brain. Biochem. Soc. Trans. 14, 80-81.

Clark, M.J., Gagnon, J., Williams, A.F. and Barclay, A.N. (1985) MRC OX-2 antigen: a lymphoid/neuronal membrane glycoprotein with a structure like a single immunoglobulin light chain. Embo J 4, 113-8.

Cocchi, F., Lopez, M., Menotti, L., Aoubala, M., Dubreuil, P. and Campadelli-Fiume, G. (1998a) The V domain of herpesvirus Ig-like receptor (HIgR) contains a major functional region in herpes simplex virus-1 entry into cells and interacts physically with the viral glycoprotein D. Proc Natl Acad Sci U S A 95, 15700-5.

Cocchi, F., Menotti, L., Mirandola, P., Lopez, M. and Campadelli-Fiume, G. (1998b) The ectodomain of a novel member of the immunoglobulin subfamily related to the poliovirus receptor has the attributes of a bona fide receptor for herpes simplex virus types 1 and 2 in human cells. J Virol 72, 9992-10002.

Cohen, B., Yoakim, M., Piwnica-Worms, H., Roberts, T.M. and Schaffhausen, B.S. (1990) Tyrosine phosphorylation is a signal for the trafficking of pp85, an 85- kDa phosphorylated polypeptide associated with phosphatidylinositol kinase activity. Proc Natl Acad Sci U S A 87, 4458-62.

Cohen, J.I. and Straus, S.E. (1995) Varicella-Zoster virus and its replication in Virology 3rdEd Edited by B. Fields volume 2 chapter 78. Lippinott-Raven Publishers.

Consortium, T.C.e.s. (1998) Genome sequence of the nematode C. elegans: A platform for investigating biology. Science 282.

Cyster, J.G., Shotton, D.M. and Williams, A.F. (1991) The dimensions of the T lymphocyte glycoprotein leukosialin and identification of linear protein epitopes that can be modified by glycosylation. Embo J 10, 893-902.

Davis, S.J. and van der Merwe, P.A. (1996) The structure and ligand interactions of CD2: implications for T-cell function. Immunol Today 17, 177-87.

Davis, S.J., Davies, E.A., Tucknott, M.G., Jones, E.Y. and van der Merwe, P.A. (1998a) The role of charged residues mediating low affinity protein-protein recognition at the cell surface by CD2. Proc Natl Acad Sci U S A 95, 5490-4.

Davis, S.J., Ikemizu, S., Wild, M.K. and van der Merwe, P.A. (1998) CD2 and the nature of protein interactions mediating cell-cell recognition. Immunol Rev 163, 217-36.

Dominguez, G., Dambaugh, T.R., Stamey, F.R., Dewhurst, S., Inoue, N. and Pellett, P.E. (1999) Human herpesvirus 6B genome sequence: coding content and comparison with human herpesvirus 6A [In Process Citation]. J Virol 73, 8040-52.

Dower, S.K., Kronheim, S.R., March, C.J., Conlon, P.J., Hopp, T.P., Gillis, S. and Urdal, D.L. (1985) Detection and characterization of high affinity plasma membrane receptors for human interleukin 1. J Exp Med 162, 501-15.

Dustin, M.L. and Springer, T.A. (1991) Role of lymphocyte adhesion receptors in transient interactions and cell locomotion. Annu Rev Immunol 9, 27-66.

Eberle, F., Dubreuil, P., Mattei, M.G., Devilard, E. and Lopez, M. (1995) The human PRR2 gene, related to the human poliovirus receptor gene (PVR), is the true homolog of the murine MPH gene. Gene 159, 267-72.

Edelman, G.M. (1970) The covalent structure of a human gamma G-immunoglobulin. XI. Functional implications. Biochemistry 9, 3197-205.

Fan, Q.R., Mosyak, L., Winter, C.C., Wagtmann, N., Long, E.O. and Wiley, D.C. (1997) Structure of the inhibitory receptor for human natural killer cells resembles haematopoietic receptors [published erratum appears in Nature 1997 Nov 20;390(6657):315]. Nature 389, 96-100.

Finnemann, S.C., Marmorstein, A.D., Neill, J.M. and Rodriguez-Boulan, E. (1997) Identification of the retinal pigment epithelium protein RET-PE2 as CE- 9/OX-47, a member of the immunoglobulin superfamily. Invest Ophthalmol Vis Sci 38, 2366-74.

Friedrichson, T. and Kurzchalia, T.V. (1998) Microdomains of GPI-anchored proteins in living cells revealed by crosslinking. Nature 394, 802-5.

Garboczi, D.N., Ghosh, P., Utz, U., Fan, Q.R., Biddison, W.E. and Wiley, D.C. (1996) Structure of the complex between human T-cell receptor, viral peptide and HLA-A2. Nature 384, 134-41.

Garcia, K.C., Degano, M., Stanfield, R.L., Brunmark, A., Jackson, M.R., Peterson, P.A., Teyton, L. and Wilson, I.A. (1996) An alphabeta T cell receptor structure at 2.5 A and its orientation in the TCR-MHC complex [see comments]. Science 274, 209-19.

Garman, S.C., Kinet, J.P. and Jardetzky, T.S. (1998) Crystal structure of the human high-affinity IgE receptor. Cell 95, 951-61.

Garnett (1993) Characterisation of leukocyte glycoproteins with reference to their mode of membrane attachment. D.Phil thesis, Oxford University.

Gaytan, O., Swann, A. and Dafny, N. (1998) Diurnal differences in rat's motor response to amphetamine. Eur J Pharmacol 345, 119-28.

Geraghty, R.J., Krummenacher, C., Cohen, G.H., Eisenberg, R.J. and Spear, P.G. (1998) Entry of alphaherpesviruses mediated by poliovirus receptor-related protein 1 and poliovirus receptor. Science 280, 1618-20.

Goffeau, A., Barrell, B.G., Bussey, H., Davis, R.W., Dujon, B., Feldmann, H., Galibert, F., Hoheisel, J.D., Jacq, C., Johnston, M., Louis, E.J., Mewes, H.W., Murakami, Y., Philippsen, P., Tettelin, H. and Oliver, S.G. (1996) Life with 6000 genes [see comments]. Science 274, 546, 563-7.

Gompels, U.A., Nicholas, J., Lawrence, G., Jones, M., Thomson, B.J., Martin, M.E., Efstathiou, S., Craxton, M. and Macaulay, H.A. (1995) The DNA sequence of human herpesvirus-6: structure, coding content, and genome evolution. Virology 209, 29-51.

Gorczynski, L., Chen, Z., Hu, J., Kai, Y., Lei, J., Ramakrishna, V. and Gorczynski, R.M. (1999a) Evidence that an OX-2-positive cell can inhibit the stimulation of type 1 cytokine production by bone marrow-derived B7-1 (and B7-2)-positive dendritic cells. J Immunol 162, 774-81.

Gorczynski, R.M., Cattral, M.S., Chen, Z., Hu, J., Lei, J., Min, W.P., Yu, G. and Ni, J. (1999b) An immunoadhesin incorporating the molecule OX-2 is a potent immunosuppressant that prolongs allo- and xenograft survival [In Process Citation]. J Immunol 163, 1654-60.

Gorczynski, R.M., Chen, Z., Fu, X.M. and Zeng, H. (1998) Increased expression of the novel molecule OX-2 is involved in prolongation of murine renal allograft survival. Transplantation 65, 1106-14.

Gorczynski, R.M., Cohen, Z., Fu, X.M. and Lei, J. (1999c) Anti-rat OX-2 blocks increased small intestinal transplant survival after portal vein immunization. Transplant Proc 31, 577-8.

Gordon, S. (1995) The macrophage. Bioessays 17, 977-86.

Grakoui, A., Bromley, S.K., Sumen, C., Davis, M.M., Shaw, A.S., Allen, P.M. and Dustin, M.L. (1999) The immunological synapse: a molecular machine controlling T cell activation [see comments]. Science 285, 221-7.

Greene, J.L., Leytze, G.M., Emswiler, J., Peach, R., Bajorath, J., Cosand, W. and Linsley, P.S. (1996) Covalent dimerization of CD28/CTLA-4 and oligomerization of CD80/CD86 regulate T cell costimulatory interactions. J Biol Chem 271, 26762-71.

Halaby, D.M., Poupon, A. and Mornon, J. (1999) The immunoglobulin fold family: sequence analysis and 3D structure comparisons. Protein Eng 12, 563-71.

Hall, C.B., Long, C.E., Schnabel, K.C., Caserta, M.T., McIntyre, K.M., Costanzo, M.A., Knott, A., Dewhurst, S., Insel, R.A. and Epstein, L.G. (1994) Human herpesvirus-6 infection in children. A prospective study of complications and reactivation. N Engl J Med 331, 432-8.

Harpaz, Y. and Chothia, C. (1994) Many of the immunoglobulin superfamily domains in cell adhesion molecules and surface receptors belong to a new structural set which is close to that containing variable domains. J Mol Biol 238, 528-39.

Heldin, C.H. (1995) Dimerization of cell surface receptors in signal transduction. Cell 80, 213-23.

Hortsch, M. (1996) The L1 family of neural cell adhesion molecules: old proteins performing new tricks. Neuron 17, 587-93.

Hsiung, L., Barclay, A.N., Brandon, M.R., Sim, E. and Porter, R.R. (1982) Purification of human C3b inactivator by monoclonal-antibody affinity chromatography. Biochem J 203, 293-8.

Isegawa, Y., Mukai, T., Nakano, K., Kagawa, M., Chen, J., Mori, Y., Sunagawa, T., Kawanishi, K., Sashihara, J., Hata, A., Zou, P., Kosuge, H. and Yamanishi, K. (1999) Comparison of the complete DNA sequences of human herpesvirus 6 variants A and B [In Process Citation]. J Virol 73, 8053-63.

Jefferies, W.A., Green, J.R. and Williams, A.F. (1985) Authentic T helper CD4 (W3/25) antigen on rat peritoneal macrophages. J Exp Med 162, 117-27.

Jentoft, N. (1990) Why are proteins O-glycosylated? [see comments]. Trends Biochem Sci 15, 291-4.

Johnsson, B., Lofas, S. and Lindquist, G. (1991) Immobilization of proteins to a carboxymethyldextran-modified gold surface for biospecific interaction analysis in surface plasmon resonance sensors. Anal Biochem 198, 268-77.

Jonsson, U., Fagerstam, L., Ivarsson, B., Johnsson, B., Karlsson, R., Lundh, K., Lofas, S., Persson, B., Roos, H., Ronnberg, I. and et al. (1991) Real-time biospecific interaction analysis using surface plasmon resonance and a sensor chip technology. Biotechniques 11, 620-7.

Juel, C. and Halestrap, A.P. (1999) Lactate transport in skeletal muscle - role and regulation of the monocarboxylate transporter. J Physiol (Lond) 517, 633-42.

Kief, E. (1995) Epstain-Barr virus and its replication in Virology 3rdEd Edited by B. Fields volume 2 chapter 74. Lippinott-Raven Publishers.

Kirshner, J.R., Staskus, K., Haase, A., Lagunoff, M. and Ganem, D. (1999) Expression of the open reading frame 74 (G-protein-coupled receptor) gene of Kaposi's sarcoma (KS)-associated herpesvirus: implications for KS pathogenesis. J Virol 73, 6006-14.

Kohler, G. and Shulman, M.J. (1978) Cellular and molecular restrictions of the lymphocyte fusion. Current Topics in Microbiology and Immunology 81, 143-48.

Kohler, G., Howe, S.C. and Milstein, C. (1976) Fusion between immunoglobulin-secreting and nonsecreting myeloma cell lines. Eur J Immunol 6, 292-5.

Koike, S., Horie, H., Ise, I., Okitsu, A., Yoshida, M., Iizuka, N., Takeuchi, K., Takegami, T. and Nomoto, A. (1990) The poliovirus receptor protein is produced both as membrane-bound and secreted forms. Embo J 9, 3217-24.

Kondo, K., Kondo, T., Okuno, T., Takahashi, M. and Yamanishi, K. (1991) Latent human herpesvirus 6 infection of human monocytes/macrophages. J Gen Virol 72, 1401-8.

Kornfeld, R. and Kornfeld, S. (1985) Assembly of asparagine-linked oligosaccharides. Annu Rev Biochem 54, 631-64.

Kozak, M. (1987) An analysis of 5'-noncoding sequences from 699 vertebrate messenger RNAs. Nucleic Acids Res 15, 8125-48.

Kroese, F.G., Wubbena, A.S. and Nieuwenhuis, P. (1986) Germinal centre formation and follicular antigen trapping in the spleen of lethally X-irradiated and reconstituted rats. Immunology 57, 99-104.

Kroese, F.G., Wubbena, A.S., Kuijpers, K.C. and Nieuwenhuis, P. (1987) The ontogeny of germinal centre forming capacity of neonatal rat spleen. Immunology 60, 597-602.

Kumar, S. and Hedges, S.B. (1998) A molecular timescale for vertebrate evolution. Nature 392, 917-20.

Kunkel, T.A., Bebenek, K. and McClary, J. (1991) Efficient site-directed mutagenesis using uracil-containing DNA. Methods Enzymol 204, 125-39.

Kunkel, T.A., Roberts, J.D. and Zakour, R.A. (1987) Rapid and efficient site-specific mutagenesis without phenotypic selection. Methods Enzymol 154, 367-82.

Lange, G., Lewis, S.J., Murshudov, G.N., Dodson, G.G., Moody, P.C., Turkenburg, J.P., Barclay, A.N. and Brady, R.L. (1994) Crystal structure of an extracellular fragment of the rat CD4 receptor containing domains 3 and 4. Structure 2, 469-81.

Lanier, L.L. (1998) NK cell receptors. Annu Rev Immunol 16, 359-93.

Lanier, L.L., Corliss, B.C., Wu, J., Leong, C. and Phillips, J.H. (1998) Immunoreceptor DAP12 bearing a tyrosine-based activation motif is involved in activating NK cells [see comments]. Nature 391, 703-7.

Lesley, J., Hyman, R. and Kincade, P.W. (1993) CD44 and its interaction with extracellular matrix. Adv Immunol 54, 271-335.

Lopez, M., Aoubala, M., Jordier, F., Isnardon, D., Gomez, S. and Dubreuil, P. (1998) The human poliovirus receptor related 2 protein is a new hematopoietic/endothelial homophilic adhesion molecule. Blood 92, 4602-11.

Maenaka, K., Juji, T., Nakayama, T., Wyer, J.R., Gao, G.F., Maenaka, T., Zaccai, N.R., Kikuchi, A., Yabe, T., Tokunaga, K., Tadokoro, K., Stuart, D.I., Jones, E.Y. and van der Merwe, P.A. (1999) Killer Cell Immunoglobulin Receptors and T Cell Receptors Bind Peptide- Major Histocompatibility Complex Class I with Distinct Thermodynamic and Kinetic Properties. J Biol Chem 274, 28329-28334.

Maisner, A., Liszewski, M.K., Atkinson, J.P., Schwartz-Albiez, R. and Herrler, G. (1996) Two different cytoplasmic tails direct isoforms of the membrane cofactor protein (CD46) to the basolateral surface of Madin-Darby canine kidney cells. J Biol Chem 271, 18853-8.

Manley, J.L., Yu, H. and Ryner, L. (1985) RNA sequence containing hexanucleotide AAUAAA directs efficient mRNA polyadenylation in vitro. Mol Cell Biol 5, 373-9.

Mason, D.W. and Williams, A.F. (1986) Kinetics of antibody reactions and the analysis of cell surface antigens. In handbook of Experimental Immunology, D.M. Weir et al.,eds. (Oxford: Blackwell Scientific Publications), Volume 1, Chapter 38.

Mathew, P.A., Garni-Wagner, B.A., Land, K., Takashima, A., Stoneman, E., Bennett, M. and Kumar, V. (1993) Cloning and characterization of the 2B4 gene encoding a molecule associated with non-MHC-restricted killing mediated by activated natural killer cells and T cells. J Immunol 151, 5328-37.

Matyszak, M.K., Denis-Donini, S., Citterio, S., Longhi, R., Granucci, F. and Ricciardi-Castagnoli, P. (1999) Microglia induce myelin basic protein-specific T cell anergy or T cell activation, according to their state of activation. Eur. J. Immunol. 29, 3063-3076.

McCaughan, G.W., Clark, M.J. and Barclay, A.N. (1987a) Characterization of the human homolog of the rat MRC OX-2 membrane glycoprotein. Immunogenetics 25, 329-35.

McCaughan, G.W., Clark, M.J., Hurst, J., Grosveld, F. and Barclay, A.N. (1987b) The gene for MRC OX-2 membrane glycoprotein is localized on human chromosome 3. Immunogenetics 25, 133-5.

McGeoch, D.J., Cook, S., Dolan, A., Jamieson, F.E. and Telford, E.A. (1995) Molecular phylogeny and evolutionary timescale for the family of mammalian herpesviruses. J Mol Biol 247, 443-58.

McIntosh, A.A. and Smith, G.L. (1996) Vaccinia virus glycoprotein A34R is required for infectivity of extracellular enveloped virus. J Virol 70, 272-81.

McMaster, W.R. and Williams, A.F. (1979) Identification of Ia glycoproteins in rat thymus and purification from rat spleen. Eur J Immunol 9, 426-33.

McMichael, A.J. and O'Callaghan, C.A. (1998) A new look at T cells. J Exp Med 187, 1367-71.

Mizushima, S. and Nagata, S. (1990) pEF-BOS, a powerful mammalian expression vector. Nucleic Acids Res 18, 5322.

Mocarski, E.S. (1995) Cytomegaloviruses and their replication in Virology 3rdEd Edited by B. Fields volume 2 chapter 76. Lippinott-Raven Publishers.

Moran, M. and Miceli, M.C. (1998) Engagement of GPI-linked CD48 contributes to TCR signals and cytoskeletal reorganization: a role for lipid rafts in T cell activation. Immunity 9, 787-96.

Morris, R.J. and Beech, J.N. (1987) Sequential expression of OX2 and Thy-1 glycoproteins on the neuronal surface during development. An immunohistochemical study of rat cerebellum. Dev Neurosci 9, 33-44.

Nadler, L.M., Anderson, K.C., Marti, G., Bates, M., Park, E., Daley, J.F. and Schlossman, S.F. (1983) B4, a human B lymphocyte-associated antigen expressed on normal, mitogen-activated, and malignant B lymphocytes. J Immunol 131, 244-50.

Nicholson, M.W., Barclay, A.N., Singer, M.S., Rosen, S.D. and van der Merwe, P.A. (1998) Affinity and kinetic analysis of L-selectin (CD62L) binding to glycosylation-dependent cell-adhesion molecule-1. J Biol Chem 273, 763-70.

Nielsen, H., Engelbrecht, J., Brunak, S. and von Heijne, G. (1997) Identification of prokaryotic and eukaryotic signal peptides and prediction of their cleavage sites. Protein Eng 10, 1-6.

O'Callaghan C, A., Byford, M.F., Wyer, J.R., Willcox, B.E., Jakobsen, B.K., McMichael, A.J. and Bell, J.I. (1999) BirA enzyme: production and application in the study of membrane receptor-ligand interactions by site-specific biotinylation. Anal Biochem 266, 9-15.

Ogg, G.S. and McMichael, A.J. (1998) HLA-peptide tetrameric complexes. Curr Opin Immunol 10, 393-6.

Okuno, T., Takahashi, K., Balachandra, K., Shiraki, K., Yamanishi, K., Takahashi, M. and Baba, K. (1989) Seroepidemiology of human herpesvirus 6 infection in normal children and adults. J Clin Microbiol 27, 651-3.

Oosterwegel, M.A., Greenwald, R.J., Mandelbrot, D.A., Lorsbach, R.B. and Sharpe, A.H. (1999) CTLA-4 and T cell activation. Curr Opin Immunol 11, 294-300.

Ottemann, K.M., Xiao, W., Shin, Y.K. and Koshland, D.E., Jr. (1999) A piston model for transmembrane signaling of the aspartate receptor [In Process Citation]. Science 285, 1751-4.

Padawar, J. and Gordon, A.S. (1956) Cellular elements in the peritoneal fluid of some mammals. Anatomical Records 124, 209.

Paterson, D.J., Jefferies, W.A., Green, J.R., Brandon, M.R., Corthesy, P., Puklavec, M. and Williams, A.F. (1987) Antigens of activated rat T lymphocytes including a molecule of 50,000 Mr detected only on CD4 positive T blasts. Mol Immunol 24, 1281-90.

Perry, V.H. and Gordon, S. (1991) Macrophages and the nervous system. Int Rev Cytol 125, 203-44.

Pfuhl, M. and Pastore, A. (1995) Tertiary structure of an immunoglobulin-like domain from the giant muscle protein titin: a new member of the I set. Structure 3, 391-401.

Preston, S., Wright, G.J., Starr, K., Barclay, A.N. and Brown, M.H. (1997) The leukocyte/neuron cell surface antigen OX2 binds to a ligand on macrophages. Eur J Immunol 27, 1911-8.

Preston. (1996) Interactions of immunoglobulin superfamily leukocyte cell surface molecules. D.Phil thesis, Oxford University.

Rabinowitz, S.S. and Gordon, S. (1991) Macrosialin, a macrophage-restricted membrane sialoprotein differentially glycosylated in response to inflammatory stimuli [published erratum appears in J Exp Med 1992 Jan 1;175(1):309]. J Exp Med 174, 827-36.

Ranheim, T.S., Edelman, G.M. and Cunningham, B.A. (1996) Homophilic adhesion mediated by the neural cell adhesion molecule involves multiple immunoglobulin domains. Proc Natl Acad Sci U S A 93, 4071-5.

Reeves, R.H., Rue, E.E., Citron, M.P. and Cabin, D.E. (1997) High-resolution recombinational map of mouse chromosome 16. Genomics 43, 202-8.

Renne, R., Zhong, W., Herndier, B., McGrath, M., Abbey, N., Kedes, D. and Ganem, D. (1996) Lytic growth of Kaposi's sarcoma-associated herpesvirus (human herpesvirus 8) in culture. Nat Med 2, 342-6.

Rettig, M.B., Ma, H.J., Vescio, R.A., Pold, M., Schiller, G., Belson, D., Savage, A., Nishikubo, C., Wu, C., Fraser, J., Said, J.W. and Berenson, J.R. (1997) Kaposi's sarcoma-associated herpesvirus infection of bone marrow dendritic cells from multiple myeloma patients [see comments]. Science 276, 1851-4.

Roizman, B. and Seers, A.E. (1995) Herpes viruses and their replication in Virology 3rdEd Edited by B. Fields volume 2 chapter 72. Lippinott-Raven Publishers.

Russo, J.J., Bohenzky, R.A., Chien, M.C., Chen, J., Yan, M., Maddalena, D., Parry, J.P., Peruzzi, D., Edelman, I.S., Chang, Y. and Moore, P.S. (1996) Nucleotide sequence of the Kaposi sarcoma-associated herpesvirus (HHV8). Proc Natl Acad Sci U S A 93, 14862-7.

Sambrook, J., Fritsch, E.F. and Maniatis, T. (1989) Molecular cloning. A laboratory Manual. 2nd Edition, Cold Spring Harbour Laboratory Press.

Sanchez-Madrid, F., Szklut, P. and Springer, T.A. (1983) Stable hamster-mouse hybridomas producing IgG and IgM hamster monoclonal antibodies of defined specificity. J Immunol 130, 309-12.

Seed, B. and Aruffo, A. (1987) Molecular cloning of the CD2 antigen, the T-cell erythrocyte receptor, by a rapid immunoselection procedure. Proc Natl Acad Sci U S A 84, 3365-9.

Sewell, W.A., Palmer, R.W., Spurr, N.K., Sheer, D., Brown, M.H., Bell, Y. and Crumpton, M.J. (1988) The human LFA-3 gene is located at the same chromosome band as the gene for its receptor CD2. Immunogenetics 28, 278-82.

Sharp, P.A. (1981) Speculations on RNA splicing. Cell 23, 643-6.

Simmons, D. (1993) Cloning cell surface molecules by transient expression in mammalian cells. Cellular Interactions in Development: A Practical Approach, D.Hartley, eds. (Oxford: IRL Press), 93-128.

Simons, K. and Ikonen, E. (1997) Functional rafts in cell membranes. Nature 387, 569-72.

Singer, O. and Frenkel, N. (1997) Human herpesvirus 7 (HHV-7) DNA: analyses of clones spanning the entire genome. Arch Virol 142, 287-303.

Smith, G.L., Symons, J.A., Khanna, A., Vanderplasschen, A. and Alcami, A. (1997) Vaccinia virus immune evasion. Immunol Rev 159, 137-54.

Spielman, R.S., Lee, J., Bodmer, W.F., Bodmer, J.G. and Trowsdale, J. (1984) Six HLA-D region alpha-chain genes on human chromosome 6: polymorphisms and associations of DC alpha-related sequences with DR types. Proc Natl Acad Sci U S A 81, 3461-5.

Spriggs, M.K. (1996) One step ahead of the game: viral immunomodulatory molecules. Annu Rev Immunol 14, 101-30.

Springer, T.A. (1981) Monoclonal antibody analysis of complex biological systems. Combination of cell hybridization and immunoadsorbents in a novel cascade procedure and its application to the macrophage cell surface. J Biol Chem 256, 3833-9.

Stephens, P.E. and Cockett, M.I. (1989) The construction of a highly efficient and versatile set of mammalian expression vectors. Nucleic Acids Res 17, 7110.

Stryer, L. (1988) Biochemistry. 3rd Ed. W.H. Freeman and Company. New York.

Stumbles, P. and Mason, D. (1995) Activation of CD4+ T cells in the presence of a nondepleting monoclonal antibody to CD4 induces a Th2-type response in vitro. J Exp Med 182, 5-13.

Su, X.D., Gastinel, L.N., Vaughn, D.E., Faye, I., Poon, P. and Bjorkman, P.J. (1998) Crystal structure of hemolin: a horseshoe shape with implications for homophilic adhesion. Science 281, 991-5.

Sunderland, C.A., McMaster, W.R. and Williams, A.F. (1979) Purification with monoclonal antibody of a predominant leukocyte-common antigen and glycoprotein from rat thymocytes. Eur J Immunol 9, 155-9.

Takaya, R., Fukaya, T., Sasano, H., Suzuki, T., Tamura, M. and Yajima, A. (1997) Macrophages in normal cycling human ovaries; immunohistochemical localization and characterization. Hum Reprod 12, 1508-12.

Tanaka, H., Matsui, T., Agata, A., Tomura, M., Kubota, I., McFarland, K.C., Kohr, B., Lee, A., Phillips, H.S. and Shelton, D.L. (1991) Molecular cloning and expression of a novel adhesion molecule, SC1. Neuron 7, 535-45.

Tedder, T.F., Zhou, L.J. and Engel, P. (1994) The CD19/CD21 signal transduction complex of B lymphocytes. Immunol Today 15, 437-42.

Thomas, M.L. (1989) The leukocyte common antigen family. Annu Rev Immunol 7, 339-69.

Unkeless, J.C. and Jin, J. (1997) Inhibitory receptors, ITIM sequences and phosphatases. Curr Opin Immunol 9, 338-43.

Unwin, N. (1995) Acetylcholine receptor channel imaged in the open state. Nature 373, 37-43.

van der Merwe, P.A. and Barclay, A.N. (1994) Transient intercellular adhesion: the importance of weak protein- protein interactions. Trends Biochem Sci 19, 354-8.

van der Merwe, P.A. and Barclay, A.N. (1996) Analysis of cell-adhesion molecule interactions using surface plasmon resonance. Curr Opin Immunol 8, 257-61.

van der Merwe, P.A., Barclay, A.N., Mason, D.W., Davies, E.A., Morgan, B.P., Tone, M., Krishnam, A.K., Ianelli, C. and Davis, S.J. (1994) Human cell-adhesion molecule CD2 binds CD58 (LFA-3) with a very low affinity and an extremely fast dissociation rate but does not bind CD48 or CD59. Biochemistry 33, 10149-60.

van der Merwe, P.A., Bodian, D.L., Daenke, S., Linsley, P. and Davis, S.J. (1997) CD80 (B7-1) binds both CD28 and CTLA-4 with a low affinity and very fast kinetics. J Exp Med 185, 393-403.

van der Merwe, P.A., Bodian, D.L., Daenke, S., Linsley, P. and Davis, S.J. (1997) CD80 (B7-1) binds both CD28 and CTLA-4 with a low affinity and very fast kinetics. J Exp Med 185, 393-403.

van der Merwe, P.A., Brown, M.H., Davis, S.J. and Barclay, A.N. (1993) Affinity and kinetic analysis of the interaction of the cell adhesion molecules rat CD2 and CD48. Embo J 12, 4945-54.

van der Merwe, P.A., McNamee, P.N., Davies, E.A., Barclay, A.N. and Davis, S.J. (1995) Topology of the CD2-CD48 cell-adhesion molecule complex: implications for antigen recognition by T cells. Curr Biol 5, 74-84.

van der Merwe, P.A., McPherson, D.C., Brown, M.H., Barclay, A.N., Cyster, J.G., Williams, A.F. and Davis, S.J. (1993) The NH2-terminal domain of rat CD2 binds rat CD48 with a low affinity and binding does not require glycosylation of CD2. Eur J Immunol 23, 1373-7.

Varma, R. and Mayor, S. (1998) GPI-anchored proteins are organized in submicron domains at the cell surface. Nature 394, 798-801.

Viola, A., Schroeder, S., Sakakibara, Y. and Lanzavecchia, A. (1999) T lymphocyte costimulation mediated by reorganization of membrane microdomains [see comments]. Science 283, 680-2.

Vleminckx, K. and Kemler, R. (1999) Cadherins and tissue formation: integrating adhesion and signaling. Bioessays 21, 211-20.

Wagers, A.J., Waters, C.M., Stoolman, L.M. and Kansas, G.S. (1998) Interleukin 12 and interleukin 4 control T cell adhesion to endothelial selectins through opposite effects on alpha1, 3-fucosyltransferase VII gene expression. J Exp Med 188, 2225-31.

Wang, J.H., Smolyar, A., Tan, K., Liu, J.H., Kim, M., Sun, Z.Y., Wagner, G. and Reinherz, E.L. (1999) Structure of a heterophilic adhesion complex between the human CD2 and CD58 (LFA-3) counterreceptors. Cell 97, 791-803.

Warner, M.S., Geraghty, R.J., Martinez, W.M., Montgomery, R.I., Whitbeck, J.C., Xu, R., Eisenberg, R.J., Cohen, G.H. and Spear, P.G. (1998) A cell surface protein with herpesvirus entry activity (HveB) confers susceptibility to infection by mutants of herpes simplex virus type 1, herpes simplex virus type 2, and pseudorabies virus. Virology 246, 179-89.

Webb, M. and Barclay, A.N. (1984) Localisation of the MRC OX-2 glycoprotein on the surfaces of neurones. J Neurochem 43, 1061-7.

Weisman, H.F., Bartow, T., Leppo, M.K., Marsh, H.C., Jr., Carson, G.R., Concino, M.F., Boyle, M.P., Roux, K.H., Weisfeldt, M.L. and Fearon, D.T. (1990) Soluble human complement receptor type 1: in vivo inhibitor of complement suppressing post-ischemic myocardial inflammation and necrosis. Science 249, 146-51.

Weiss, A. and Schlessinger, J. (1998) Switching signals on or off by receptor dimerization. Cell 94, 277-80.

Wild, M.K., Cambiaggi, A., Brown, M.H., Davies, E.A., Ohno, H., Saito, T. and van der Merwe, P.A. (1999) Dependence of T cell antigen recognition on the dimensions of an accessory receptor-ligand complex. J Exp Med 190, 31-41.

Willcox, B.E., Gao, G.F., Wyer, J.R., Ladbury, J.E., Bell, J.I., Jakobsen, B.K. and van der Merwe, P.A. (1999) TCR binding to peptide-MHC stabilizes a flexible recognition interface. Immunity 10, 357-65.

Williams, A.F. (1984) The immunoglobulin superfamily takes shape [news]. Nature 308, 12-3.

Williams, A.F. (1985) Immunoglobulin-related domains for cell surface recognition [news]. Nature 314, 579-80.

Williams, A.F. and Barclay, A.N. (1986) Glycoprotein antigens of the lymphocyte surface and their purification by antibody affinity chromatography. Handbook of Experimental Immunology. Volume 1. D.M. Weir, eds. (Oxford: Blackwell Scientific Publications)., 22.1-24.

Williams, A.F. and Barclay, A.N. (1988) The immunoglobulin superfamily--domains for cell surface recognition. Annu Rev Immunol 6, 381-405.

Williams, A.F. and Gagnon, J. (1982) Neuronal cell Thy-1 glycoprotein: homology with immunoglobulin. Science 216, 696-703.

Williams, A.F., Galfre, G. and Milstein, C. (1977) Analysis of cell surfaces by xenogeneic myeloma-hybrid antibodies: differentiation antigens of rat lymphocytes. Cell 12, 663-73.

Wong, Y.W., Williams, A.F., Kingsmore, S.F. and Seldin, M.F. (1990) Structure, expression, and genetic linkage of the mouse BCM1 (OX45 or Blast-1) antigen. Evidence for genetic duplication giving rise to the BCM1 region on mouse chromosome 1 and the CD2/LFA3 region on mouse chromosome 3. J Exp Med 171, 2115-30.

Woollett, G.R., Barclay, A.N., Puklavec, M. and Williams, A.F. (1985) Molecular and antigenic heterogeneity of the rat leukocyte-common antigen from thymocytes and T and B lymphocytes. Eur J Immunol 15, 168-73.

Yasukawa, M., Inoue, Y., Ohminami, H., Sada, E., Miyake, K., Tohyama, T., Shimada, T. and Fujita, S. (1997) Human herpesvirus 7 infection of lymphoid and myeloid cell lines transduced with an adenovirus vector containing the CD4 gene. J Virol 71, 1708-12.